The transport of organic vapours through polyorganosiloxane membranes

Preece, S. W.

Award date:
1989

Awarding institution:
University of Bath

THE TRANSPORT OF ORGANIC VAPOURS THROUGH POLYORGANOSILOXANE MEMBRANES

submitted by S.W.Preece

for the degree of PhD

of the University of Bath

1989

ProQuest LLC
789 East Eisenhower Parkway
P.O. Box 1346
Ann Arbor, MI 48106-1346

Acknowledgements

A.J.Ashworth for his help and supervision and his voice of encouragement when the apparatus wouldn't work.

E.J.Stainer for his technical advice and helping hand when the apparatus wouldn't work.

My fellow workers in the Chemistry department, particularly P.J.Lawrence and G.Bond for accompanying me to the bar when my apparatus wouldn't work and M.M^{c}Collom and P.Smith for moral support whilst writing up.

S.C.Parker for allowing access to his computer terminals whilst writing up.

My mother and father who helped my grant stretch for another three years and would love to be mentioned in print.

Summary

The transport properties of acetone, ethanol, tetrachloroethylene and nitrobenzene were investigated in three polyorganosiloxane membranes with the aim of finding a membrane which preferentially transported nitrobenzene with respect to the other permeants. The membranes used were a commercially available poly(dimethylsiloxane) (PDMS) membrane containing silica as a filler, an unfilled PDMS membrane and a membrane made from a polyorganosiloxane containing ester functionalities substituted onto the sidechains of the polymer. A dynamic method was used to measure the permeation and diffusion coefficients of the organic vapours in the membranes over a range of temperatures and vapour pressures to investigate the variation of transport properties with temperature and concentration.

Arrhenius plots for diffusivity and permeability were found to be curved, showing that the activation energies varied with temperature. Permeability and diffusivity coefficients were found to vary with concentration. All polymer/permeant systems showed an increase in permeability with increasing concentration except for the systems involving nitrobenzene which showed a decrease. Diffusion coefficients generally increased with concentration except for the systems involving tetrachloroethylene where there appeared to be a decrease in diffusivity. The permeability and

diffusivity of the membranes increased in the order filled PDMS < unfilled PDMS < ester-substituted polysiloxane for all four permeants. The permeability of the vapours increased in the order acetone < ethanol < tetrachloroethylene < nitrobenzene and the diffusion coefficients increased in the order nitrobenzene < tetrachloroethylene < acetone < ethanol in all of the membranes at similar relative pressures. Solubilities were calculated from the permeability and diffusivity coefficients.

The permeability selectivity of nitrobenzene over the permeants at 90°C increases in the membranes in the order filled PDMS < unfilled PDMS < ester-substituted polysiloxane, although the effect is smallest for the selectivity of nitrobenzene over tetrachloroethylene. The increase in permeability selectivity of nitrobenzene over acetone and ethanol from the filled PDMS through to the ester-substituted membrane is due to a large increase in the solubility selectivity, where as the smaller increase in the permeability selectivity relative to tetrachloroethylene is due to an increase in the diffusivity selectivity.

CONTENTS

Appendix containing tables and graphs appears at the end of the text.

FIGURES

TABLES

APPENDIX - TABLES

Permeability and Diffusivity

Variation of Transport Properties with Permeant Pressure

Solubility

Variation of Solubility with Permeant Pressure

APPENDIX - FIGURES

LnP against 1/T Plots

Figure A1,A1a	Acetone/Filled PDMS
Figure A2	Ethanol/Filled PDMS
Figure A3	Tetrachloroethylene/Filled PDMS
Figure A4	Nitrobenzene/Filled PDMS
Figure A5	Acetone/M1
Figure A6	Ethanol/M1
Figure A7	Tetrachloroethylene/M1
Figure A8	Nitrobenzene/M1
Figure A9,A9a	Acetone/M18
Figure A10.A10a	Ethanol/M18
Figure A11,A11a	Tetrachloroethylene/M18
Figure A12,A12a	Nitrobenzene/M18

LnD against 1/T Plots

Figure A13	Acetone/Filled PDMS
Figure A14,A14a	Ethanol/Filled PDMS
Figure A15,A15a	Tetrachloroethylene/Filled PDMS
Figure A16,A16a	Nitrobenzene/Filled PDMS
Figure A17,A17a	Acetone/M1
Figure A18,A18a	Ethanol/M1
Figure A19,A19a	Tetrachloroethylene/M1
Figure A20,A20a	Nitrobenzene/M1
Figure A21,A21a	Acetone/M18

LnS against 1/T Plots

LnP against Permeant Pressure

LnD against Permeant Pressure

LnS against Permeant Pressure

INTRODUCTION

Chapter 1 : Introduction.

1.1 Objectives.

When searching for a membrane to be used in a separation process, the two most important criteria to consider are the permeability of the membrane to a gas or vapour and the selectivity. The permeability gives a measure of the amount of a given permeant which will be transported across the membrane in a given time, and the selectivity shows how the transport of the permeant is favoured in relation to the movement of other unwanted gases or vapours across the membrane. For a membrane to be commercially viable, it must have both high permeability and high selectivity, with high permeability to ensure a sufficient yield of the permeant over a reasonable timespan and high selectivity so that enough of the unwanted contaminants are removed to give a permeate (i.e. the gas and vapour which has passed through the membrane) of the required purity.

The problem in finding such a membrane is that these criteria are not necessarily compatible, a change in the structure of the polymer which produces an increase in the permeability may also result in an unacceptable decrease in selectivity. The aim of this

research programme was to formulate a membrane which had an acceptable balance between these two properties when applied to the selective permeation of nitro-organic compounds in the atmosphere relative to undesirable species such as chloro-organics, acetone and ethanol; a membrane which had a sufficiently high permeability for organic nitro-compounds, whilst also showing selectivity for nitro-compounds in preference to any unwanted compounds that are present.

Of the possible materials which may have been considered as potential membranes for this purpose, the polysiloxanes[1] appear the most appropriate in view of their high permeability and stability. Poly(dimethylsiloxane) (PDMS) was chosen as the material for the first membranes to be studied due to its ready commercial availability. These membranes contained an amount of silica as filler which would affect the transport properties, it was therefore decided to study a PDMS membrane without filler for comparison and to study a polysiloxane with a modified structure in an attempt to enhance the membrane properties. The modification chosen was the addition of ester-groupings to the side-chains of the polymer backbone giving the third membrane for investigation. The structure and synthesis of these membranes is discussed later in section 1.7. The organic vapours chosen for investigation with the three membranes were

acetone, ethanol, tetrachloroethylene and nitrobenzene.

1.2 Transport through Polymer Membranes.

Transport of gases and vapours across a polymer film has been found to occur via a solution-diffusion mechanism first suggested by Graham[2] in 1866. The permeant coming into contact with the surface of the film dissolves into the polymer, moves across the quasi-liquid environment formed by the mobile polymer chains by a diffusion mechanism and finally 'evaporates' from the polymer into the atmosphere at the other side of the film. By analogy with the transfer of heat by conduction, the rate of transfer of a permeant across unit cross-sectional area of the polymer can be expressed as being proportional to the gradient of its concentration at any point within the polymer to give Fick's first law of diffusion:

$$F = -D \frac{dc}{dx} \qquad (1.1)$$

where F is the rate of transfer or flux per unit cross-sectional area, D is the proportionality constant defined as the mutual diffusion coefficient, c is the concentration of the diffusing substance and x is the space co-ordinate normal to the reference plane. For uni-directional diffusion, which occurs in the case of

transport across thin films, the rate of change of permeant concentration at any point within an isotropic polymer is given by Fick's second law of diffusion:

$$\frac{dc}{dt} = D \frac{d^2c}{dx^2} \qquad (1.2)$$

This is for cases where the diffusion coefficient is independent of time and concentration.

If steady-state diffusion (i.e. $d^2c/dx^2=0$) through a thin polymer film of thickness l is considered, where the concentration of the permeant at the surfaces of the film is c_1 at x=0 and c_2 at x=l, then equation (1.1) can be integrated between the two concentrations;

$$F \int_0^l dx = -D \int_{c_2}^{c_1} dc \qquad (1.3)$$

to give:

$$F = \frac{D(c_1-c_2)}{l} \qquad (1.4)$$

However, in most experimental methods the surface concentrations of the permeant in the polymer film, c_1 and c_2, are not known, but the partial pressures of the gas or vapour, p_1 and p_2, in equilibrium with the surface permeant concentration, can be found. If it is assumed that the system obeys Henry's law, where the concentration of permeant absorbed in the

surface polymer is proportional to the partial pressure of the permeant at the surface with proportionality constant S, being defined as the solubility constant of the permeant in the polymer,

$$c = Sp \qquad (1.5)$$

then equation (1.4) can be rewritten as:

$$F = \frac{DS(p_1-p_2)}{l} \qquad (1.6)$$

The product D.S is defined as the permeability,

$$P = DS \qquad (1.7)$$

Thus showing that the permeability of a polymer to a permeant is dependent on both the diffusion and solubility coefficients.

1.3 Effect of Temperature on Transport Properties

The diffusion of gases and vapours in rubbery polymers has been found to be an activated process[3-6] with the diffusion coefficient often being strongly dependent on temperature. An increase in

temperature leads to greater mobility of the polymer chains so that it is easier for the permeant molecules to pass through the polymer giving a higher diffusion rate. An Arrhenius activation energy for diffusion E_D, is defined by

$$E_D = -R \frac{d\ln D}{d(1/T)} \qquad (1.8)$$

which, if E_D is independent of temperature, gives the linear Arrhenius relationship

$$D = D_o \exp\left\{\frac{-E_D}{RT}\right\} \qquad (1.9)$$

where D_O is the pre-exponential factor. Studies of the temperature dependence of permeability coefficients have shown that these follow a similar relationship with an Arrhenius activation energy for permeation E_P, being defined by

$$E_P = -R \frac{d\ln P}{d(1/T)} \qquad (1.10)$$

which, if E_P is independent of temperature, gives the linear Arrhenius relationship

$$P = P_o \exp\left\{\frac{-E_P}{RT}\right\} \qquad (1.11)$$

where P_O is the pre-exponential factor. The temperature dependence of the solubility of a penetrant in a polymer can be represented by a Clausius-Clapeyron equation

$$S = S_o \exp\left\{\frac{-\Delta H_S^o}{RT}\right\} \qquad (1.12)$$

where ΔH_s is the enthalpy of solution and S_o is a pre-exponential constant which, as S is an equilibrium constant, can be written as

$$S_o = \exp\left\{\frac{\Delta S^o}{R}\right\} \qquad (1.13)$$

where ΔS^o is the standard entropy of solution.

From the definition of P=DS it follows that

$$E_P = E_D + \Delta H_S \qquad (1.14)$$

Thus the temperature dependence of the permeability is dependent on the temperature dependence of both the diffusion coefficient and the solubility coefficient. When E_D is small and there is a negative heat of solution it is possible to have a negative

activation energy for permeation so that the permeability decreases with increasing temperature.

This situation, where LnD varies linearly with 1/T, is that which is presented by the simplest form of the solution-diffusion model which applies over small temperature ranges for simple gases in rubbery polymers. Experimentally it has been shown that Arrhenius plots may deviate markedly from a straight line. Van Amerongen[6] found that even inert gases in natural rubber, above its glass transition temperature, over a large temperature range (-18 to 100°C) showed curvature in the Arrhenius plot for diffusion, and similar curvature has been found, over a smaller temperature range, for paraffin hydrocarbons[7] and benzene[8,9] in natural rubber. In each case the plot shows a convex curvature upwards such that the diffusion coefficient is lower at higher temperatures than would be expected from a linear relationship, and the apparent activation energy for diffusion, taken from the gradient of the plot, decreases with increasing temperature.

The temperature dependence of E_D shows that equations (1.8) and (1.9) are oversimplifications of the situation. The empirical relationship[6]

$$\frac{d(\ln D)}{d(1/T)} = \frac{-(E_o + aT)}{R} \qquad (1.15)$$

gives a better representation of the problem, where it is assumed that

$$E_D = E_o + aT \qquad (1.16)$$

and

$$a = \frac{dE_D}{dT} \qquad (1.17)$$

Integration of equation (1.15) gives

$$D = CT^{a/R} \exp\left\{\frac{-E_o}{RT}\right\} \qquad (1.18)$$

The situation where E_D varies with temperature becomes more clear if the activation energy for diffusion is considered to be the energy required to separate the polymer chains to a given distance[6] so that a sufficiently large passage is formed to allow a diffusive jump of the penetrant molecule. This energy would then correspond to the cohesive energy of the chain element concerned, which is itself a function of temperature. This still remains an oversimplification of the problem, but it does demonstrate that a

variation of activation energy with temperature should be expected. More suitable approximations have been made by using statistical methods where there is consideration of either the probability of the polymer chains assuming a configuration where a successful diffusive jump of the penetrant molecule can occur, or the energy required for a critical volume disturbance to allow the movement of the penetrant. These models depend greatly on the availability of data for input parameters and are limited by the complexity of the calculation procedures involved. The activation energy for permeation E_P, has also been found to vary with temperature. This has very little theoretical value, but can be used in conjunction with measured values of E_D in equation (1.14) to yield the heat of solution for a permeant/polymer system.

1.4 Effect of Concentration

Ideally, the diffusion coefficient of a permeant in a polymer should be independent of the permeant concentration. However, many workers have found that diffusion of organic vapours in polymers is greatly affected by the concentration[8-13]. As stated in the previous section, the diffusion of a permeant in a polymer is dependent on the free volume of the polymer and the mobility of the polymer chain segments allowing

the redistribution of the free volume to enable permeant molecules to complete successful diffusive jumps. For permeants with low solubility there is little or no effect on this, but for permeants with higher solubilities, such as easily condensable organic vapours, the higher concentration of permeant present in the polymer causes a change in the free volume of the polymer thus affecting the diffusion.

The solubility of the permeant depends largely on the specific interactions between the permeant and the polymer, which can be expressed in terms of the Flory interaction parameter χ[14]. For large values of χ (>2.5), the solvation power of the permeant is small and the membrane properties are unaffected by concentration. For lower values of χ (<2.5) the interactions are much stronger causing swelling of the polymer as the permeant concentration increases. As the polymer swells there is an increase in free volume and polymer chain segment mobility (i.e. plasticization) thus leading to an increase in the diffusivity. For systems in which the solubility obeys Henry's law, the dependence of the diffusion coefficient on the sorbed permeant concentration has been found to follow the empirical relationship

$$D = D(0)\exp(kc) \qquad (1.20)$$

where D(0) is the diffusion coefficient at zero concentration and k is a constant at a given temperature relating to the permeant-polymer interaction. For systems where Henry's law is not obeyed, the concentration dependence of the diffusion coefficient can be better represented by using the dependence on the vapour activity[10,15]

$$D = D(0)\exp(\alpha a) \qquad (1.21)$$

where a is the vapour activity, essentially the ratio of the presure of the vapour to the saturated vapour pressure ($a=p/p^{o}$), and α is a characteristic parameter of the system.

If the pre-exponential factor D_o, in equation 1.9, is considered to be independent of permeant concentration, then comparison of equations 1.20, 1.21 and 1.9 suggests that the activation energy for diffusion will be affected by permeant concentration according to the relationship

$$E_D = E_D(c \to 0) - \gamma RT \qquad (1.22)$$

where y is kc or αa and $E_D(c \rightarrow 0)$ is the activation energy for diffusion expected when the polymer is unaffected by the presence of the penetrant. The k and α are measures of the plasticizing ability of the penetrant causing a reduction in the activation energy by a quantity yRT.

1.5 Methods of Measurement

Diffusion and permeation coefficients are usually determined by observing the flow of a permeant through a membrane. The method can be divided into two categories: (i) permeation into a closed chamber[4-7,16-18] (ii) permeation into a flowing stream (open chamber)[19-22]. In the first category the cumulative mass of permeant that permeates through the membrane into a closed chamber is measured as a function of time, either by observing the increase of pressure at constant volume, the increase of volume at constant pressure or the change in composition of the atmosphere in the chamber. The method most commonly used is that involving the measurement of pressure in the chamber[4].

The permeant is brought into contact with the upstream face of the membrane either from a closed reservoir held at constant pressure or, in the case of condensable vapours, as a gas stream containing the

permeant passed over the surface of the membrane. This can then pass through the membrane into an evacuated receiving chamber where a barometric device is used to measure the pressure. A plot of accumulated permeant against time takes the form of that shown in figure (1.1). There is an initial gradual rise and then, when steady-state is reached, the pressure increases linearly with time. The permeability can then be calculated from the slope of the linear section of the plot and the diffusion coefficient can be found from the intercept θ, of the line on the time axis, also known as the time lag. There are several disadvantages to this method. To maintain steady-state conditions the pressure difference between the upstream and downstream faces of the membrane must be kept constant. This difference has to be large in order that the pressure from build-up of the permeant in the collecting reservoir is negligible in comparison with that at the upstream face of the membrane. Due to the large pressure difference the membrane requires a support which may affect the permeability by reducing the effective surface of the membrane, and there is the possibility of the membrane being damaged as it is forced against the support. It has also been observed[23] that for high pressure measurements the hydrostatic pressure may cause a decrease in the free volume of the polymer thus affecting the transport properties. The

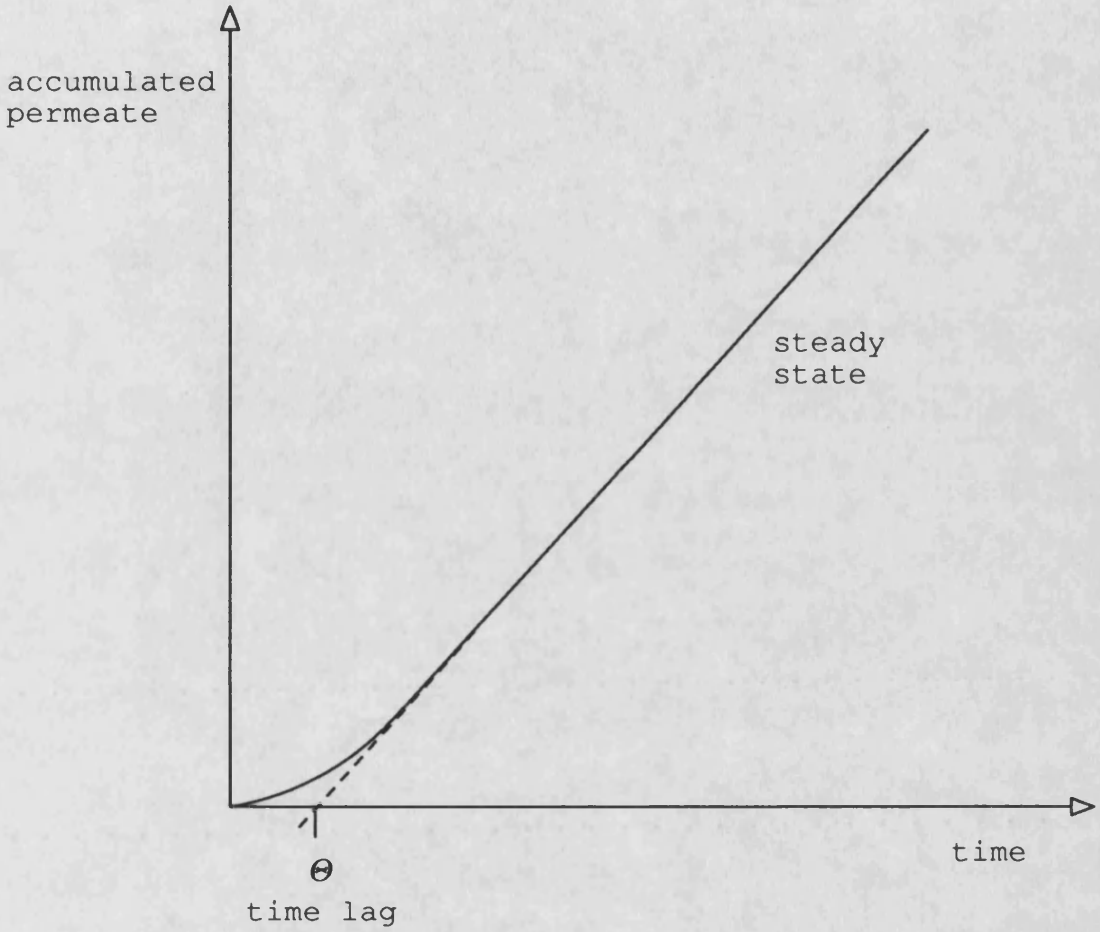

Figure 1.1 : Typical Plot Found from Experiments In Permeation into a Closed Chamber.

method also requires close attention to vacuum-seals to ensure there is no leakage.

The open receiving volume method is free from the disadvantages of the closed chamber method and has the added advantage of yielding data which is relatively free of cumulative error. In this research, a recently developed dynamic method has been used[22]. The membrane is clamped in a permeation cell separating upstream and downstream chambers. The feed stream containing the penetrant gas or vapour is passed across the face of the membrane, any penetrant which permeates through the membrane is picked up by a carrier gas stream (nitrogen) and carried to a detector. The signal from the detector, produced as a trace on a recorder (see figure 2.5), shows an initial increase from which the diffusion coefficient can be found and, when the system reaches steady-state, a plateau from which the permeability can be calculated.

The calculation of the permeability is straight forward. Provided the thickness of the membrane, the surface area of the membrane and the pressure difference across the membrane are known, the permeability can be found if equations (1.6) and (1.7) are combined and written as

$$P = \frac{F.l}{(p_1 - p_2)} \qquad (1.23)$$

In this method, any penetrant reaching the downstream face of the membrane is immediately removed by the carrier stream. The pressure of penetrant in the downstream chamber is therefore effectively zero and the pressure difference across the membrane is given by the pressure of the penetrant in the upstream chamber, p. The flux, F is given by

$$F = \frac{S_\infty K}{A} \qquad (1.24)$$

where S_∞ is the plateau height of the recorder trace, A is the surface area of the membrane available for permeation and K is a calibration constant calculated for the detector. Therefore the permeability is given by

$$P = \frac{S_\infty . K . l}{A . p} \qquad (1.25)$$

Three methods have been proposed for the estimation of a diffusion coefficient from the trace recording generated by a permeation run with an open receiving volume. The first and simplest method is to find the time, $t_{1/2}$ at which the height of the recorder

signal, S reaches half its asymptotic value, S_∞. The diffusion coefficient is then given by[24]

$$D \approx \frac{l^2}{7.199\, t_{\frac{1}{2}}} \qquad (1.26)$$

Another estimation technique is a moment method proposed by Felder et al[25-27]. A quantity, τ_p given by

$$\tau_p = \int_0^\infty \left[1 - \frac{S(t)}{S_\infty} \right] dt \qquad (1.27)$$

has been shown to be equal to the time lag of the closed volume experiment. τ_p can be calculated by numerical integration and used in the estimation of the diffusion coefficient thus

$$\tau_p = \frac{l^2}{6D} \qquad (1.28)$$

A third method is to use an asymptotic solution of the diffusion equation valid at small times. Both Rogers et al[28] and Pasternak et al[22] have used methods based on this, but the method used by Pasternak is valid over a wider range of times and has been adopted as the method for this work.

The following mathematical treatment is given by

Pasternak et al[22].

The permeation flux, F through a membrane of thickness l is given by

$$F(x) = -D \frac{dc}{dx} \qquad (1.29)$$

where c is the concentration of the permeant in the membrane at position x. In this treatment it is assumed that the diffusion coefficient, D is not a function of concentration, that the surface concentration is proportional to the pressure of the permeant and that the swelling of the membrane is negligible.

The following generalised boundary conditions are characteristic for permeation studies:

$c = 0$	$x = l$	$t \leq 0$
$c = c_i$	$x = 0$	$t = 0$
$c = c_f$	$x = 0$	$t > 0$
$c = c_i(l - x)/l$	$0 \leq x \leq l$	$t = 0$
$c = c_f(l - x)/l$	$0 \leq x \leq l$	$t = \infty$

These boundary conditions represent the change from one steady-state to another, with the pressure of the permeant on the downstream side of the membrane always kept at zero. Either c_i or c_f, the initial and

final concentrations at x = 0, can be zero. Two useful solutions of the differential equation, which were obtained by generalizing expressions in the literature[28,29] are

$$F = \frac{Dc_i}{l} + \frac{D(c_i-c_f)}{l}\left[1 + 2\sum_{}^{\infty}(-1)^n \exp\left\{\frac{-n^2\pi^2 Dt}{l^2}\right\}\right] \qquad (1.30)$$

$$F = \frac{Dc_i}{l} + \frac{D(c_i-c_f)}{l}\,\frac{4}{\sqrt{\pi}}\sqrt{\frac{l^2}{4Dt}}\sum_{n=1,3,5..}^{\infty}\exp\left\{\frac{-n^2l^2}{4Dt}\right\} \qquad (1.31)$$

where F is the flux at x = l and Dc_i/l and Dc_f/l are the steady-state fluxes at time t = 0 and t = ∞ respectively. Equation (1.31) was found to be more useful, converging at small values of t and giving a first order approximation of

$$\Delta F = \Delta F_\infty \;\frac{4}{\sqrt{\pi}}\sqrt{\frac{l^2}{4Dt}}\;\exp\left\{\frac{-l^2}{4Dt}\right\} \qquad (1.32)$$

where $\Delta F = F - Dc_i/l$ represents the change in flux during the experiment. If it is assumed that the first order approximation is reasonable when the second term contributes less than 2% to the sum, then equation (1.32) holds over a wide range (i.e. $\Delta F/\Delta F_\infty < 0.97$). Equation (1.32) can be written in a more convenient form

$$\frac{\Delta F}{\Delta F_\infty} = \frac{4}{\sqrt{\pi}} X \exp(-X^2) \qquad (1.33)$$

where $X^2 = l^2/4Dt$. A plot of $\Delta F/\Delta F_\infty$ against $1/X^2$ gives a theoretical curve comparable to the experimental curves obtained from permeation runs. The plot has an extended linear range with an empirical slope of $d(\Delta F/\Delta F_\infty)/d(1/X^2) = 1.42$. When the definition of X is introduced this gives

$$D = 0.176\, l^2 \frac{dS}{dt} \cdot \frac{1}{S_\infty} \qquad (1.34)$$

where dS/dt is the gradient of the linear part of the experimental curve and S_∞ is the height of the plateau. Thus if the slope of the experimental curve and the maximum signal height are known, both the diffusivity and permeability can be calculated from the same experiment.

1.6 Criteria for Separation Membranes

As stated previously, the two most important criteria when selecting a material for use as a separation membrane are the permeability of a particular penetrant and the selectivity for that penetrant over others. Unfortunately, with many

commercially available membranes, the dual properties of high permeability and high selectivity seem to be mutually exclusive, as demonstrated by poly(dimethylsiloxane) which is one of the most permeable materials but also has one of the lowest selectivities for many gas mixtures[30-34]. The aim of many workers is now to synthesise a material which optimises the desirable properties.

Providing that the downstream pressure is much lower than the upstream pressure, a guide to the selectivity of a material to two components of a mixture can be found by considering the ideal separation factor[35]

$$\alpha^*_{AB} = \frac{P_A}{P_B} \qquad (1.35)$$

which is equal to the ratio of the permeabilities of the two pure components, P_A and P_B. This is a very simplistic view as in many cases, especially with vapours, the permeability of each component of the mixture may not be independent of the other components. However, it is useful as a starting point for material selection. As permeation takes place by a solution-diffusion mechanism, it is often useful to split the separation into two by combining equation (1.35) with equation (1.7) to give[35-37]

$$\alpha^*_{AB} = \frac{P_A}{P_B} = \frac{D_A}{D_B}\,\frac{S_A}{S_B} \qquad (1.36)$$

From this it is apparent that separation is dependent upon a kinetic factor D_A/D_B, which can be called the mobility or diffusivity selectivity, and a thermodynamic factor S_A/S_B, which can be called the solubility selectivity.

The diffusivity selectivity is based on the inherent ability of the polymer to restrict the mobility of a penetrant molecule on the basis of size and shape. This ability is dependent upon factors which affect the free volume of the polymer, such as the rigidity of the polymer chain backbone and the packing of the polymer segments. Any attempt to influence the selectivity of a membrane material by chemically modifying the polymer structure to bring about a change in diffusivity selectivity, is limited to gas or vapour mixtures where the components can be differentiated by size and shape. As polymers are designed with more rigid back bones and closer intersegmental packing, thus reducing the free volume, the membranes tend to act more as molecular sieves, discriminating between penetrants solely by their bulk. There is also the disadvantage that the transport of all components of the mixture is inhibited, not just that of the

undesirable penetrants. For separations where their there is little difference in the size and shape of the components of the mixture, this approach is obviously unsatisfactory.

The solubility selectivity is dependent upon the molecular interactions between the polymer and the penetrant. If a substituent is added to the polymer chain containing a functional group which will interact specifically with the penetrant to be separated, this will result in an increase in the solubility of penetrant with respect to the other components of the mixture. Therefore, providing there is no compensating decrease in the diffusivity selectivity, the overall selectivity will be improved in favour of the penetrant. The foreseeable problem is that the requirement for a good plasticizer is also that there are specific interactions with the polymer so that the plasticizer is a good solvent. Care has to be exercised that the penetrant will not act as a plasticizer for the chemically modified polymer thus causing an increase in polymer chain mobility and free volume. This would enhance the diffusion of all components of a mixture which may lead to decrease in diffusivity selectivity that could outweigh any benefits from the favourable solubility.

1.7 Synthesis of Polymer Membranes

Three polymer membranes have been used in this research, one of which was commercially available. The two other membranes were synthesised at the University of Bath for a SERC research project[38]. The commercially available membrane was made of poly(dimethylsiloxane) (PDMS), of thickness 5.33×10^{-3}cm obtained from ESCO (Rubber) Ltd. No information is available on the manufacture of these PDMS films, the only known property is that the polymer contains 28% by weight of filler. One of the membranes made at the University was also a PDMS film, but without filler so that a comparison could be made between the transport properties of penetrants in filled and unfilled membranes. This film had a measured average thickness of 1.65×10^{-2}cm. The third membrane, also made at the University, consisted of a polyorganosiloxane containing an ester functionality, it had a measured average thickness of 3.33×10^{-2}cm and once again no filler was added.

The polyorganosiloxane containing an ester functionality (M18) was synthesised by the platinum catalysed addition of the unsaturated ester, $CH_2=CHCH_2COOCH_3$, to a linear poly(methylhydridosiloxane), $Me_3SiO[MeSi(H)O]_nSiMe_3$ (where n ~ 40). The polymer had the structure

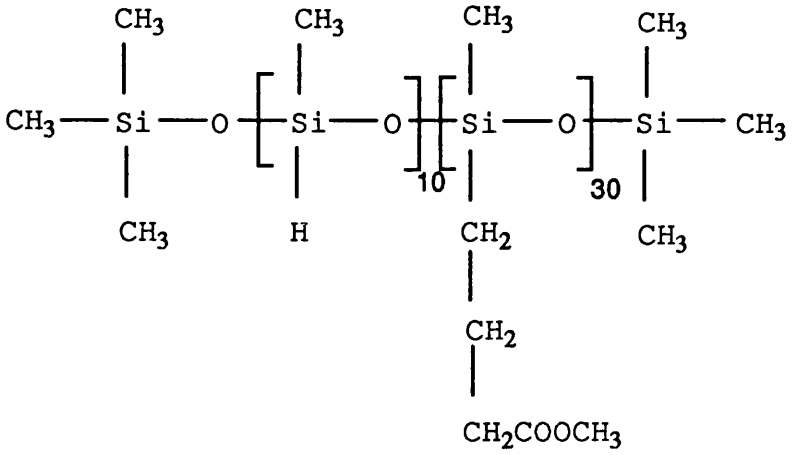

and a number average molecular weight (Mn) of 5360 and still contained some Si-H linkages[39]. The solid polymer dissolved in the minimum amount of toluene was crosslinked with a α,ω-dihydroxypoly(dimethylsiloxane) (Mn=1350) using dibutyltinlaurate as a catalyst and tetramethoxysilane to ensure complete reaction of the Si-H linkages. The clear liquid polymer mixtures contained 3g ester functionalised polymer, 5g PDMS, 0.5g tetramethylsilane and 0.75g catalyst. The crosslinking was carried out at ambient temperature in a press using a 50 ton force, with the liquid polymer being held between sheets of cellulose acetate to produce a film having an ester functionality of 17.3 mol% of Si atoms.

The unfilled PDMS membrane (M1) was prepared from a higher molecular weight α,ω-dihydroxypoly(dimethylsiloxane) (Mn=71000) with dibutyltinlaurate catalyst and tetramethoxysilane. As before the reaction was carried out at ambient

temperature in a press using a 50 ton force, with the mixture held between sheets of cellulose acetate. The number average molecular weights were determined at the Rubber and Plastics Research Association, Shrewsbury by gel permeation chromatography based on calibration with polystyrene and toluene as solvent.

Differential calorimetry scans of the M1 and M18 membranes were taken in the course of the SERC research project. In the scan of the M1 membrane (figure 1.2) the first feature to take account of is at -117°C which represents the transformation of the polymer from the glassy to the rubbery state, i.e. the glass transition temperature. At approximately -95°C there is an increase in the heat flow caused by the exothermic process of crystallisation occurring in the polymer. At approximately -50°C there is a trough in the scan due to heat absorbed as the crystals melt. The scan of the M18 polymer (figure 1.3) takes a very similar form, with the glass transition appearing at -118°C, crystallisation occuring at -95.5°C and the crystals melting at -55.5°C. These scans show that that the membranes used in the permeation experiments are composed of siloxane polymers which are above the glass transition temperature and do not contain crystallites, i.e. the research is concerned with amorphous, rubbery polymers.

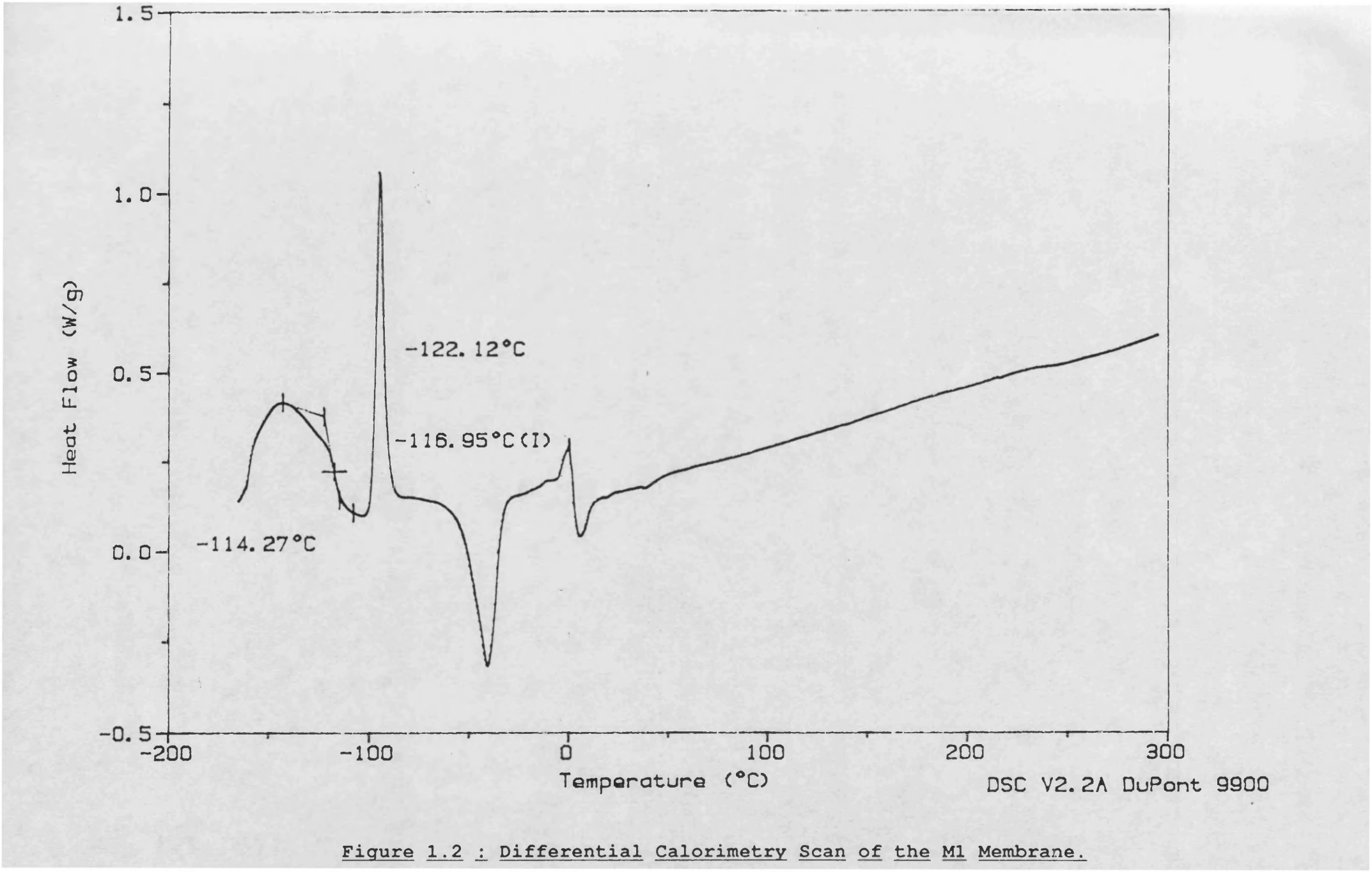

Figure 1.2 : Differential Calorimetry Scan of the M1 Membrane.

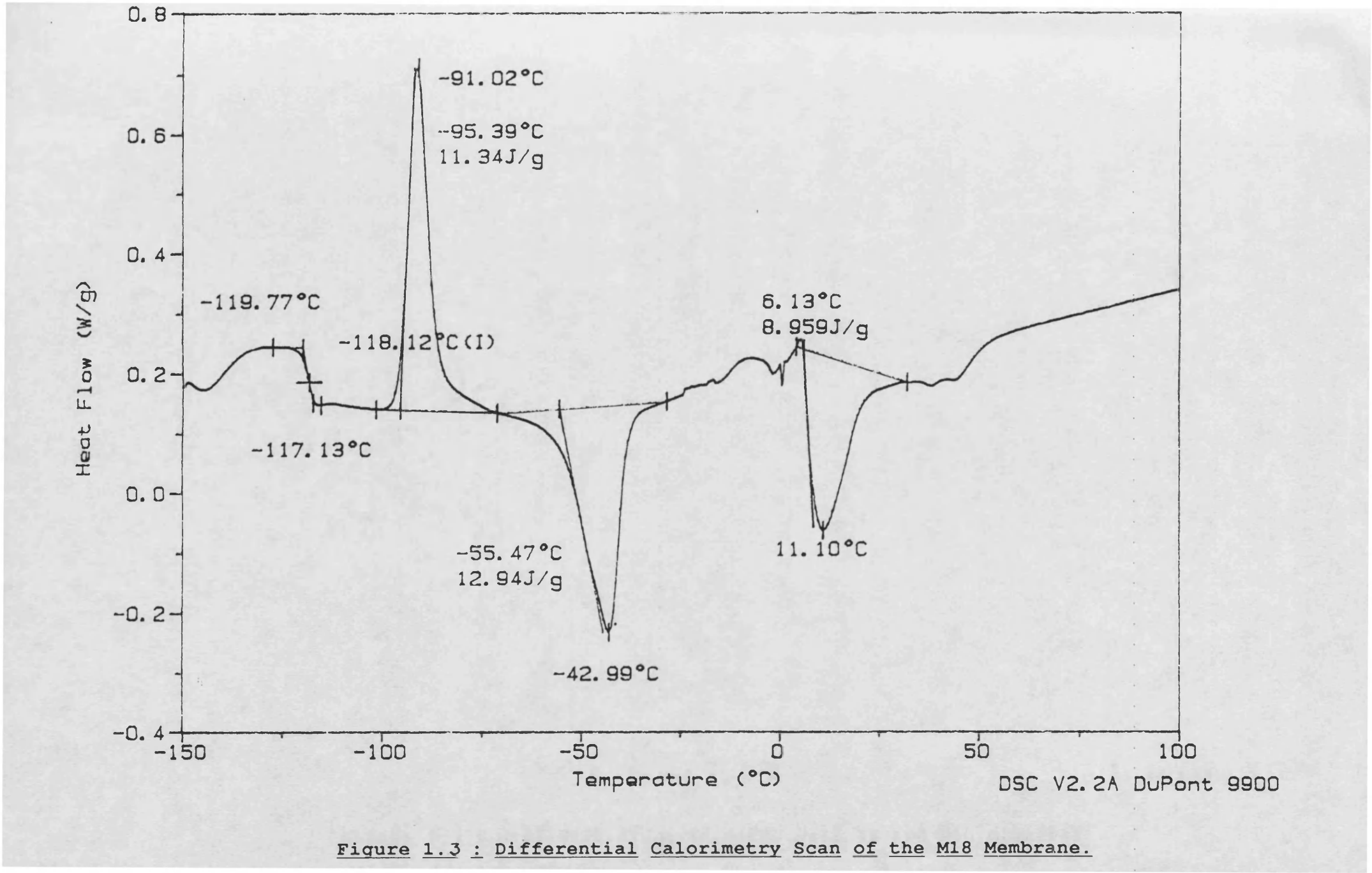

Figure 1.3 : Differential Calorimetry Scan of the M18 Membrane.

1.8 Work Performed in this Research

A membrane was needed which would selectively transport organic vapours containing nitro-groups over organic vapours containing chloro-groups and other contaminants such as acetone and ethanol vapour. Hence acetone and ethanol were used as permeants and nitrobenzene and tetrachloroethylene were chosen to represent the nitro- and chloro- compounds respectively. Poly(dimethylsiloxane) (PDMS) was chosen as the material to use as a basis for transport measurements. PDMS is known to be highly permeable to penetrants, a property which is desirable in a separation membrane, but it has also shown an inability to distinguish between permeants and thus generally has a very poor selectivity. It was intended to produce chemically modified polymers, using PDMS as a basis, which improved upon the poor selectivity of PDMS, but retained its high permeability. Research by Stern and co-workers[40] was reported during this project, which used the same basic ideas to influence the transport of eight gaseous penetrants ranging from helium to propane.

Stern used twelve different polysiloxanes membranes, one of which was PDMS, the other eleven, although polymerised from different monomers, could be visualised as formed by the substitution of different

functional groups in the side or backbone chains of PDMS. Substitution into the backbone chain was found to restrict the mobility afforded by the Si-O linkages in PDMS, thus a significant drop in diffusivity was observed. More favourable results were achieved by substitution into the side chains where, providing the substituting group was not too bulky, there was no significant loss in polymer chain mobility. Therefore, in this research project, it was decided to substitute functional groups into the sidechains of PDMS in an attempt to enhance the transport of nitro-organic vapours.

At first a commercially available PDMS membrane, of thickness 5.33×10^{-3}cm, containing 28% filler by weight was studied. Ideally, a membrane without filler was required, but this was not available initially. Once the SERC funded research project[38] was underway, a source of unfilled and chemically modified membranes became available. A PDMS membrane containing no filler (M1), of thickness 1.65×10^{-2}cm, was acquired to give a comparison to the filled PDMS membrane. The choice of functional group to substitute onto the PDMS sidechain was difficult, but, at the time, the SERC project was involved with substituting ester functionalities, therefore, considering the possible favourable interaction between the nitro-group of the permeant and the ester group of the polymer, it was decided to

investigate the transport properties of a membrane containing an ester functionality of 17.3 mol% of Si atoms, of thickness 3.33×10^{-2}cm (M18). The synthesis of the M1 and M18 membranes is described in section 1.7.

The concentration and temperature dependence of the penetrants in the membranes was examined. As there were three membranes, each to be examined with four permeants over a range of concentration and temperature, it was necessary to find a rapid and easy method of transport property determination. An apparatus was built based on the dynamic method, described in section 1.6, which was run at atmospheric pressure and required no vacuum-tight seals. The permeant feed streams were produced by passing a nitrogen stream through the liquid permeant in a thermostatted gas saturator. Each permeant/polymer system was investigated at five or six different concentrations over a temperature range between 50 and 120°C, with permeability and diffusivity coefficients being calculated for each set of conditions.

The reliability of the method and apparatus was checked by measuring the transport properties of some previously studied systems. Transport results were checked using methane and dichloromethane in poly(hexafluoropropylene-co-tetrafluoroethylene) (FEP) and showed good agreement with previous work by

Wickham[41]. Finally, density measurements were made on each of the polymers used.

EXPERIMENTAL

Chapter 2 : Experimental

2.1 The Flow System

A dynamic method was used to determine the transport properties of the various organic vapours through the polysiloxane membranes. A schematic representation of the apparatus constructed to carry out this research is shown in figure 2.1

A cylinder of high purity nitrogen supplied two gas streams. One was used as a flush to purge the permeation cell (described in section 2.2) of any organic vapour or contaminant, the other was directed through a gas saturator (described in section 2.3) where the nitrogen became saturated with an organic vapour to give the permeant stream. Accurate flow control of the streams was achieved by the use of Brookes extra low flow controllers incorporated into the gas line after the cylinder head regulator. From the gas saturator the permeant stream passed into a 3-way valve, which allowed the vapour stream to be switched to a standard gas/vapour mixture for calibration purposes.

Both flush and permeant streams then passed through a gas chromatographic switching valve, which enabled the stream passing through the upstream chamber

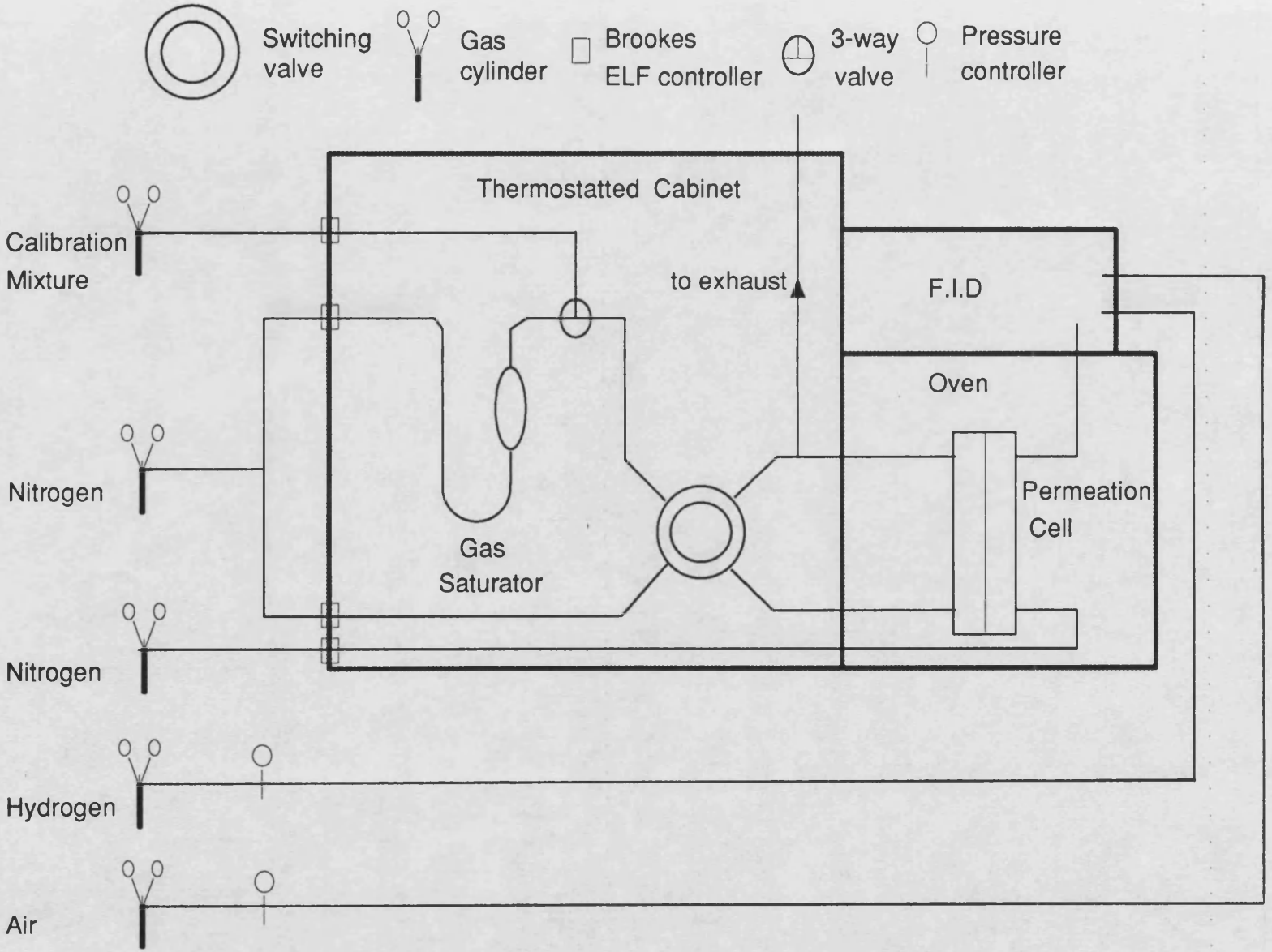

Figure 2.1 : Schematic Diagram of the Flow System.

of the permeation cell to be switched between flush and permeant, with the other stream being vented to the atmosphere. Venting the vapour stream whilst the flush gas was passing through the permeation cell allowed constant nitrogen flow through the gas saturator, so that equilibrium was maintained and constant vapour loading of the stream was achieved. The stream passing through the upstream chamber of the permeation cell was also vented to the atmosphere after passing across the face of the membrane. In the downstream chamber of the cell, a constant flow of high purity nitrogen, from another gas cylinder, carried any permeant which passed through the membrane to a flame ionisation detector. Accurate flow control was again achieved by the use of Brookes extra low flow controllers.

The signal generated by the detector in response to the organic permeate, that is the permeant which has permeated through the membrane, was amplified and recorded on a Gould BS-271 chart recorder. The flame for the detector was fed by air and hydrogen streams supplied by gas cylinders and controlled by diaphragm pressure controllers positioned before flow restrictors. All pipework and fittings downstream of the gas saturator, which came into contact with the vapour, were made of stainless steel or aluminium to prevent the vapour attacking the metal. Other pipework and fittings were made of copper or brass.

EXPERIMENTAL

2.2 The Permeation Cell

A diagram of the permeation cell is shown in figure 2.2. The cell consisted of two cylinders of stainless steel, each with a shallow cylindrical depression machined into one of the flat faces. These could be fastened together by six bolts, with a polymer film sandwiched between, to give an enclosed chamber,divided into two by the membrane. Each subdivision of the chamber had a narrow bore inlet and outlet pipe at its face to allow the passage of flush or permeant streams (upstream chamber) or carrier stream (downstream chamber) across the face of the membrane. The downstream chamber also contained a small step around its circumference to allow a 1mm stainless steel mesh to be placed against the membrane.

When the cell was assembled and secured firmly with the bolts, the portion of the membrane trapped by the faces of the outer rim of each section acted as a gasket, forming an effective seal against leakage of gas or vapour from the permeation chamber. The area of the chamber, and thus the area of the membrane available for permeation, was 8.55 cm^2, with the depth of the chamber on either side being 2 mm. The step around the circumference of the downstream chamber was 1 mm deep.

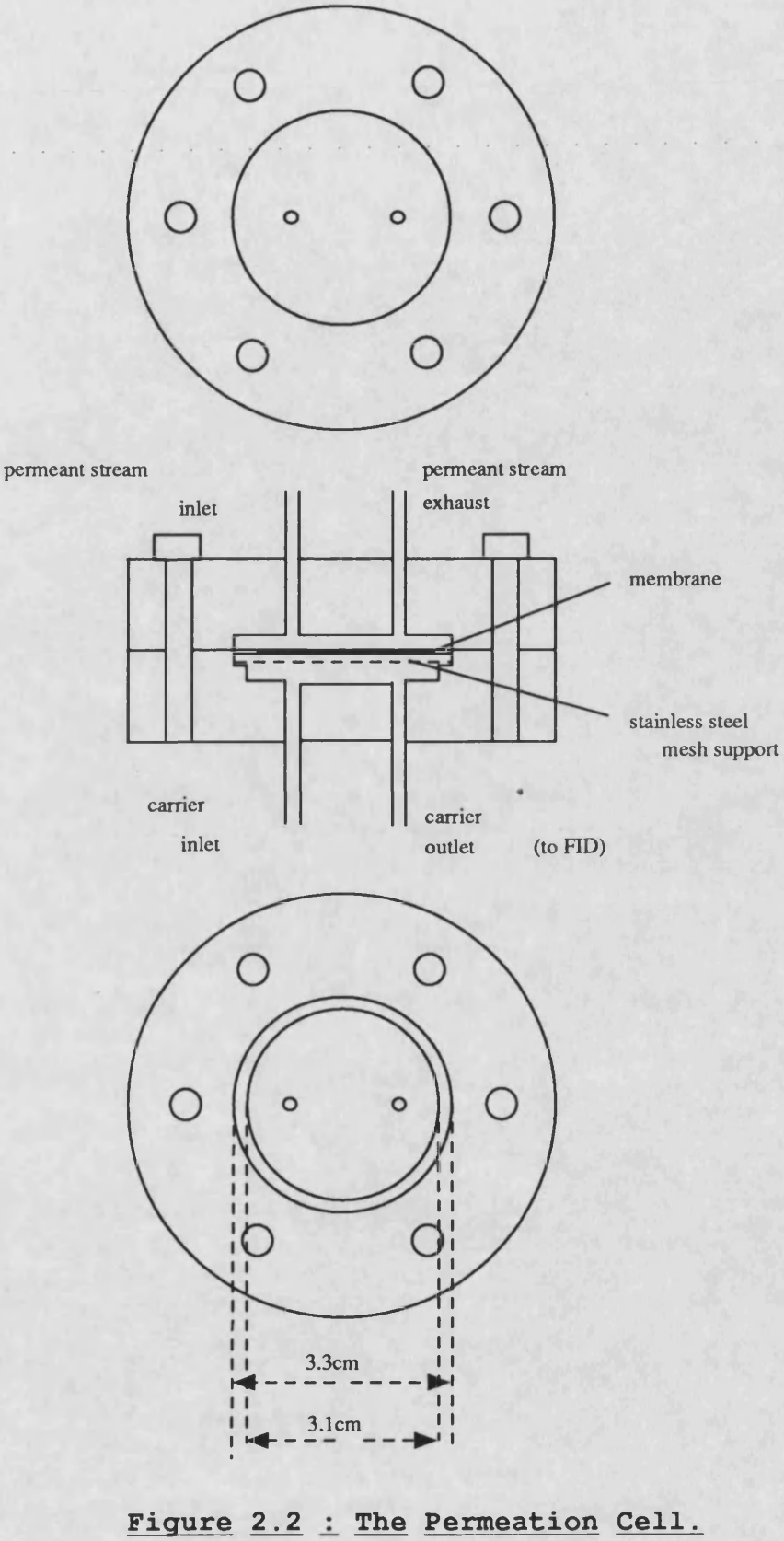

Figure 2.2 : The Permeation Cell.

Due to the flexibility of the thin membranes used, it was found that at higher temperatures the polymer expanded and any slight pressure difference between the upstream and downstream chambers could cause the membrane to bulge to such an extent that it touched the face of the permeation chamber, thus affecting the area of the membrane exposed to the permeant. Metal supports have been used in research by other workers[4,5,42,43] and the 1mm stainless steel mesh, which was fitted on the downstream side of the membrane, was found to be the most successful method of support. Any form of support placed on the upstream side was found to disrupt the flow of the permeant stream across the face of the membrane and to therefore affect the permeation of the vapour through the membrane. Other workers[40] have also suggested the use of filter paper as a means of support. As any pressure differences across the membrane would have been likely to be small, the filter paper could have been used on its own, clamped into the cell with the membrane, or it could be used in conjunction with a metal mesh support, where the paper is placed between the membrane and the mesh to prevent the polymer adhering to the metal. However, the filter paper was found to affect the transport of vapour across the membrane. There was also the possibility of absorption of the permeant vapours into the paper which would affect the measurement of diffusion coefficients.

Experimental runs carried out using just the stainless steel mesh as support showed that there was no problem of the polymer adhering to the metal with the membranes used in this work. To ensure that if there was a pressure difference across the membrane then the pressure in the upstream chamber was higher, constrictions were placed in the outlet pipe. This counteracted any increased pressure in the downstream chamber due to the narrow bore of the jet in the flame ionisation detector and ensured that the membrane was held against the support.

The assembled cell was placed in a Pye 104 series chromatograph oven from which the chromatographic columns had been removed. This provided temperature control of the cell and membrane to ±0.1°C at temperatures above 50°C. The temperature was measured using a mercury in glass thermometer with 0.1°C graduations.

2.3 The Gas Saturator

The permeant stream for the experiments was provided by a gas saturator based on a design shown by Weissberger[44]. A diagram of the apparatus is shown in figure 2.3. The saturator was in effect a glass U-tube containing the organic permeant as a liquid. A stream of high purity nitrogen was passed through the liquid

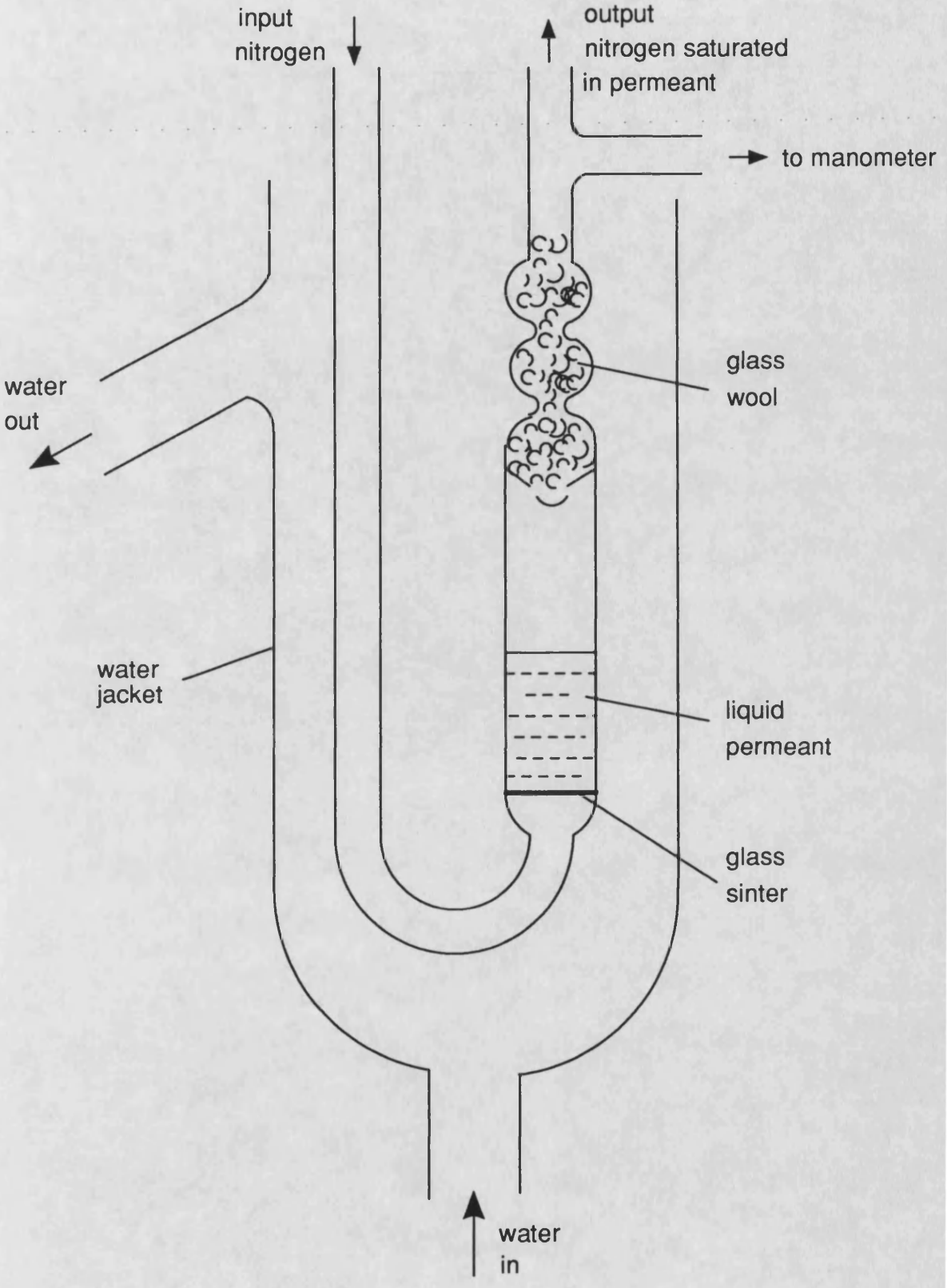

Figure 2.3 : Gas Saturator.

at a sufficiently slow rate to ensure complete saturation of the gas with organic vapour. A glass sinter situated below the liquid caused the nitrogen to pass through as small bubbles to facilitate saturation. A wad of solvent washed glass wool filled the chamber at the outlet of the saturator to ensure that any droplets of liquid suspended in the gas stream, due to the agitation of the reservoir, were filtered out before the stream passed into the pipes leading to the permeation cell.

The concentration of vapour in the gas stream could be changed by altering the temperature of the organic liquid. Temperature control was achieved by immersing the saturator in a thermostatted water jacket, supplied with water by a pump from a water bath, with the water temperature being regulated using a Techne Tempunit TU-16A temperature controller for temperatures above room temperature. For temperatures near to or below room temperature, the Tempunit was used in conjunction with a Grant cooling coil, with ethylene glycol being added to the water for experiments requiring temperatures below 0°C, to prevent freezing. A mercury in glass thermometer, with 0.1°C graduations, was used to measure the temperature of the water jacket.

The gas saturator and all of the pipework downstream of it were enclosed in a thermostatted

cabinet so that, if the saturator was at a temperature near or above room temperature, the cabinet could be heated to a temperature approximately 5°C higher to prevent vapour from condensing out in the pipes. The cabinet was constructed from asbestolux board, with the temperature being controlled using two heating mats,the output of which could be varied by using a variable voltage controller. The mats were mounted on a partition within the cabinet, with the air being circulated around the interior of the cabinet by two fans.

For the calculation of permeabilities, it is necessary to know the concentration of the vapour stream supplied by the gas saturator, so that the partial pressure of the vapour in the upstream chamber of the permeation cell can be found. Assuming that the nitrogen stream is completely saturated in the gas saturator and that both the nitrogen and the organic vapour behave ideally, it is possible to find the partial pressure of the vapour in the upstream chamber (p_c) if the saturated vapour pressure (p_v) of the organic liquid in the saturator, the total pressure above the gas saturator (P_s) and the total pressure in the upstream chamber of the permeation cell (P_c) are known. The saturated vapour pressure of the organic liquid can be calculated from the Antoine equation, using reported values of the constants. The total

pressure above the gas saturator was equal to the sum of the atmospheric pressure and the excess pressure in the saturator caused by the restrictions of gas flows due to narrow bore pipes and valves in the flow system. The atmospheric pressure was measured to ±0.1mmHg using a mercury barometer, whilst the excess pressure was measured using a mercury manometer attached above the liquid level at the exit from the gas saturator.

If it is assumed that Dalton's Law applies, then the ratio of the partial pressure of the vapour to the total pressure above the saturator is equal to the ratio of the volume of vapour in the gas stream to the total volume of the permeant stream (vapour and nitrogen) leaving the gas saturator in unit time. Therefore, the partial pressure of vapour in the upstream chamber of the permeation cell is given by:

$$p_c = \frac{p_v}{P_s} \cdot P_c$$

The total pressure in the permeation cell, P_C was originally taken to be equal to the atmospheric pressure, as the cell was vented directly to the atmosphere. However, once constrictions were placed in the vent, for reasons discussed in section 2.2, the total pressure upstream of the membrane was increased. Measurement of the pressure in the permeation cell, using a mercury manometer, showed that the

total pressure in the upstream chamber was equal to the total pressure above the gas saturator. Therefore, the partial pressure of the organic vapour in the permeation cell, p_C was equal to the saturated vapour of the organic liquid in the gas saturator, p_V.

The organic vapours of interest in this research were ethanol, acetone, nitrobenzene and tetrachloroethylene. The transport properties of each of them were investigated in three different membranes over a range of concentrations. The theoretical vapour pressures for ethanol, acetone and nitrobenzene were calculated from the following Antoine equations:

Ethanol[45]:

$$\log_{10}p = 8.24739 - \frac{1670.409}{232.959 + t}$$

Acetone[46]:

$$\log_{10}p = 7.23157 - \frac{1277.03}{237.23 + t}$$

Nitrobenzene[47]:

$$\log_{10}p = 7.55755 - \frac{2026}{225 + t}$$

In each case t is the temperature of the liquid in °C and p is the saturated vapour pressure in mmHg. For tetrachloroethylene a set of tabulated vapour pressure data was found[48]:

T(K)	270	275	280	285	290
$p(kNm^{-2})$	0.447	0.622	0.854	1.158	1.550

T(K)	295	300	305	310
$p(kNm^{-2})$	2.053	2.689	3.468	4.476

The saturated vapour pressure at a particular temperature was calculated by interpolating between two temperatures using the equation:

$$\log p_2 = \log p_1 + \frac{T_3}{T_1}\left\{\frac{T_2-T_1}{T_3-T_1}\right\}(\log p_3 - \log p_1)$$

where p_2 is the saturated vapour pressure to be calculated at a temperature of T_2. T_1 and p_1 are the temperature and vapour pressure, in the table, closest below the required temperature and T_3 and p_3 are the closest values above the required temperature. The calculated vapour pressure could then be converted to mmHg by multiplying by 0.1333.

To ensure that the calculated vapour pressures were accurate and that the gas stream was completely saturated, it was necessary to check the concentration of vapour in the permeant stream. This was achieved, in the cases of acetone, ethanol and tetrachloroethylene, by passing the permeant stream through a glass trap immersed in a dry-ice/acetone slurry where the vapour condensed out. In the case of nitrobenzene, the permeant stream was passed through a glass tube containing TENAX absorbent which removed the vapour

from the stream. The TENAX was used in preference to cold trapping in this case due to nitrobenzene's low vapour pressure which led to a small weight of liquid being collected; the TENAX trap was much smaller and lighter than that used for cold trapping and thus reduced errors in weighing the permeant trapped. After the vapour had been removed, the remaining nitrogen stream was bubbled through water in a Drechsel bottle at room temperature and onto a bubble flowmeter. The Drechsel bottle was used to saturate the nitrogen stream with water vapour, thus preventing the gas from taking an unknown amount of moisture from the bubble flowmeter. Knowing the saturated vapour pressure of the water allowed the nitrogen flow rate to be measured with a correction for the amount of water vapour present. The relative volumes of nitrogen and organic vapour in the stream could be found from the measured flow rate of nitrogen and from the weight of liquid trapped over a given period of time. The partial vapour pressure could then be calculated if the following factors were known:

P_A, atmospheric pressure

T, room temperature

R, gas constant

p_w, saturated vapour pressure of water at T

f, flow rate measured at P_A and T

t, duration of trapping

W, weight of organic liquid trapped

MW, molecular weight of the liquid

The volume of nitrogen passing through the trap during the trapping run, with a correction for the amount of water vapour, is given by:

$$V_{N2} = \left\{ \frac{P_A - P_w}{P_A} \right\} f.t$$

The volume of organic vapour passing into the trap over the same period is given by:

$$V_{vap} = \frac{W}{MW} \cdot \frac{R\,T}{P_A}$$

The partial pressure can then be calculated by using the ratio of the volume of vapour to the total volume of the permeant stream and the total pressure, thus:

$$p_v = \frac{V_{vap}}{V_{vap} + V_{N2}} \cdot P_A$$

This procedure was repeated for each permeant, at each saturator temperature used in the experiments.

Nitrobenzene was used at several saturator temperatures within the range 11.1 to 43.3°C. At all temperatures, the partial vapour pressure calculated from trapping the permeant agreed with the theoretical values calculated from the Antoine equation to within ±1%. The permeabilities were then calculated using the

vapour pressure given by the Antoine equation.

Tetrachloroethylene was used at several temperatures within the range 1.7 to 32.1°C. As with nitrobenzene, the partial vapour pressure found from trapping agreed with the calculated value to within ±1% at all temperatures. The partial pressures calculated from the tabulated vapour pressure data were considered to be sufficiently accurate to be used for the calculation of permeability.

Acetone and ethanol partial pressures showed some deviation from the calculated theoretical values, with ethanol in particular showing some quite large deviations. Table 2.1 shows the saturator temperatures used for acetone and ethanol for each membrane and gives the deviation from the theoretical value as a percentage. When making any calculations involving the partial vapour pressure, such as finding permeabilities and calibration constants, these deviations were taken into account and the values were corrected.

2.4 The Flame Ionisation Detector.

Any organic vapour which permeated through the membrane was picked up by a nitrogen carrier stream in the downstream chamber of the permeation cell and carried to a Pye 104-series flame ionisation detector. The flame ionisation detector was selected due to its

Permeant : Acetone

Membrane :	ESCO(filled PDMS)		M1(unfilled PDMS)		M18(ester func)	
	Saturator Temperature /°C	% of Theory	Saturator Temperature /°C	% of Theory	Saturator Temperature /°C	% of Theory
	-4.8	98.9	-2.7	98.5	-4.1	98.7
	1.7	98.5	2.9	98.5	2.0	98.5
	6.9	97.5	8.6	97.7	7.0	97.5
	11.2	98.4	13.7	98.1	11.6	98.3
	16.5	98.1	18.5	98.1	16.9	98.1

Permeant : Ethanol

Membrane :	ESCO(filled PDMS)		M1(unfilled PDMS)		M18(ester func)	
	Saturator Temperature /°C	% of Theory	Saturator Temperature /°C	% of Theory	Saturator Temperature /°C	% of Theory
	1.7	109.0	1.8	109.0	2.1	109.0
	7.0	103.9	7.1	103.9	7.7	104.5
	11.5	101.2	12.3	101.2	12.1	101.2
	17.5	100	18.3	100	18.2	100
	25.0	95.7	25.1	95.7	25.1	95.7

Table 2.1 : Saturator Efficiency for Acetone and Ethanol.

high sensitivity to organic compounds. The signal generated by the detector passed through a Pye ionisation amplifier and was recorded as a pen trace on a Gould BS-271 chart recorder.

To be able to interpret the signal it was necessary to calibrate the detector for each of the organic permeants used. Gas chromatographic detectors, like the flame ionisation detector, are usually calibrated by passing a plug of the relevant compound, of known volume and concentration, through the detector and measuring the area under the resulting peak given by the chart recorder. This plug would be supplied from the sample loop of a gas chromatographic sampling valve. However, when permeation measurements were being carried out on this apparatus, the detector was subjected to a constant flow of permeant carried by the nitrogen stream. It would therefore appear reasonable to simulate the same conditions, as near as possible, during the calibration of the detector. It was also necessary to ensure that the detector gave a linear response over the whole vapour concentration range found during the permeation experiments, i.e. that the sensitivity of the detector was constant over the concentration range. This required the generation of at least two permeant streams for the calibration of the detector for each organic vapour; one at a vapour concentration slightly higher than the upper end of the

concentration range found in the permeation experiments and the other slightly below the lower end of that range.

Due to the low vapour pressure of nitrobenzene, most permeation runs were carried out with the gas saturator held at a relatively high temperature (>11.0°C). It was therefore possible to lower the temperature of the saturator to produce vapour streams of similar concentrations to the permeate streams generated by transport of the vapour across the membranes. Nitrogen flowing at a rate of 27.8 cm^3min^{-1} (the same flow rate as that of the carrier stream) was passed through the nitrobenzene in the saturator, which was thermostatted at 1.5°C (p^o= 0.041mmHg) and at 29.9°C (p^o=0.41mmHg) to give permeant streams of concentrations slightly above and below the concentration range found in the permeation runs. Each vapour stream was passed directly to the detector producing a constant signal in response, which was recorded as a plateau by the chart recorder. A calibration constant, K with units cm^3(STP)(cm chart)$^{-1}s^{-1}$, was calculated by dividing the flow rate of the vapour at standard temperature and pressure in cm^3s^{-1} by the height of the plateau in cm of chart paper. Saturator temperatures of 1.5°C and 29.9°C gave an average calibration constant of 7.5×10^{-10} (±1%) cm^3(STP)(cm chart)$^{-1}s^{-1}$. Checks carried out at other

saturator temperatures within this range all gave a similar calibration constant, showing that the detector gave a linear response across the whole concentration range.

The three remaining permeants (acetone, ethanol and tetrachloroethylene) all have much higher vapour pressures, therefore permeation runs at the lower end of the concentration range were carried out with low saturator temperatures. To use the gas saturator to simulate the permeant streams produced by these conditions, after transport across a membrane, would have required that the saturator be thermostatted at temperatures below -20°C. It was not possible, with the equipment available, to achieve accurate control at these temperatures, therefore alternative methods of producing vapour streams of the required concentration had to be considered. These methods included gas mixing, diffusion tubes and permeation tubes[49-52].

Gas mixing involves the dilution of a permeant stream with a nitrogen stream. Mixing takes place in a large volume vessel, with the concentration of the outlet stream being determined by the relative flow rates of the incoming streams. It was considered doubtful whether sufficiently accurate control could be achieved for the purposes of calibration, so the method was discarded. Diffusion tubes have a reservoir

containing the permeant as a liquid which diffuses through a capillary into a gas stream, with the flux of the permeant vapour depending upon the bore and length of the capillary. This a useful and accurate method of introducing a vapour into a gas stream, but it provides only low vapour loadings. The vapour concentrations produced would have been much lower than those required for calibration of the detector and this method was also discarded.

Permeation tubes consist of a length of polymer tubing, containing the permeant as a liquid, which is plugged at each end[52]. The vapour flux through such a tube is given by[53]:

$$q = 2\pi LP(p_i - p_o)/\ln(d_o/d_i)$$

where L is the length of the tube (cm), P is the permeability of the organic vapour in the polymer ($cm^3(STP)cm/cm^{-2}s.cmHg$), p_i and p_o are the partial pressures of the permeant inside and outside the tube (cmHg) and d_i and d_o are the inner and outer diameters of the tube (cm). If the vapour permeating from the tube is removed continuously by a flow of carrier, then the partial pressure of the permeant outside of the tube, p_o, is equal to 0 and the partial pressure inside the tube will be equal to the saturated vapour pressure, p^o. Thus the flux is given by:

$$q = 2\pi LPp^{o}/\ln(d_o/d_i)$$

Most examples of permeation tubes found in the literature were made of FEP or PTFE. These are glassy polymers having a low permeability and permeation tubes made from them gave fluxes which were lower than those required for calibration purposes. However, it was obvious that a rubbery polymer, with greater permeability, would give a higher flux. It was found that silicone rubber tubing was suitable for making a permeation tube for ethanol.

A 6.5 cm long piece of silicone rubber tubing, with an internal diameter of 6 mm and an external diameter of 9 mm, was filled with ethanol and plugged at each end with aluminium stoppers. This was enclosed in a glass tube through which a constant stream of nitrogen was passed and which was immersed in thermostatted water bath. The flux produced depended strongly upon the temperature as it affected both the vapour pressure and the permeability of the vapour in the polymer. It was found that if the permeation tube was equilibrated at 25°C for 24 hours, with a continuous stream of nitrogen passing over it, a constant flux of permeant was produced which was suitable for calibration measurements at the lower end of the concentration range. The permeation tube was weighed at hourly intervals until a steady weight loss

was observed over a period of 3 hours. It was then inserted into the flow system in place of the gas saturator, using the saturator water jacket to maintain a temperature of 25°C. Determination of the calibration constant of the detector for ethanol, using the permeation tube for the lower end of the vapour concentration range and the gas saturator at a temperature of 13.5°C for the upper end of the range, gave an average value of $3.45 \times 10^{-9}(\pm 5\%)$ $cm^3(STP)(cm\ chart)^{-1}s^{-1}$.

For acetone and tetrachloroethylene, the use of permeation tubes proved unsuccessful. The flux required for acetone was too great for any permeation tube of practical size to have a reasonable lifetime and tetrachloroethylene was too highly permeable in the silicone rubber, giving a much larger flux than required. Instead it was decided to have cylinders of standard vapour mixtures made up containing acetone/nitrogen and tetrachloroethylene/nitrogen. However, vapour mixtures of the required concentration could not be obtained because, at the minimum working pressure of the cylinders and the temperature of the laboratory, the vapours would have condensed out in the cylinders. Therefore, the maximum concentration of vapour in nitrogen, which would not condense out under the conditions, was obtained. This was calculated to be 1000ppm acetone in nitrogen and 400ppm

tetrachloroethylene in nitrogen. For calibration purposes these standard mixtures were passed into the flow system via the 3-way valve, mentioned in section 2.1, and then taken directly to the detector at a flow rate of 27.8 cm^3s^{-1}; the same flow rate as that experienced by the detector in the permeation runs.

Calibration of the detector for acetone at the upper end of the concentration range was carried out using the gas saturator at a temperature of -4.1°C. The calibration constants calculated at the upper and lower ends of the range agreed to within 5% and gave an average of 2.0×10^{-9} $cm^3(STP)(cm\ chart)^{-1}s^{-1}$. For tetrachloroethylene, the higher concentration stream was provided by the saturator at a temperature of 17.6°C. The calibration constant determinations agreed to within 4%, with an average value of 1.85×10^{-9} $cm^3(STP)(cm\ chart)^{-1}s^{-1}$.

2.5 Membrane Treatment.

Before being used in permeation experiments, all of the membranes had to undergo some pretreatment. As received, the membranes were assumed to contain some contaminants such as low molecular weight siloxanes or solvents , used in the polymer preparation, which would have to be removed to prevent them from fouling or interfering with the detector. This was particularly

evident with the unfilled PDMS (M1) and the ester-substituted siloxane (M18) membranes which were prepared in the University laboratories, as these had a characteristic smell before pretreatment and were observed to lose weight over a period of days. Previous workers studying siloxanes had found that refluxing with acetone[32,54] or ethylacetate[55] was suitable for removing such contaminants. In this research, prior to carrying out transport measurements, the membranes were refluxed in ethylacetate for 3 hours and then allowed to dry under vacuum.

It was also necessary to measure the thickness of the membranes before they were mounted into the permeation cell. This was initially accomplished by the use of an electronic micrometer. The commercially available filled PDMS film was found to have a reasonably uniform thickness which could be found from a small number of measurements across the membrane. The unfilled PDMS and ester-substituted siloxane membranes however, were found to have a very irregular thickness and often had a wedge-shaped cross-section. The thicknesses of these membranes were estimated by taking many measurements across a section of film and then taking an average of the values in close proximity to the area of film exposed to the permeant stream in the permeation cell (see figure 2.4).

Due to the obvious errors in this technique, it

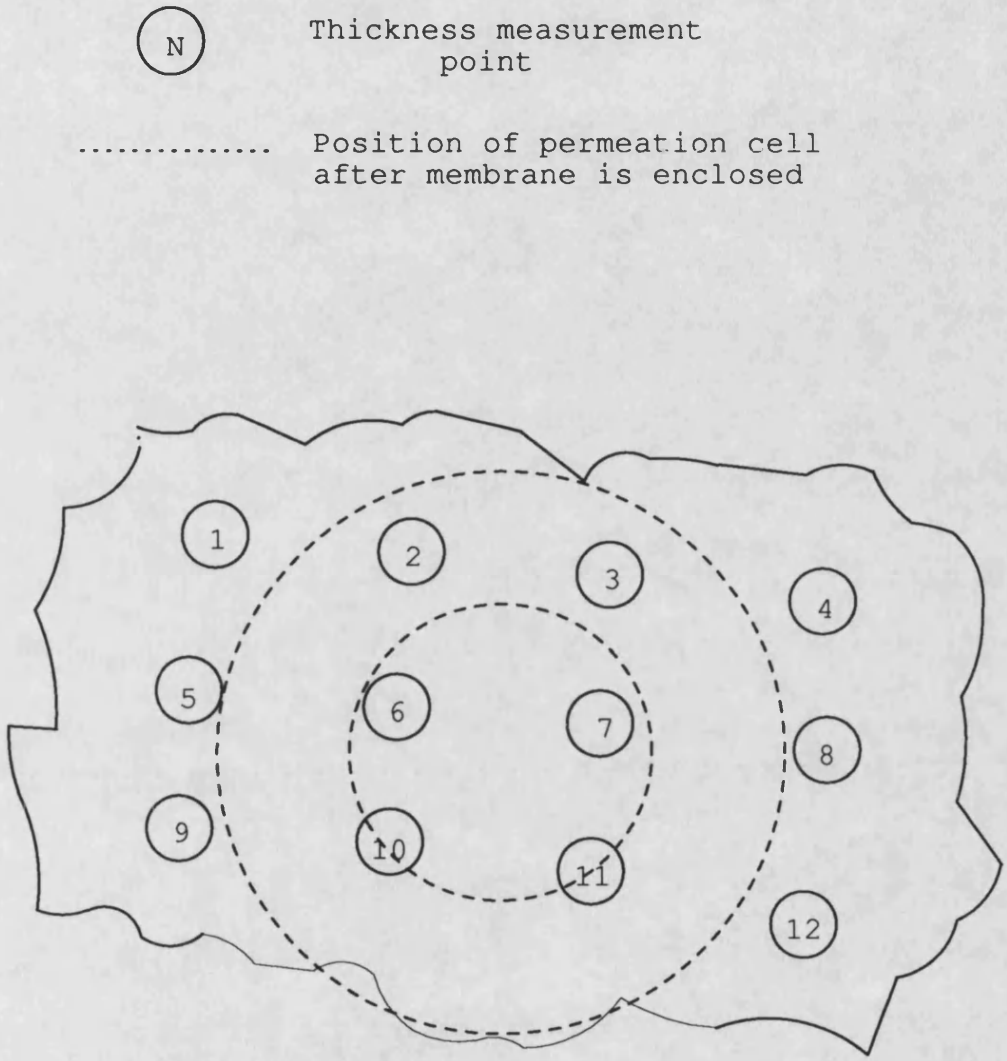

Figure 2.4 : Measurement of Membrane Thickness.

was necessary to find an independent method of estimating the membrane thickness. This was accomplished by measuring the density of the polymer, using a method described in section 2.7, and weighing the section of membrane that was exposed to the permeant in the permeation cell. As the area of the membrane was known and the volume of the section could be found from the weight and the density, then the average thickness could be calculated.

2.6 Measurement of Transport Properties.

With the membrane clamped firmly in the cell, the flow of each of the gas and gas/vapour streams were set and measured accurately using a bubble flowmeter. The permeant stream was set at $35cm^3min^{-1}$, for reasons described later in this section, and the flow of the flush stream was set at the same rate. The carrier flow rate, downstream of the membrane, was set at $27.8cm^3min^{-1}$. Theoretically, this flowrate should have been relatively unimportant, as the response of the detector depends on the mass flow of the organic vapour, which is determined by the rate of permeation through the membrane. However, a variation in response with change in carrier flow rate was found, which meant that the flowrate had to be constant throughout the permeation experiments, and calibration of the detector

had to be carried out under similar conditions. The hydrogen and air streams supplying the flame ionisation detector were set according to the instructions in the Pye manual; the hydrogen flowrate was set at $27.8cm^3min^{-1}$, the same as the carrier flowrate, and the air was set at $500cm^3min^{-1}$, which was the minimum recommended flowrate.

The gas saturator thermostat was set at the required temperature and, if this was near to or above room temperature, the thermostat for the heated cabinet containing the saturator was set approximately 5°C higher. The oven containing the permeation cell was set at the lowest temperature being used for permeation runs, generally about 50°C, and the oven for the flame ionisation detector was set at 150°C, a higher temperature than any used in the permeation cell oven. The apparatus was then left to equilibrate overnight with the flush stream passing through the cell.

When ready to begin a permeation run, the baseline of the recorder was set to zero using the controls on the recorder, and the backing-off control on the ionisation amplifier and the attenuation of the amplifier were set at the required level. Changing the position of the switching valve vented the flush stream to the atmosphere and allowed the permeant stream to pass through the permeation cell and over the face of the membrane. Any permeant which passed through the

membrane (the permeate) was picked up by the nitrogen carrier stream and transported to the detector. A typical trace produced on the chart recorder is shown in figure 2.5. There is a period after the time when the switching valve is changed to allow the permeant into the cell where there is no response from the detector. This is where the permeant stream is replacing the nitrogen of the flush stream in the pipes leading up to the permeation cell and in the chamber upstream of the membrane. There is a further delay as the permeant front crosses the membrane and time is taken for the carrier to move the initial permeate emerging from the downstream face of the membrane to the detector. From this point the detector signal begins to rise and continues to rise until a steady state equilibrium is reached in the system, which is recorded on the trace as a plateau of height, S_∞. From this plateau height, in cm of chart paper adjusted to unit attenuation, and from the calibration constant, K (cm^3(STP)(cm chart)$^{-1}s^{-1}$) calculated previously, the flux of the vapour through the membrane can be given, in units of cm^3s^{-1}, by:

$$F = S_\infty . K$$

From this, a permeability coefficient for the permeant/polymer system can be calculated if the thickness of the membrane, L(cm), the area of the

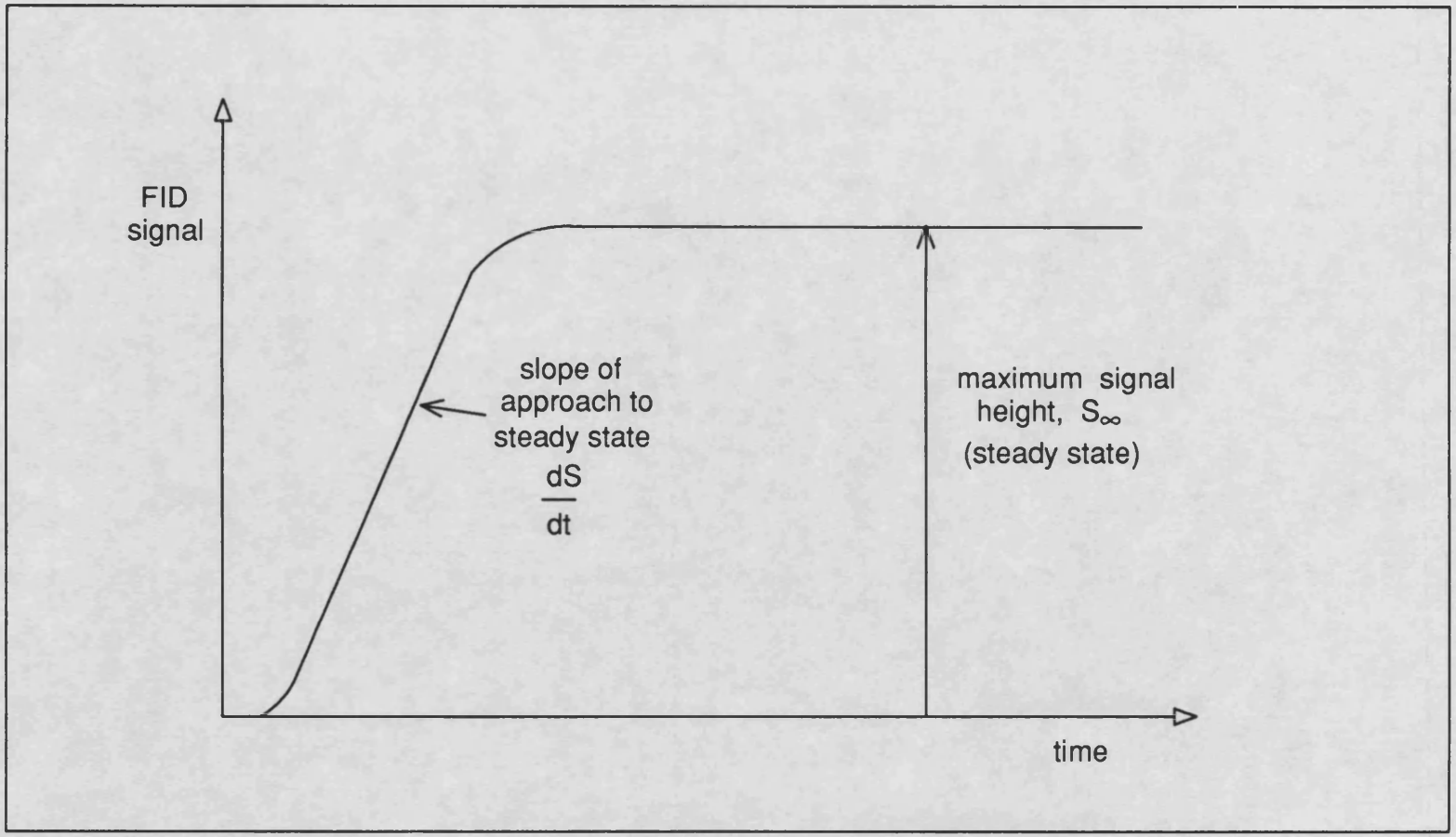

Figure 2.5 : Typical Chart Recording Produced during Permeation Run.

membrane exposed to the permeant stream, A(cm^2), and the partial pressure of the permeant in the upstream chamber, p_c(cmHg), are known. The following equation gives the permeability, P in units of cm^3(STP)cm/cm^2s.cmHg:

$$P = \frac{S_\infty . K L}{A p_c}$$

A more suitable unit for the permeability is the Barrer (B), and this has been used to record the results in this work. A simple conversion is given by:

$$1B = 10^{-10} cm^3(STP)cm/cm^2 s\ cmHg$$

Information about the diffusion coefficient of the permeant/polymer system can be found from the approach to steady state as described in section 1.5. The mutual diffusion coefficient of the permeant polymer system, in cm^2s^{-1}, is given by:

$$D = 0.176\, L^2 \frac{dS}{dt} \cdot \frac{1}{S_\infty}$$

where dS/dt is the gradient of the linear region of the approach to steady state of the permeation curve. Care had to be taken with the experimental conditions as the gradient, dS/dt could be affected by the flowrate of the permeant stream[22]. This has been attributed to the permeant stream only gradually

replacing the flush stream at lower flow rates, whereas at higher flow rates the boundary between the two streams is much sharper and the gradient is seen to approach a maximum. Although experimentally there can never be an instantaneous change from flush to permeant and therefore the experimental values will, in principle, always be lower than the theoretical values. The error is only significant for a very fast approach to steady state. Design of the flow system to incorporate only small volumes between the switching valve and the membrane will also reduce errors. Previous research[41] showed that dS/dt reached a maximum at a permeant stream flow rate of $35cm^3min^{-1}$. This flow rate was adopted for transport measurements in this research. The validity of the diffusion coefficients for organic vapours found using the dynamic method has been checked[41] using the polymer/penetrant systems used in this previous research by an independent method of determining diffusivity using sorption kinetics. The sorption method confirmed diffusivity values found for a dichloromethane/FEP using the dynamic method.

2.7 Density Measurements.

Density measurements were taken on each of the membranes so that, if the section of the membrane exposed to the permeant in the permeation cell was

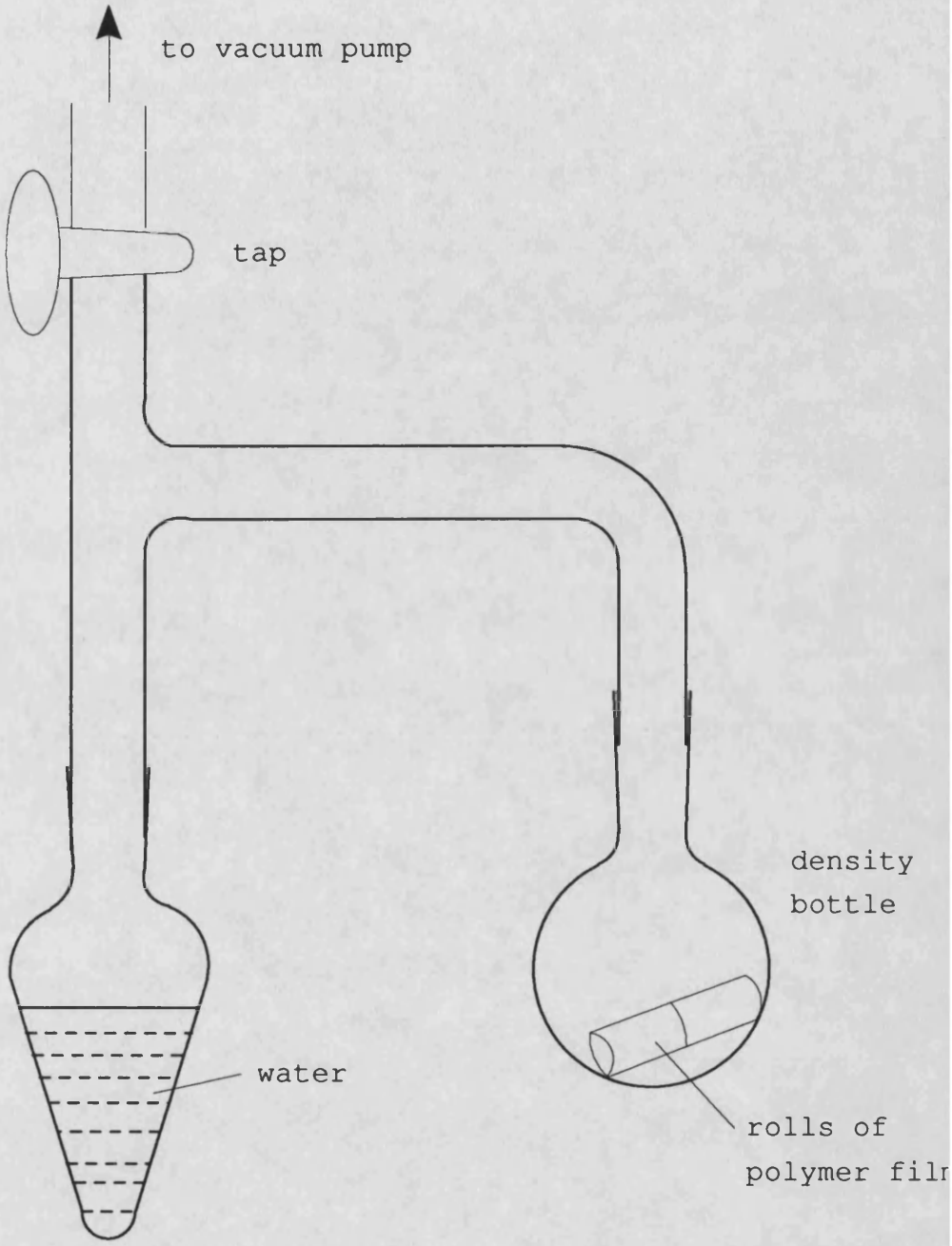

Figure 2.6 : Apparatus Used for Density Measurement.

weighed, an average thickness could be calculated. The density was found by using a displacement of water method. To ensure complete wetting of the polymer, and to prevent the trapping of any air bubbles, the immersion of the polymer in water was carried out under vacuum, using the apparatus shown in figure 2.6.

The polymer film was cut into strips of width 2.5cm and rolled up tightly into rolls which would fit into a $10cm^3$ density bottle, with a total weight of polymer of approximately 1.5g. If the strips of polymer would not remain tightly rolled, they were fastened by a short length of platinum wire. The rolls were weighed accurately (with and without the platinum wire if necessary) and placed into the density bottle which was then attached to the vacuum frame. The flask attached to the other arm of the frame contained in excess of $10cm^3$ of de-ionised water.

The water was frozen by placing a Dewar flask of nitrogen around the vessel and the apparatus was evacuated using rotary and mercury diffusion vacuum pumps. After closing the tap, to shut the apparatus off from the vacuum pump, the water was thawed, using a hot air blower, to allow degassing and was then refrozen to prevent any water vapour from being drawn off under vacuum. The tap was re-opened and the apparatus was evacuated again. This procedure was repeated until no pressure change was recorded on opening the tap. With

the tap closed, the water reservoir was heated gently using the hot air blower and a Dewar flask of nitrogen was placed around the density bottle to encourage the water to condense around the polymer. This was carried out until the polymer was completely immersed. The vacuum was released and the density bottle was removed from the frame, topped up with de-ionised water and the stopper placed in it. This was then equilibrated in a water bath at 25°C for 30 minutes. The bottle, water and film were weighed every 10 minutes until a steady weight was found. Measurements were also taken with the density bottle containing just de-ionised water also equilibrated at 25°C

The following information is required to find the density of the polymer:

W_p= the weight of polymer

W_1= the weight of the density bottle filled with de-ionised water @ 25°C

W_2= the weight of the density bottle, polymer and water @ 25°C

ρ_{25}= the density of water @ 25°C

The weight of water displaced is given by:

$$W = W_1-(W_2-W_p)$$

The volume of water displaced is given by:

$$V = \frac{W_1-(W_2-W_p)}{\rho_{25}}$$

This is equal to the volume of the polymer. The density of the polymer is then given by:

$$\rho = \frac{W_p}{V}$$

Once the permeation runs with a particular membrane had been completed, it was removed from the permeation cell and the section of membrane which had been exposed to the permeant was weighed. From this weight and the measured density of the polymer, the volume of the section could be calculated and, as the area of the membrane was known, an average thickness could be found.

The densities found for each of the polymers at 25°C were: filled PDMS (ESCO) 1.135gcm^{-3}, unfilled PDMS (M1) 0.9917gcm^{-3} and ester-substituted siloxane (M18) 0.9847gcm^{-3}. Average thicknesses calculated using these densities were; ESCO 5.57x10^{-3}cm, M1 1.79x10^{-2} and M18 3.54x10^{-2cm}. These agreed closely with values estimated from measurements taken with the electronic micrometer. There are obviously errors in both methods. Taking the average of thickness measurements taken at various points across an uneven membrane must lead to uncertainties, and it was found to be difficult to cut

out the section of membrane from the permeation cell very accurately for weighing.

2.8 Materials.

The filled poly(dimethylsiloxane) membrane was 5.33×10^{-3}cm thick and contained 28% silica filler by weight. The membrane was supplied by ESCO (Rubber) Ltd.

The unfilled poly(dimethylsiloxane) membrane (M1) had an average thickness of 1.65×10^{-2}cm and was produced for a SERC funded project by Dr. B.Reddy at the University of Bath.

The ester-substituted polysiloxane membrane was supplied from the same source. It had a thickness of 3.33×10^{-2}cm and contained no filler. The preparation of the M1 and M18 membranes is described in section 1.7.

The high purity nitrogen, used as the carrier gas, and the hydrogen and air supplying the flame ionisation detector were supplied by the British Oxygen Company Ltd. The calibration mixtures of acetone, ethanol and tetrachloroethylene in nitrogen were specially prepared by Electrochem Ltd.

The four organic permeants were all supplied by BDH Chemicals Ltd. The ethanol, which was absolute ethanol, and the acetone were 'Analar' grade and the tetrachloroethylene and nitrobenzene were 'Aristar' grade.

RESULTS

Chapter 3 : Results

3.1 Filled Poly(dimethylsiloxane)

Tables A1-A22 show the transport properties of the four permeants in the filled PDMS membrane from ESCO (Rubber) Ltd. The experiments were carried out with a membrane of a relatively uniform thickness of 5.33×10^{-3}cm with the same piece of membrane being used for experiments with all four permeants without being disturbed. Each table shows the transport properties for the PDMS/permeant system at a particular concentration at six temperatures over a range from approximately 47 to 115°C. Tables A1-A5 show the permeation and diffusion coefficients of acetone with partial pressures of acetone of 5.40, 7.59, 9.76, 12.14 and 15.50cmHg supplied by the gas saturator thermostatted respectively at -4.8, 1.7, 6.5, 11.2 and 16.5°C. The partial pressures quoted for each saturator temperature are those found by weighing the acetone frozen out in a cold trap over a given period of time and measuring the nitrogen flow rate (see section 2.3). In each case the value was between 97.5 and 99% of that calculated using an Antoine equation; this was taken into consideration when calculating the permeabilities for the polymer/permeant system and the

calibration constant for the detector.

Tables A6-A10 show the permeation and diffusion coefficients of ethanol in the same filled PDMS membrane. As with acetone, trapping runs showed that the vapour loading of the permeant stream did not agree with the theoretical values derived from the Antoine equation. Saturator temperatures of 1.7, 7.0, 11.5, 17.5 and 25.0°C were used. The only temperature which gave a partial pressure which agreed with the theoretical value was 17.5°C, the other temperatures gave partial pressures from 109.0% of the expected value at the lower end of the temperature range to 97.5% at the higher end (see section 2.3). The partial pressure found from the trapping runs was used in the calculation of the calibration constant for the detector and for the permeabilities of the ethanol/filled PDMS system. Saturator temperatures of 1.7, 11.5, 17.5 and 25.0°C gave ethanol partial pressures of 1.47, 2.01, 2.63, 3.78 and 5.66cmHg respectively, the permeation and diffusion coefficients at these pressures are shown in table A6-A10.

Tables A11-A16 show the permeability and diffusivity of tetrachloroethylene in the filled PDMS membrane. Partial pressures calculated by interpolation of tabulated vapour data for tetrachloroethylene agreed to within 1% of values found by trapping out the vapour at all saturator temperatures used, therefore values

derived from the tabulated data were used in the relevant calculations. Saturator temperatures of 1.9, 8.5, 15.7, 20.9, 26.2, and 31.5°C were used for the tetrachloroethylene, giving partial vapour pressures of 0.46, 0.70, 1.08, 1.50, 1.95 and 2.59cmHg respectively. The transport properties calculated at these vapour pressures are shown in tables A11-A16.

The transport properties of the nitrobenzene/ filled PDMS system were determined at six permeant concentrations. The vapour loading of the permeant stream, predicted using an Antoine equation for nitrobenzene, was confirmed by trapping out the vapour using TENAX absorbent, therefore the values calculated from the Antoine equation were used in the calculation of permeabilities and calibration constants. Saturator temperatures of 11.1, 17.3, 23.8, 31.7, 35.9 and 43.0°C were used giving nitrobenzene partial pressures of 0.010, 0.016, 0.026, 0.046, 0.062 and 0.10cmHg, and the permeabilities and diffusivities of nitrobenzene at these pressures are given in tables A17-A22.

Density measurements, described in section 2.7, showed that the filled PDMS film had a density of $1.135 gcm^{-3}$ at 25°C. Once the permeation runs were completed with all four permeants, the membrane was removed from the cell and the area of film exposed to the permeant was cut out and weighed. Using the weight found, the density of the film and the area of membrane

exposed, the average thickness of the membrane was found to be 5.57×10^{-3}cm, which agrees closely with the value of 5.33×10^{-3}cm found by using the electronic micrometer.

3.2 Unfilled Poly(dimethylsiloxane) (M1)

The density of the unfilled PDMS membrane (M1) at 25°C was found to be $0.9917 gcm^{-3}$. After transport measurements had been completed for all four permeants in the same piece of membrane, the thickness was calculated by the same method as before and found to be 1.79×10^{-2}cm. This showed good agreement with the value of 1.65×10^{-2}cm estimated from measurements using the electronic micrometer.

The permeabilities and diffusivities of the four permeants, at various concentrations, in the unfilled PDMS membrane are shown in tables A23-A42. The concentrations of vapour in the permeant stream were determined by trapping and were found once again to agree with values found from the literature and Antoine equations for tetrachloroethylene and nitrobenzene, but to deviate from theoretical values in the cases of ethanol and acetone. For tetrachloroethylene the partial vapour pressures found from tabulated vapour pressure data were used in calculations, and for nitrobenzene the values calculated from the Antoine

equation were satisfactory. Deviations of between 97.5 and 99% for acetone and 95.7 and 109.0% for ethanol were taken into consideration in calculating the permeabilities and calibration constants.

The permeability and diffusion coefficients of acetone in the unfilled PDMS membrane are shown in tables A23-A27 with the gas saturator thermostatted at -2.7, 2.9, 8.6, 13.7 and 18.5°C giving vapour pressures of acetone of 6.03, 8.07, 10.63, 13.62 and 16.97cmHg respectively.

Tables A28-A32 show the permeability and diffusion coefficients for ethanol in the same unfilled PDMS membrane with the gas saturator thermostatted at 1.8, 7.1, 12.3, 18.3 and 25.1°C giving vapour pressures of ethanol of 1.48, 2.01, 2.77, 3.97 and 5.69cmHg respectively.

Tables A33-A37 show the permeability and diffusion coefficients for tetrachloroethylene in the same unfilled PDMS membrane with the gas saturator thermostatted at 2.4, 9.1, 15.6, 24.2 and 32.1°C giving vapour pressures of tetrachloroethylene of 0.48, 0.73, 1.08, 1.75 and 2.64cmHg respectively.

Tables A38-A42 show the permeability and diffusion coefficients for nitrobenzene in the same unfilled PDMS membrane with the gas saturator thermostatted at 11.2, 17.2, 27.7, 36.3 and 43.3°C giving vapour pressures of 0.010, 0.016, 0.035, 0.064 and 0.10cmHg respectively.

3.3 Ester-substituted Polysiloxane (M18)

The ester-substituted polysiloxane film (M18) was found to have a density of 0.9847gcm^{-3} at 25°C. The section of membrane exposed to the permeant stream was weighed and, as the area of the section was known, a thickness of 3.54×10^{-2}cm was calculated. This compared well with the average thickness of 3.33×10^{-2}cm which was estimated from measurements taken with an electronic micrometer. The permeability and diffusion coefficients for the four permeants in the membrane are shown in tables A43-A64. The concentration of vapour in the permeant stream, supplied by the gas saturator at various temperatures, was found, once again, to deviate from the theoretical values for acetone and ethanol. These deviations were taken into account for calculations involving the vapour pressure. The vapour pressures of tetrachloroethylene and nitrobenzene showed good agreement (to within 1%) with predicted values.

The permeability and diffusion coefficients of acetone in the ester-substituted polysiloxane membrane are shown in tables A43-A47 with the gas saturator thermostatted at -4.1, 2.0, 7.0, 11.6 and 16.9°C giving vapour pressures of acetone of 5.60, 7.71, 9.81, 12.36 and 15.78cmHg respectively.

Tables A48-A52 show the permeability and diffusion coefficients for ethanol in the same ester-substituted polysiloxane membrane with the gas saturator thermostatted at 2.1, 7.7, 12.1, 18.2 and 25.1°C giving vapour pressures of ethanol of 1.51, 2.12, 2.73, 3.95 and 5.69cmHg respectively.

Tables A53-A58 show the permeability and diffusion coefficients for tetrachloroethylene in the same ester-substituted polysiloxane membrane with the gas saturator thermostatted at 1.9, 8.5, 15.7, 20.9, 26.2 and 31.5°C giving vapour pressures of tetrachloroethylene of 0.47, 0.71, 1.09, 1.46, 1.95 and 2.57cmHg respectively.

Tables A59-A64 show the permeability and diffusion coefficients for nitrobenzene in the same ester-substituted polysiloxane membrane with the gas saturator thermostatted at 11.8, 17.4, 24.3, 31.5, 36.6 and 43.2°C giving vapour pressures of nitrobenzene of 0.010, 0.016, 0.027, 0.046, 0.065 and 0.10cmHg respectively.

In each of the polymer/permeant systems the permeability and diffusion coefficients have been calculated using the thickness found by using the electronic micrometer (filled PDMS: 5.33×10^{-3}cm, unfilled PDMS: 1.65×10^{-2}cm and ester-substituted polysiloxane: 3.33×10^{-2}cm). This was because it was thought the errors in finding the thickness by cutting

out the membrane and weighing it were much higher due to the difficulty in cutting out the area accurately when the membrane adhered to the cell.

3.4 General

The results for studies on the concentration dependence of the transport properties of the vapours in the polymer membranes are shown in tables A65-A79. Tables A65-A73 show the variation of transport properties of acetone, ethanol and tetrachloroethylene in the three membranes, with each table showing activation energies for permeation and diffusion and the permeability and diffusivity at 90°C for a particular system. The data was calculated from the LnP against 1/T and LnD against 1/T Arrhenius plots for each system. Activation energies for permeation and diffusion are given at both ends of the temperature range used because, although straight line plots are expected for gas/polymer systems, when systems involving heavier organic vapours are used there is often marked deviation from this, and in all cases in this study the Arrhenius plots were found to be curved, so that the activation energies varied with temperature. Therefore activation energies are given at 50 and 110°C for the systems involving acetone, ethanol and tetrachloroethylene. The variation of permeability

and diffusivity with concentration is demonstrated by showing the permeability and diffusion coefficients at 90°C for each concentration; this temperature was chosen as it is near the middle of the temperature range used. Tables A65, A66 and A67 show the activation energies and transport data for acetone in the filled PDMS, unfilled PDMS and ester-substituted polysiloxane membranes respectively, tables A68, A69 and A70 show the activation energies and transport properties for ethanol in the filled PDMS, unfilled PDMS and ester-substituted polysiloxane membranes and tables A71, A72 and A73 show the activation energies and transport data for tetrachloroethylene in the filled PDMS, unfilled PDMS and ester-substituted polysiloxane membranes.

As with the other systems, the activation energies, permeabilities and diffusivities are shown for the permeant/polymer systems involving nitrobenzene, but at different temperatures. A higher temperature range was used, due to practical difficulties with working with nitrobenzene, therefore activation energies are shown at 60 and 110°C to cover this range. The LnD against 1/T Arrhenius plots for the nitrobenzene systems are similar to those for the systems involving the other permeants, and the diffusivity at 90°C is used again to show the variation of diffusivity with concentration. The LnP against 1/T

plots, however, are very different from those found for other systems, and the variation of permeability with concentration is dependent upon the temperature. Therefore, the permeability of nitrobenzene in the membranes is shown at 60 and 110°C so that the variation is shown at both ends of the temperature range. Tables A74, A75 and A76 show the activation energies for permeation and the permeabilities at 60 and 110°C for nitrobenzene in filled PDMS, unfilled PDMS and ester-substituted polysiloxane respectively. Tables A77, A78 and A79 show the activation energies for diffusion at 60 and 110°C and the diffusivity at 90°C for nitrobenzene in the filled PDMS, unfilled PDMS and ester-substituted polysiloxane membranes.

Uncertainties in the reported values were difficult to determine accurately. The permeation measurements in the commercially available filled PDMS film were estimated to have an uncertainty of up to 10%, with the main source of error being the permeant partial pressure, which is used directly in the calculation of the permeability and in the calculation of the calibration constant of the detector. The uncertainty in permeation measurements for the unfilled PDMS and ester-substituted polysiloxane films, however, was much higher due to the errors involved in the determination of the film thickness. An uncertainty of up to 16% has been

estimated for permeabilities in systems involving these membranes. The diffusion coefficients in the filled PDMS/permeant systems were estimated to have an uncertainty of 15%, which was due mainly to the difficulty in obtaining the gradient of the approach to steady-state (dS/dt) with accuracy. The linear section of the approach to steady-state was often small and difficult to determine, especially with the slower approach to steady-state observed for the systems involving nitrobenzene. For the systems involving the unfilled PDMS and ester-substituted polysiloxane membranes the uncertainty increases to 25% due to the dependency of the diffusion on the square of the film thickness. Any other statistical analysis of the results was not possible as time limitations prevented any measurements from being repeated to any extent. The uncertainties in the activation energies and the permeabilities and diffusion coefficients at a particular temperature have not been estimated. These values have been taken from the best curve drawn through the Arrhenius plots derived from the transport data and are only meant as a guide to the trends in transport properties with permeant concentration.

DISCUSSION

Chapter 4 : Discussion.

4.1 The Transport of Acetone.

i) Filled Poly(dimethylsiloxane).

The permeability and diffusivity data for the acetone/filled PDMS system in tables A1-A5 are shown in graphical form as plots of LnP against 1/T and LnD against 1/T in figures A1 and A1a and figure A13. Although linear relationships might be expected for both plots, giving constant activation energies for permeation and diffusion over the temperature ranges considered, this situation usually only occurs for the transport of some gases in polymers over a limited range of temperature. As the diffusivity increases with temperature, the LnD against 1/T plots have a negative gradient which, using the Arrhenius relationship expressed in equation (1.9), gives a positive activation energy for diffusion. The plots show a marked curvature which is concave to the 1/T axis, showing that the activation energy for diffusion decreases with increasing temperature. Values for the activation energy at 50 and 110°C are given in table A65. Several other workers have found a similar curvature for LnD against 1/T plots[6-8]. The variation

of the activation energy for diffusion can be explained if this quantity is considered to be the energy required to separate the polymer chains to form a void which is large enough to allow the penetrant molecule to complete a successful diffusive jump. This energy is related to the cohesive energy of the chain segments involved which, like the heat of vaporisation of a substance, is dependent on the temperature and likely to decrease with temperature.

The LnP against 1/T plots have a positive gradient yielding a negative activation energy for permeation. The plots are slightly curved and are convex to the 1/T axis so that the activation energy increases (i.e. becomes less negative) with increasing temperature. Values for the activation energy for permeation at 50 and 110°C have been taken from the experimental curves and are shown in table A65. These energies are of little theoretical value and are merely a combination of the activation energy for diffusion and the heat of solution of the permeant in the polymer (see equation 1.14) which gives a useful method for estimating the heats of solution. The solubility data estimated from the permeability values are considered later in this chapter.

ii) Unfilled Poly(dimethylsiloxane) (M1).

Plots of LnP against 1/T and LnD against 1/T representing the results for the acetone/M1 system in tables A23-A27 are shown in figure A5 and figures A17 and A17a. The shapes of the curves are very similar to those for the acetone/filled PDMS system with the activation energies for diffusion decreasing with temperature. The activation energies for permeation are negative and become less negative as the temperature is raised. Both the permeability and the diffusivity of acetone are higher in the unfilled membrane, the permeability is increased by a factor of approximately 1.7 and the diffusivity is improved by a factor of approximately 5. The activation energies at 50 and 110°C are shown in table A66 and are found to be higher for diffusion but lower for permeation.

iii) Ester-substituted Polysiloxane (M18).

The substitution of ester functional groups on to the sidechains of the polysiloxane structure gave a polymer membrane with enhanced transport properties. The diffusivity was approximately doubled, while the permeability was increased by a factor of approximately 1.25 compared with the unfilled PDMS membrane. As with the two PDMS membranes, the activation energy for diffusion decreased with increasing temperature and the activation energy for permeation was negative and

increased with temperature. The activation energies at 50 and 110°C, which are shown in table A67, were found to be higher for diffusion but lower for permeation than for the PDMS membranes. Plots of LnP against 1/T and LnD against 1/T are shown in figures A9 and A9a and figures A21 and A21a .

4.2 The Transport of Ethanol.

i) Filled Poly(dimethylsiloxane).

The permeability and diffusivity data for the ethanol/filled PDMS system, listed in tables A6-A10, are shown as plots of LnP against 1/T and LnD against 1/T in figure A2 and figures A14 and A14a. The shape of the curves is very similar to that of the acetone/polysiloxane systems, with the LnD against 1/T plots being concave to the 1/T axis with a negative gradient and the LnP against 1/T plots being concave to the 1/T axis with a positive gradient. Therefore, as with the systems involving acetone, the activation energy for diffusion is positive and decreases with increasing temperature and the activation energy for permeation is negative and increases (becomes less negative) with increasing temperature. Activation energies for permeation and diffusion at 50 and 110°C are shown in table A68. The permeabilities and

diffusivities are very similar to those found for the acetone/filled system. The diffusivity of ethanol is slightly higher than that of acetone in the PDMS membrane if compared at similar partial pressures and at similar relative pressures (p/p^o). Ethanol is also a better permeant than acetone in the filled PDMS when compared at similar partial and relative pressures.

ii) Unfilled Poly(dimethylsiloxane) (M1).

Plots of LnP against 1/T and LnD against 1/T, representing the transport data for the ethanol/M1 system listed in tables A28-A32, are shown in figure A6 and figures A18 and A18a. The curve shapes and variation of activation energies with temperature are similar to those in the previously discussed systems. The activation energies for permeation and diffusion at 50 and 110°C are shown in table A69. As with acetone, ethanol is more easily transported across the unfilled membrane, with the diffusivity increasing by a factor of approximately 5.8 and the permeability increasing by a factor of approximately 1.6. The activation energies for permeation are less in the unfilled PDMS, but the activation energies for diffusion are increased. The permeabilities and diffusivities are similar to those found for the acetone/M1 system.

iii) Ester-substituted Polysiloxane (M18).

Once again, a similar trend to that found with the acetone/polysiloxane systems is found. Transport across the M18 membrane is enhanced with respect to the filled and unfilled membranes. The diffusion coefficient was increased by a factor of approximately 2.4 by the addition of the ester groups, whilst there was a 25% increase in the permeability. The variation of transport properties with temperature is shown as plots of LnP against 1/T and LnD against 1/T in figures A10 and A10a and figures A22 and A22a, with the activation energies at 50 and 110°C being listed in table A70. As with the other membranes, ethanol has a higher permeability through M18 than does acetone when values are compared at similar permeant partial pressures and relative pressures. Ethanol also has a higher diffusivity than acetone in M18 at similar partial and relative pressures.

4.3 The Transport of Tetrachloroethylene.

i) Filled PDMS.

The plot of LnD against 1/T shown in figures A15 and A15a demonstrates a similar trend to that found

with the systems involving acetone and ethanol. The plot has a concave curvature towards the 1/T axis giving an activation energy for diffusion which decreases with increasing temperature, but the plot of LnP against 1/T, shown in figure A3, is different from those found with the other systems. The plots are curved with a negative activation energy, but the curves are convex to the 1/T axis showing that the activation energy for permeation decreases (becomes more negative) with increasing temperature. The activation energies at 50 and 110°C are listed in table A71. The filled membrane is more permeable to tetrachloroethylene than to ethanol or acetone. At a comparable permeant partial pressure, the permeability of tetrachloroethylene is approximately 50% greater than that of ethanol, with the activation energy for permeation being greater for tetrachloroethylene. The diffusivity of tetrachloroethylene is less than that for ethanol and acetone with a corresponding higher activation energy for diffusion, as would be expected for a larger permeant. The diffusion coefficient for the tetrachloroethylene/filled PDMS system is approximately 2.5 times less than that for the ethanol/filled PDMS system at comparable vapour pressures. A direct comparison between the transport properties of tetrachloroethylene, acetone and ethanol in the filled PDMS membrane can be made if the relative

pressures of the permeants are considered. At similar relative pressures the permeabilities of the penetrants increase in the order acetone < ethanol < tetrachloroethylene, the diffusivity, however, increases in the order tetrachloroethylene < acetone < ethanol. The order of decreasing diffusivity is an indication of the increasing size of the penetrant molecules whereas the the different order of increasing permeability shows a relatively high solubility for tetrachloroethylene in the filled PDMS.

ii) Unfilled PDMS (M1).

The tetrachloroethylene/M1 system has similar characteristics to the tetrachloroethylene/filled PDMS system, but with enhanced transport parameters. The diffusion coefficient of tetrachloroethylene in the M1 membrane is approximately 3 times greater than that in the filled membrane and the permeability is greater by a factor of approximately 2.5. The LnP against 1/T and LnD against 1/T plots, in figure A7 and figures A19 and A19a, show an activation energy for diffusion which decreases with increasing temperature and a negative activation energy for permeation which also decreases with increasing temperature. Activation energies at 50 and 110°C are shown in table A72. As with the filled membrane, tetrachloroethylene is more permeable than

ethanol or acetone in the M1 membrane, with the permeability for tetrachloroethylene being more than double that for ethanol at a comparable permeant vapour pressure. The diffusion coefficient for the larger molecule is less than 0.25 of that for ethanol with a much larger activation energy for diffusion. As with the filled membrane, when the transport properties of the penetrant/M1 systems are considered at similar relative pressures the permeabilities increase in the order acetone < ethanol < tetrachloroethylene and the diffusivities increase in the order tetrachloroethylene < acetone < ethanol.

iii) Ester-substituted Polysiloxane (M18).

LnP against 1/T and LnD against 1/T plots for the tetrachloroethylene/M18 system are shown in figures A11 and A11a and figures A23 and A23a. The variation of diffusion with temperature is similar to that found with all of the other systems, having an activation energy for diffusion which decreases with increasing temperature. The diffusion coefficients for this system are higher than for tetrachloroethylene in the M1 membrane by a factor of approximately 2.4, but this permeant has a smaller diffusion coefficient than the smaller acetone and ethanol molecules in the same membrane. The diffusion coefficient of ethanol is

approximately 4.5 times greater than that of tetrachloroethylene in M18.

The LnP against 1/T plots are the same shape as those for the other two systems involving tetrachloroethylene, but are different from the systems involving acetone and ethanol. The negative activation energy for permeation of the tetrachloroethylene/M18 decreases with increasing temperature. The activation energies for permeation and diffusion at 50 and 110°C are given in table A73. The M18 membrane is more permeable to tetrachloroethylene than is the M1 membrane by a factor of approximately 1.6 and, as with the other membranes, M18 is more permeable to tetrachloroethylene than to acetone or ethanol. The permeability of ethanol in M18 is approximately 2.8 times less than that of tetrachloroethylene. Once again, comparison at similar relative pressures shows the permeabilities increase in the order acetone < ethanol < tetrachloroethylene and the diffusivities increase in the order tetrachloroethylene < acetone < ethanol.

4.4 The Transport of Nitrobenzene.

Plots of LnP against 1/T and LnD against 1/T for nitrobenzene in the filled PDMS, M1 and M18 membranes are shown in figures A4, A8, A12 and A12a and in

figures A16, A16a, A20, A20a, A24 and A24a. The variation of diffusivity with temperature in the three systems is very similar and all three show trends which match those in the systems involving acetone, ethanol and tetrachloroethylene. As with the other permeants, the diffusivity of nitrobenzene in each membrane increases in the order filled PDMS < M1 < M18, with the diffusion coefficient being increased by a factor of approximately 3.5 from the filled PDMS to the M1 membrane and by a factor of approximately 3 from the M1 to the M18 membrane. As would be expected for such a large molecule, nitrobenzene has much smaller diffusion coefficients than the other permeants, although direct comparison is not possible at similar permeant partial pressures due to the low volatility of nitrobenzene. However, if the transport properties are considered at similar relative pressures the diffusivity can be seen to increase in the order nitrobenzene < tetrachloroethylene < acetone < ethanol so that the diffusivity increases with decreasing size of the penetrant molecule. The activation energies for diffusion decrease with increasing temperature, values for the activation energy at 50 and 110°C are shown in tables A77, A78 and A79.

The LnP against 1/T plots for nitrobenzene in the three membranes show similar characteristics to each other, yet are very different from those found for

acetone, ethanol and tetrachloroethylene. For the other three permeants the permeability plots at each permeant concentration lie approximately parallel to each other with the permeability generally increasing with increase in concentration. For nitrobenzene however, the permeability plots at lower concentrations lie very close together and give very small activation energies which are usually negative, whereas at higher concentrations the permeability decreases with the activation energy increasing from a negative to a positive value with increase in temperature, or remaining positive over the entire temperature range covered. The activation energies for permeation at 60 and 110°C are shown in tables A74, A75 and A76. The variation in the activation for permeation is due to a combination of the variation of both the activation energy for diffusion and the heat of solution, which will be discussed later in this section. At similar relative pressures the permeabilities of the penetrants are found to increase in the order acetone < ethanol < tetrachloroethylene < nitrobenzene in all of the membranes studied. The higher permeabilities of tetrachloroethylene and nitrobenzene are due to their greater solubilities.

4.5 Solubility.

The variation of solubility with temperature for each of the permeants in the three membranes is shown in tables A80-A91 and as plots of LnS against 1/T in figures A25-A36a. The solubilities were calculated from the experimental permeability and diffusivity results using the relationship S=P/D. Solubilities for the four permeants at 90°C were calculated from the permeabilities and diffusivities at 90°C taken from the LnP against 1/T and LnD against 1/T plots. Values for the heat of solution, ΔH_S, at 60 and 110°C for nitrobenzene and 50 and 110°C for the other three permeants, were calculated from the activation energies for permeation, E_P and the activation energies for diffusion, E_D using the relationship $\Delta H_S=E_P-E_D$. Due to cumulative errors from the permeability measurements and particularly from the diffusion measurements, the solubility data are likely to have very large errors. The values are not meant to be used as accurate measurements, but they are useful as a guide to the relative solubilities of each system. The solubilities of the permeants in all three membranes increase in the order acetone ≈ ethanol < tetrachloroethylene < nitrobenzene. As the solubility depends on the condensability of the vapour and also the interaction of the permeant and the polymer, it seems likely that the high solubility of both tetrachloroethylene and nitrobenzene is due to their being more condensable. It

is unlikely to be due to a much stronger interaction than acetone and ethanol as these are both polar molecules and are likely to have a strong attraction for the oxygen bonds in the polymer.

The solubilities in the polymer/permeant systems, with respect to the polymer, increases in the order M18 < M1 < filled PDMS. Acetone and ethanol are much more soluble in the filled PDMS membrane than in the other membranes (approximately 3.5 times more soluble in the filled PDMS than in the unfilled M1) however, there is little difference between the solubilities of tetrachloroethylene and nitrobenzene in the filled PDMS and M1 membranes. The enhanced solubility of acetone and ethanol must be due to an interaction between the filler and the permeant which does not affect the solubility of tetrachloroethylene and nitrobenzene. The overall effect is that the solubility selectivity of nitrobenzene over acetone and ethanol is enhanced by the omission of filler from the PDMS membrane. The solubility selectivity of nitrobenzene with respect to tetrachloroethylene however, is unaffected.

The solubility of all the permeants is decreased by the addition of ester groups into the PDMS. Ethanol is approximately half as soluble in the M18 membrane as in the M1 membrane, acetone is less soluble by a factor of approximately 0.59 and nitrobenzene and tetrachloroethylene are approximately 0.62 and 0.67

times less soluble in the M18 membrane respectively. Again, this means that the solubility selectivity of the nitrobenzene over acetone and ethanol is enhanced, but the relative solubilities of nitrobenzene and tetrachloroethylene remain relatively unchanged.

4.6 Effect of Penetrant on Transport Properties.

The transport of a permeant across a polymer membrane depends on characteristics of both the permeant molecules and the polymer. The effect of the characteristics of the penetrant molecules will be considered here, whilst the effect of the polymer will be discussed in the next section. The properties of the penetrant molecules can be divided into two, those which affect diffusion and those which affect solubility.

The diffusion of a molecule through a polymer is dependent mainly upon the molecular size. For a large molecule, a larger 'hole' has to be made between the polymer chains to allow a successful diffusive jump and this results in a higher activation energy for diffusion and a lower diffusion coefficient. The relative size of the molecules can be judged by using the van der Waals volume, which can be calculated by using group contributions to the van der Waals volume given by Bondi[56]. It is important that care is taken

when considering the diffusion of 'non-spherical' molecules. A long chain hydrocarbon, for example, will diffuse through a polymer 'headfirst' so that there is the smallest disturbance of the polymer chains, then the dimension which should be considered is the kinetic diameter, that is the largest diameter of the molecule perpendicular to its direction of diffusion.

Van der Waals volumes for the permeants in this research have been calculated from Bondi's values giving a volume for ethanol of $31.94 cm^3 mol^{-1}$, for acetone $39.94 cm^3 mol^{-1}$, for tetrachloroethylene $56.62 cm^3 mol^{-1}$ and for nitrobenzene $62.64 cm^3 mol^{-1}$. The volume for ethanol does not include a correction for hydrogen bonding as single molecules are being considered in the diffusion process and the volume for nitrobenzene may only be used as an approximate guide as the group contribution to the volume from a nitro group attached to an aromatic ring was not available, so the value for a nitro group attached to an alkyl group was used. Although acetone and ethanol have quite different van der Waals volumes, neither molecule can be considered spherical. If models of the two molecules are studied, their kinetic diameters appear quite similar, which accounts for the similarity of the diffusion coefficients of the two permeants at similar concentrations, although ethanol has a slightly higher diffusion coefficient due to its slightly smaller size.

Tetrachloroethylene and nitrobenzene, being much larger molecules, have smaller diffusion coefficients.

The diffusion can also be affected by interactions between the penetrant and the polymer. If there are strong specific interactions between the penetrant molecules and groups in the polymer chain then the diffusion of some molecules may be retarded. If the interaction between the penetrant molecules is much greater than that between the penetrant and the polymer, there may be a tendency for the penetrant to cluster within the polymer causing molecules to be less mobile. This has been observed particularly with hydrogen-bonding species such as water[54,57] and methanol[58] in polyorganosiloxanes.

The solubility of the permeant in the polymer is dependent upon both the condensability of the permeant and the interaction between the permeant and the polymer. The condensability, which is related to the normal boiling point, increases for each permeant in the order acetone < ethanol < tetrachloroethylene < nitrobenzene, so that the sorption of nitrobenzene should be favoured above the other permeants if this is the only factor to be taken into account. However, as the condensability of the vapours is a constant factor, to achieve an improvement in the solubility selectivity it is necessary to chemically modify the polymer to increase the attractive forces between the desired

permeant and the polymer, leaving the interactions between the other permeants and the polymer relatively unchanged or even reduced.

4.7 Effect of Polymer on Transport Properties.

The properties of a polymer which affect the transport of permeants are the interaction of the polymer with permeant, which is mentioned in the previous section, the free volume of the polymer and the polymer chain segment mobility. A larger free volume generally indicates wider polymer chain separation, so that a permeant molecule has more freedom of movement resulting in a higher diffusion coefficient. However, if there is low polymer chain segment mobility, the reduction in chain fluctuations results in there being a lower chance of there being a localisation of free volume to form a 'hole' of sufficient size to allow a successful diffusive jump, giving a lower diffusion coefficient. Moreover, as the energy required to separate the segments to a sufficient distance is greater for the more rigid polymer chains, a higher activation energy is needed for diffusion. PDMS is known to have high polymer chain flexibility, which is due to the ease of segmental rotation about the Si-O linkages in the polymer backbone. The resulting high diffusivity has led to

the siloxanes being some of the most permeable polymers known.

The effect of adding an ester group to the side chains of the PDMS can be seen by comparing the diffusivities of the M1 and M18 membranes. The diffusion coefficients of all of the permeants are higher in the ester-substituted M18 polymer with the diffusivity of acetone being doubled, the diffusivities of ethanol and tetrachloroethylene increasing by a factor of approximately 2.4 and the diffusion coefficient for nitrobenzene increasing by a factor of 3. The enhanced diffusion is likely to be caused by an increase in the free volume due to the large $-(CH_2)_3COOCH_3$ group preventing the polymer chains from packing so closely together. It is possible that the polymer chain mobility may be restricted by such a large group, although the Si-O linkages are still present in the backbone. If this is the case then the effect is easily outweighed by the increase in free volume. This increase will obviously have a greater effect on larger penetrant molecules which are more restricted by the polymer network, which explains the greater increase in the diffusivity of nitrobenzene than of the other permeants in the M18 polymer. The increase in diffusivity for ethanol is greater than would be expected when compared to that for acetone and tetrachloroethylene, as ethanol is the smallest

permeant molecule and would therefore be expected to be affected the least by any change in free volume of the polymer. The solubility results show that the solubility of ethanol in M18 is decreased from that in M1 to a greater degree than the solubilities of acetone and tetrachloroethylene, i.e. ethanol is relatively more soluble in the M1 membrane. This indicates that there is either a strong interaction between ethanol and the M1 membrane, retarding the diffusion process, which is not present to such an extent in the M18 membrane, or there is a retarding interaction between both acetone and tetrachloroethylene in the M18 membrane. It is possible that there is a strong attraction between the hydroxy group of the ethanol and the oxygen in the backbone of the M1 polymer which is reduced in the M18 due to steric effects of the bulky ester group, or there may be an increased affinity for acetone and tetrachloroethylene due to the substitution of the ester group in the M18 polymer.

The difference between the permeant/filled PDMS systems and the permeant/M1 (unfilled PDMS) systems is due largely to the large amount of filler in the commercially available filled polymer. The filled polymer contains 28 weight% of silica as a filler. The diffusion of all four permeants was much lower in the filled membrane, but the diffusion of acetone and ethanol was affected to a much greater extent than that

of tetrachloroethylene and nitrobenzene. The diffusivities of tetrachloroethylene and nitrobenzene were approximately 3.0 and 3.5 times higher in the M1 membrane, whereas those of acetone and ethanol were increased by factors of 5.0 and 5.8 respectively.

For the two larger permeants, the filler particles act purely as obstructions to diffusion within the polymer network which restrict the passage of the permeant, just as obstructions in a pipe of flowing liquid would obstruct the flow. It is also possible that a different degree of crosslinking in the two polymers may cause differences in diffusivity, as crosslinking results in reduced polymer chain mobility and thus decreases diffusion, however, the degree of crosslinking in the commercial filled PDMS membrane could not be determined. In either case the diffusivity of the larger nitrobenzene molecules is affected to a greater extent than that of tetrachloroethylene, as would be expected.

The decrease in the diffusivity in the filled membrane of the smaller acetone and ethanol molecules, however, is greater than would be expected if the only effect of the filler was as an inert barrier to molecular motion. If the relative solubilities of each permeant in the two membranes is considered, it can be seen that the addition of filler has a much greater effect on acetone and ethanol. The solubilities of

these two permeants are increased by factors of approximately 3.1 and 3.5 respectively, whereas the solubility of the two larger permeants is increased by only 25%. From this it can be seen that ethanol and acetone have a high affinity for the silica which would be expected when the high polarities of the filler and the two permeants are considered. A large amount of acetone or ethanol can be adsorbed by the silica resulting in greatly enhanced solubility in the filled membrane, but once the permeant molecules are adsorbed their diffusive motion is restricted, resulting in a large decrease in diffusion coefficient.

4.8 Effect of Permeant Concentration.

In the simplest solution-diffusion system, neither the solubility nor the diffusivity of the permeant in the polymer is affected by the concentration of the penetrant present in the polymer. Henry's law would be obeyed giving a constant solubility coefficient at a given temperature and the penetrant would be randomly dispersed in the polymer, as neither penetrant-penetrant interactions nor penetrant-polymer interactions would be preferred. This simple behaviour is observed for some permanent gases in polymers for pressures below and about an atmosphere, where weak polymer-penetrant interactions result in a low

solubility so that penetrant-penetrant interactions are negligible due to the low concentration of gas in the polymer. This low solubility also results in a negligible change in the free volume of the system so that the diffusion of the penetrant is unaffected. For vapours in polymers however, the situation is more complex.

In this research, the behaviour of the four permeants in the polysiloxane membranes was studied over a range of concentrations. The concentration range of each permeant is different due to the very different volatilities of organic liquids and to the method of producing the permeant stream in the experimental apparatus. Over the ranges studied, the permeability increased with concentration for the polymer/vapour systems involving acetone, ethanol and tetrachloroethylene. Plots of LnP at 90°C against the permeant partial pressure for these three permeants in each of the membranes are shown in figures A37-A40, all of the plots have curvature concave to the pressure axis indicating that the effect on permeability decreases at higher permeant pressures and the permeability begins to level off. The only exception is for acetone in the filled PDMS membrane where the permeation appears to be hardly affected by the permeant pressure, but this may be due to an inaccurate result at the lowest pressure, which is higher than

expected, as these results were obtained at an early stage in the experimental work when errors were more likely. Similar results for acetone and ethanol in PDMS have been reported by Baker et al[59] and other workers[60,61], and also by Paul et al[62] who have reported work on acetone in PDMS.

The nitrobenzene/polysiloxane systems however, appear to be much more complex. The LnP against 1/T plots discussed earlier were very different from those for the other systems and, as a result the permeability appears to be relatively constant at lower concentrations, or it may even pass through a maximum, and at higher concentrations the permeability decreases. Due to the unusual LnP against 1/T plots, the concentration dependence of the permeability also varies with temperature, therefore plots of LnP at 60, 90 and 110°C against permeant pressure are shown in figures A40 and A40a. This variation of the permeability appears to be due to the unusual solubility behaviour of nitrobenzene which will be discussed later.

Plots of LnD at 90°C against permeant pressure are shown in figures A41-A44. There is a marked increase in diffusivity with concentration for the acetone/polymer and nitrobenzene/polymer systems but for the ethanol/polymer systems there is very little change in diffusion coefficient and for tetrachloroethylene an

increase in concentration leads to a decrease in diffusivity. It is generally accepted that diffusivity increases with concentration for vapours in polymers. The sorption of a vapour into a polymer leads to an increase in free volume and often weakens the inter-molecular attraction between the polymer segments leading to greater chain mobility, this facilitates the transport of the penetrant molecules through polymer, giving a greater diffusivity.

The only documented accounts of a true decrease in diffusion with increase in permeant concentration in polyorganosiloxanes are for water[55,57] and other strongly hydrogen-bonded species such as methanol[58]. The decrease in diffusivity is due to the formation of clusters of the penetrant molecules which restricts their mobility. Antiplasticisers[63-65] can also cause a decrease in diffusivity, these are low molecular weight penetrants which at low concentrations appear to fill the free volume of a glassy polymer resulting in a loss of chain mobility. However, as the siloxanes are not glassy polymers, this effect can be discounted. As ethanol is a hydrogen-bonding species, it is possible that association may occur leading to a fall in diffusivity as the concentration increases, however, the effect of clustering for water and methanol has been found to be much greater than the effect seen here. It is possible that a reduced tendency to

cluster may give rise to the lesser effect. No such explanation can be used for the tetrachloroethylene systems as tetrachloroethylene is obviously not a hydrogen-bonding species.

An alternative explanation is offered in work by Suwandi and Stern[31]. Here a maximum was found in the experimental diffusion against penetrant volume-fraction curves for halothane ($CF_3CHClBr$) and methoxyflurane ($CHCl_2CF_2OCH_3$) in silicone rubber, so that at some concentrations there was a decrease in diffusivity with increasing concentration. The explanation offered was that the mutual diffusion coefficients used were defined with respect to the volume of unswollen polymer (i.e. contains no penetrant), the swelling of the polymer during the experiments caused a mass-flow of polymer and dissolved penetrant in the opposite direction to that of penetrant transport. At higher concentrations the swelling was greater causing a larger effect which gave the appearance of a decrease in diffusion coefficient. Suwandi and Stern argued that in order to obtain the true, or molecular, diffusion of the penetrants in the polymer, it was necessary to determine their intrinsic diffusion coefficient $\mathcal{D}$, which is defined with respect to a frame of reference which follows the mass flow. If it assumed that the intrinsic diffusion coefficient of the polymer is negligible, the relation between the

intrinsic diffusion coefficient of the penetrant and the mutual diffusion coefficient is given by

$$\mathcal{D} = \frac{D}{(1-\nu)^3}$$

where ν is the volume fraction of the penetrant in the polymer. For halothane and methoxyflurane in silicone rubber, $\mathcal{D}$ was found to increase over the whole concentration range studied. Due to the high solubility of tetrachloroethylene in the siloxanes it is quite possible that the diffusion-concentration relation is affected by swelling of the polymer. The effect is also likely to be present in the other systems, especially for nitrobenzene due to its high solubility, which means that the true diffusion coefficient would increase to an even greater extent with concentration.

Data for the variation of solubility with permeant concentration are given in tables A92-A103 and these are represented in graphical form as plots of LnS at 90°C against permeant pressure in figures A45-A48. The solubilities of the polymer/penetrant systems generally increase with penetrant concentration, the only exceptions being the nitrobenzene/polymer systems and acetone in the filled PDMS membrane. For the systems where the solubility increases with concentration, this is usually because the first molecules sorbed tend to loosen the polymer structure locally facilitating the

sorption of subsequent molecules. This occurs for systems with strong polymer-penetrant interactions where the penetrant acts as a plasticiser for the polymer. An alternative explanation, which is possible in the case of ethanol, is that if the penetrant-penetrant interactions are strong, then the solubility of a system may increase as the permeant concentration increases due to the attraction of free penetrant molecules for those absorbed in the polymer. If this is true and limited clustering of ethanol molecules occurs in the polymer, this may also help to explain the limited effect that increasing concentration has on the diffusivity due to the opposing effects of plastcization and clustering. The acetone/filled PDMS system shows a sharp decrease in solubility at lower concentrations. If the enhanced solubility of acetone in the filled PDMS, when compared to the unfilled M1 and M18 membranes, is taken into account the effect of the concentration can be explained by assuming that the acetone is preferentially sorbed onto the filler particles in the polymer, once the filler is saturated then the acetone is just sorbed into the polymer itself and the solubility-concentration curve assumes the characteristics of the acetone/unfilled PDMS system. It seems surprising however, that the ethanol/filled PDMS system does not exhibit similar characteristics.

4.9 Selectivity.

The differences in the transport properties of each membrane for the four permeants were intended to give improved permeation of nitrobenzene relative to the other permeants. Table 4.1 shows the permeability selectivities for nitrobenzene with respect to the other permeants for each of the three membranes, these selectivities are the ratio of the permeability of nitrobenzene and the permeants at 90°C, using the lowest permeant pressure in each case. As was mentioned in section 1.6, the permeability selectivity can be separated into a solubility selectivity S_A/S_B, and a diffusivity selectivity D_A/D_B. As the diffusion process is dependent mainly upon the size and the shape of the permeating species, which cannot be altered, it was thought that altering the membrane to enhance the solubility of nitro-compounds, represented by nitrobenzene, with respect to the other permeants would be the most suitable method of increasing the selectivity of the membranes for nitrobenzene. Both solubility selectivities and diffusivity selectivities for nitrobenzene with respect to the other permeants are also shown in table 4.1 to show how the sorption and diffusion processes are affected by changes in the membrane, and how they affect the relative

Table 4.1 : Membrane Selectivity for Nitrobenzene @ 90°C.

Solubility Selectivity

	Filled PDMS	M1	M18
$C_6H_5NO_2/C_2H_5OH$	23.35	59.72	76.88
$C_6H_5NO_2/(CH_3)_2CO$	24.30	65.64	76.88
$C_6H_5NO_2/C_2Cl_4$	7.38	7.26	7.00

Diffusivity Selectivity

	Filled PDMS	M1	M18
$C_6H_5NO_2/C_2H_5OH$	0.07	0.05	0.06
$C_6H_5NO_2/(CH_3)_2CO$	0.07	0.05	0.07
$C_6H_5NO_2/C_2Cl_4$	0.17	0.20	0.26

Permeability Selectivity

	Filled PDMS	M1	M18
$C_6H_5NO_2/C_2H_5OH$	1.69	2.97	4.70
$C_6H_5NO_2/(CH_3)_2CO$	1.75	3.48	5.71
$C_6H_5NO_2/C_2Cl_4$	1.23	1.45	1.85

permeabilities of the polymer/penetrant systems.

The selectivity, or ideal separation factor P_A/P_B, increases for nitrobenzene with respect to the other permeants in the membranes in the order filled PDMS < M1 < M18 and is accompanied by an increase in permeability. The increased permeability is due solely to an increase in diffusivity in the membranes as the solubility decreases in the order filled PDMS > M1 > M18, but the increased selectivity for nitrobenzene over acetone and ethanol is due mainly to an increased relative solubility. It can be seen from table 4.1 that the diffusion process actually favours the smaller molecules and, due to the low diffusivity of acetone and ethanol in the filled PDMS when compared to the unfilled M1 membrane, the diffusivity selectivity actually decreases with the omission of filler. The diffusivity selectivity increases slightly from the M1 to M18 membrane due to the greater effect of the increased free volume on the diffusion of the larger nitrobenzene, indicating that a more open polymer network favours the transport of nitrobenzene. The main reason for the higher total selectivity for nitrobenzene is its high solubility and, although the solubility of nitrobenzene decreases in the order filled PDMS > M1 > M18, the solubility selectivity increases due to the greater decrease in the solubility of acetone and ethanol.

For the selectivity of nitrobenzene over tetrachloroethylene, the situation is different. As with acetone and ethanol, tetrachloroethylene has a greater diffusivity but a lower solubility than nitrobenzene, but the increase in the overall selectivity in the M18 membrane is due to an increase in the diffusivity selectivity rather than solubility effects, which is not what was expected. The diffusivity selectivity was expected to increase, as the diffusivity of the larger nitrobenzene molecules would be affected to a greater extent an easier diffusion pathway, but the solubility selectivity of nitrobenzene was actually found to decrease slightly in the order filled PDMS > M1 > M18 which was the opposite of the desired effect.

It is obvious from these results that a membrane with greater free volume and greater chain mobility is desirable to improve the diffusivity of the large nitrobenzene molecules. However, if a smaller nitro compound was the desired species, or if larger contaminants were present, then the increase in diffusivity would not necessarily favour transport of the required penetrant, although the increased diffusivity would be desirable for an increase in permeability. The selectivity must be governed by solubility if a useful separation is to occur and, if the solubility selectivity of nitrobenzene over

tetrachloroethylene is considered, it appears that the substitution of the ester group into the PDMS does not favour the sorption of the nitro compound relative to the chloro compound. For a more satisfactory selectivity, the substitution of a different functional group is necessary.

4.10 Future Work.

The results of this research can easily be built upon by further investigation of the same systems to increase understanding. Examining these systems over wider temperature range to give a better idea of the effect of temperature on the transport properties would be useful, especially considering the unusual characteristics of the nitrobenzene systems. Extending the concentration range would also be useful for further examination of the concentration dependence of the system, with nitrobenzene again having unusual characteristics which require further clarification.

Due to the large errors estimated for the solubility coefficients, independent sorption experiments should be carried out using a different experimental method to give more accurate results. The most common method is the measurement of the uptake of the penetrant by the polymer gravimetrically. Finally, as the increase in selectivity was not as great as was

hoped, especially with respect to tetrachloroethylene, the synthesis of other polymer membranes containing other functional groups is required. The possibility of substituting a group which a nitro functionality into a PDMS should be considered for the enhancement of the transport of nitro-organic species.

REFERENCES

References.

1) W.J.Schell, J.Membrane Sci. (1985), 22, 217

2) T.Graham, Phil. Mag. (1866), 32, 401

3) G.S.Park, Transport Principles - Solution, Diffusion and Permeation in Polymer Membranes, in: P.M.Bungay, H.K.Lonsdale, and M.N.De Pinho, Synthetic Membranes: Science, Engineering and Applications. p57, NATO ASI Series, Series C, Mathematical and Physical Sciences, Vol.181 (Proceedings of the NATO Advanced Study Institute, Alcabideche, Portugal, June 26- July 8, 1983) D.Reidel Publishing Co., Durdrecht, Neth. 1986.

4) R.M.Barrer, Trans. Faraday Soc. (1939), 35, 628

5) G.J.Van Amerongen, J.Appl. Phys. (1946), 17, 972

6) G.J.Van Amerongen, J.Polym. Sci. (1950), 5, 307

7) R.M.Barrer and G.Skirrow, J.Polym. Sci. (1948), 3, 549

8) M.J.Hayes and G.S.Park, Trans. Faraday Soc. (1955), 51, 1134

9) M.J.Hayes and G.S.Park, Trans. Faraday Soc. (1956), 52, 949

10) C.E.Rogers, V.Stannett and M.Szwarc, J.Polym. Sci. (1960), 45, 61

11) G.S.Park, Trans. Faraday Soc. (1950), 46, 684

12) A.T.Hutcheon, R.J.Kokes, J.L.Hoard and F.A.Long,

J.Chem. Phys. (1952), 20, 1232

13) S.Prager and F.A.Long, J.Am. Chem. Soc. (1951), 73, 4072

14) Encyclopedia of Polymer Science and Engineering, 2nd Edition, Vol.9, p509, (1987)

15) C.E.Rogers, Permeation of Gases and Vapours in Polymers, in: J.Comyn (Ed), Polymer Permeability, London: Elsevier Applied Science Publishers Ltd., 1985.

16) R.M.Barrer, Trans. Faraday Soc. (1947), 43, 3

17) D.W.Brubaker and K.Kammermeyer, Ind. Eng. Chem. (1952), 44, 1465

18) D.W.Brubaker and K.Kammermeyer, Ind. Eng. Chem. (1953), 45, 1148

19) T.L.Caskey, Modern Plastics (1967), 45, 148

20) A.Phatak, C.M.Burns and R.Y.M.Huang, J.Appl. Polym. Sci. (1987), 34, 1835

21) D.G.Pye, H.H.Hoehn and M.Panar, J.Appl. Polym. Sci. (1976), 20, 287

22) R.A.Pasternak, J.F.Schimscheimer and J.Heller, J.Polym. Sci. A2 (1970), 8, 467

23) S.A.Stern, S-M.Fang and H.L.Frisch, J.Polym. Sci. A2 (1972), 10, 201

24) K.D.Zeigel, H.K.Frensdorff and D.E.Blair, J.Polym. Sci. A2 (1969), 7, 809

25) R.M.Felder, J.Membrane Sci. (1978), 3, 15

26) R.M.Felder, R.D.Spence and J.K.Ferrell, J.Appl.

Polym. Sci. (1975), 19, 3193

27) R.M.Felder, C-C.Ma and J.K.Ferrell, AIChEJ (1976), 22, 724

28) W.A.Rogers, R.J.Buritz and D.Alpert, J.Appl. Phys. (1954), 25, 868

29) J.Crank, The Mathematics of Diffusion, Clarendon Press, Oxford, 1956, p.47.

30) K.Kammermeyer, Ind. Eng. Chem. (1957), 49, 1685

31) M.S.Suwandi and S.A.Stern, J.Polym. Sci. Polym. Phys. (1973), 11, 663

32) R.M.Barrer, J.A.Barrie and N.K.Raman, Polymer (1962), 3, 595

33) H.Strathmann, C-M.Bell and K.Kimmerle, Pure and Appl. Chem. (1986), 58, 1663

34) W.L.Robb, Ann. N.Y.Acad. Sci. (1968), 146 Pt1, 119

35) R.T.Chern, W.J.Koros, H.B.Hopfenberg and V.T.Stannett, Material Selection for Membrane-Based Gas Separations, in: D.R.Lloyd (Ed), Materials Science of Synthetic Membranes, ACS Symposium Series 269, ACS, Washington, (1985) Chap2.

36) W.J.Koros, J.Polym. Sci. Polym. Phys. (1985), 23, 1611

37) W.J.Koros, B.J.Story, S.M.Jordan, K.O'Brien and G.R.Husk, Polym. Eng. Sci. (1987), 27, 603

38) A.J.Ashworth, B.J.Brisdon and R.England, "Functionalised Polysiloxane Membranes for Gas, Vapour and Liquid Separations.", SERC Research

Grant, GR/D7518, April 1986.

39) A.J.Ashworth, B.J.Brisdon, R.England, B.S.R.Reddy and I.Zafar, "Polyorganosiloxanes containing both ester and hydride functionalities. A detailed study by ^{1}H and ^{13}C nmr spectroscopy.", British Polym. J. in press.

40) S.A.Stern, V.M.Shah and B.J.Hardy, J.Polym. Sci. Polym. Phys. (1987), 25, 1263

41) i) M.D.Wickham, "Transport Properties of Selected Polymer Films.", PhD thesis, University of Bath, (1983)

ii) A.J.Ashworth and M.D.Wickham, J.Membrane Sci. (1987), 34, 225

42) H.A.Daynes, Proc. Roy. Soc.(London) (1920), 97A, 287

43) E.Casur and T.G.Smith, J.Appl. Polym. Sci. (1986), 31, 1425

44) A.Weissberger (Ed), Technique of Organic Chemistry Vol.1, Physical Methods Pt1, 3rd Edition, Chap IX, p447, Interscience Publishers Inc., New York, 1959.

45) S.Ohe, Computer Aided Data Book of Vapour Pressure, Data Book Publishing Publishing Company, Tokyo, Japan, 1976.

46) Selected Values of Properties of Chemical Compounds, Thermodynamic Research Center Data Project, Texas A and M University, College Station, Texas, 1957, table 23-2-1(1.1130)k.

47) R.R.Dreisbach, Physical Properties of Chemical Compounds, ACS, Washington D.C., 1955, Vol.1

48) Engineering Sciences Data Unit, Physical Data, Chemical Engineering, 1976, Vol.2f

49) R.S.Barratt, Analyst, (1981), 106, 817

50) J.Namiesnik, J.Chromatography (1984), 300, 79

51) D.P.Lucero, Anal. Chem. (1971), 43, 1744

52) A.E.O'Keefe and G.C.Ortman, Anal. Chem. (1966), 38, 760

53) J.Crank and G.S.Park, Methods of Measurement, in: J.Crank and G.S.Park (Eds), Diffusion in Polymers, Academic Press, London and New York, 1981, Chap.1.

54) J.A.Barrie and D.Machin, J.Macromol. Sci. (1969), B3, 673

55) J.A.Barrie, M.J.L.Williams and H.G.Spencer, J.Membrane Sci. (1984), 21, 185

56) A.Bondi, J.Phys. Chem. (1964), 68, 441

57) J.A.Barrie and D.Machin, J.Macromol. Sci. (1969), B3, 645

58) J.A.Barrie, J.Polym. Sci. A1 (1966), 4, 3081

59) R.W.Baker, N.Yoshioka, J.M.Mohr and A.J.Khan, J.Membrane Sci. (1987), 31, 259

60) G.E.Spangler, Amer. Lab. (1975), 7, 3

61) C.E.Rogers, M.Fels and N.N.Li, Separation by Permeation through Polymer Membranes, in: Recent Developments in Separation Science, Vol.II, Chemical Rubber Company, Ohio, 1972.

62) H.Paul, C.Philipsen, F.J.Gerner and H.Strathmann, J.Membrane Sci. (1988), 36, 363

63) Y.Maeda and D.R.Paul, J.Polym. Sci. (1987), 25, 957

64) Y.Maeda and D.R.Paul, J.Polym. Sci. (1987), 25, 981

65) Y.Maeda and D.R.Paul, J.Polym. Sci. (1987), 25, 1005

APPENDIX

Permeability and Diffusivity

T/°C	P/B	$D/cm^2s^{-1}\times10^7$
48.0	13976	6.909
62.3	12647	7.347
72.1	11465	7.671
81.6	10696	7.938
96.9	9751	8.417
113.4	8923	8.623

Table A1 : Permeability and Diffusivity of Acetone in Filled PDMS, p=5.40cmHg.

T/°C	P/B	$D/cm^2s^{-1}\times10^7$
49.4	12279	7.318
63.2	11270	7.774
72.5	10681	8.202
81.7	10219	8.069
96.9	9420	8.455
113.3	8852	8.997

Table A2 : Permeability and Diffusivity of Acetone in Filled PDMS, p=7.59cmHg.

T/°C	P/B	$D/cm^2s^{-1}\times10^7$
49.3	13173	7.803
63.1	11964	8.433
73.0	11114	8.913
82.0	10559	8.896
97.3	9676	9.384
113.5	8957	9.658

Table A3 : Permeability and Diffusivity of Acetone in Filled PDMS, p=9.76cmHg

T/°C	P/B	$D/cm^2s^{-1}\times10^7$
49.1	13043	8.400
62.9	11886	8.779
72.2	11176	9.120
81.0	10571	9.213
97.4	9572	9.954
113.6	8862	10.093

Table A4 : Permeability and Diffusivity of Acetone in Filled PDMS, p=12.14cmHg.

T/°C	P/B	$D/cm^2s^{-1}\times10^7$
49.0	13677	8.509
63.5	12358	8.818
72.1	11535	9.601
82.1	10834	10.159
97.4	9887	9.921
113.4	9145	10.145

Table A5 : Permeability and Diffusivity of Acetone in Filled PDMS, p=15.50cmHg

T/°C	P/B	$D/cm^2s^{-1}\times10^7$
48.8	13605	6.631
63.4	12385	7.284
73.0	11635	7.467
82.1	11025	8.183
97.5	10133	8.267
114.1	9453	8.862

Table A6 : Permeability and Diffusivity of Ethanol in Filled PDMS, p=1.47cmHg.

T/°C	P/B	$D/cm^2s^{-1}\times10^7$
48.7	14395	6.614
62.9	13024	7.310
73.6	12150	7.836
81.1	11585	8.218
97.5	10539	8.338
113.6	9828	8.950

Table A7 : Permeability and Diffusivity of Ethanol in Filled PDMS, p=2.01cmHg.

T/°C	P/B	$D/cm^2s^{-1}\times10^7$
49.0	15876	6.347
63.7	14199	7.096
73.2	13099	7.692
82.0	12261	7.914
97.8	11134	8.715
114.1	10243	9.134

Table A8 : Permeability and Diffusivity of Ethanol in Filled PDMS, p=2.63cmHg

T/°C	P/B	$D/cm^2s^{-1}\times10^7$
48.8	17278	5.848
63.8	15787	6.400
72.8	14987	6.742
83.1	14259	6.713
97.7	13241	7.849
113.0	12368	8.170

Table A9 : Permeability and Diffusivity of Ethanol in Filled PDMS, p=3.78cmHg.

T/°C	P/B	$D/cm^2s^{-1}\times10^7$
49.0	19796	8.190
63.8	17583	8.664
72.6	16294	9.046
82.6	15146	9.488
97.6	13692	9.868
113.0	12549	9.938

Table A10 : Permeability and Diffusivity of Ethanol in Filled PDMS, p=5.66cmHg.

T/°C	P/B	D/$cm^2s^{-1}x10^7$
48.9	15543	1.269
63.4	15303	1.973
72.6	15065	2.450
82.3	14758	3.055
97.6	14228	4.119
113.7	13670	4.859

Table A11 : Permeability and Diffusivity of Tetrachloroethylene in Filled PDMS, p=0.46cmHg.

T/°C	P/B	D/$cm^2s^{-1}x10^7$
49.2	16146	1.249
63.1	15831	1.971
71.9	15569	2.476
82.7	15202	3.079
97.5	14678	4.058
113.8	14058	4.664

Table A12 : Permeability and Diffusivity of Tetrachloroethylene in Filled PDMS, p=0.70cmHg.

T/°C	P/B	D/$cm^2s^{-1}x10^7$
48.6	16815	1.105
63.4	16508	1.751
72.6	16235	2.284
82.2	15928	2.677
97.8	15280	3.488
113.2	14564	3.903

Table A13 : Permeability and Diffusivity of Tetrachloroethylene in Filled PDMS, p=1.08cmHg

T/°C	P/B	$D/cm^2s^{-1}\times10^7$
48.5	17226	1.113
62.8	17029	1.847
71.8	16783	2.358
82.3	16391	2.994
97.1	15753	3.994
114.0	15017	4.806

Table A14 : Permeability and Diffusivity of Tetrachloroethylene in Filled PDMS, p=1.50cmHg.

T/°C	P/B	$D/cm^2s^{-1}\times10^7$
48.1	17941	1.099
63.6	17563	1.924
71.7	17335	2.481
81.1	17033	2.924
96.9	16352	3.858
114.3	15670	4.645

Table A15 : Permeability and Diffusivity of Tetrachloroethylene in Filled PDMS, p=1.95mHg.

T/°C	P/B	$D/cm^2s^{-1}\times10^7$
49.6	17817	1.205
63.9	17532	1.986
72.7	17189	2.517
82.9	16846	3.198
97.5	16218	4.401
114.0	15533	5.106

Table A16 : Permeability and Diffusivity of Tetrachloroethylene in Filled PDMS, p=2.59cmHg

T/°C	P/B	D/$cm^2s^{-1}x10^8$
48.5	17816	1.383
63.8	17717	2.756
72.4	17816	3.488
82.1	18013	4.743
97.6	17914	6.937
113.1	17914	8.479

Table A17 : Permeability and Diffusivity of Nitrobenzene in Filled PDMS, p=0.010cmHg.

T/°C	P/B	D/$cm^2s^{-1}x10^8$
50.7	17511	1.500
63.9	17391	2.642
72.6	17391	3.171
81.7	17391	4.228
97.8	17391	6.137
112.9	17272	7.663

Table A18 : Permeability and Diffusivity of Nitrobenzene in Filled PDMS, p=0.016cmHg.

T/°C	P/B	D/$cm^2s^{-1}x10^8$
50.7	19565	1.621
63.7	19421	2.982
73.3	19421	4.572
82.9	19421	5.716
98.0	19493	9.318
113.5	19421	12.860

Table A19 : Permeability and Diffusivity of Nitrobenzene in Filled PDMS, p=0.026mHg

T/°C	P/B	D/$cm^2s^{-1}\times10^8$
48.0	17568	1.524
63.4	17892	3.142
73.1	17972	5.214
81.6	18216	6.498
97.7	18499	10.130
112.5	18621	15.097

Table A20 : Permeability and Diffusivity of Nitrobenzene in Filled PDMS, p=0.046mHg.

T/°C	P/B	D/$cm^2s^{-1}\times10^8$
49.5	12488	1.766
63.6	13785	3.199
72.9	14841	4.705
81.8	15927	6.576
97.9	16711	10.028
113.1	16892	16.534

Table A21 : Permeability and Diffusivity of Nitrobenzene in Filled PDMS, p=0.062cmHg.

T/°C	P/B	D/$cm^2s^{-1}\times10^8$
49.0	9500	1.657
63.1	10697	3.469
72.3	11408	4.739
82.2	12343	7.652
97.4	13428	11.904
112.9	14737	15.667

Table A22 : Permeability and Diffusivity of Nitrobenzene in Filled PDMS, p=0.10cmHg

T/°C	P/B	D/$cm^2s^{-1}\times10^6$
48.3	22449	2.470
63.0	19335	3.163
72.2	17697	3.555
82.8	16386	3.993
97.5	14747	4.662
112.0	13600	5.229

Table A23 Permeability and Diffusivity of Acetone in Unfilled PDMS, p=6.03cmHg.

T/°C	P/B	D/$cm^2s^{-1}\times10^6$
48.6	23505	2.633
64.7	20016	3.213
73.1	18486	3.673
82.3	17200	4.119
97.6	15425	4.802
113.2	14140	5.238

Table A24 : Permeability and Diffusivity of Acetone in Unfilled PDMS, p=8.07cmHg.

T/°C	P/B	D/$cm^2s^{-1}\times10^6$
47.6	24622	2.989
63.2	21046	3.526
72.1	19466	3.812
81.8	17840	4.244
97.4	15982	4.939
111.9	14727	5.477

Table A25 : Permeability and Diffusivity of Acetone in Unfilled PDMS, p=10.63cmHg

T/°C	P/B	D/$cm^2s^{-1}x10^6$
48.5	26051	2.781
63.3	22133	3.538
72.6	20319	3.961
81.7	18772	4.552
97.4	16690	5.425
112.4	15312	5.914

Table A26 Permeability and Diffusivity of Acetone in Unfilled PDMS, p=13.62cmHg.

T/°C	P/B	D/$cm^2s^{-1}x10^6$
48.2	26906	2.881
63.0	22713	3.657
72.6	20558	4.189
82.1	18927	4.550
97.5	16773	5.232
113.1	15200	6.120

Table A27 : Permeability and Diffusivity of Acetone in Unfilled PDMS, p=16.97cmHg.

T/°C	P/B	D/$cm^2s^{-1}\times10^6$
48.4	24666	2.848
63.3	21926	3.550
72.5	20267	3.947
82.2	18896	4.354
97.4	17274	4.977
113.0	16084	5.426

Table A28 : Permeability and Diffusivity of Ethanol in Unfilled PDMS, p=1.48cmHg.

T/°C	P/B	D/$cm^2s^{-1}\times10^6$
48.3	26131	3.038
63.6	22865	3.539
72.6	21284	3.953
81.7	19914	4.401
97.4	18070	5.061
113.8	16648	5.616

Table A29 : Permeability and Diffusivity of Ethanol in Unfilled PDMS, p=2.02cmHg.

T/°C	P/B	D/$cm^2s^{-1}\times10^6$
48.5	27344	2.922
63.7	23878	3.680
72.5	22106	4.033
82.8	20489	4.481
97.4	18717	5.301
113.5	17215	5.763

Table A30 : Permeability and Diffusivity of Ethanol in Unfilled PDMS, p=2.77cmHg

T/°C	P/B	$D/cm^2s^{-1}\times10^6$
49.0	28736	2.921
63.5	24822	3.539
72.6	22892	3.896
82.2	21230	4.291
97.5	19193	5.070
113.2	17638	5.517

Table A31 : Permeability and Diffusivity of Ethanol in Unfilled PDMS, p=3.97cmHg.

T/°C	P/B	$D/cm^2s^{-1}\times10^6$
48.0	31586	2.867
63.6	26945	3.578
72.2	24849	4.009
81.8	22903	4.500
97.5	20658	5.167
113.5	18862	5.762

Table A32 : Permeability and Diffusivity of Ethanol in Unfilled PDMS, p=5.69cmHg.

T/°C	P/B	D/$cm^2s^{-1}\times10^6$
48.6	45509	0.330
63.4	42546	0.593
72.6	40650	0.751
82.5	38516	1.003
97.4	35317	1.374
113.2	32354	1.714

Table A33 : Permeability and Diffusivity of Tetrachloroethylene in Unfilled PDMS, p=0.48cmHg.

T/°C	P/B	D/$cm^2s^{-1}\times10^6$
49.0	46694	0.333
63.8	43581	0.548
73.0	41558	0.777
82.2	49535	0.953
97.7	36033	1.327
113.6	33309	1.696

Table A34 : Permeability and Diffusivity of Tetrachloroethylene in Unfilled PDMS, p=0.73cmHg.

T/°C	P/B	D/$cm^2s^{-1}\times10^6$
48.6	48887	0.308
63.3	45614	0.521
72.9	43080	0.687
81.8	40757	0.900
97.7	36956	1.268
113.2	33999	1.653

Table A35 : Permeability and Diffusivity of Tetrachloroethylene in Unfilled PDMS, p=1.08cmHg.

T/°C	P/B	D/$cm^2s^{-1}\times10^6$
49.0	51532	0.280
63.3	48000	0.500
72.3	45646	0.663
82.1	43030	0.899
97.6	38976	1.276
112.8	35837	1.766

Table A36 : Permeability and Diffusivity of Tetrachloroethylene in Unfilled PDMS, p=1.75cmHg.

T/°C	P/B	D/$cm^2s^{-1}\times10^6$
48.9	51564	0.260
63.7	47584	0.484
72.9	46200	0.660
82.3	41182	0.873
97.4	37894	1.157
112.6	43951	1.519

Table A37 : Permeability and Diffusivity of Tetrachloroethylene in Unfilled PDMS, p=2.64cmHg.

T/°C	P/B	$D/cm^2s^{-1}\times10^8$
50.4	55332	0.473
68.0	54578	0.961
77.7	54427	1.536
85.9	54276	2.054
97.7	53522	2.941
115.9	51563	4.324

Table A38 Permeability and Diffusivity of Nitrobenzene in Unfilled PDMS, p=0.010cmHg.

T/°C	P/B	$D/cm^2s^{-1}\times10^8$
56.9	54184	0.500
68.2	54184	1.079
77.1	53070	1.489
86.4	52885	1.926
97.5	52885	2.595
116.1	51586	3.830

Table A39 : Permeability and Diffusivity of Nitrobenzene in Unfilled PDMS, p=0.016cmHg.

T/°C	P/B	$D/cm^2s^{-1}\times10^8$
56.2	56255	0.659
68.7	56560	1.190
77.4	56059	1.704
86.8	55058	2.645
97.9	54057	3.572
116.5	53056	6.201

Table A40 : Permeability and Diffusivity of Nitrobenzene in Unfilled PDMS, p=0.035cmHg

T/°C	P/B	D/$cm^2s^{-1}\times10^8$
52.0	46897	0.552
67.9	53078	1.200
77.5	53805	1.817
86.3	53260	2.569
97.6	52532	4.005
118.2	50896	6.791

Table A41 Permeability and Diffusivity of Nitrobenzene in Unfilled PDMS, p=0.064cmHg.

T/°C	P/B	D/$cm^2s^{-1}\times10^8$
52.0	29922	0.416
67.6	34966	1.071
77.8	38520	1.761
86.6	40928	2.486
97.6	44367	3.821
117.9	47462	5.845

Table A42 : Permeability and Diffusivity of Nitrobenzene in Unfilled PDMS, p=0.10cmHg.

T/°C	P/B	$D/cm^2s^{-1}\times10^6$
47.7	28932	5.177
62.9	24481	6.633
71.8	22256	7.506
82.0	20386	8.878
97.1	18072	10.450
113.4	16469	11.467

Table A43 : Permeability and Diffusivity of Acetone in Ester-substituted Polysiloxane, p=5.60cmHg.

T/°C	P/B	$D/cm^2s^{-1}\times10^6$
48.7	30657	5.418
64.1	25547	6.588
72.3	23478	7.792
82.0	21408	8.934
97.6	18886	10.780
113.3	17204	12.228

Table A44 : Permeability and Diffusivity of Acetone in Ester-substituted Polysiloxane, p=7.71cmHg.

T/°C	P/B	$D/cm^2s^{-1}\times10^6$
48.5	32822	5.300
62.9	27233	6.743
72.6	24693	8.031
82.9	22355	9.241
97.7	19713	10.935
112.8	17884	12.053

Table A45 : Permeability and Diffusivity of Acetone in Ester-substituted Polysiloxane, p=9.81cmHg

T/°C	P/B	$D/cm^2s^{-1}x10^6$
48.5	33238	5.482
63.8	27268	6.793
72.6	24686	7.972
82.4	22427	9.117
97.5	19604	10.568
114.1	17664	12.377

Table A46 : Permeability and Diffusivity of Acetone in Ester-substituted Polysiloxane, p=12.36cmHg.

T/°C	P/B	$D/cm^2s^{-1}x10^6$
48.3	35760	5.473
63.6	29000	6.970
72.8	26030	7.895
82.3	23630	8.997
97.5	20471	10.756
114.3	18386	12.654

Table A47 : Permeability and Diffusivity of Acetone in Ester-substituted Polysiloxane, p=15.78cmHg.

T/°C	P/B	$D/cm^2s^{-1}\times10^6$
48.7	33568	6.474
63.4	29078	7.972
73.0	26513	9.204
82.5	24660	10.847
97.5	22094	12.591
113.6	20383	13.648

Table A48 Permeability and Diffusivity of Ethanol in Ester-substituted Polysiloxane, p=1.51cmHg.

T/°C	P/B	$D/cm^2s^{-1}\times10^6$
49.0	33731	6.680
63.8	28957	8.454
73.0	26721	9.514
82.1	24791	10.809
97.6	22251	12.731
113.5	20473	14.244

Table A49 : Permeability and Diffusivity of Ethanol in Ester-substituted Polysiloxane, p=2.12cmHg.

T/°C	P/B	$D/cm^2s^{-1}\times10^6$
49.0	34650	6.721
63.4	29768	8.328
72.3	27405	9.347
81.4	25358	10.450
97.6	22759	12.506
114.0	20790	14.217

Table A50 : Permeability and Diffusivity of Ethanol in Ester-substituted Polysiloxane, p=2.73cmHq

T/°C	P/B	D/$cm^2s^{-1}\times10^6$
49.0	35705	6.686
63.5	30480	8.298
73.0	27758	9.334
82.1	25690	10.881
97.6	23404	12.608
113.4	21188	13.972

Table A51 : Permeability and Diffusivity of Ethanol in Ester-substituted Polysiloxane, p=3.95cmHg.

T/°C	P/B	D/$cm^2s^{-1}\times10^6$
48.6	40785	6.231
63.0	33987	8.031
72.5	30815	9.567
81.6	28290	10.437
97.3	25000	12.284
113.0	22809	14.049

Table A52 : Permeability and Diffusivity of Ethanol in Ester-substituted Polysiloxane, p=5.69cmHg.

T/°C	P/B	$D/cm^2s^{-1}x10^6$
49.5	79983	0.881
63.5	72824	1.345
72.5	67640	1.885
81.9	62209	2.285
97.8	55173	3.164
114.0	49002	3.997

Table A53 : Permeability and Diffusivity of Tetrachloroethylene in Ester-substituted Polysiloxane, p=0.47cmHg.

T/°C	P/B	$D/cm^2s^{-1}x10^6$
50.0	80552	0.838
63.8	72562	1.354
73.0	67344	1.750
82.8	61800	2.259
97.8	54462	3.142
114.4	47940	4.255

Table A54 Permeability and Diffusivity of Tetrachloroethylene in Ester-substituted Polysiloxane p=0.71cmHg.

T/°C	P/B	$D/cm^2s^{-1}x10^6$
49.0	86887	0.763
64.0	76715	1.302
72.8	70993	1.719
82.8	64847	2.192
97.8	56794	3.073
113.4	50013	3.829

Table A55 : Permeability and Diffusivity of Tetrachloroethylene in Ester-substituted Polysiloxane,p=1.09cmHg

T/°C	P/B	D/$cm^2s^{-1}\times10^6$
49.2	91849	0.755
63.6	81117	1.064
73.3	73858	1.695
82.4	67861	2.101
97.8	58707	3.015
113.9	51290	4.003

Table A56 : Permeability and Diffusivity of Tetrachloroethylene in Ester-substituted Polysiloxane, p=1.46cmHg

T/°C	P/B	D/$cm^2s^{-1}\times10^6$
49.2	96248	0.701
64.3	83951	1.222
73.2	77329	1.686
81.9	71181	2.098
97.6	61012	2.932
112.9	53209	3.614

Table A57 : Permeability and Diffusivity of Tetrachloroethylene in Ester-substituted Polysiloxane, p=1.95cmHg

T/°C	P/B	D/$cm^2s^{-1}\times10^6$
49.0	98648	0.643
63.5	86631	1.203
72.8	79636	1.628
82.6	72821	2.108
97.6	63135	3.030
113.9	54705	3.950

Table A58 : Permeability and Diffusivity of Tetrachloroethylene in Ester-substituted Polysiloxane, p=2.57cmHg

T/°C	P/B	D/$cm^2s^{-1}x10^7$
52.7	115674	1.383
69.8	114973	3.241
77.3	112899	4.686
87.1	110299	6.563
97.6	107027	9.105
117.5	99316	13.427

Table A59 : Permeability and Diffusivity of Nitrobenzene in Ester-substituted Polysiloxane, p=0.010cmHg

T/°C	P/B	D/$cm^2s^{-1}x10^7$
50.3	114771	1.383
67.5	114771	3.176
78.0	112405	4.755
86.3	110334	6.056
97.7	107376	8.785
117.0	99981	13.366

Table A60 : Permeability and Diffusivity of Nitrobenzene in Ester-substituted Polysiloxane, p=0.016cmHg

T/°C	P/B	D/$cm^2s^{-1}x10^7$
52.5	112515	1.643
67.3	112861	3.261
77.8	112168	5.312
86.4	110437	7.232
97.5	106629	11.001
118.1	99013	18.955

Table A61 : Permeability and Diffusivity of Nitrobenzene in Ester-substituted Polysiloxane, p=0.027cmHg

T/°C	P/B	D/$cm^2s^{-1}\times10^7$
50.7	112742	1.456
59.6	113972	2.199
75.0	113972	4.697
86.3	111922	7.171
97.6	108642	10.744
116.2	101263	17.075

Table A62 : Permeability and Diffusivity of Nitrobenzene in Ester-substituted Polysiloxane, p=0.046cmHg.

T/°C	P/B	D/$cm^2s^{-1}\times10^7$
50.7	84845	1.414
68.1	99226	3.454
77.4	103540	5.193
86.7	106416	7.326
97.9	106991	11.210
116.8	102390	16.920

Table A63 : Permeability and Diffusivity of Nitrobenzene in Ester-substituted Polysiloxane, p=0.065cmHg.

T/°C	P/B	D/$cm^2s^{-1}\times10^7$
51.2	60156	1.408
65.0	64784	2.923
74.2	68486	4.651
82.9	70337	7.133
97.7	73668	11.351
116.9	76815	18.662

Table A64 : Permeability and Diffusivity of Nitrobenzene in Ester-substituted Polysiloxane, p=0.01cmHg

Variation of Transport Properties

with Permeant Pressure

Vapour Pressure /cmHg	Activation Energy for Permeation /kJmol^{-1} 50°C	110°C	Permeability at 90°C /B	Activation Energy for Diffusion /kJmol^{-1} 50°C	110°C	Diffusivity at 90°C /cm^{2}s^{-1} x10^7
5.40	-8.5	-6.3	10209	4.8	2.4	8.24
7.59	-5.4	-4.8	9750	4.2	1.8	8.53
9.76	-6.6	-5.9	10087	5.0	1.9	9.24
12.14	-6.8	-5.5	9967	3.8	2.2	9.56
15.50	-7.4	-5.8	10311	4.2	2.0	9.88

Table A65 : Variation of Transport Properties with Permeant Pressure for Acetone in Filled PDMS.

Vapour Pressure /cmHg	Activation Energy for Permeation /kJmol^{-1} 50°C	110°C	Permeability at 90 C /B	Activation Energy for Diffusion /kJmol^{-1} Average	Diffusivity at 90 C /cm^{2}s^{-1} $\times 10^6$
6.03	-10.4	-5.9	15429	12.0	4.37
8.07	-9.2	-6.9	16236	11.4	4.41
10.63	-9.4	-6.5	16831	9.9	4.71
13.62	-9.8	-6.7	17571	12.4	4.89
16.97	-10.8	-6.7	17694	11.7	5.03

Table A66 : Variation of Transport Properties with Permeant Pressure for Acetone in Unfilled PDMS.

Vapour Pressure /cmHg	Activation Energy for Permeation /kJmol^{-1} 50°C	110°C	Permeability at 90°C /B	Activation Energy for Diffusion /kJmol^{-1} 50°C	110°C	Diffusivity at 90°C /cm^{2}s^{-1} $\times 10^6$
5.60	-11.6	-6.9	19092	17.8	8.9	9.47
7.71	-12.1	-7.1	20030	18.6	9.1	9.82
9.81	-13.1	-7.6	20889	18.6	9.4	9.99
12.36	-13.1	-7.6	20848	18.6	9.4	9.99
15.78	-14.3	-7.9	22049	18.1	9.1	10.19

Table A67 : Variation of Transport Properties with Permeant Pressure for Acetone in Ester-substituted Polysiloxane.

Vapour Pressure /cmHg	Activation Energy for Permeation /kJmol^{-1} 50°C	110°C	Permeability at 90°C /B	Activation Energy for Diffusion /kJmol^{-1} 50°C	110°C	Diffusivity at 90°C /cm^{2}s^{-1} $\times 10^7$
1.47	-6.5	-5.3	10541	5.5	3.4	8.15
2.01	-6.8	-5.8	11026	6.4	3.6	8.26
2.63	-8.5	-6.2	11696	7.9	4.3	8.32
3.78	-5.9	-5.0	13630	7.1	4.2	7.40
5.66	-8.2	-6.7	14415	5.2	1.0	9.62

Table A68 : Variation of Transport Properties with Permeant Pressure for Ethanol in Filled PDMS.

Vapour Pressure /cmHg	Activation Energy for Permeation /kJmol^{-1} 50°C	110°C	Permeability at 90°C /B	Activation Energy for Diffusion /kJmol^{-1} 50°C	110°C	Diffusivity at 90°C /cm^{2}s^{-1} $\times 10^6$
1.48	-7.8	-6.0	18088	15.8	7.1	4.66
2.02	-8.4	-6.0	18883	15.0	6.9	4.77
2.77	-8.6	-6.3	19575	16.7	7.6	4.93
3.97	-9.7	-6.5	20070	16.7	7.1	4.70
5.69	-10.4	-8.0	21590	14.9	7.6	4.86

Table A69 : Variation of Transport Properties with Permeant Pressure for Ethanol in Unfilled PDMS.

Vapour Pressure /cmHg	Activation Energy for Permeation /kJmol^{-1} 50°C	110°C	Permeability at 90°C /B	Activation Energy for Diffusion /kJmol^{-1} 50°C	110°C	Diffusivity at 90°C /cm^{2}s^{-1} $\times 10^5$
1.51	-9.2	-6.1	23179	17.2	8.8	1.12
2.12	-11.5	-6.1	23342	17.8	9.0	1.18
2.73	-11.2	-6.3	23885	17.8	9.3	1.16
3.95	-12.1	-6.4	24197	17.8	9.3	1.15
5.69	-13.4	-6.8	26370	19.9	9.3	1.15

Table A70 : Variation of Transport Properties with Permeant Pressure for Ethanol in Ester-substituted Polysiloxane.

Vapour Pressure /cmHg	Activation Energy for Permeation /kJmol^{-1} 50°C	110°C	Permeability at 90°C /B	Activation Energy for Diffusion /kJmol^{-1} 50°C	110°C	Diffusivity at 90°C /cm^{2}s^{-1} x10^7
0.46	-0.9	-3.1	14472	30.8	14.6	3.55
0.70	-0.9	-3.2	14958	34.1	12.2	3.47
1.08	-0.8	-3.6	15537	33.0	14.3	2.96
1.50	-0.2	-3.5	16027	38.5	13.0	3.35
1.95	-0.6	-3.2	16664	38.3	16.7	3.47
2.64	-0.5	-3.2	16564	38.9	16.2	3.64

Table A71 : Variation of Transport Properties with Permeant Pressure for Tetrachloroethylene in Filled PDMS.

Vapour Pressure /cmHg	Activation Energy for Permeation /kJmol^{-1} 50°C	110°C	Permeability at 90°C /B	Activation Energy for Diffusion /kJmol^{-1} 50°C	110°C	Diffusivity at 90°C /cm^{2}s^{-1} $\times 10^6$
0.48	-3.4	-7.3	36975	35.3	19.1	1.16
0.73	-4.2	-7.3	37911	37.8	19.6	1.14
1.08	-3.8	-7.7	39105	37.0	19.6	1.08
1.75	-4.2	-7.9	41069	42.0	20.7	1.10
2.64	-3.7	-6.3	42531	55.2	19.0	1.02

Table A72 : Variation of Transport Properties with Permeant Pressure for Tetrachloroethylene in Unfilled PDMS.

Vapour Pressure /cmHg	Activation Energy for Permeation /kJmol^{-1} 50°C	110°C	Permeability at 90°C /B	Activation Energy for Diffusion /kJmol^{-1} 50°C	110°C	Diffusivity at 90°C /cm^{2}s^{-1} $\times 10^6$
0.47	-6.0	-8.9	58806	31.9	17.8	2.65
0.71	-6.5	-9.3	58396	35.9	18.6	2.72
1.09	-7.4	-10.1	60779	36.1	19.2	2.55
1.46	-8.1	-10.2	63007	38.5	19.3	2.48
1.95	-8.0	-10.8	65644	35.7	19.3	2.44
2.57	-8.1	-10.7	68323	42.5	20.5	2.48

Table A73 : Variation of Transport Properties with Permeant Pressure for Tetrachloroethylene in Ester-substituted Polysiloxane.

Vapour Pressure /cmHg	Activation Energy for Permeation /kJmol^{-1} 60°C	110°C	Permeability at 60°C /B	Permeability at 110°C /B
0.010	0.1	0.1	17836	17783
0.016	-0.2	-0.2	17257	17430
0.026	-0.1	-0.1	19438	19497
0.046	0	0	18527	17694
0.064	7.2	-0.4	16950	13616
0.10	7.2	6.4	14487	10457

Table A74 : Variation of Permeability with Permeant Pressure at 60°C and 110°C for Nitrobenzene in Filled PDMS.

Vapour Pressure /cmHg	Activation Energy for Permeation /kJmol^{-1} 60°C	110°C	Permeability at 60°C /B	Permeability at 110°C /B
0.010	-0.4	-2.1	52052	55050
0.016	-0.1	-1.7	51792	54068
0.036	1.1	-0.5	53370	55715
0.064	-2.2	4.5	51586	51586
0.10	3.7	13.2	46490	31226

Table A75 : Variation of Permeability with Permeant Pressure at 60°C and 110°C for Nitrobenzene in Unfilled PDMS.

Vapour Pressure /cmHg	Activation Energy for Permeation /kJmol^{-1} 60°C	110°C	Permeability at 60°C /B	Permeability at 110°C /B
0.010	-0.7	-4.9	101519	115844
0.016	0	-4.9	102028	114920
0.027	0.4	-4.9	101215	113210
0.046	0.8	-4.5	102847	114119
0.065	7.6	-3.0	105451	93340
0.10	5.6	2.4	75433	63895

Table A76 : Variation of Permeability with Permeant Pressure at 60°C and 110°C for Nitrobenzene in Ester-substituted Polysiloxane.

Vapour Pressure /cmHg	Activation Energy for Diffusion /kJmol^{-1} 60°C	110°C	Diffusivity at 90°C /cm^{2}s^{-1} $\times 10^8$
0.010	37.1	19.0	5.92
0.016	32.3	20.1	5.00
0.026	41.2	24.6	7.60
0.046	43.8	25.3	8.42
0.062	44.3	25.2	8.92
0.10	45.2	25.8	9.40

Table A77 : Variation of Diffusivity with Permeant Pressure for Nitrobenzene in Filled PDMS.

Vapour Pressure /cmHg	Activation Energy for Diffusion /kJmol^{-1} 50°C	110°C	Diffusivity at 90°C /cm^{2}s^{-1} $\times 10^7$
0.010	43.1	27.2	2.32
0.016	55.4	25.4	2.17
0.035	49.2	30.1	2.92
0.064	49.2	30.1	2.80
0.10	52.1	31.7	3.09

Table A78 : Variation of Diffusivity with Permeant Pressure for Nitrobenzene in Unfilled PDMS.

Vapour Pressure /cmHg	Activation Energy for Diffusion /kJmol^{-1} 60°C	110°C	Diffusivity at 90°C /cm^{2}s^{-1} $\times 10^7$
0.010	44.0	26.4	7.02
0.016	44.0	26.4	7.02
0.027	47.1	31.2	8.32
0.046	50.5	28.7	8.46
0.065	50.5	28.7	8.32
0.10	52.7	29.4	9.05

Table A79 : Variation of Diffusivity with Permeant Pressure for Nitrobenzene in Ester-substituted Polysiloxane.

Solubility

Table A80 : Solubility of Acetone in Filled PDMS at Various Permeant Pressures.

T/ °C	Solubility $cm^3(STP)/cm^3cmHg$	T/ °C	Solubility $cm^3(STP)/cm^3cmHg$
p=5.40cmHg		p=12.14cmHg	
48.0	2.02	49.1	1.55
62.3	1.72	62.9	1.35
72.1	1.49	72.2	1.23
81.6	1.35	81.0	1.15
96.9	1.16	97.4	0.96
113.4	1.03	113.6	0.88
p=7.59cmHg		p=15.50cmHg	
49.4	1.68	49.0	1.61
63.2	1.45	63.5	1.40
72.5	1.30	72.1	1.20
81.7	1.27	82.1	1.07
96.9	1.11	97.4	1.00
113.3	0.98	113.4	0.90
p=9.76cmHg			
49.3	1.69		
63.1	1.42		
73.0	1.25		
82.0	1.19		
97.3	1.03		
113.5	0.93		

Table A81 : Solubility of Ethanol in Filled PDMS at Various Permeant Pressures.

T/ °C	Solubility $cm^3(STP)/cm^3cmHg$	T/ °C	Solubility $cm^3(STP)/cm^3cmHg$
p=1.47cmHg		p=3.78cmHg	
48.8	2.05	48.8	2.95
63.4	1.70	63.8	2.47
73.0	1.56	72.8	2.22
82.1	1.35	83.1	2.12
97.5	1.23	97.7	1.69
114.1	1.07	113.0	1.51
p=2.01cmHg		p=5.66cmHg	
48.7	2.18	49.0	2.42
62.9	1.78	63.8	2.03
73.6	1.55	72.6	1.80
81.1	1.41	82.6	1.60
97.5	1.26	97.6	1.39
113.6	1.10	113.0	1.26
p=2.63cmHg			
49.0	2.50		
63.7	2.00		
73.2	1.70		
82.0	1.55		
97.8	1.28		
114.1	1.12		

Table A82 : Solubility of Tetrachloroethylene in Filled PDMS at Various Permeant Pressures.

T/ °C	Solubility $cm^3(STP)/cm^3cmHg$	T/ °C	Solubility $cm^3(STP)/cm^3cmHg$
p=0.46cmHg		p=1.50cmHg	
48.9	12.25	48.5	15.48
63.4	7.76	62.8	9.22
72.6	6.15	71.8	7.12
82.3	4.83	82.3	5.47
97.6	3.45	97.1	3.94
113.7	2.81	114.0	3.12
p=0.70cmHg		p=1.95cmHg	
49.2	12.93	48.1	16.32
63.1	8.03	63.6	9.13
71.9	6.29	71.7	6.99
82.7	4.94	81.1	5.83
97.5	3.62	96.9	4.24
113.8	3.01	114.3	3.37
p=1.08cmHg		p=2.59cmHg	
48.6	15.22	49.6	14.79
63.4	9.43	63.9	8.83
72.6	7.11	72.7	6.83
82.2	5.95	81.1	5.27
97.8	4.38	97.5	3.69
113.2	3.73	114.0	3.04

Table A83 : Solubility of Nitrobenzene in Filled PDMS at Various Permeant Pressures.

T/ °C	Solubility $cm^3(STP)/cm^3cmHg$	T/ °C	Solubility $cm^3(STP)/cm^3cmHg$
p=0.010cmHg		p=0.046cmHg	
48.5	128.82	48.0	115.28
63.8	64.29	63.4	54.94
72.4	51.08	73.1	34.47
82.1	37.98	81.6	28.03
97.6	25.82	97.7	18.26
113.1	21.13	112.5	12.32
p=0.016cmHg		p=0.062cmHg	
50.7	116.74	49.5	70.71
63.9	65.83	63.6	43.09
72.6	54.84	72.9	31.54
81.7	41.13	81.8	24.21
97.8	28.34	97.9	16.66
112.9	22.54	113.1	10.22
p=0.026cmHg		p=0.01cmHg	
50.7	120.70	49.0	57.83
63.7	65.13	63.1	30.84
73.3	42.48	72.3	24.07
82.9	33.98	82.2	16.13
98.0	20.92	97.4	11.28
113.5	15.10	112.9	9.41

Table A84 : Solubility of Acetone in Unfilled PDMS at Various Permeant Pressures.

T/ °C	Solubility $cm^3(STP)/cm^3cmHg$	T/ °C	Solubility $cm^3(STP)/cm^3cmHg$
p=6.03cmHg		p=13.62cmHg	
48.3	0.909	48.5	0.937
63.0	0.611	63.3	0.626
72.2	0.498	72.6	0.513
82.8	0.410	81.7	0.411
97.5	0.319	97.4	0.308
112.0	0.260	112.4	0.259
p=8.07cmHg		p=16.97cmHg	
48.6	0.893	48.2	0.934
64.7	0.623	63.0	0.621
73.1	0.503	72.6	0.491
82.3	0.418	82.1	0.416
97.6	0.321	97.5	0.321
113.2	0.270	113.1	0.248
p=10.63cmHg			
47.6	0.824		
63.2	0.597		
72.1	0.511		
81.8	0.420		
92.4	0.324		
111.9	0.269		

Table A85 : Solubility of Ethanol in Unfilled PDMS at Various Permeant Pressures.

T/ °C	Solubility $cm^3(STP)/cm^3cmHg$	T/ °C	Solubility $cm^3(STP)/cm^3cmHg$
p=1.48cmHg		p=3.97cmHg	
48.4	0.866	49.0	0.984
63.3	0.618	63.5	0.701
72.5	0.513	72.6	0.588
82.2	0.434	82.2	0.495
97.4	0.347	97.5	0.379
113.0	0.296	113.2	0.320
p=2.02cmHg		p=5.69cmHg	
48.3	0.860	48.0	1.102
63.6	0.646	63.6	0.753
72.6	0.538	72.2	0.620
81.7	0.452	81.8	0.509
97.4	0.357	97.5	0.400
113.8	0.296	113.5	0.327
p=2.77cmHg			
48.5	0.936		
63.7	0.649		
72.5	0.548		
82.8	0.457		
97.4	0.353		
113.5	0.299		

Table A86 : Solubility of Tetrachloroethylene in Unfilled PDMS at Various Permeant Pressures.

T/ °C	Solubility $cm^3(STP)/cm^3cmHg$	T/ °C	Solubility $cm^3(STP)/cm^3cmHg$
p=0.48cmHg		p=1.75cmHg	
48.6	13.79	49.0	18.40
63.4	7.17	63.3	9.60
72.6	5.41	72.3	6.88
82.5	3.84	82.1	4.79
97.4	2.57	97.6	3.05
113.2	1.89	112.8	2.03
p=0.73cmHg		p=2.64cmHg	
49.0	14.02	48.9	19.83
63.8	7.95	63.7	9.83
73.0	5.35	72.9	7.00
82.2	4.15	82.3	4.72
97.7	2.72	97.4	3.28
113.6	1.96	112.6	2.89
p=1.08cmHg			
48.6	15.87		
63.3	8.76		
72.9	6.27		
81.8	4.53		
97.7	2.91		
113.2	2.06		

Table A87 : Solubility of Nitrobenzene in Unfilled PDMS at Various Permeant Pressures.

T/ °C	Solubility $cm^3(STP)/cm^3cmHg$	T/ °C	Solubility $cm^3(STP)/cm^3cmHg$
p=0.010cmHg		p=0.064cmHg	
50.4	116.98	52.0	84.96
68.0	56.79	67.9	44.23
77.7	35.43	77.5	22.61
85.9	26.42	86.3	20.52
97.7	18.20	97.6	13.12
115.9	11.92	118.2	7.49
p=0.016cmHg		p=0.10cmHg	
56.9	108.37	52.0	71.93
68.2	50.22	67.6	32.65
77.1	35.64	77.8	21.87
86.4	27.46	86.6	16.46
97.5	20.38	97.6	11.61
113.1	13.47	117.9	8.12
p=0.035cmHg			
56.2	83.85		
68.7	47.53		
77.4	32.90		
86.8	20.82		
97.9	15.13		
116.5	8.56		

Table A88 : Solubility of Acetone in Ester-substituted Polysiloxane at Various Permeant Pressures.

T/ °C	Solubility $cm^3(STP)/cm^3cmHg$	T/ °C	Solubility $cm^3(STP)/cm^3cmHg$
p=5.60cmHg		p=12.36cmHg	
47.7	0.559	48.5	0.606
62.9	0.369	63.8	0.401
71.8	0.297	72.6	0.310
82.0	0.230	82.4	0.246
97.1	0.173	97.5	0.186
113.4	0.144	114.1	0.143
p=7.71cmHg		p=15.78cmHg	
48.7	0.566	48.3	0.653
64.1	0.388	63.6	0.416
72.3	0.301	72.8	0.330
82.0	0.240	82.3	0.263
97.6	0.175	97.5	0.190
113.3	0.141	114.3	0.145
p=9.81cmHg			
48.5	0.619		
62.9	0.404		
72.6	0.307		
82.9	0.242		
97.7	0.180		
112.8	0.148		

Table A89 : Solubility of Ethanol in Ester-substituted Polysiloxane at Various Permeant Pressures.

T/ °C	Solubility $cm^3(STP)/cm^3cmHg$	T/ °C	Solubility $cm^3(STP)/cm^3cmHg$
p=1.51cmHg		p=3.95cmHg	
48.7	0.519	49.0	0.534
63.4	0.365	63.5	0.367
73.0	.0288	73.0	0.297
82.5	0.227	82.1	0.236
97.5	0.175	97.6	0.186
113.6	0.149	113.4	0.151
p=2.12cmHg		p=5.69cmHg	
49.0	0.505	48.6	0.655
63.8	0.343	63.0	0.423
73.0	0.281	72.5	0.322
82.1	0.229	81.6	0.271
97.6	0.175	97.3	0.204
113.5	0.144	113.0	0.162
p=2.73cmHg			
49.0	0.516		
63.4	0.357		
72.3	0.293		
81.4	0.243		
97.6	0.182		
114.0	0.146		

Table A90 : Solubility of Tetrachloroethylene in Ester-substituted Polysiloxane at Various Permeant Pressures.

T/ °C	Solubility $cm^3(STP)/cm^3cmHg$	T/ °C	Solubility $cm^3(STP)/cm^3cmHg$
p=0.47cmHg		p=1.46cmHg	
49.5	9.08	49.2	12.17
63.5	5.41	63.6	7.62
72.5	3.65	73.3	4.36
81.9	2.72	82.4	3.23
97.8	1.74	97.8	1.95
114.0	1.23	113.9	1.28
p=0.71cmHg		p=1.95cmHg	
50.0	9.64	49.2	13.73
63.8	5.36	64.3	6.87
73.0	3.85	73.2	4.59
82.8	2.74	81.9	3.39
97.8	1.73	97.6	2.08
114.4	1.13	112.9	1.47
p=1.09cmHg		p=2.57cmHg	
49.0	11.39	49.0	15.34
64.0	5.89	63.5	7.20
72.8	4.13	72.8	4.89
82.8	2.96	82.6	3.45
97.8	1.85	97.6	2.08
113.4	1.31	113.9	1.38

Table A91 : Solubility of Nitrobenzene in Ester-substituted Polysiloxane at Various Permeant Pressures.

T/ °C	Solubility $cm^3(STP)/cm^3cmHg$	T/ °C	Solubility $cm^3(STP)/cm^3cmHg$
p=0.010cmHg		p=0.046cmHg	
52.7	83.64	50.7	77.43
69.8	35.47	59.6	51.83
77.3	24.09	75.0	24.26
87.1	16.81	86.3	15.60
97.6	11.75	97.6	10.11
117.5	7.40	116.2	5.93
p=0.016cmHg		p=0.065cmHg	
50.3	82.99	50.7	60.00
67.5	36.14	68.1	28.73
78.0	23.64	77.4	19.94
86.3	18.22	86.7	14.53
97.7	12.22	97.9	9.54
117.0	7.48	116.8	6.05
p=0.027cmHg		p=0.01cmHg	
52.5	68.48	51.2	42.72
67.3	34.61	65.0	22.16
77.8	21.11	74.2	14.73
86.4	15.27	82.9	9.86
97.5	9.69	97.7	6.49
118.1	5.22	116.9	4.12

Variation of Solubility

with Permeant Pressure

Variation of Solubility with Permeant Pressure for Acetone in Polysiloxanes.

Vapour Pressure /cmHg	Heat of Solution/kJmol^{-1} 50°C	110°C	Solubility at 90°C /cm^3(STP)/cm^{3}cmHg
5.40	-13.3	-8.4	1.24
7.59	-9.6	-6.6	1.14
9.76	-11.6	-7.8	1.09
12.14	-10.6	-7.7	1.04
15.50	-11.6	-7.8	1.04

Table A92 : Filled PDMS.

Vapour Pressure /cmHg	Heat of Solution/kJmol^{-1} 50°C	110°C	Solubility at 90°C /cm^3(STP)/cm^{3}cmHg
6.03	-28.3	-14.9	0.353
8.07	-23.9	-15.4	0.368
10.63	-22.1	-13.8	0.357
13.62	-25.7	-15.6	0.359
16.97	-27.3	-15.3	0.352

Table A93 : Unfilled PDMS.

Vapour Pressure /cmHg	Heat of Solution/kJmol^{-1} 50°C	110°C	Solubility at 90°C /cm^3(STP)/cm^{3}cmHg
5.60	-29.4	-15.8	0.202
7.71	-30.7	-16.2	0.204
9.81	-31.7	-17.0	0.209
12.36	-31.7	-17.0	0.209
15.78	-32.4	-17.0	0.216

Table A94 : Ester-substituted Polysiloxane.

Variation of Solubility with Permeant Pressure for Ethanol in Polysiloxanes.

Vapour Pressure /cmHg	Heat of Solution/kJmol^{-1} 50°C	110°C	Solubility at 90°C /cm^3(STP)/cm^{3}cmHg
1.48	-12.0	-8.7	1.29
2.01	-13.2	-9.4	1.33
2.63	-16.4	-10.5	1.41
3.78	-13.0	-9.2	1.84
5.66	-13.4	-7.7	1.50

Table A95 : Filled PDMS.

Vapour Pressure /cmHg	Heat of Solution/kJmol^{-1} 50°C	110°C	Solubility at 90°C /cm^3(STP)/cm^{3}cmHg
1.48	-23.6	-13.1	0.388
2.02	-23.4	-12.9	0.397
2.77	-25.3	-13.9	0.397
3.97	-26.4	-13.6	0.427
5.69	-25.3	-15.6	0.444

Table A96 : Unfilled PDMS.

Vapour Pressure /cmHg	Heat of Solution/kJmol^{-1} 50°C	110°C	Solubility at 90°C /cm^3(STP)/cm^{3}cmHg
1.51	-26.4	-14.9	0.207
2.12	-29.3	-15.1	0.198
2.73	-29.0	-15.6	0.206
3.95	-29.9	-15.7	0.210
5.69	-33.3	-16.1	0.229

Table A97 : Ester-substituted Polysiloxane.

Variation of Solubility with Permeant Pressure for Tetrachloroethylene in Polysiloxanes.

Vapour Pressure /cmHg	Heat of Solution/kJmol^{-1} 50°C	110°C	Solubility at 90°C /cm^3(STP)/cm^{3}cmHg
0.46	-31.7	-17.7	4.08
0.70	-35.0	-15.4	4.31
1.08	-33.8	-17.9	5.25
1.50	-38.7	-16.5	4.78
1.95	-38.9	-19.9	4.80
2.64	-39.4	-19.4	4.55

Table A98 : Filled PDMS.

Vapour Pressure /cmHg	Heat of Solution/kJmol^{-1} 50°C	110°C	Solubility at 90°C /cm^3(STP)/cm^{3}cmHg
0.48	-38.7	-26.4	3.19
0.71	-42.0	-26.9	3.33
1.08	-40.8	-27.3	3.62
1.75	-46.2	-28.6	3.73
2.64	-58.9	-25.3	4.17

Table A99 : Unfilled PDMS.

Vapour Pressure /cmHg	Heat of Solution/kJmol^{-1} 50°C	110°C	Solubility at 90°C /cm^3(STP)/cm^{3}cmHg
0.47	-37.9	-26.7	2.22
0.71	-42.4	-27.9	2.15
1.09	-43.5	-29.3	2.38
1.46	-46.6	-29.5	2.54
1.95	-47.7	-30.1	2.69
2.57	-50.6	-31.2	2.75

Table A100 : Ester-substituted Polysiloxane.

Variation of Solubility with Permeant Pressure for Nitrobenzene in Polysiloxanes.

Vapour Pressure /cmHg	Heat of Solution/kJmol^{-1} 60°C	110°C	Solubility at 90°C /cm^3(STP)/cm^{3}cmHg
0.010	-37.0	-18.9	30.13
0.016	-32.5	-20.3	34.69
0.026	-41.3	-24.7	25.65
0.046	-43.8	-25.3	21.68
0.062	-37.1	-25.6	18.38
0.10	-38.1	-19.4	13.73

Table A101 : Filled PDMS.

Vapour Pressure /cmHg	Heat of Solution/kJmol^{-1} 60°C	110°C	Solubility at 90°C /cm^3(STP)/cm^{3}cmHg
0.010	-45.0	-29.3	23.17
0.016	-55.5	-27.1	24.52
0.035	-50.3	-30.6	18.91
0.064	-51.4	-25.6	19.00
0.10	-38.9	-28.0	13.71

Table A102 : Unfilled PDMS.

Vapour Pressure /cmHg	Heat of Solution/kJmol^{-1} 60°C	110°C	Solubility at 90°C /cm^3(STP)/cm^{3}cmHg
0.010	-44.7	-31.3	15.53
0.016	-44.0	-31.3	15.57
0.027	-46.7	-36.1	13.07
0.046	-49.7	-33.2	13.01
0.065	-42.9	-31.7	12.87
0.10	-47.1	-27.0	8.00

Table A103 : Ester-substituted Polysiloxane.

Arrhenius Plots for Permeation

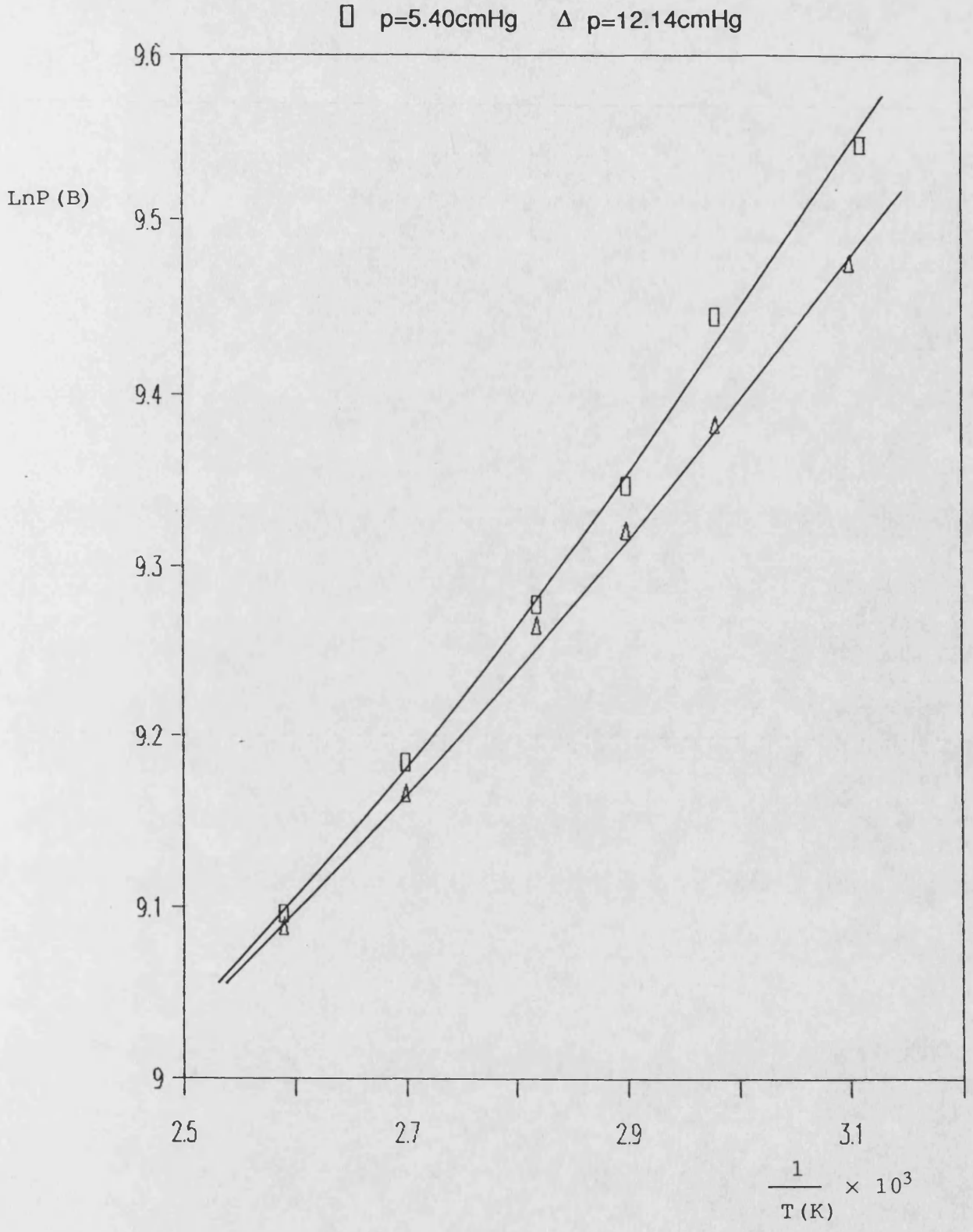

Figure A1 : LnP vs 1/T for Acetone in Filled PDMS.

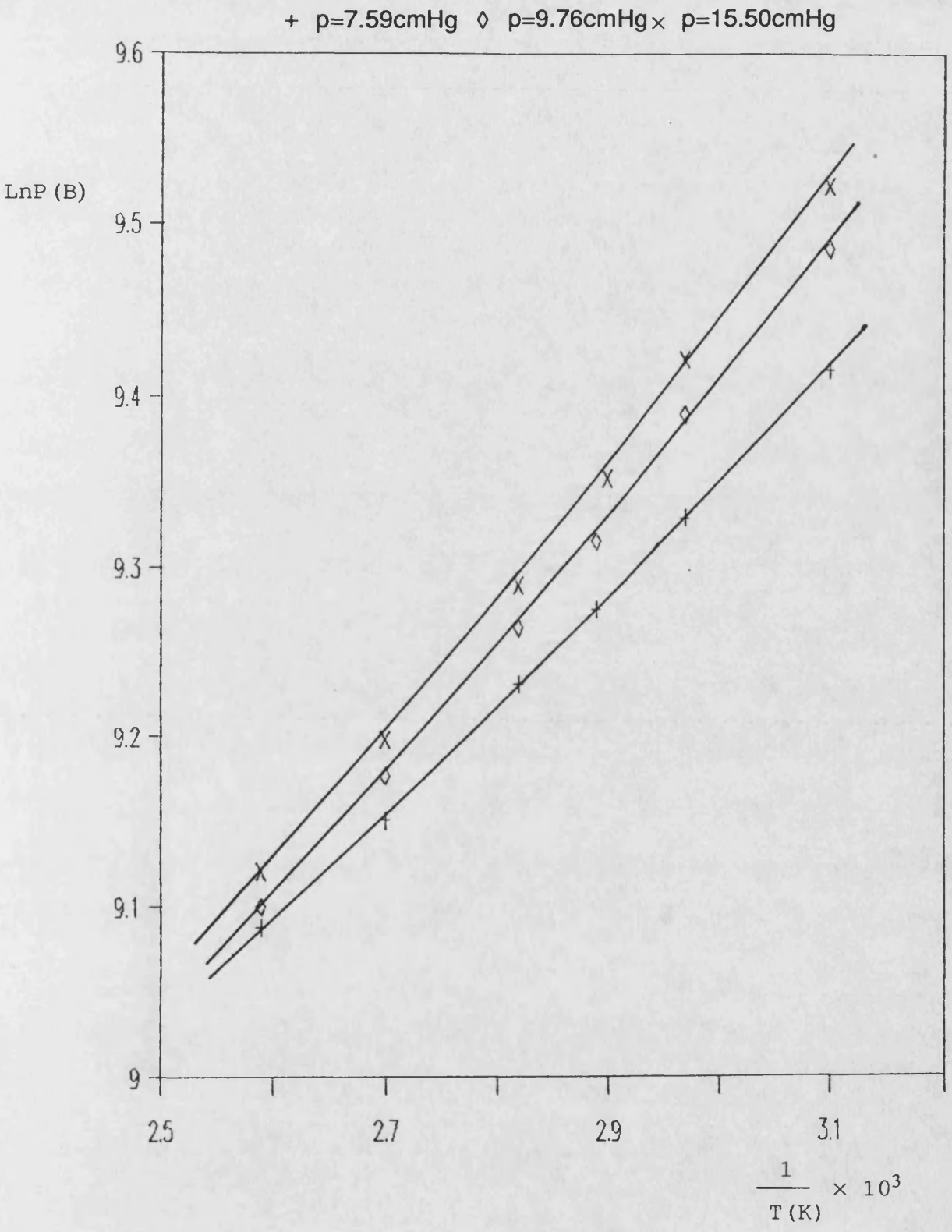

Figure A1a : LnP vs 1/T for Acetone in Filled PDMS.

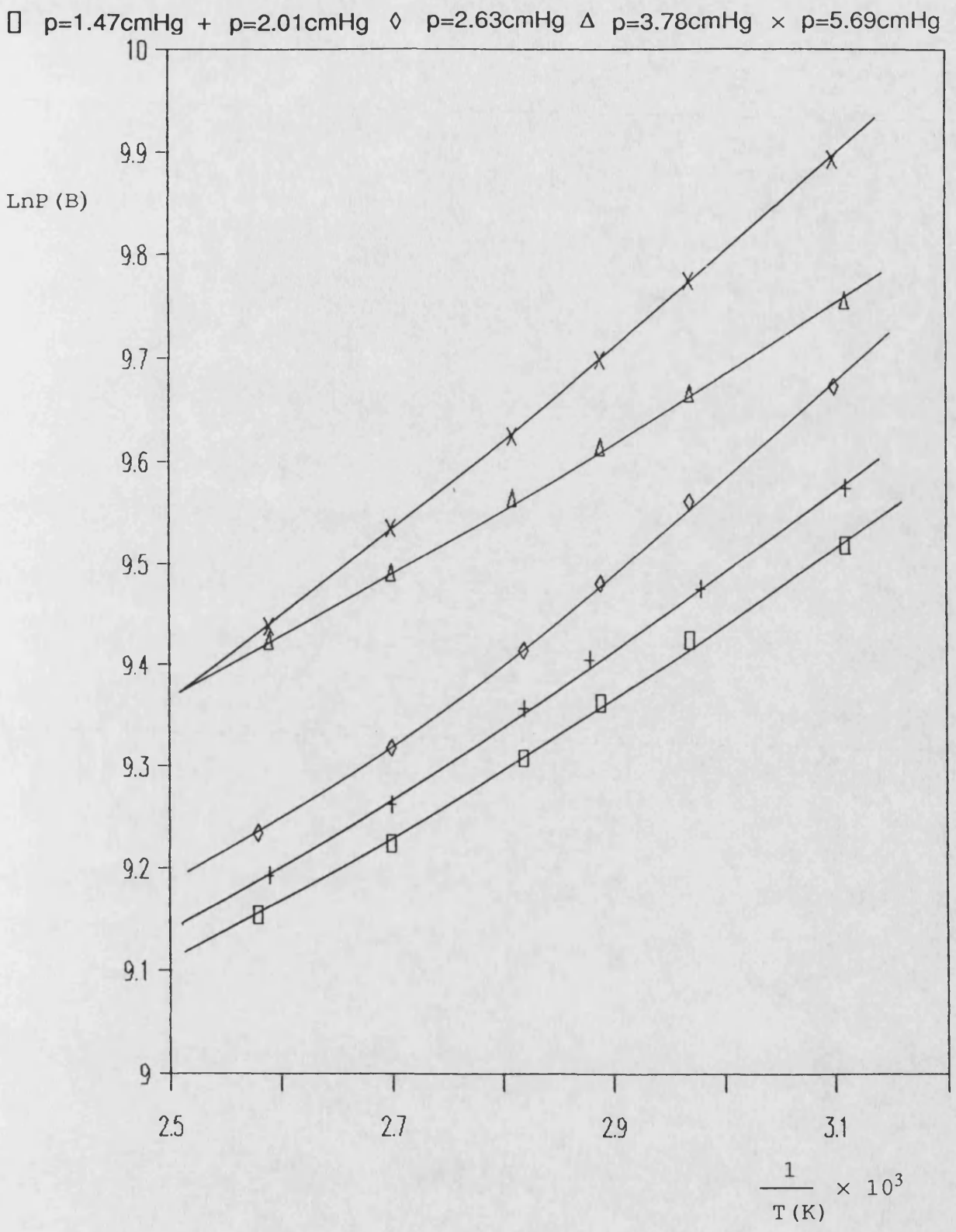

Figure A2 : LnP vs 1/T for Ethanol in Filled PDMS.

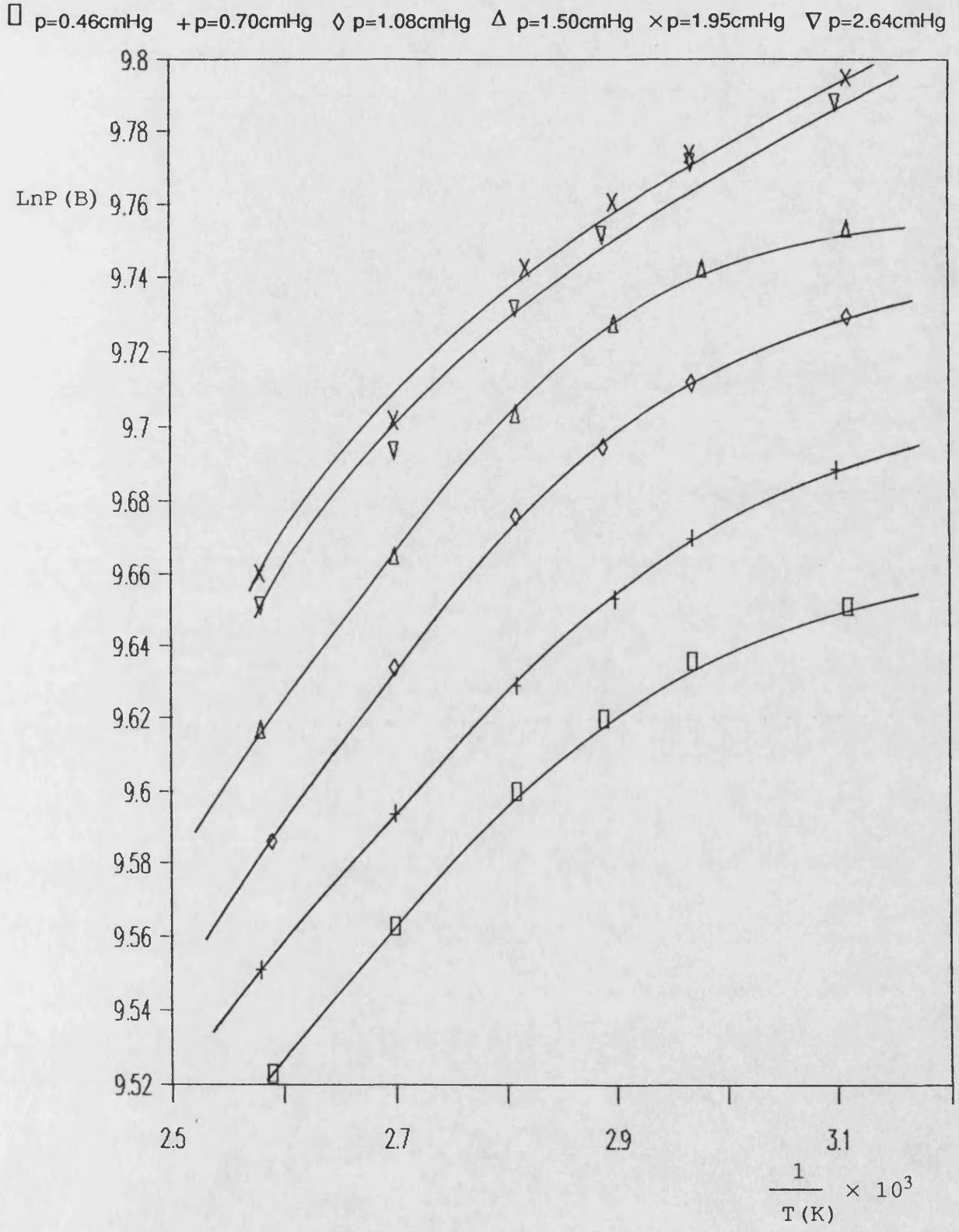

Figure A3: LnP vs 1/T for Tetrachloroethylene in Filled PDMS.

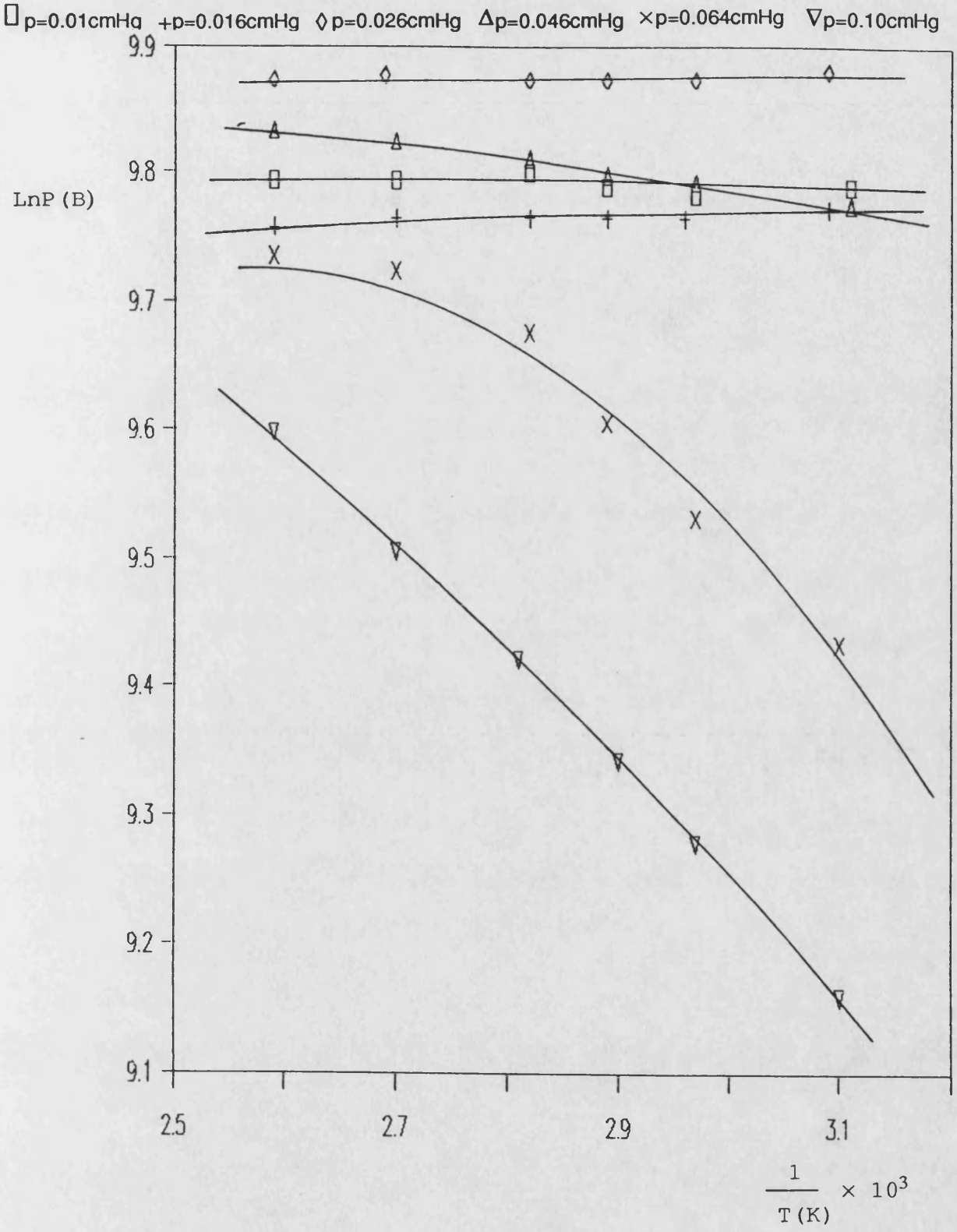

Figure A4 : LnP vs 1/T for Nitrobenzene in Filled PDMS.

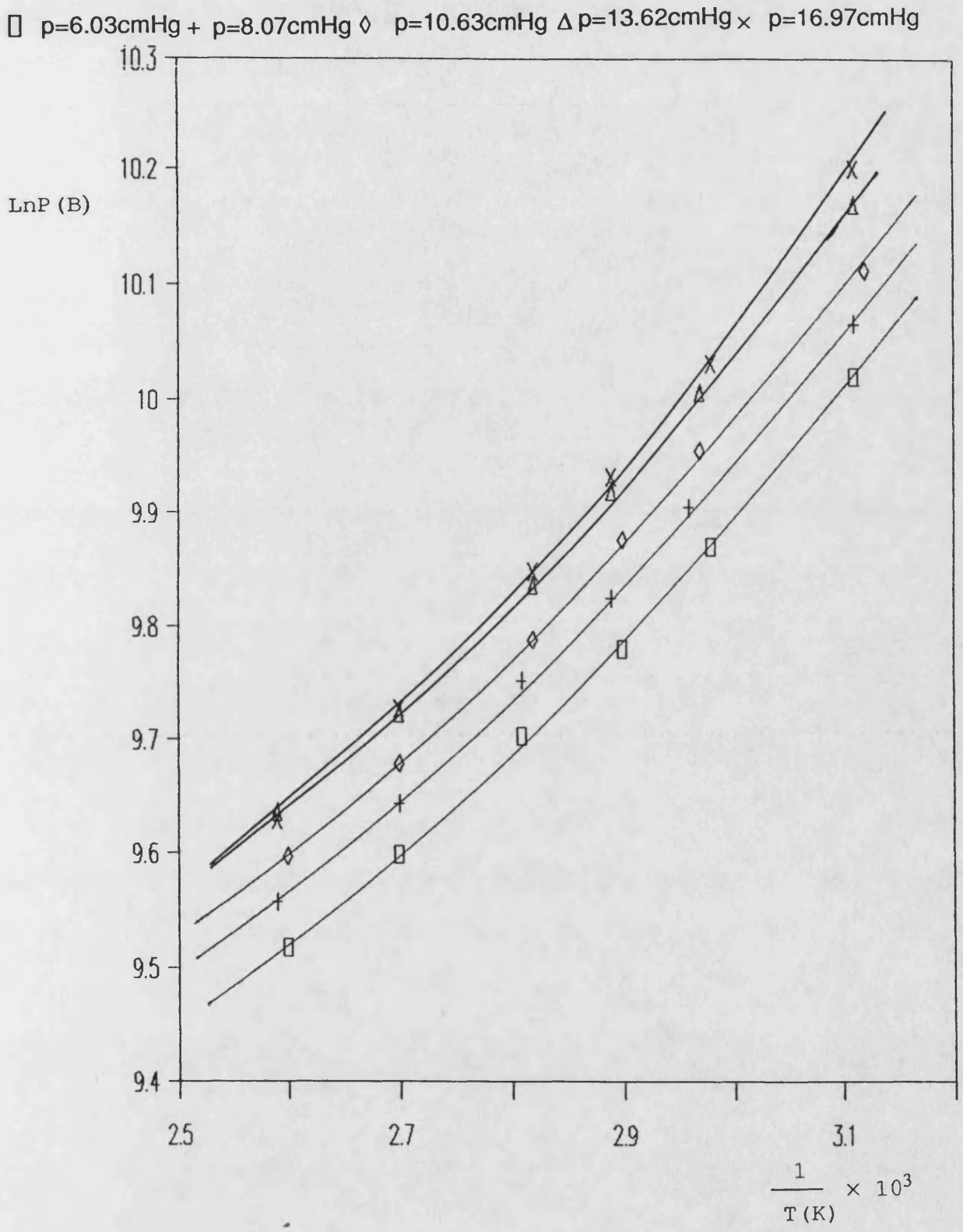

Figure A5 : LnP vs 1/T for Acetone in Unfilled PDMS.

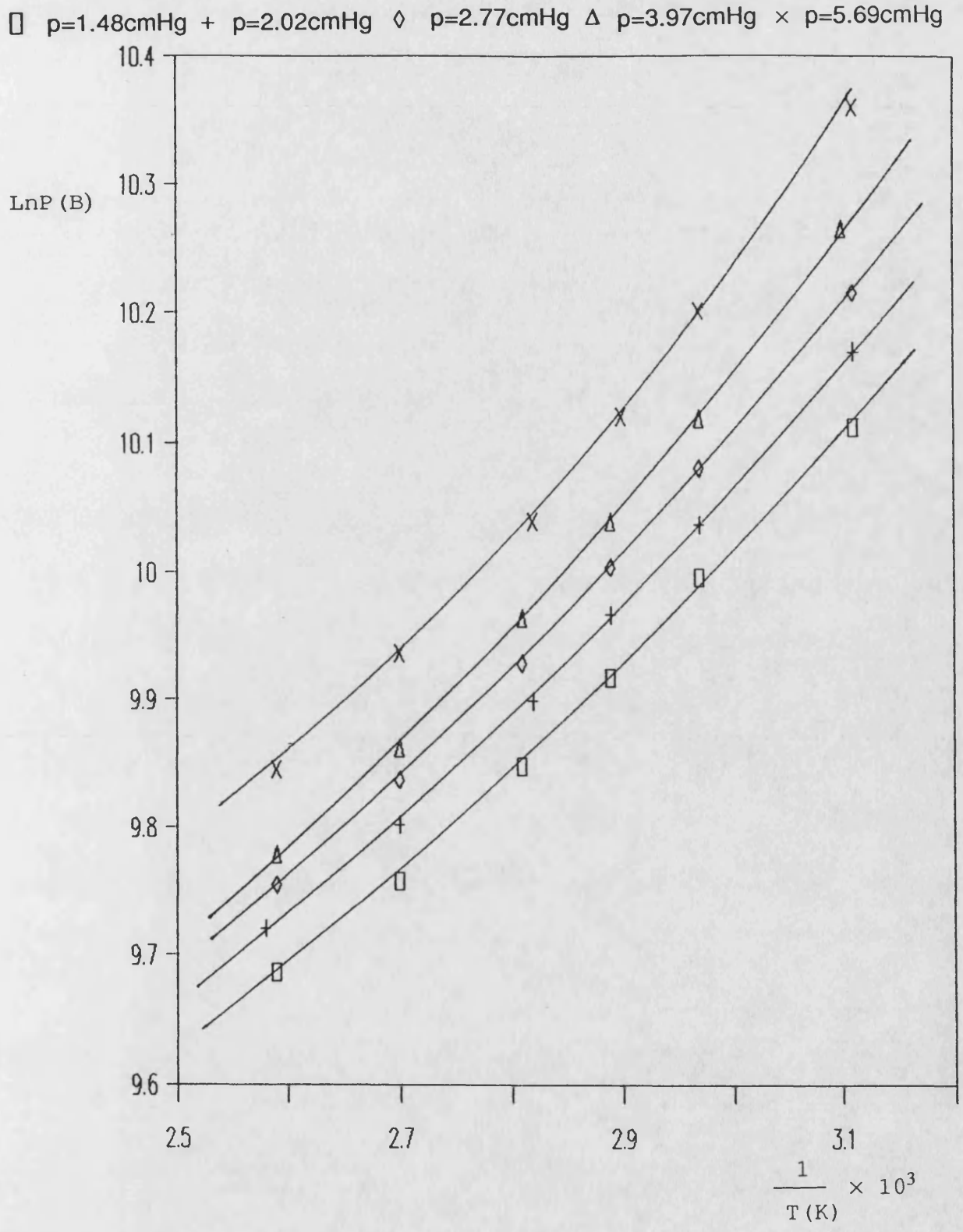

Figure A6 : LnP vs 1/T for Ethanol in Unfilled PDMS.

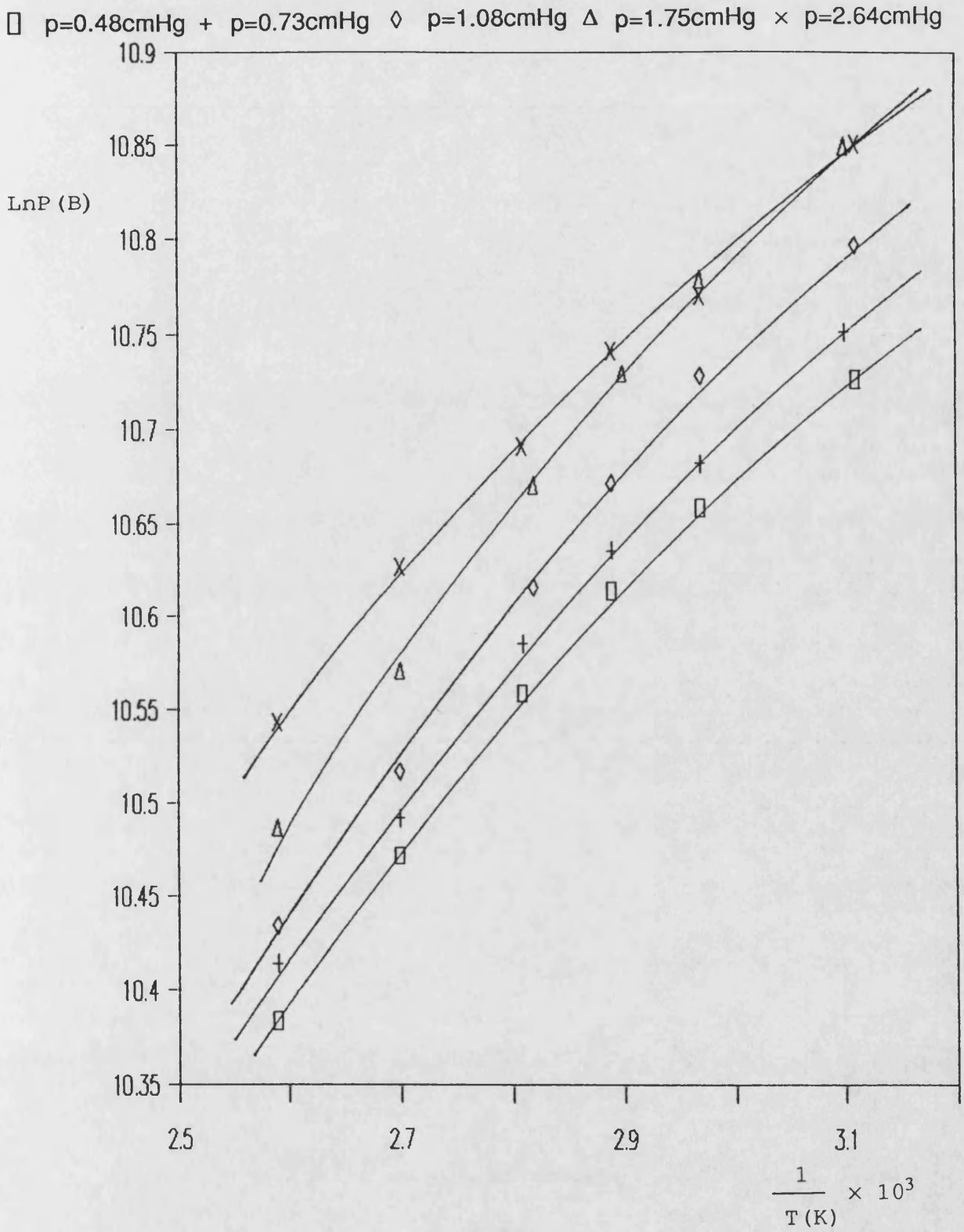

Figure A7 : LnP vs 1/T for Tetrachloroethylene in Unfilled PDMS.

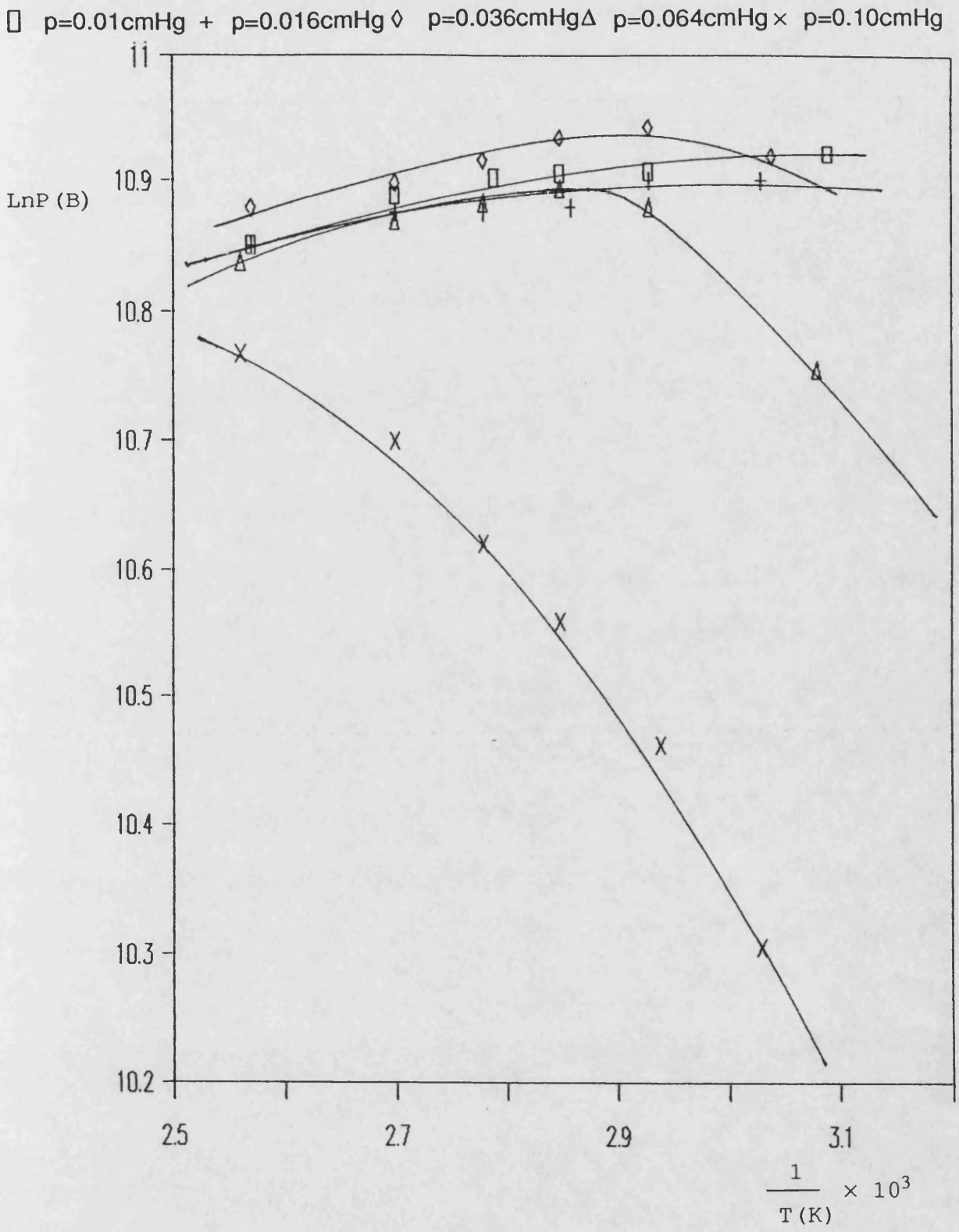

Figure A8 : LnP vs 1/T for Nitrobenzene in Unfilled PDMS.

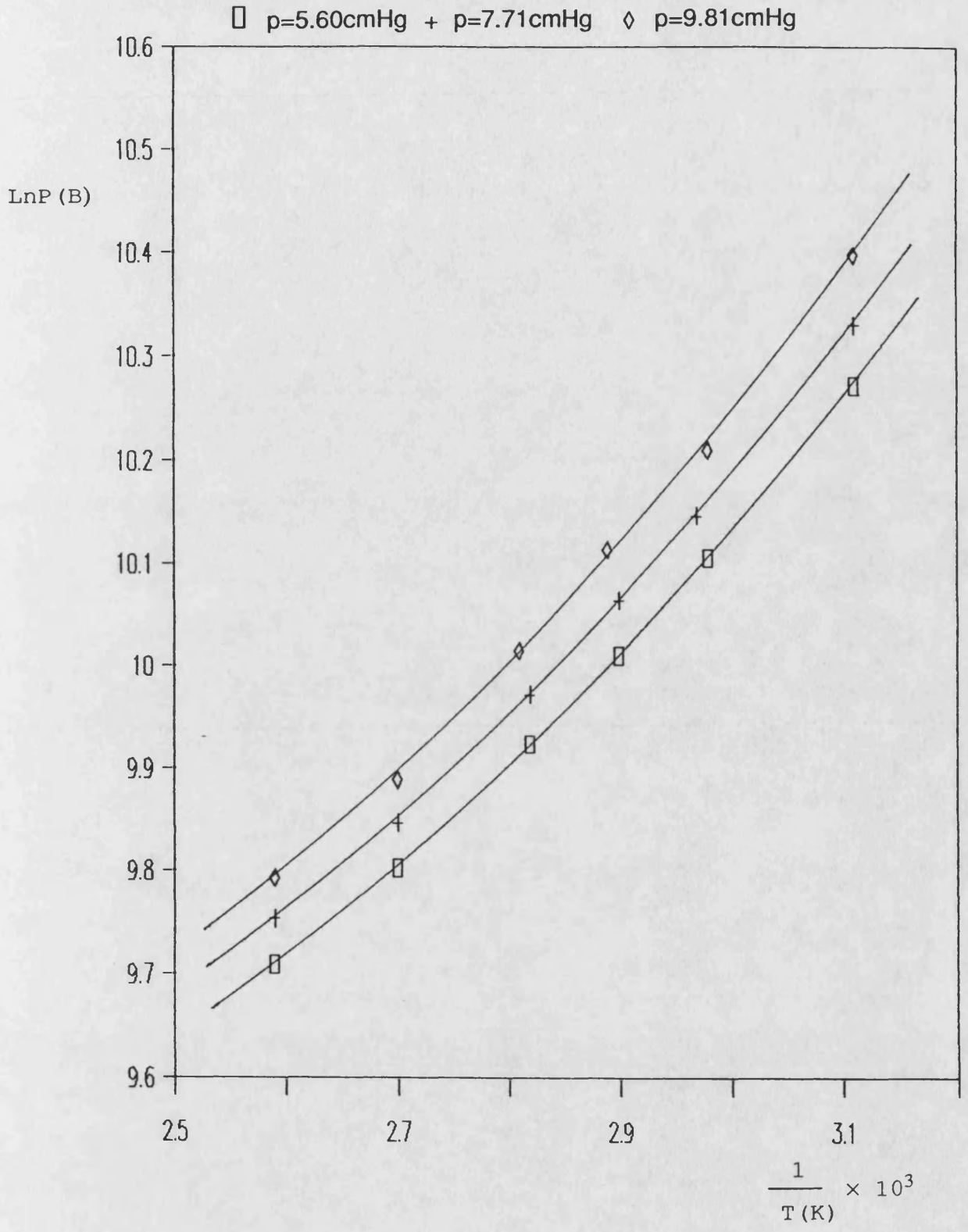

Figure A9 : LnP vs 1/T for Acetone in Ester-substituted PDMS.

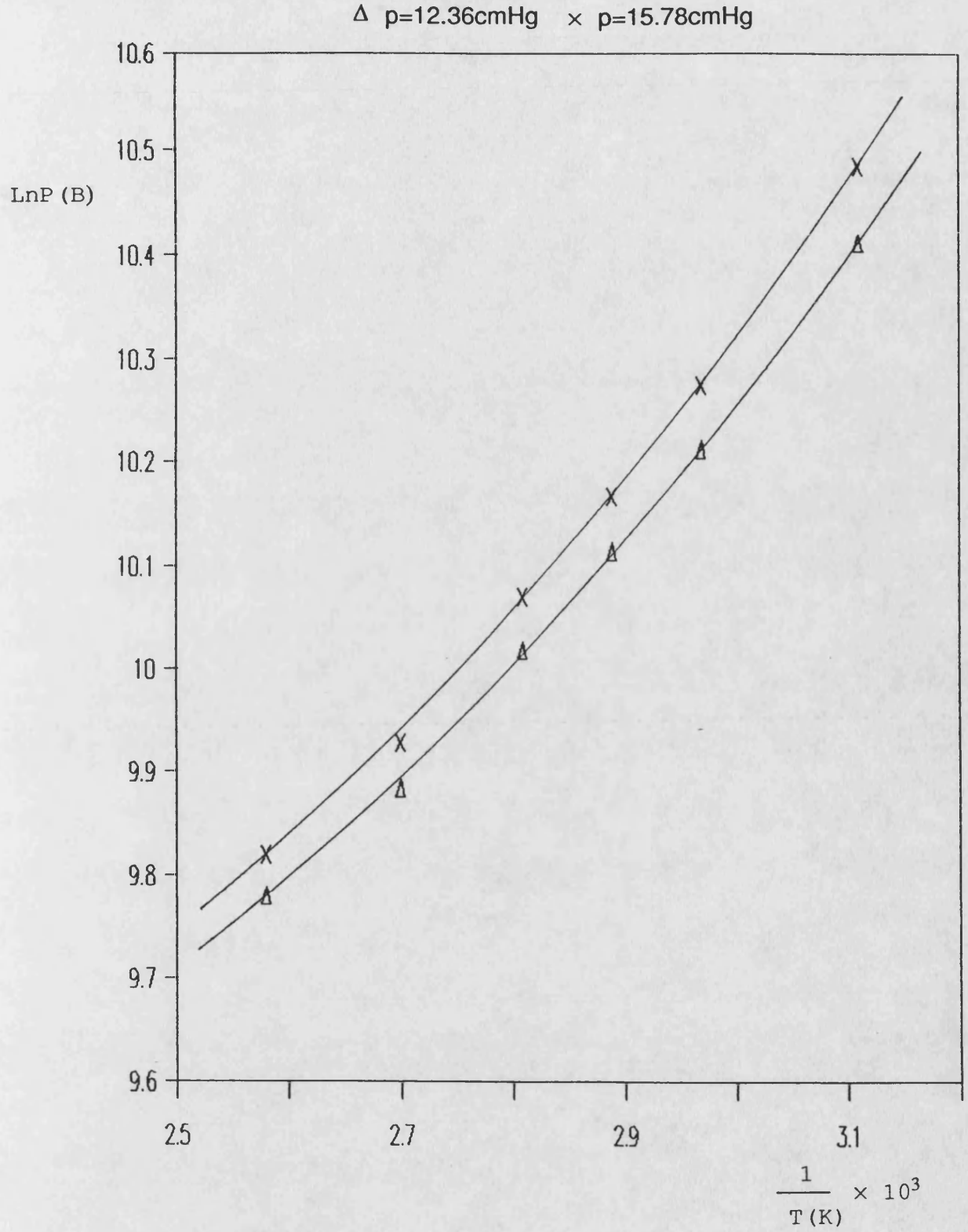

Figure A9a : LnP vs 1/T for Acetone in Ester-substituted PDMS.

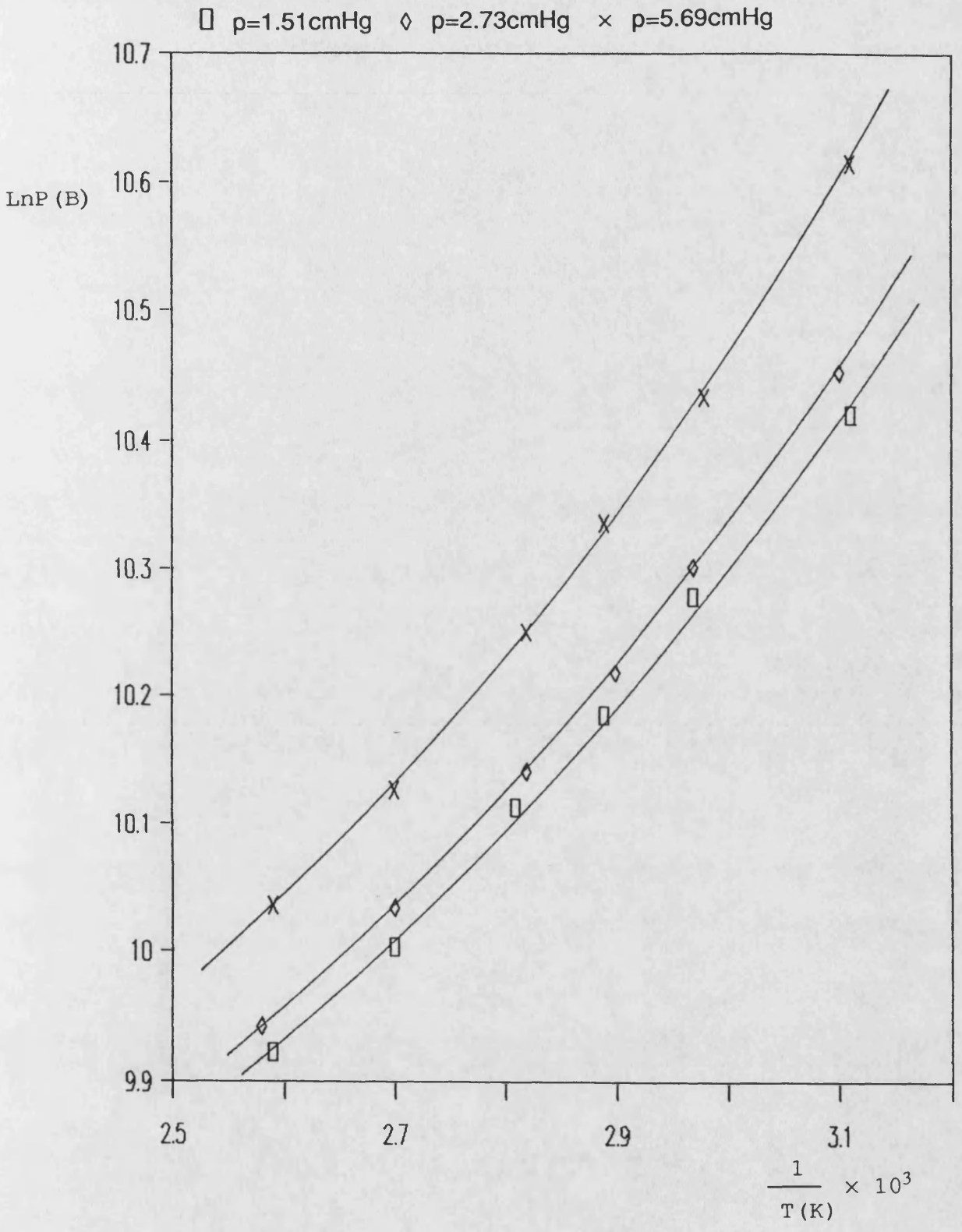

Figure A10 : LnP vs 1/T for Ethanol in Ester-substituted PDMS.

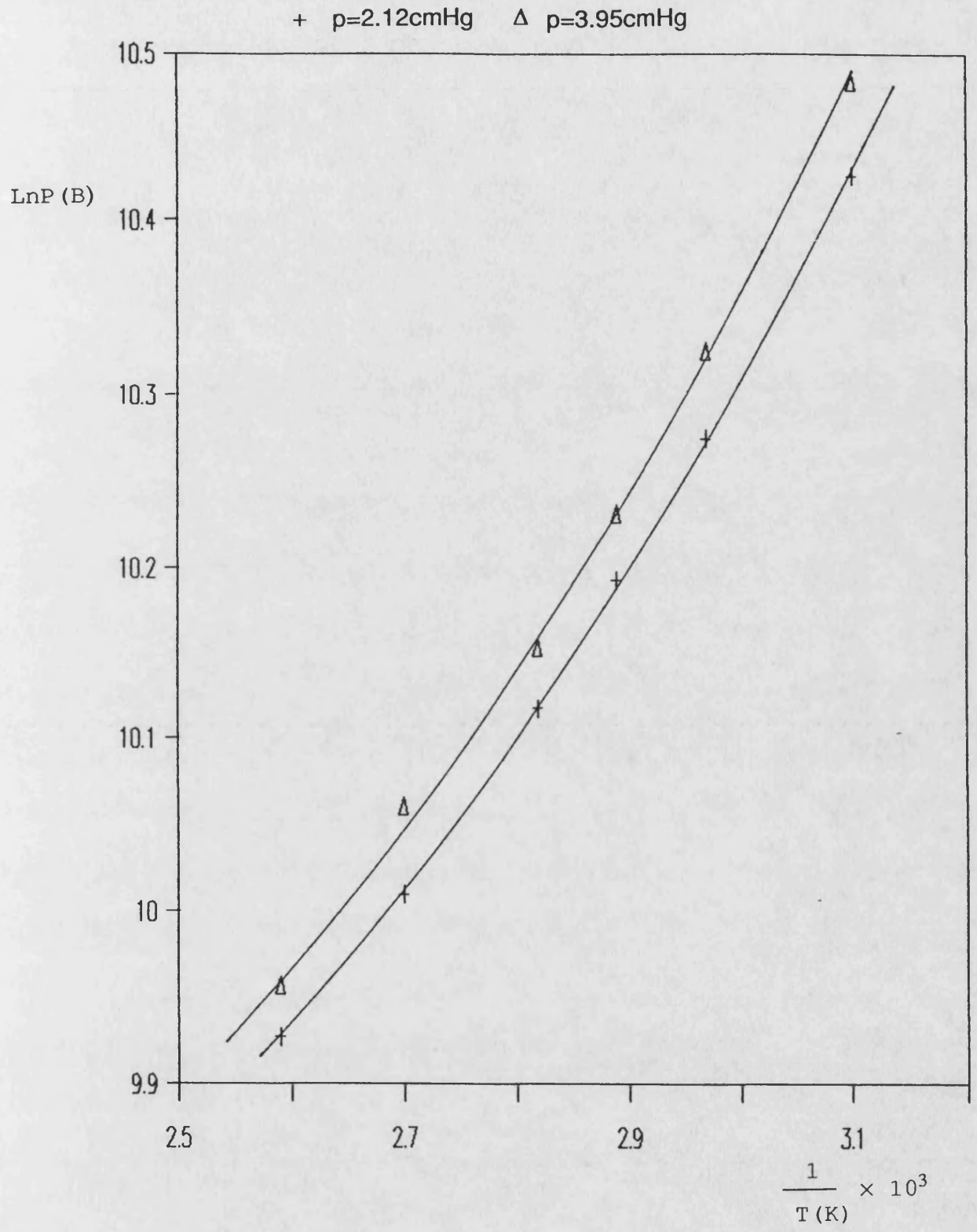

Figure A10a : LnP vs 1/T for Ethanol in Ester-substituted PDMS.

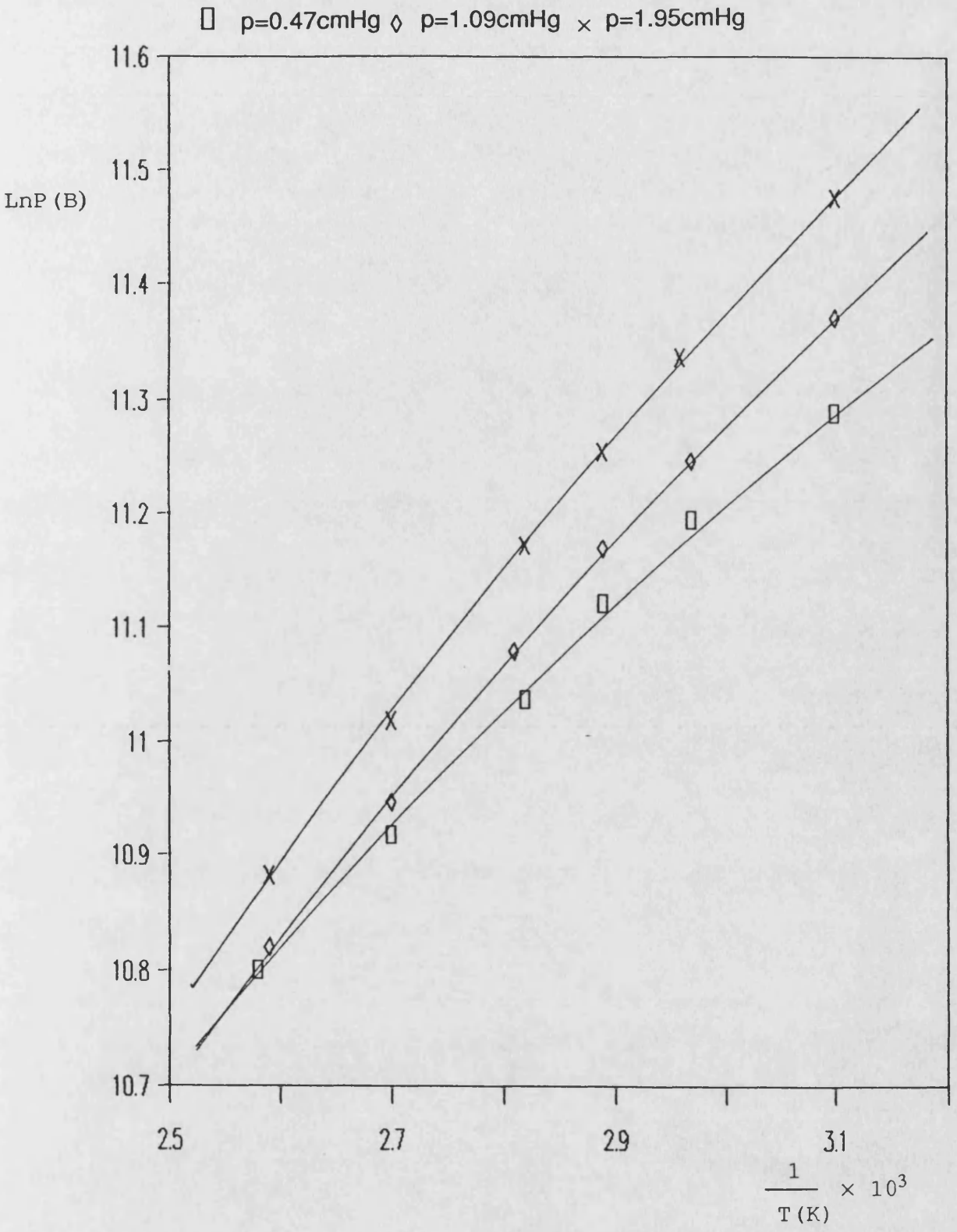

Figure A11 : LnP vs 1/T for Tetrachloroethylene in Ester-substituted PDMS.

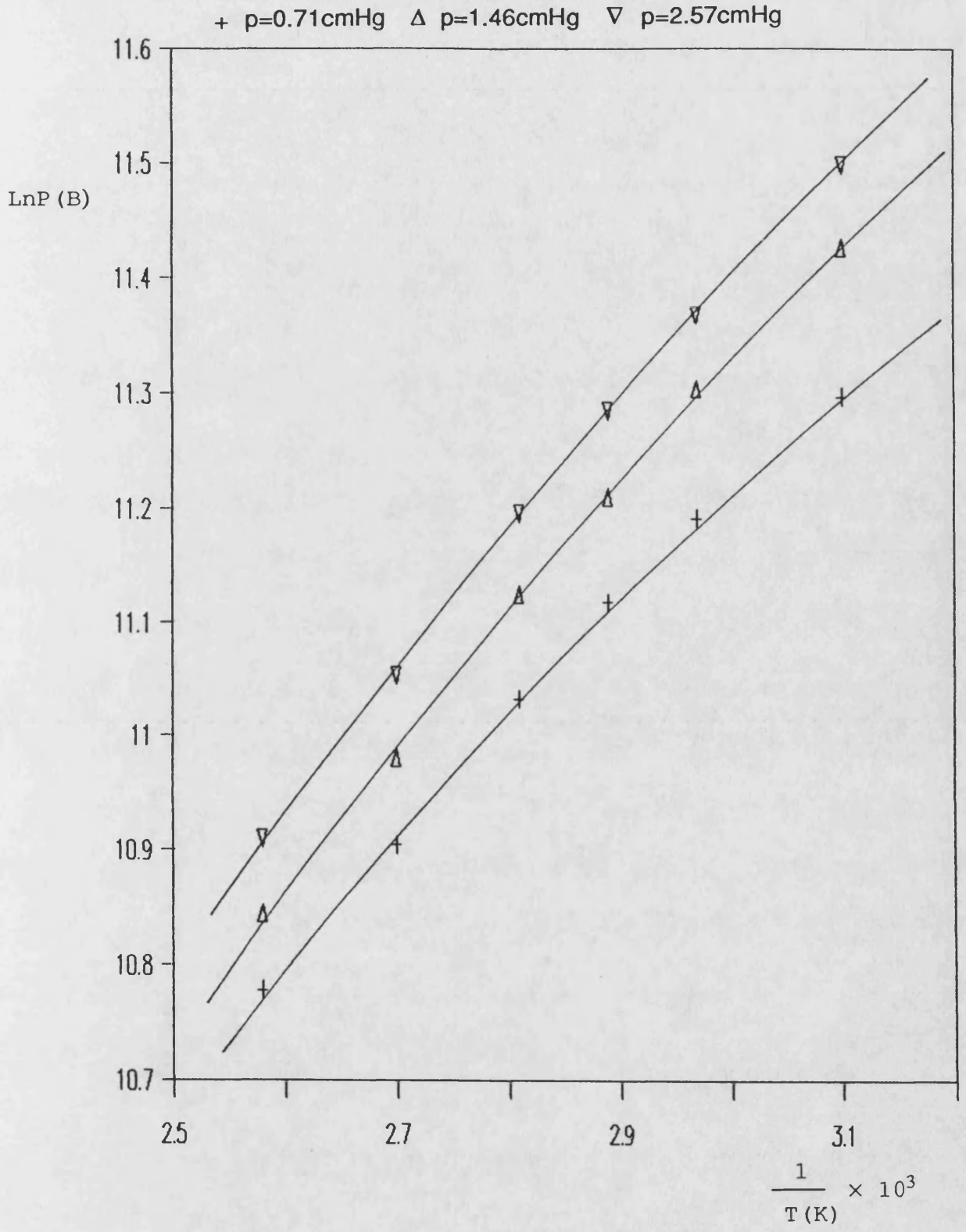

Figure A11a : LnP vs 1/T for Tetrachloroethylene in Ester-substituted PDMS.

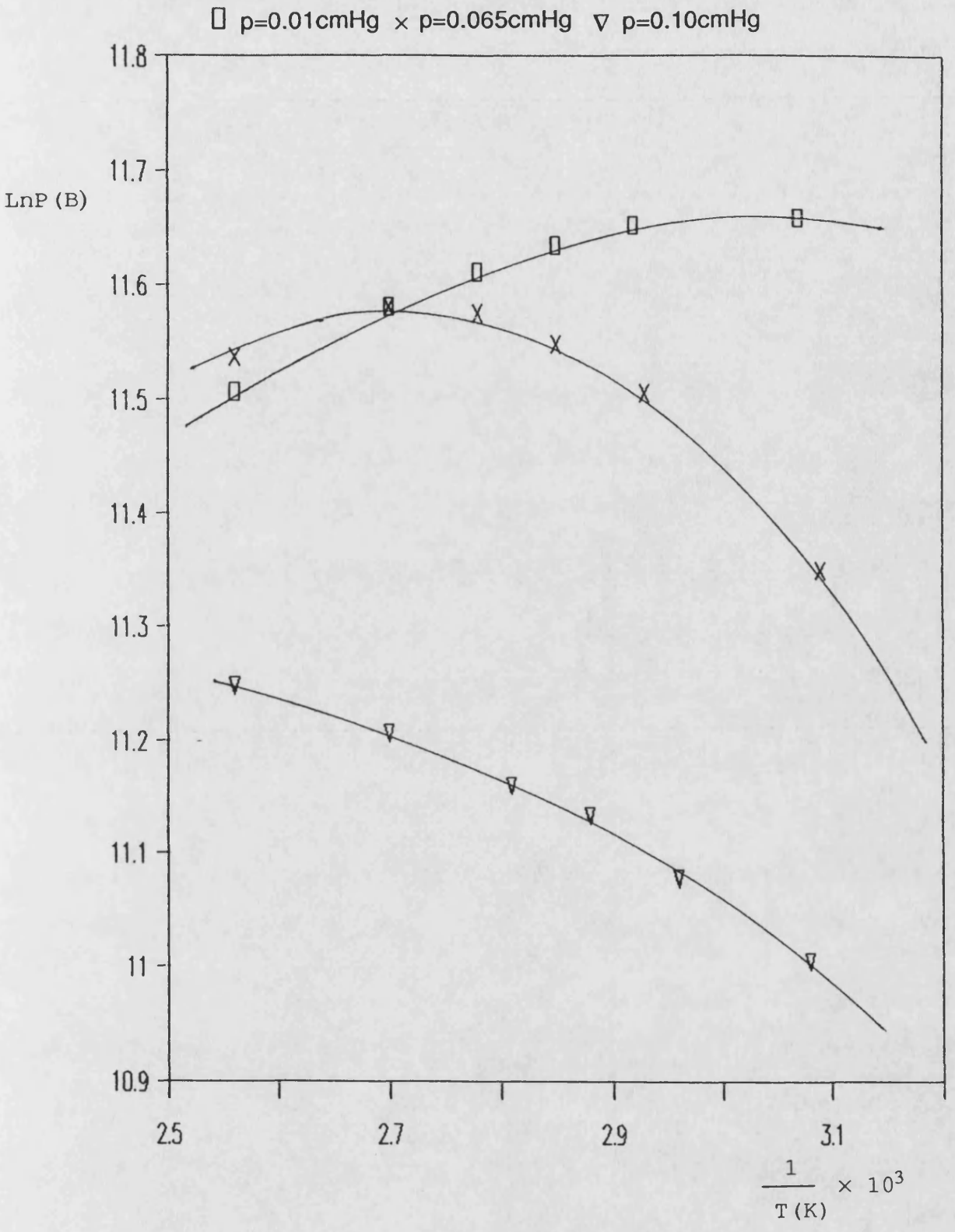

Figure A12 : LnP vs 1/T for Nitrobenzene in Ester-substituted PDMS.

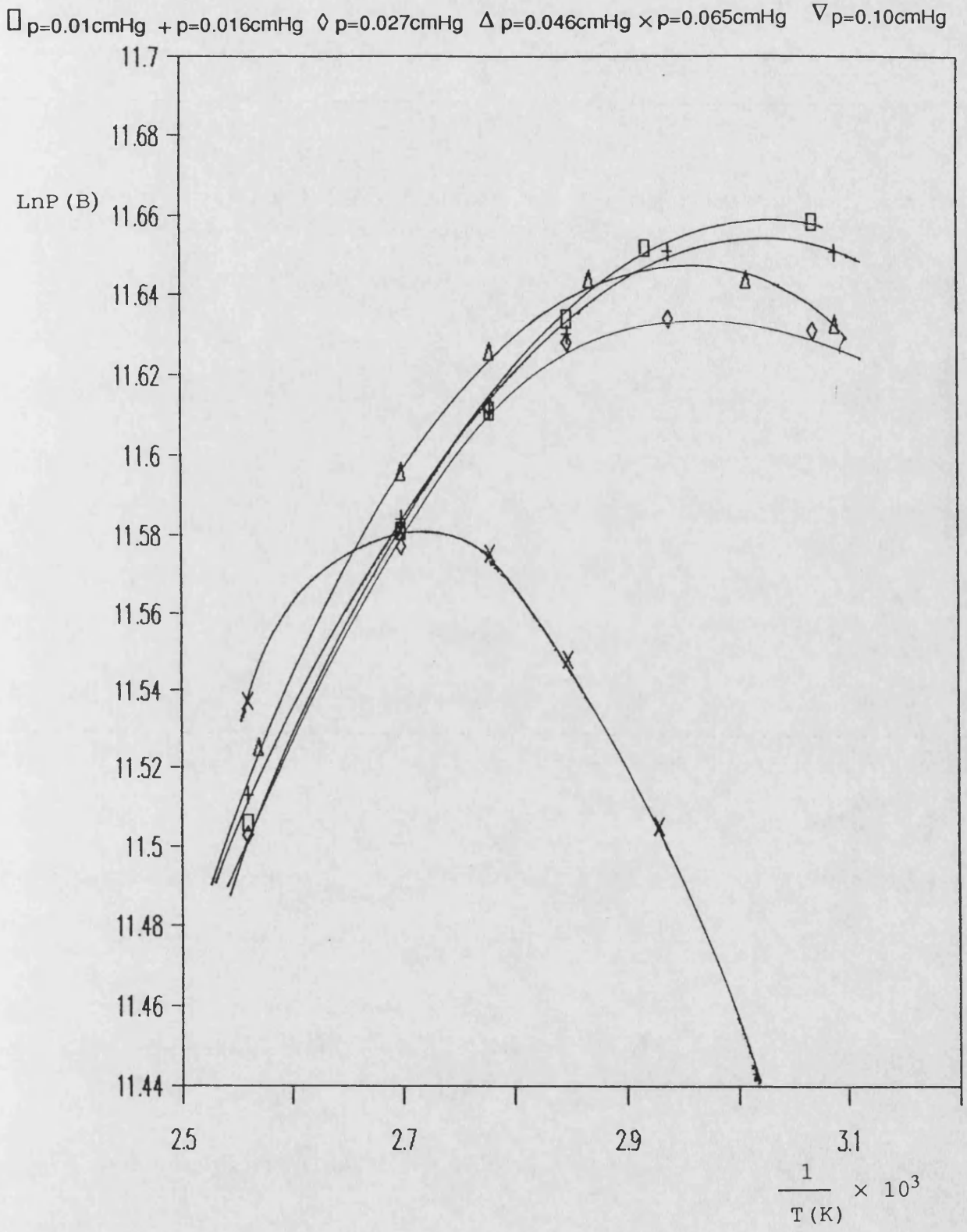

Figure A12a : LnP vs 1/T for Nitrobenzene in Ester-substituted PDMS.

Arrhenius Plots for Diffusion

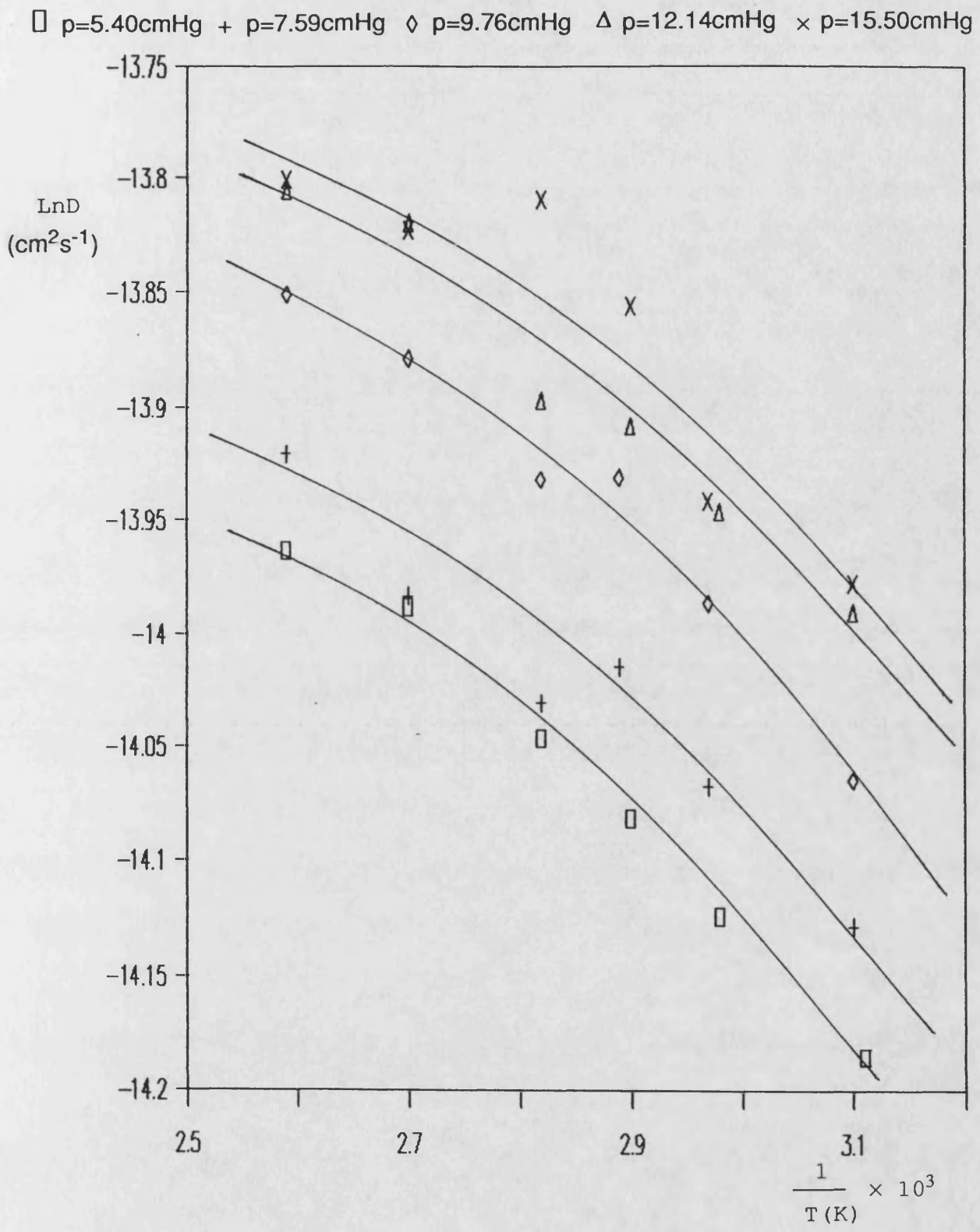

Figure A13 : LnD vs 1/T for Acetone in Filled PDMS.

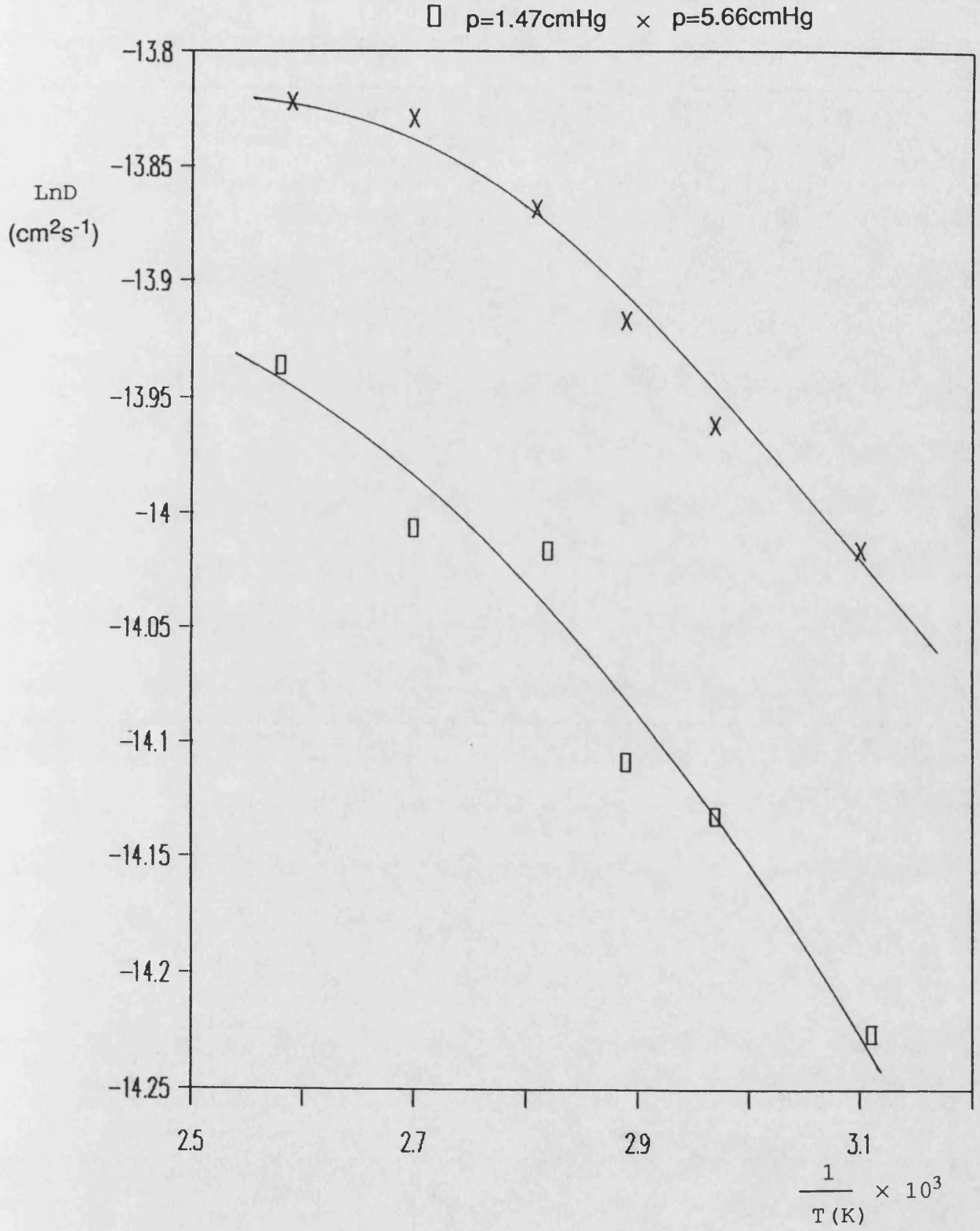

Figure A14 : LnD vs 1/T for Ethanol in Filled PDMS.

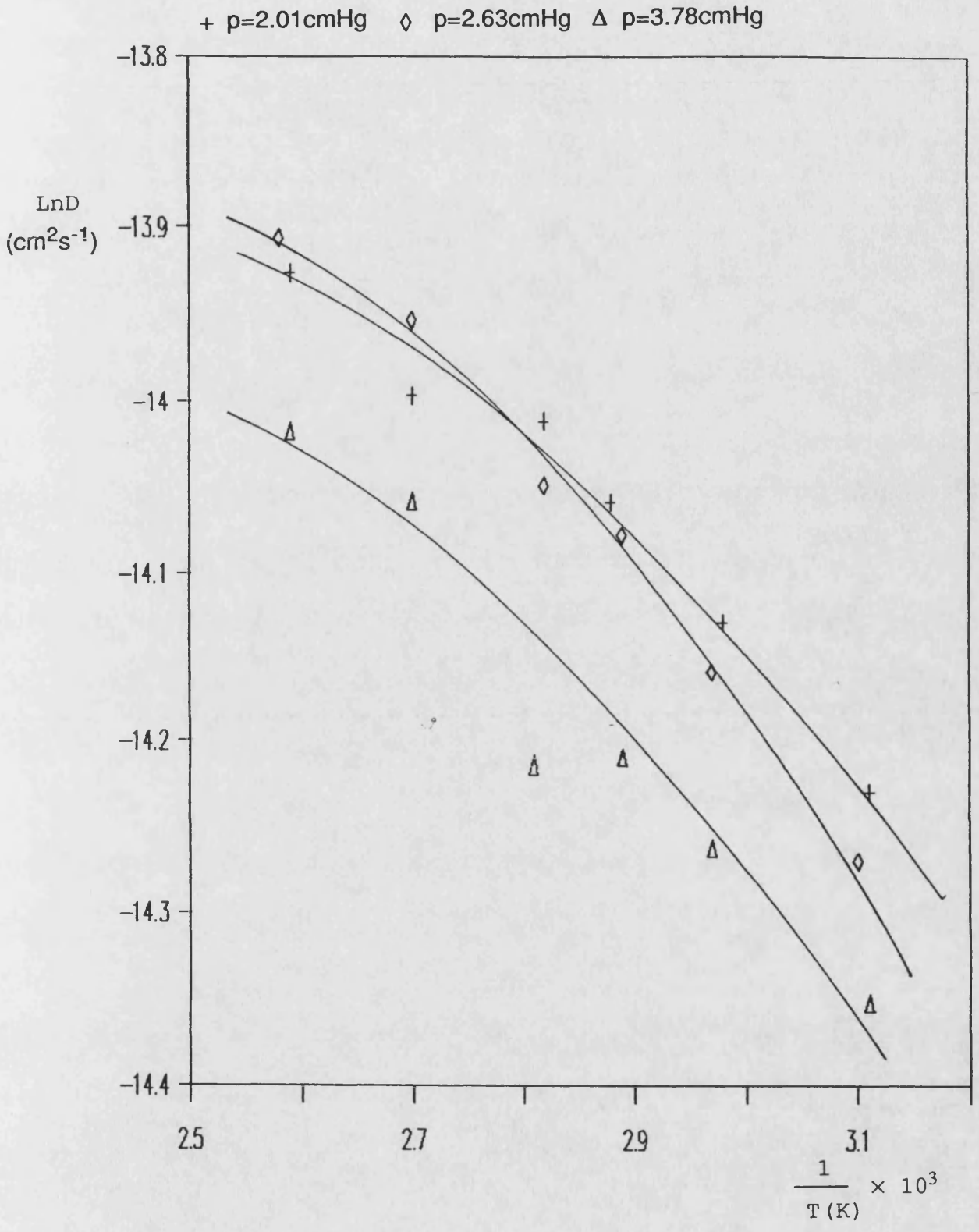

Figure A14a : LnD vs 1/T for Ethanol in Filled PDMS.

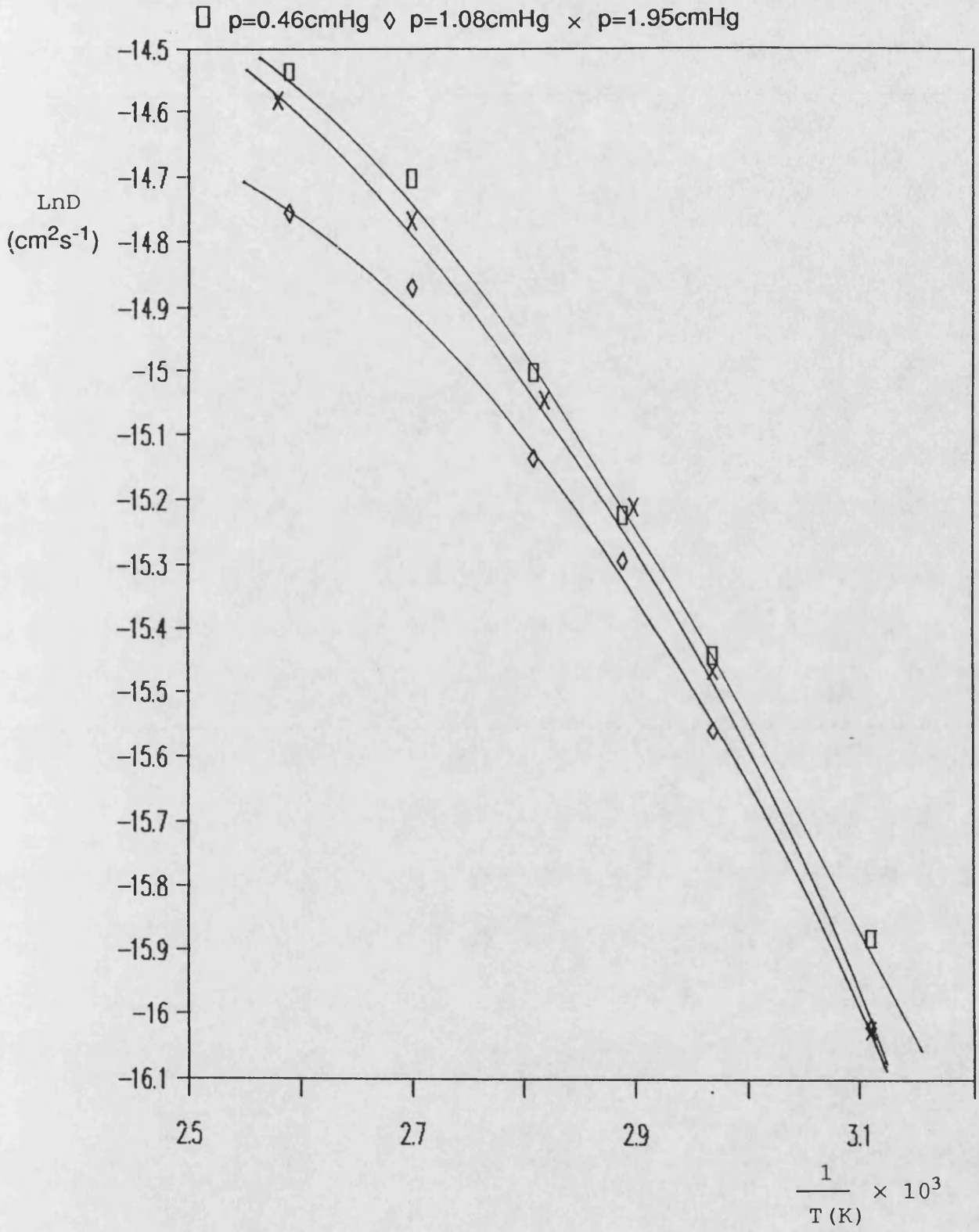

Figure A15 : LnD vs 1/T for Tetrachloroethylene in Filled PDMS.

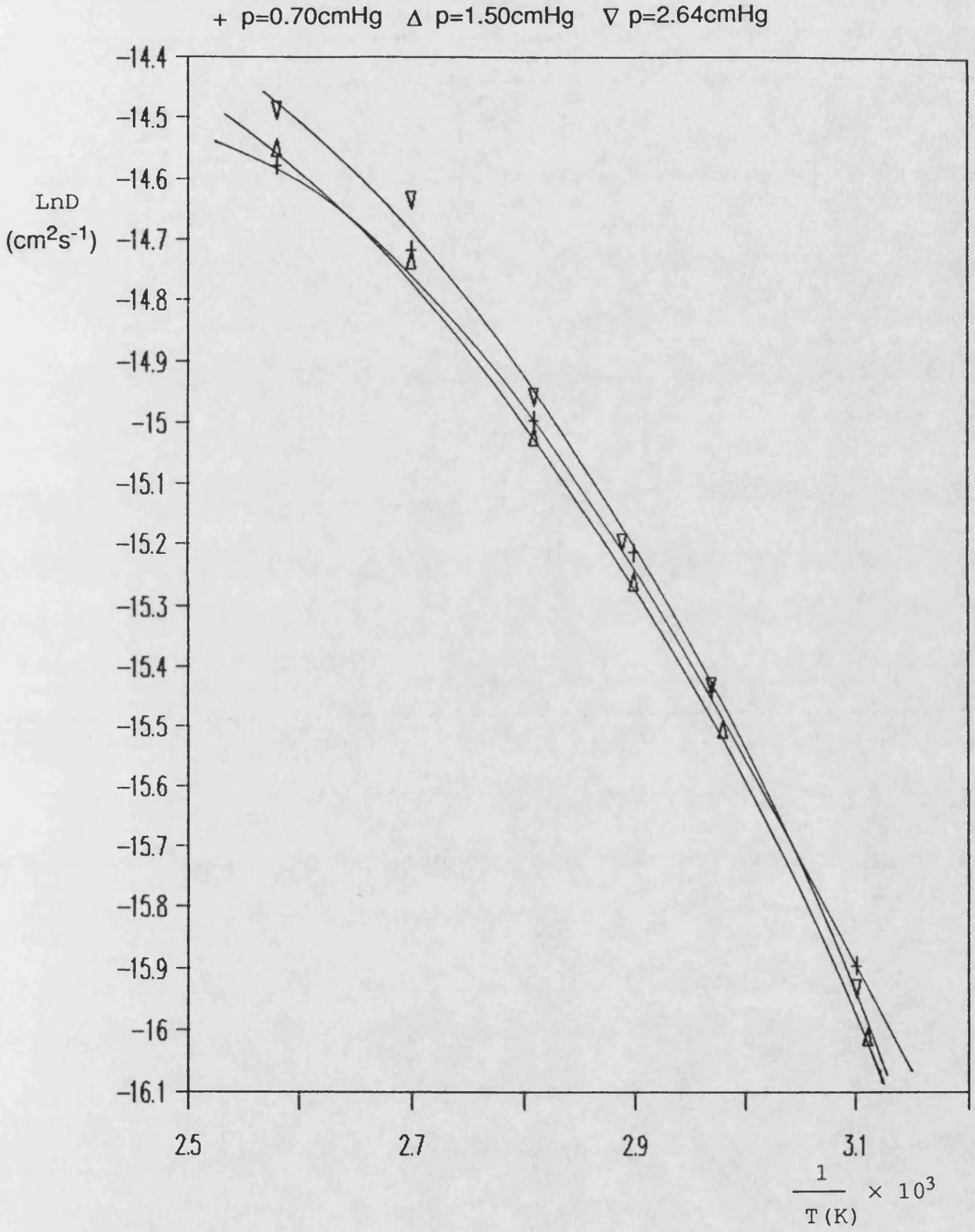

Figure A15a : LnD vs 1/T for Tetrachloroethylene in Filled PDMS.

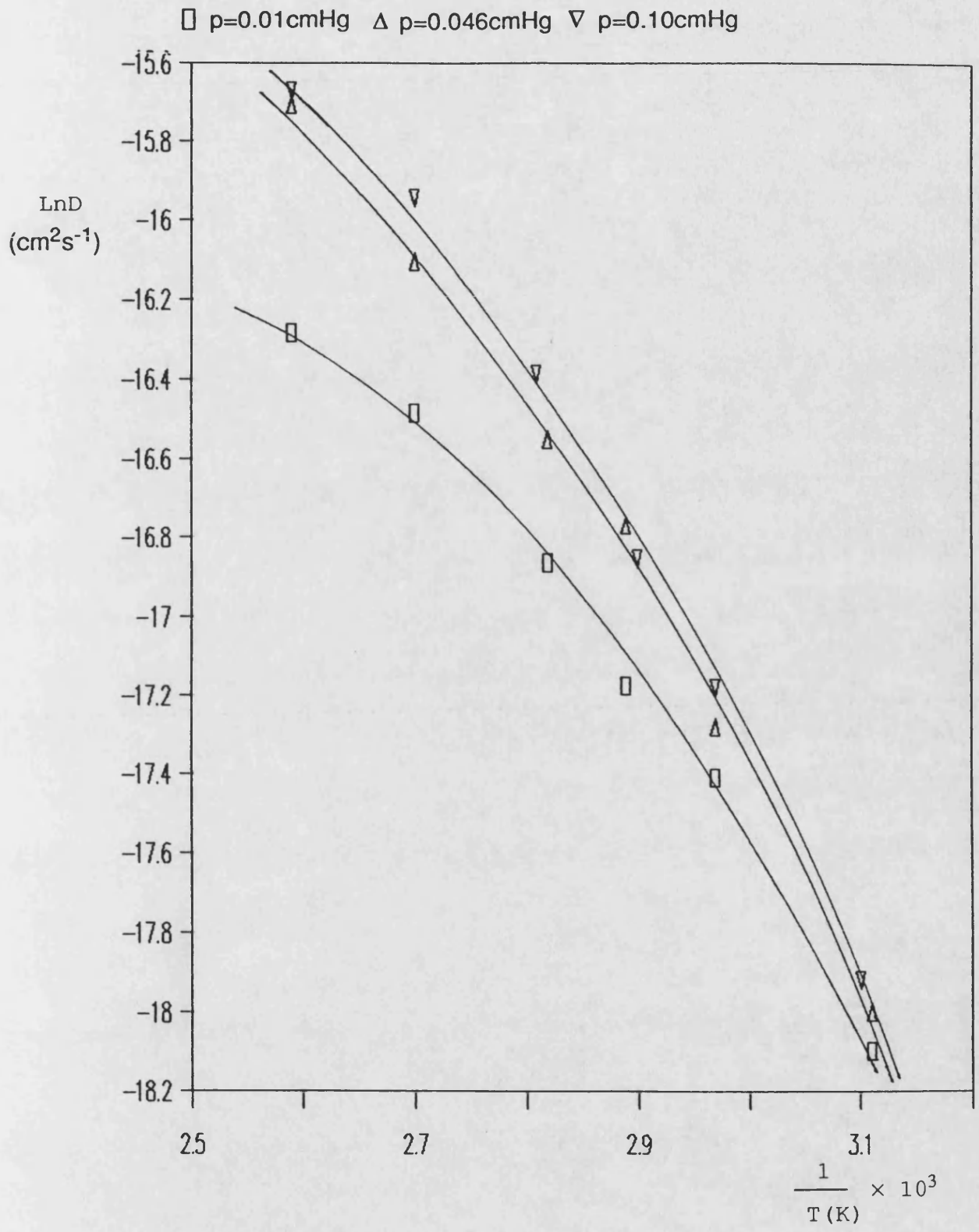

Figure A16 : LnD vs 1/T for Nitrobenzene in Filled PDMS.

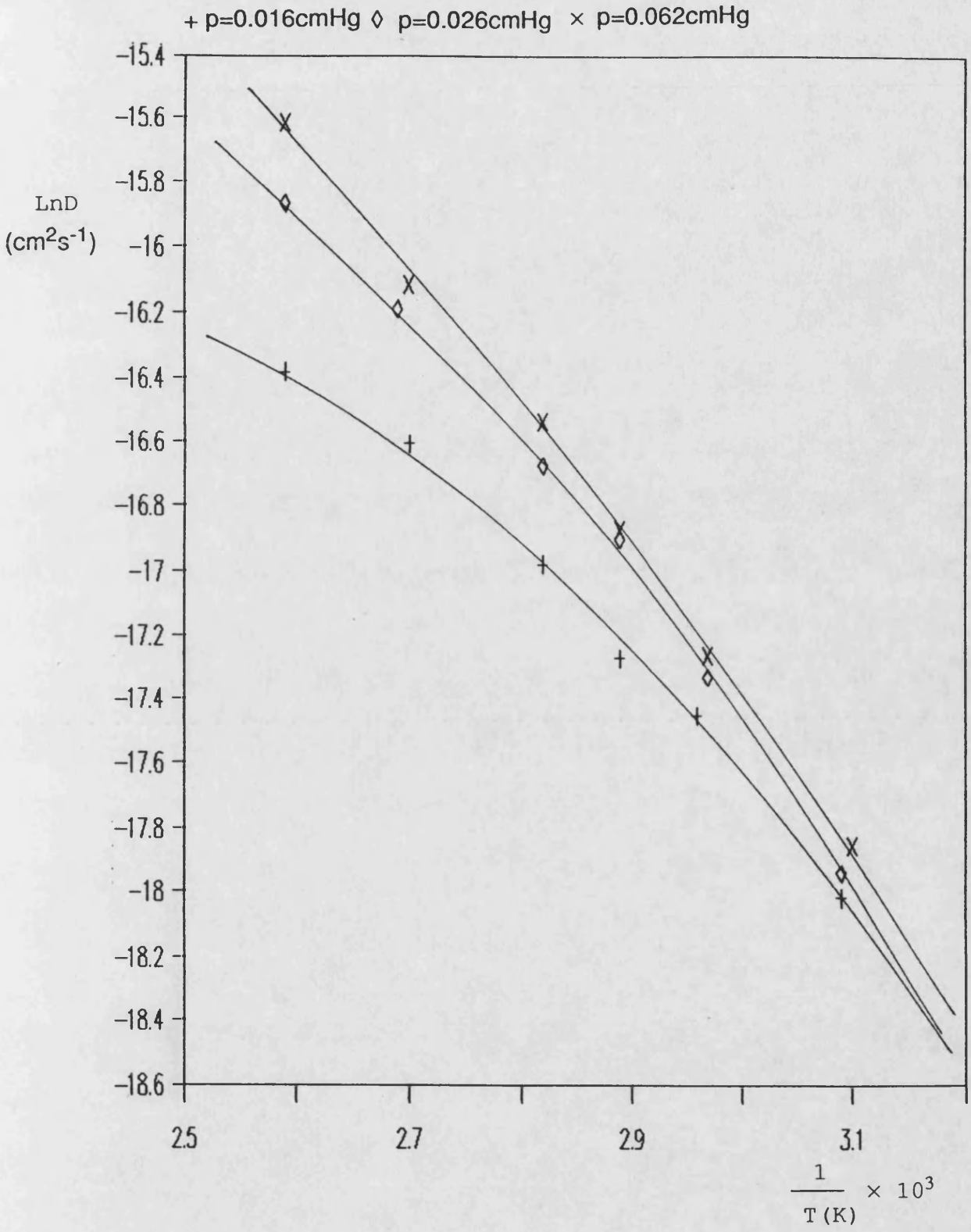

Figure A16a : LnD vs 1/T for Nitrobenzene in Filled PDMS.

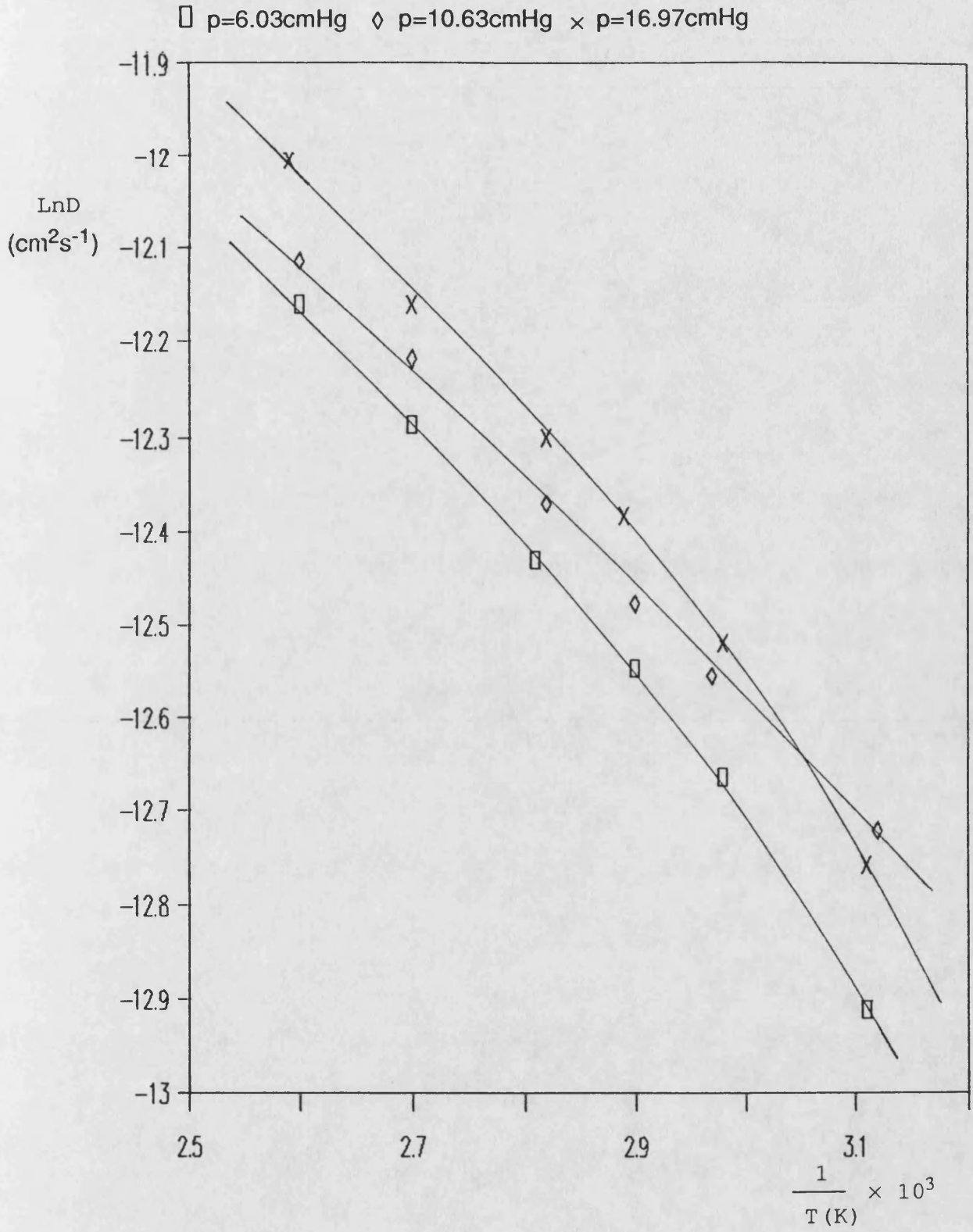

Figure A17 : LnD vs 1/T for Acetone in Unfilled PDMS.

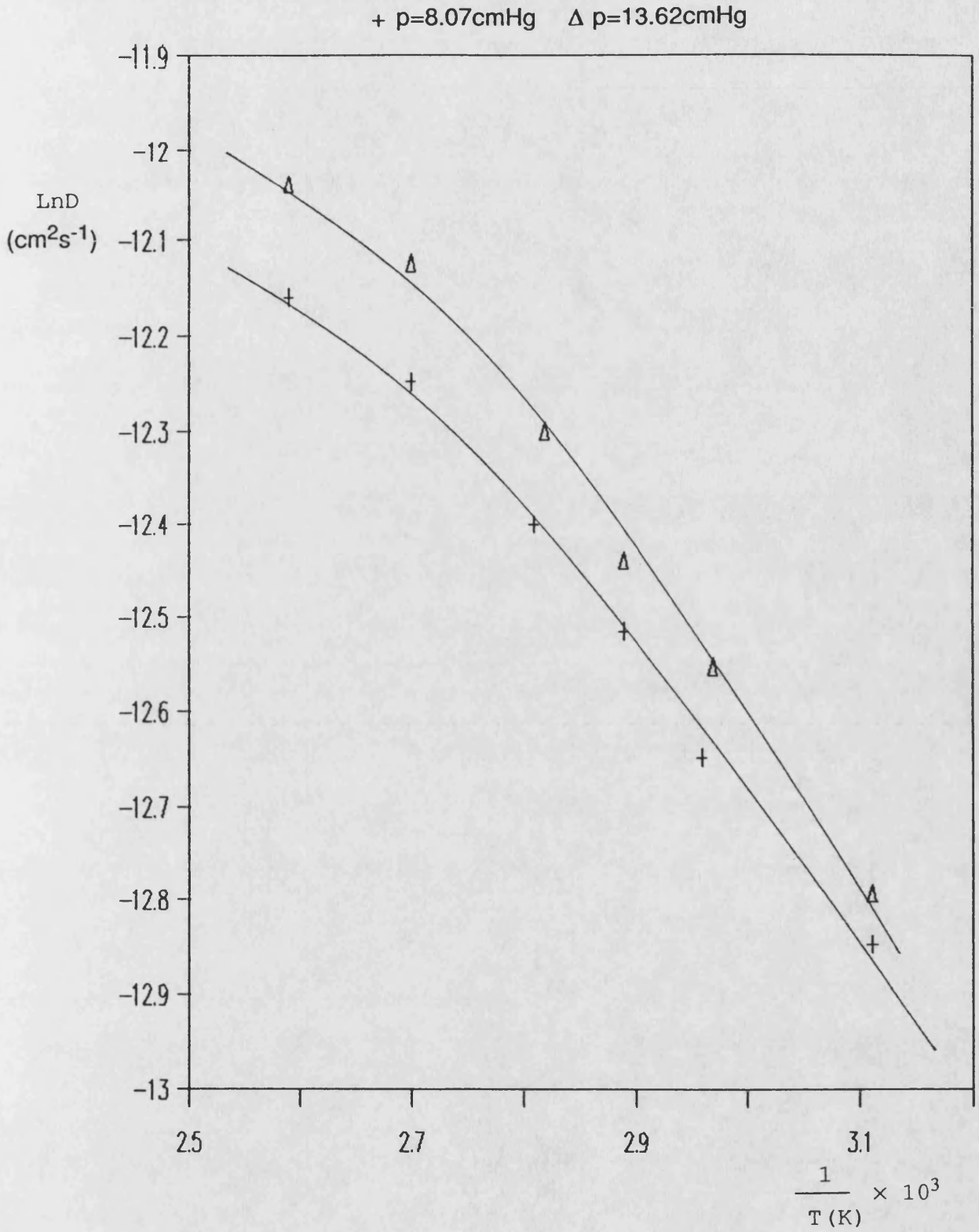

Figure A17a : LnD vs 1/T for Acetone in Unfilled PDMS.

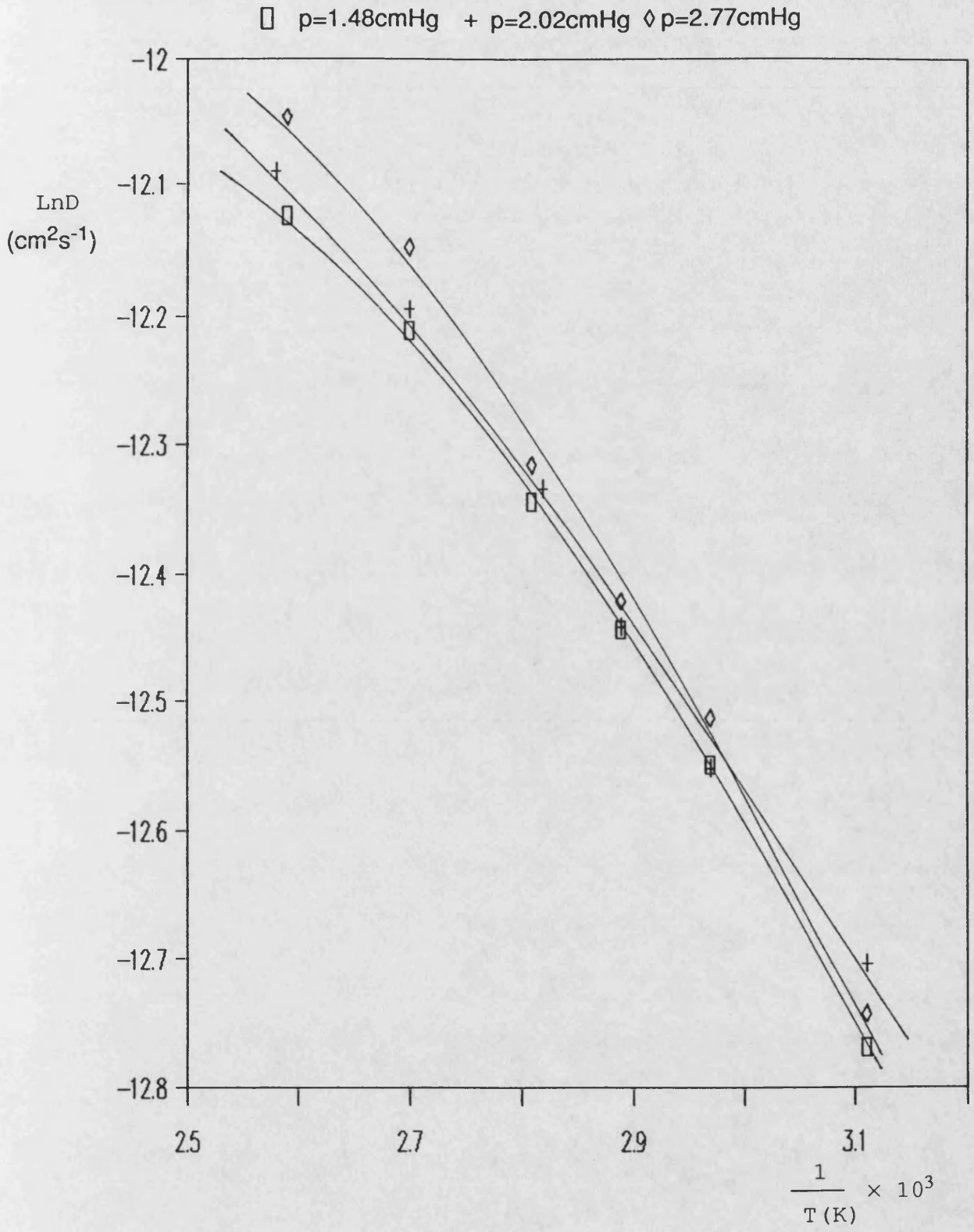

Figure A18 : LnD vs 1/T for Ethanol in Unfilled PDMS.

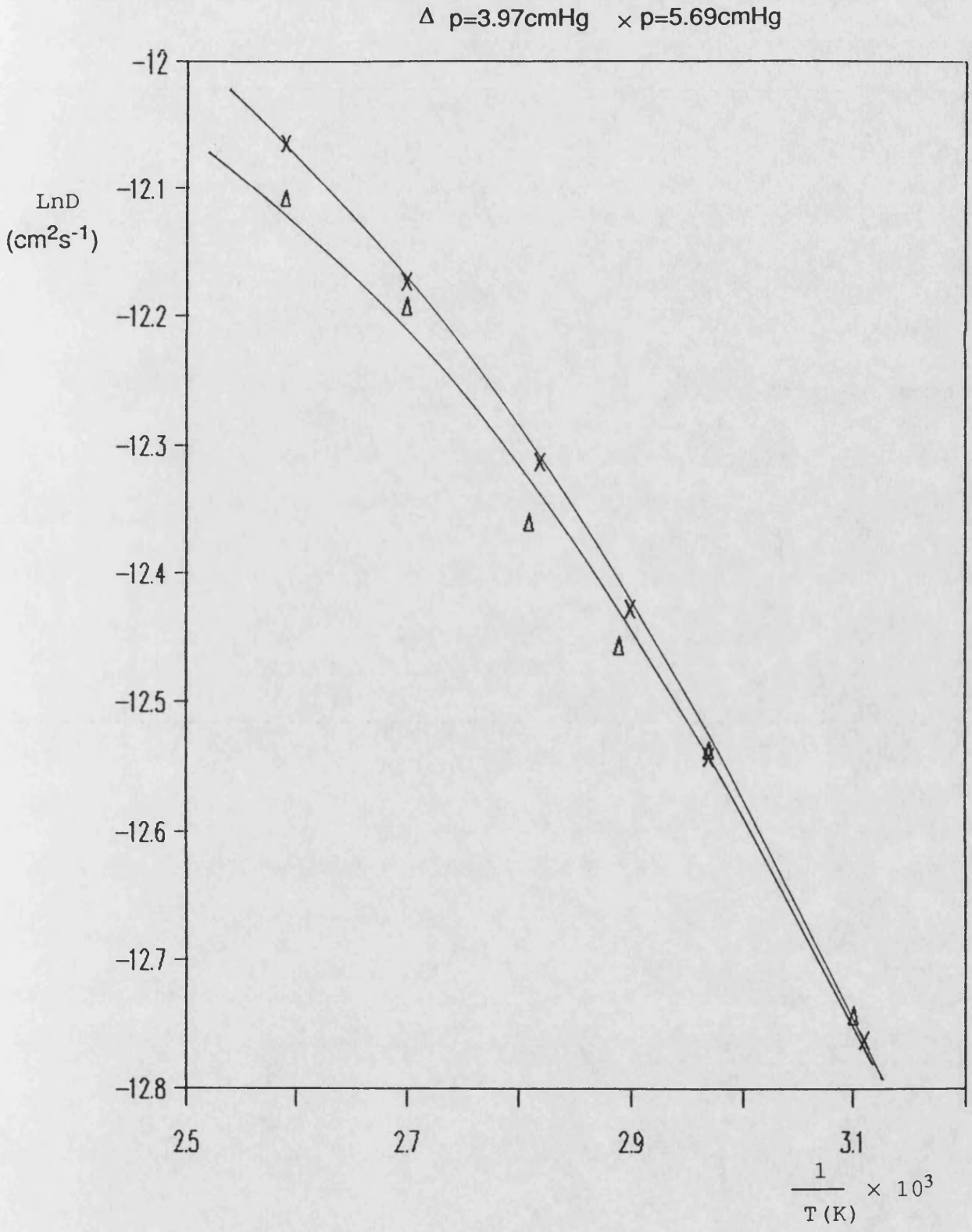

Figure A18a : LnD vs 1/T for Ethanol in Unfilled PDMS.

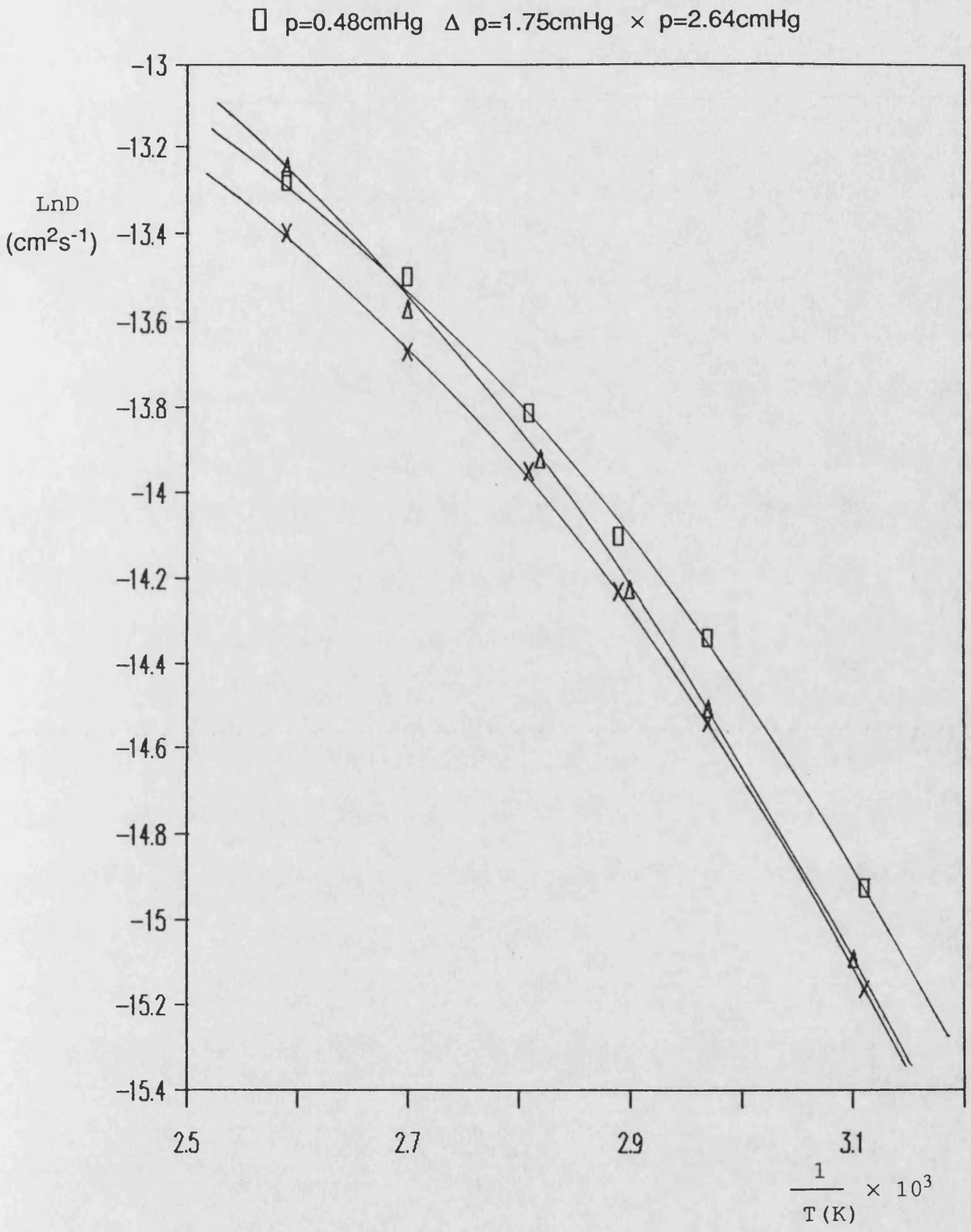

Figure A19 : LnD vs 1/T for Tetrachloroethylene in Unfilled PDMS.

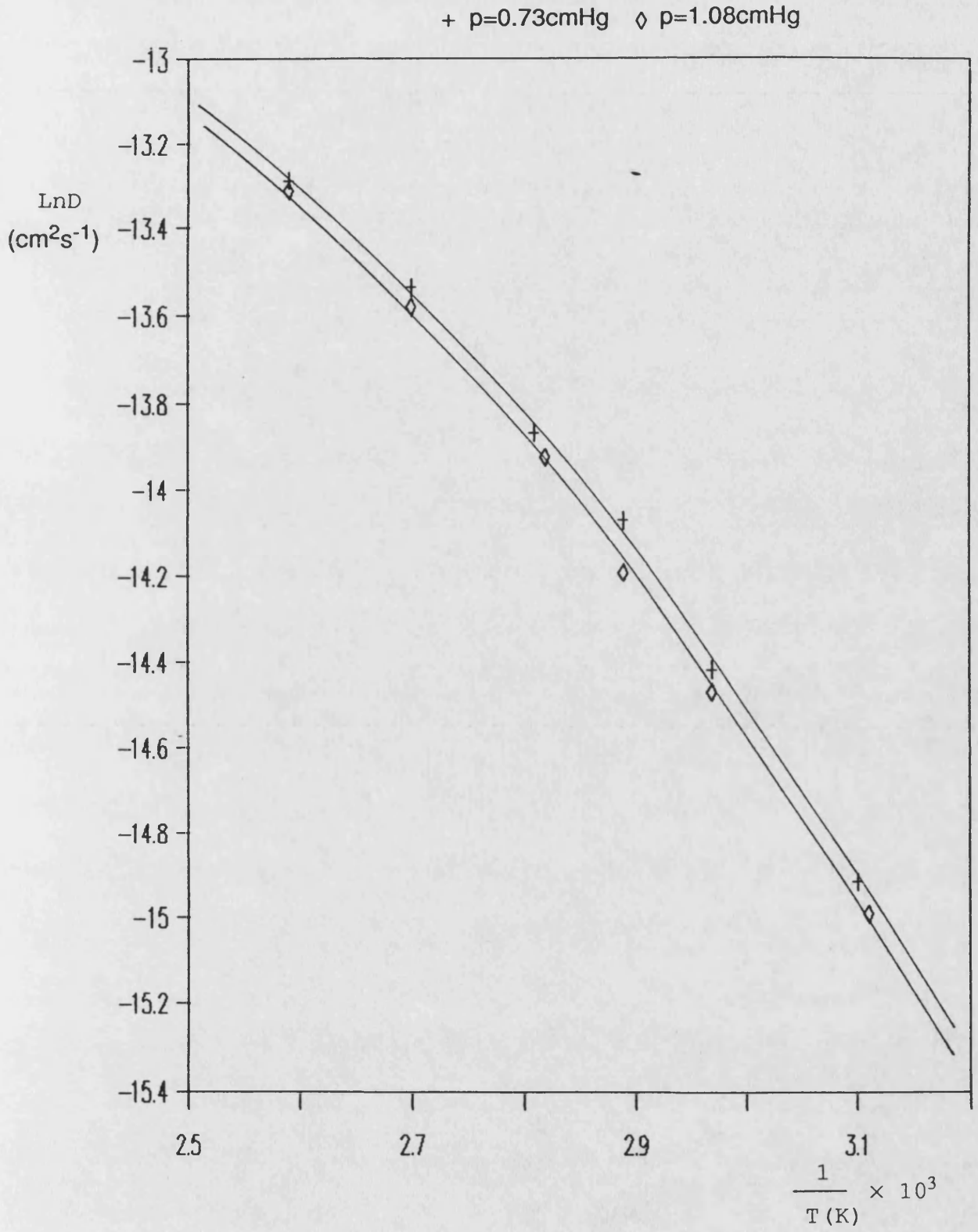

Figure A19a : LnD vs 1/T for Tetrachloroethylene in Unfilled PDMS.

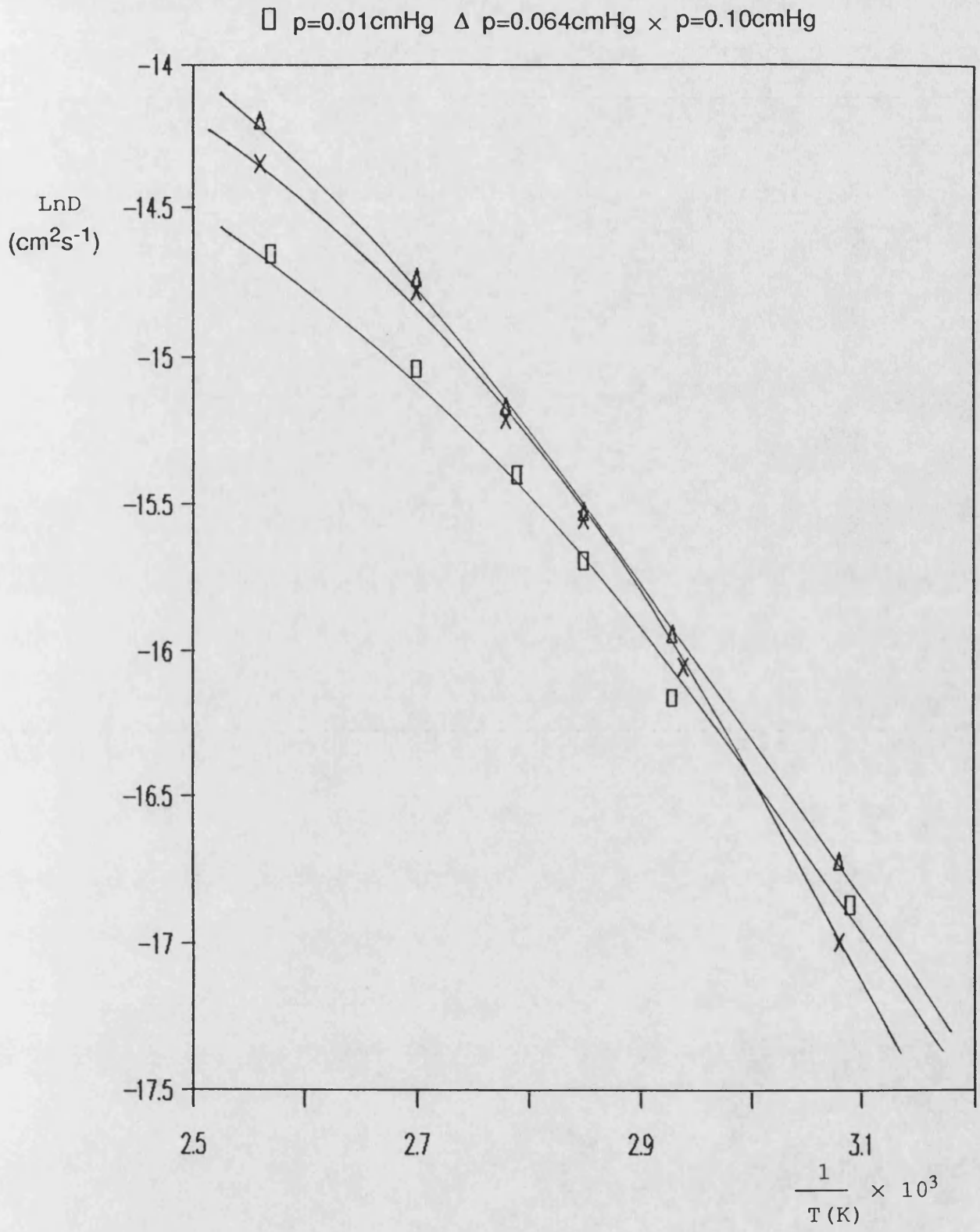

Figure A20 : LnD vs 1/T for Nitrobenzene in Unfilled PDMS.

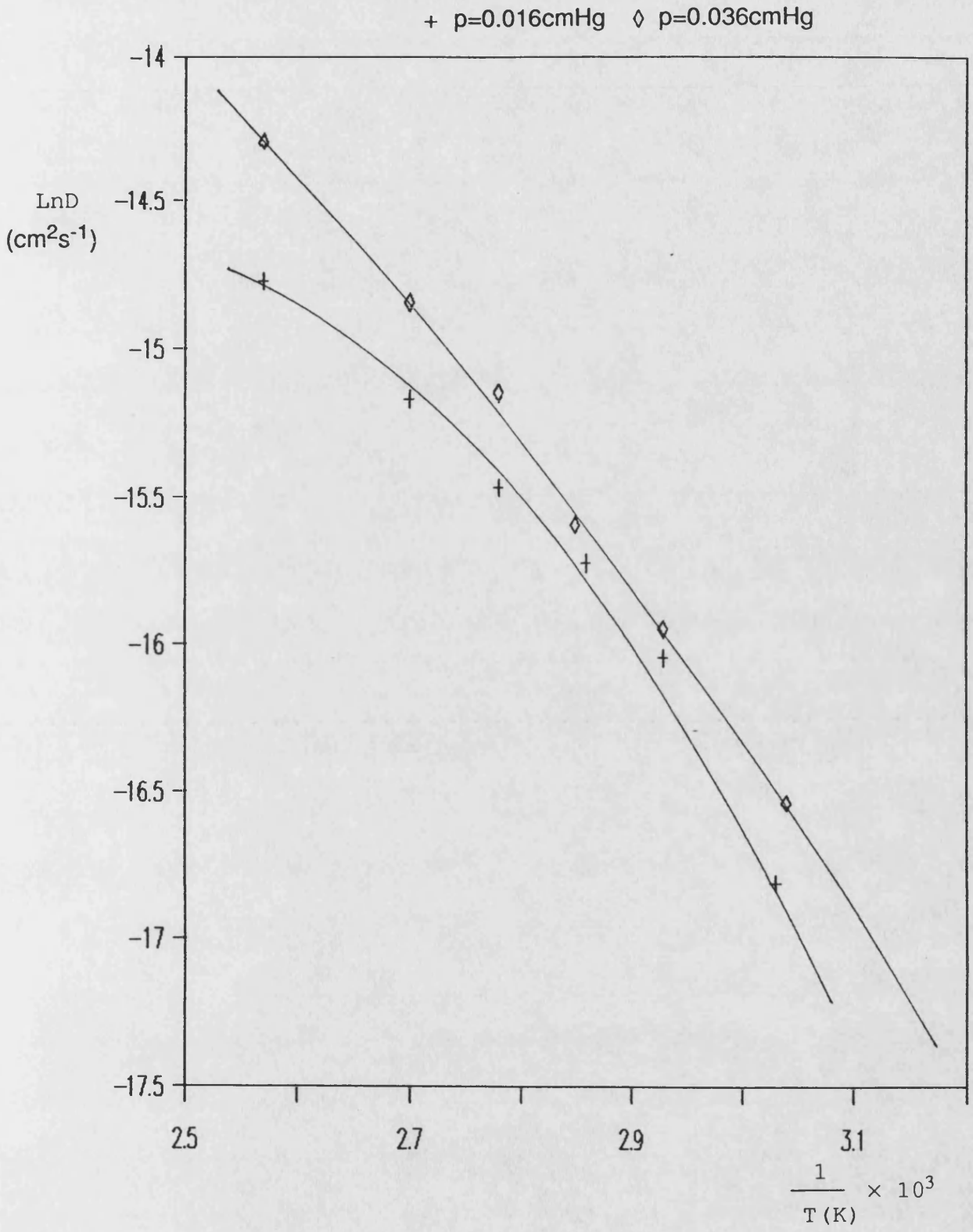

Figure A20a : LnD vs 1/T for Nitrobenzene in Unfilled PDMS.

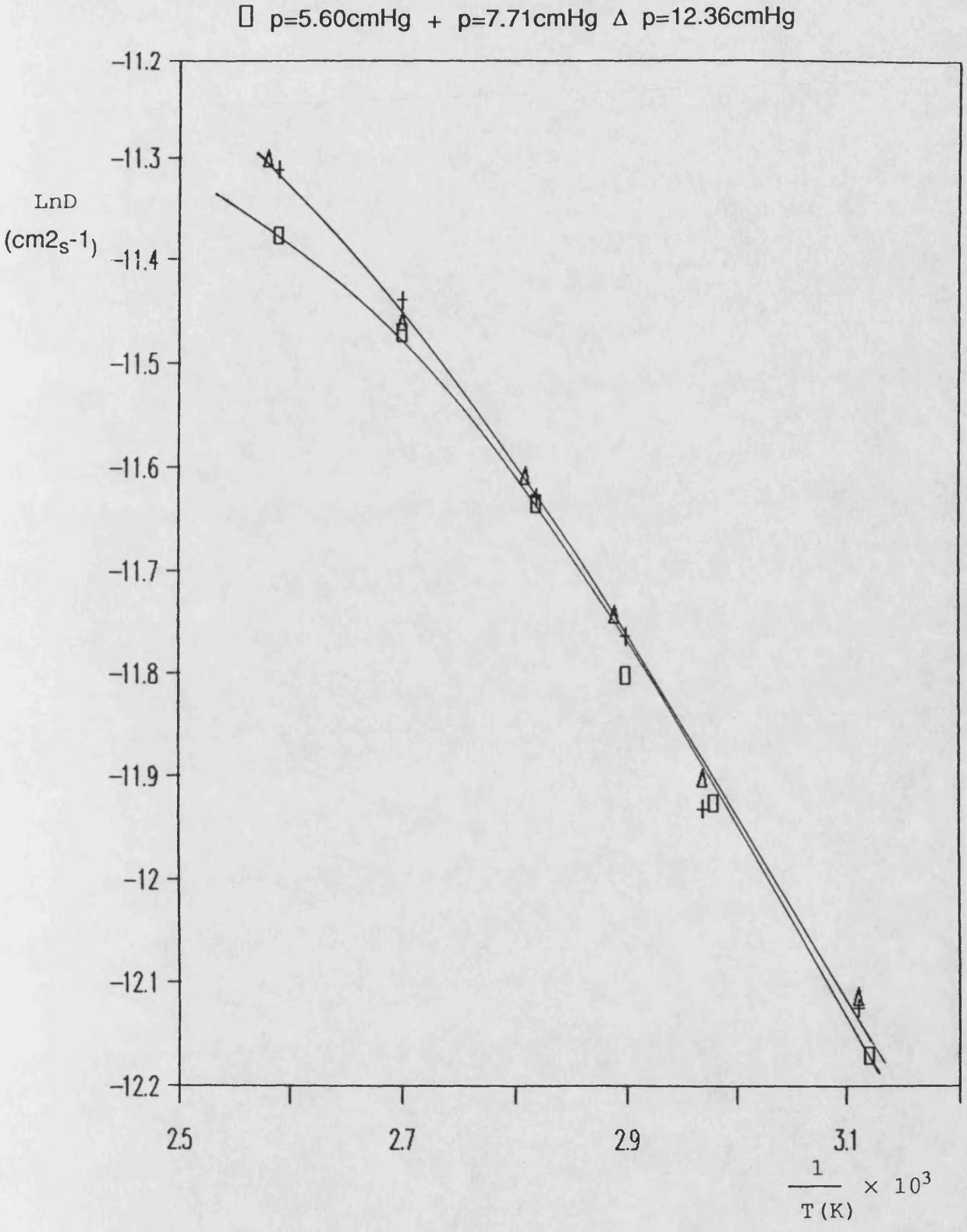

Figure A21 : LnD vs 1/T for Acetone in Ester-substituted PDMS.

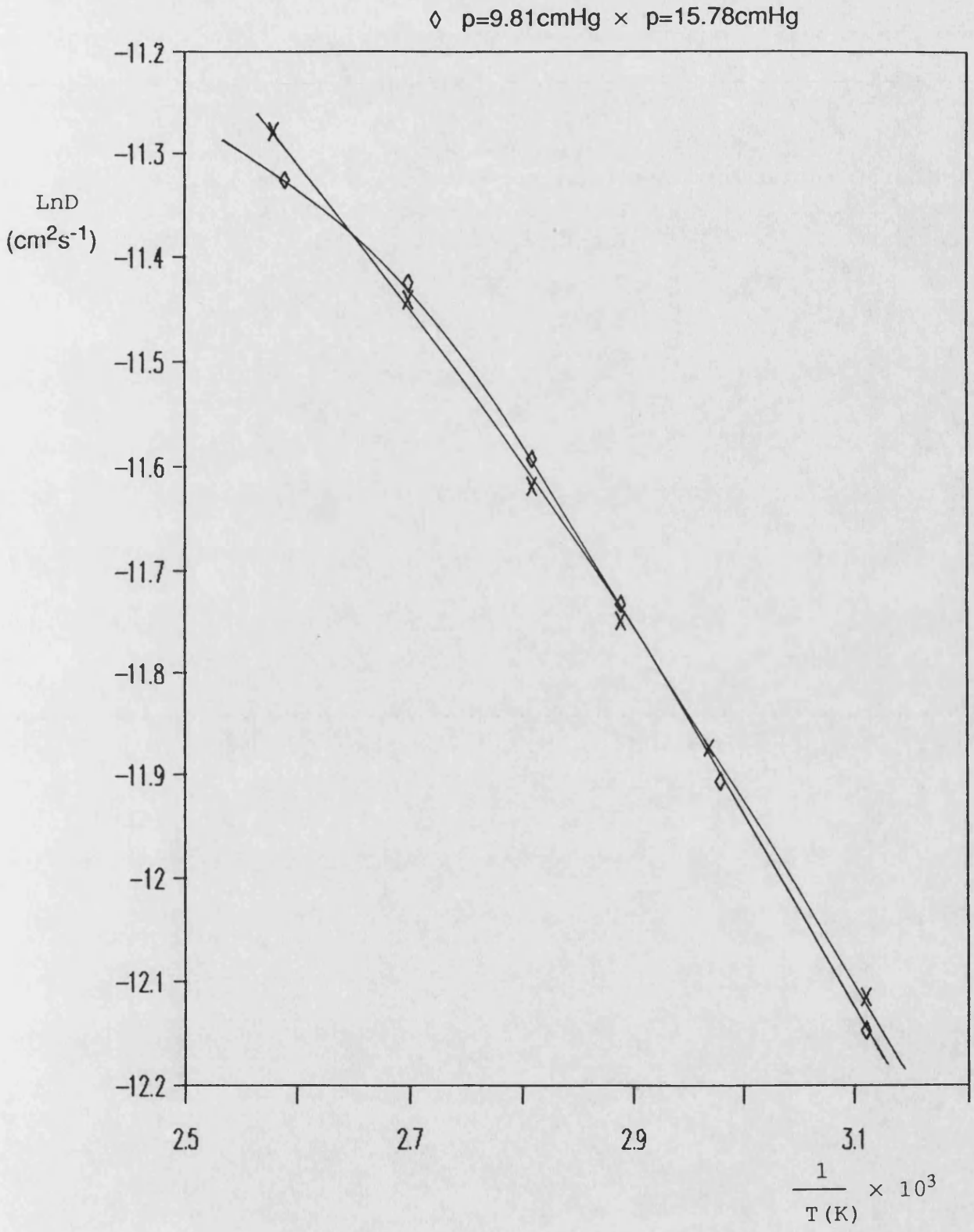

Figure A21a : LnD vs 1/T for Acetone in Ester-substituted PDMS.

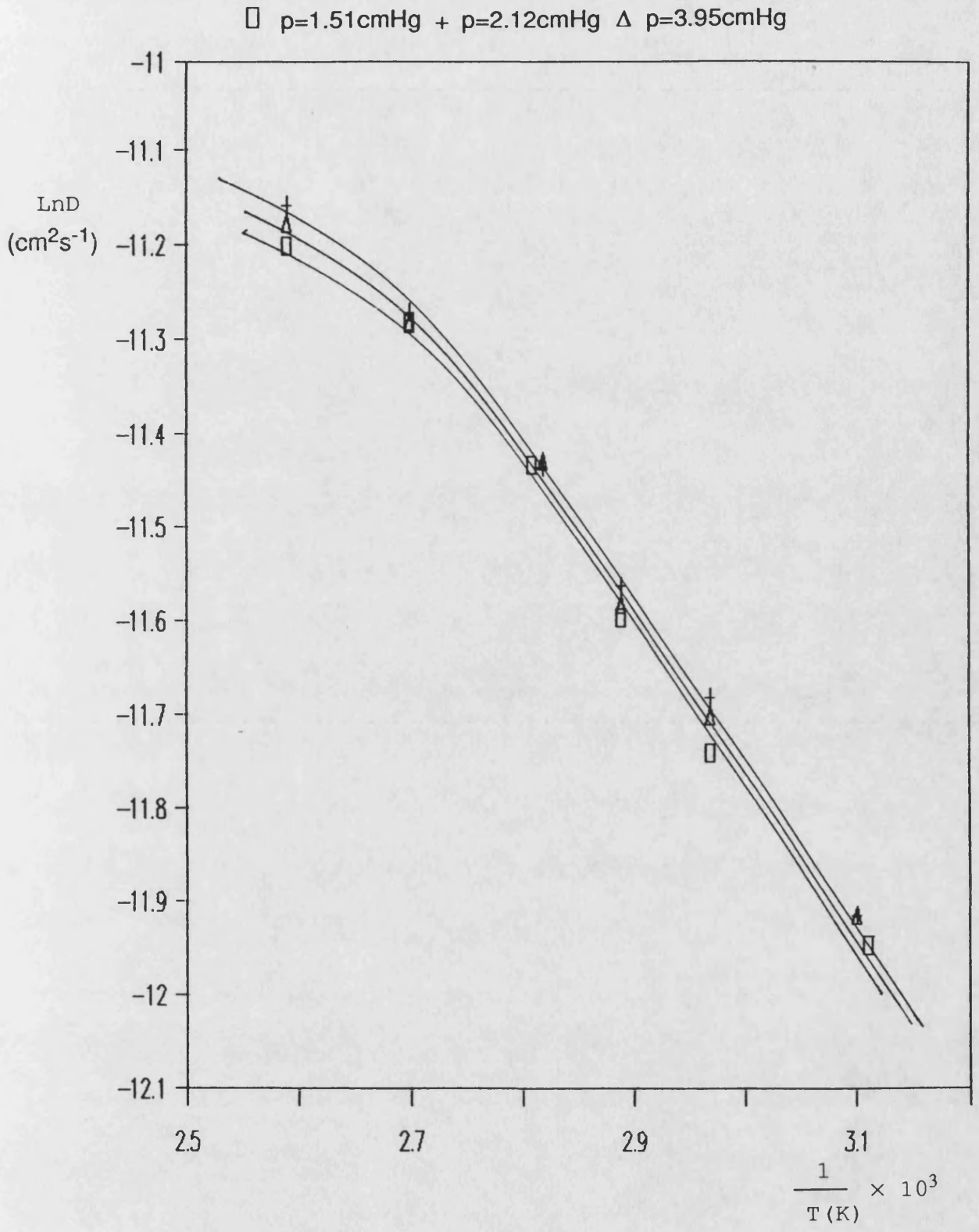

Figure A22 : LnD vs 1/T for Ethanol in Ester-substituted PDMS.

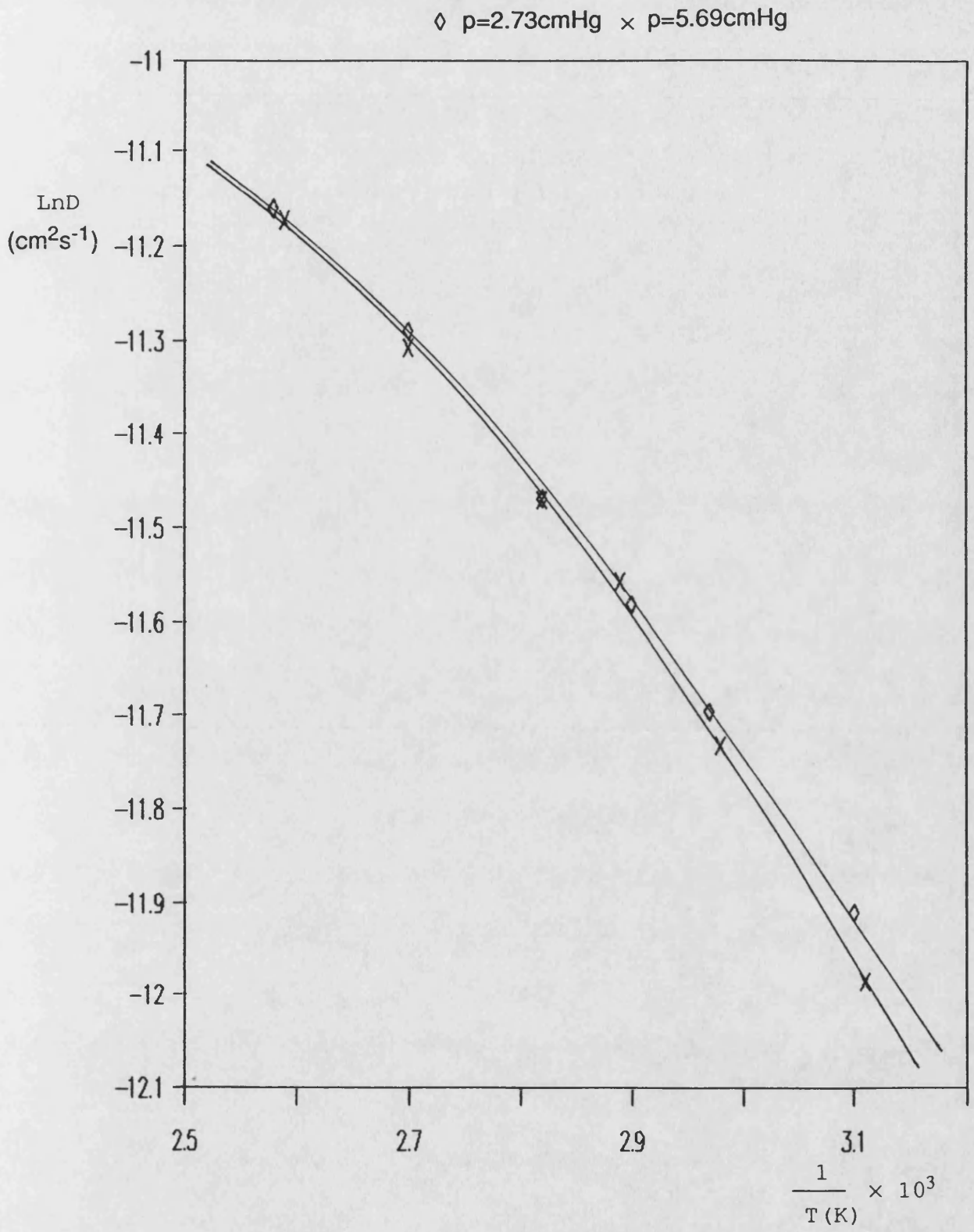

Figure A22a : LnD vs 1/T for Ethanol in Ester-substituted PDMS.

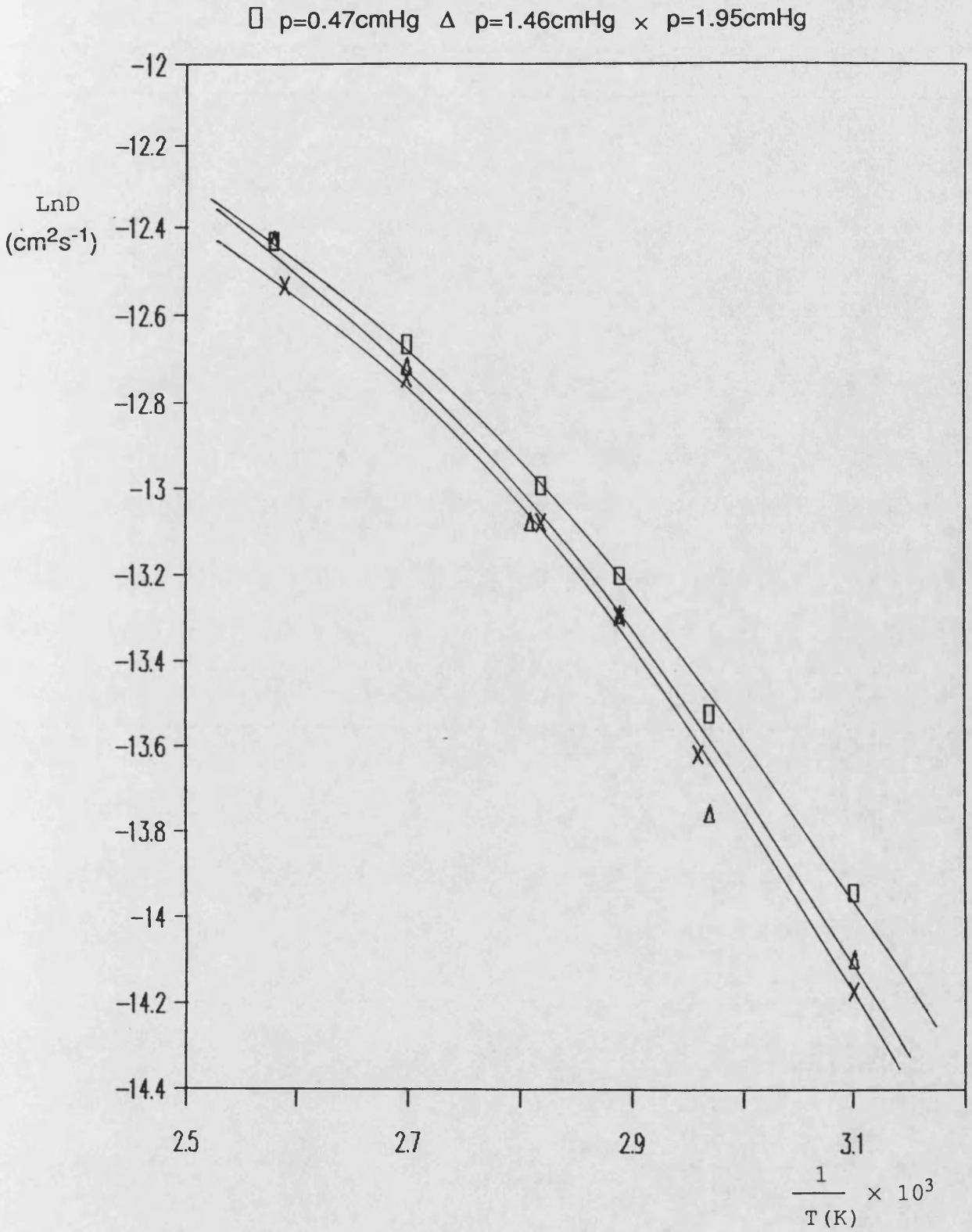

Figure A23 : LnD vs 1/T for Tetrachloroethylene in Ester-substituted PDMS.

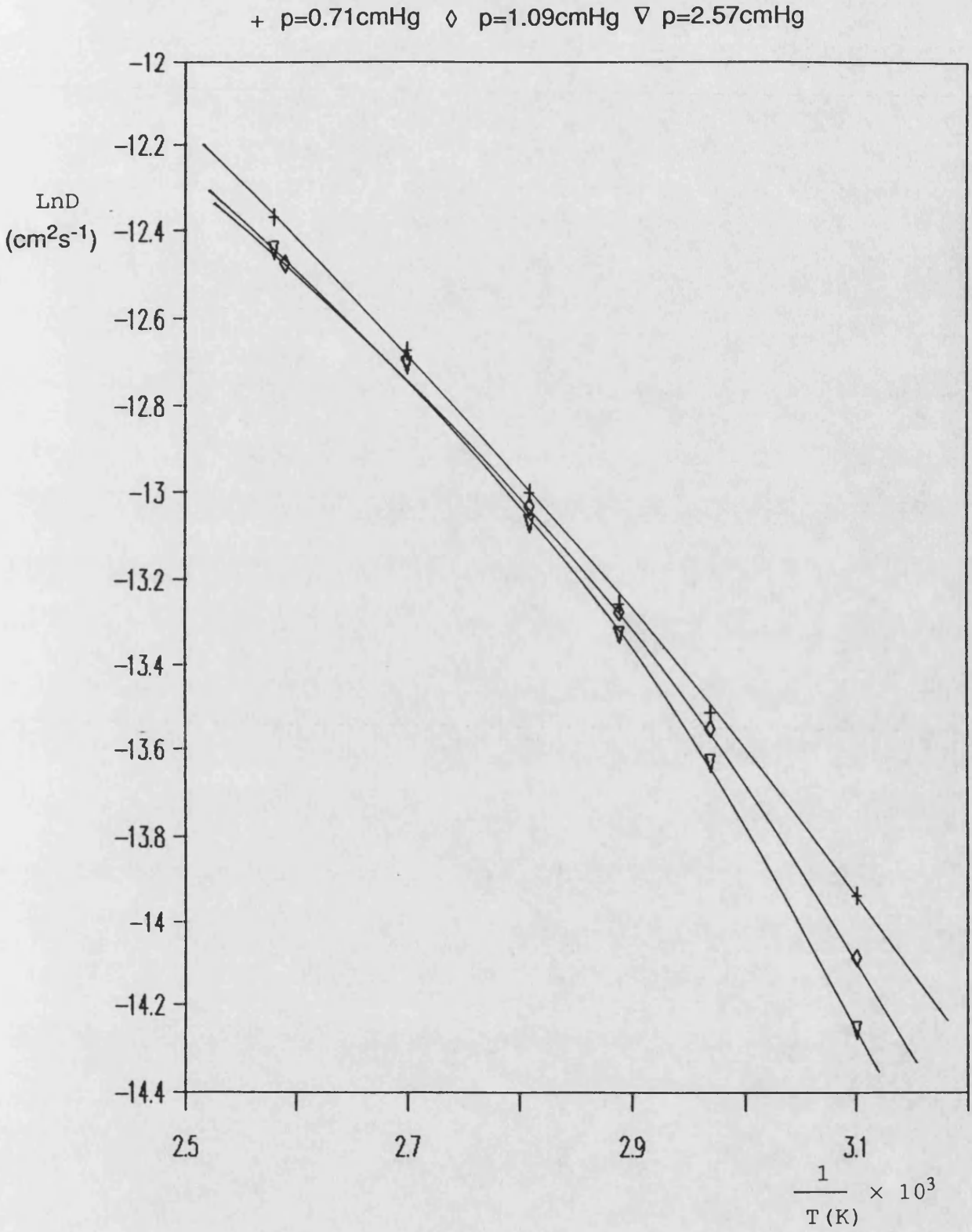

Figure A23a : LnD vs 1/T for Tetrachloroethylene in Ester-substituted PDMS.

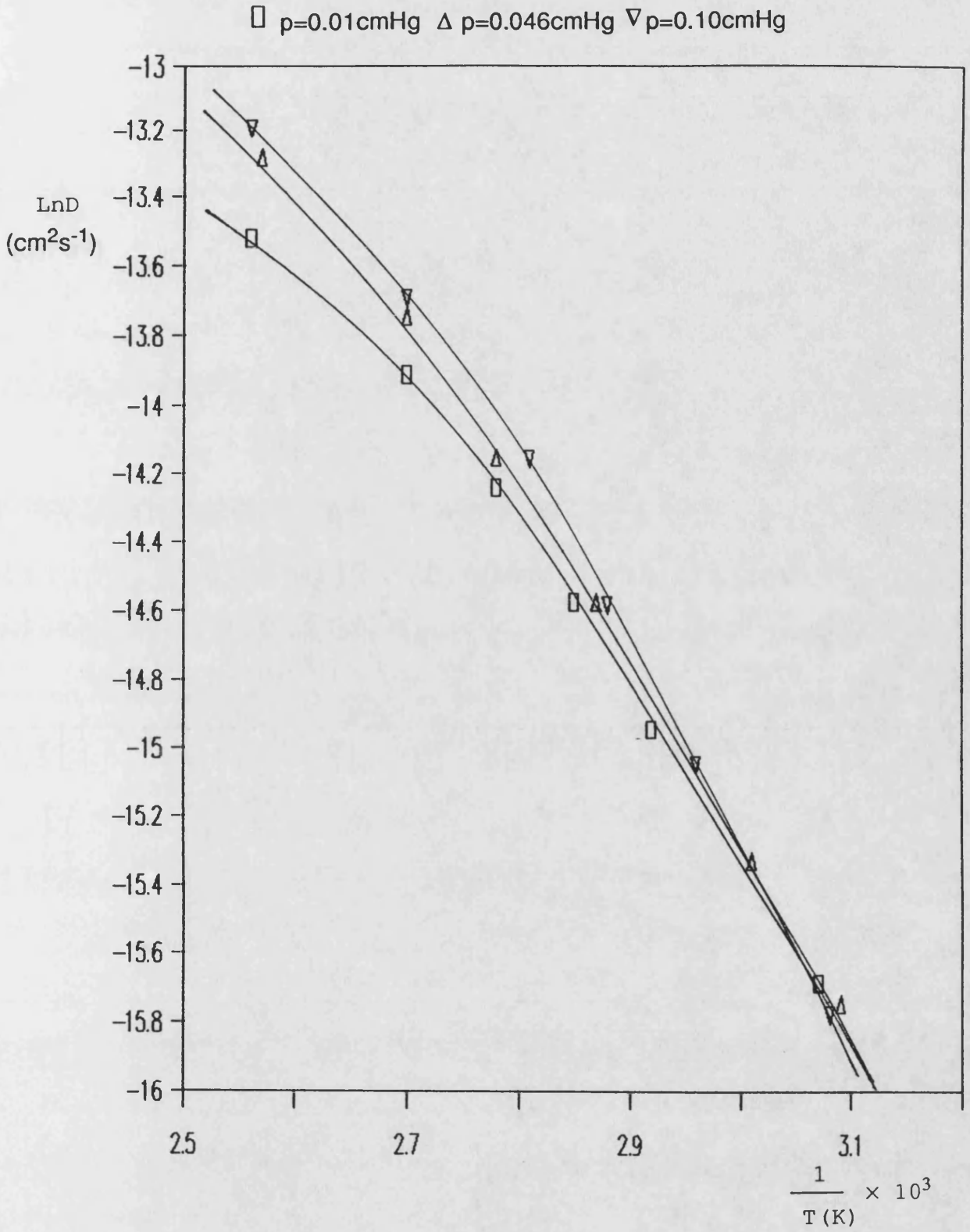

Figure A24 : LnD vs 1/T for Nitrobenzene in Ester-substituted PDMS.

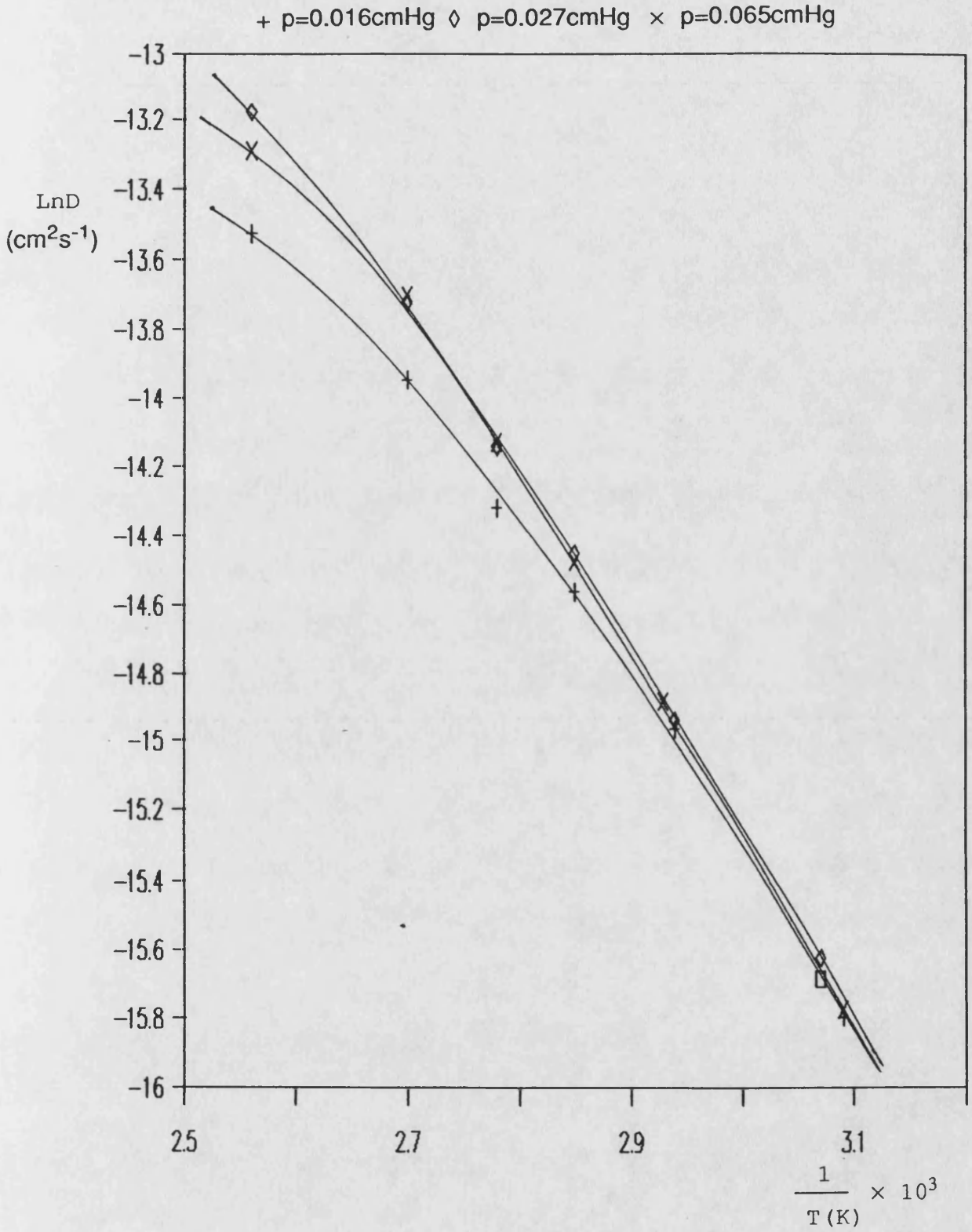

Figure A24a : LnD vs 1/T for Nitrobenzene in Ester-substituted PDMS.

Arrhenius Plots for

Solubility

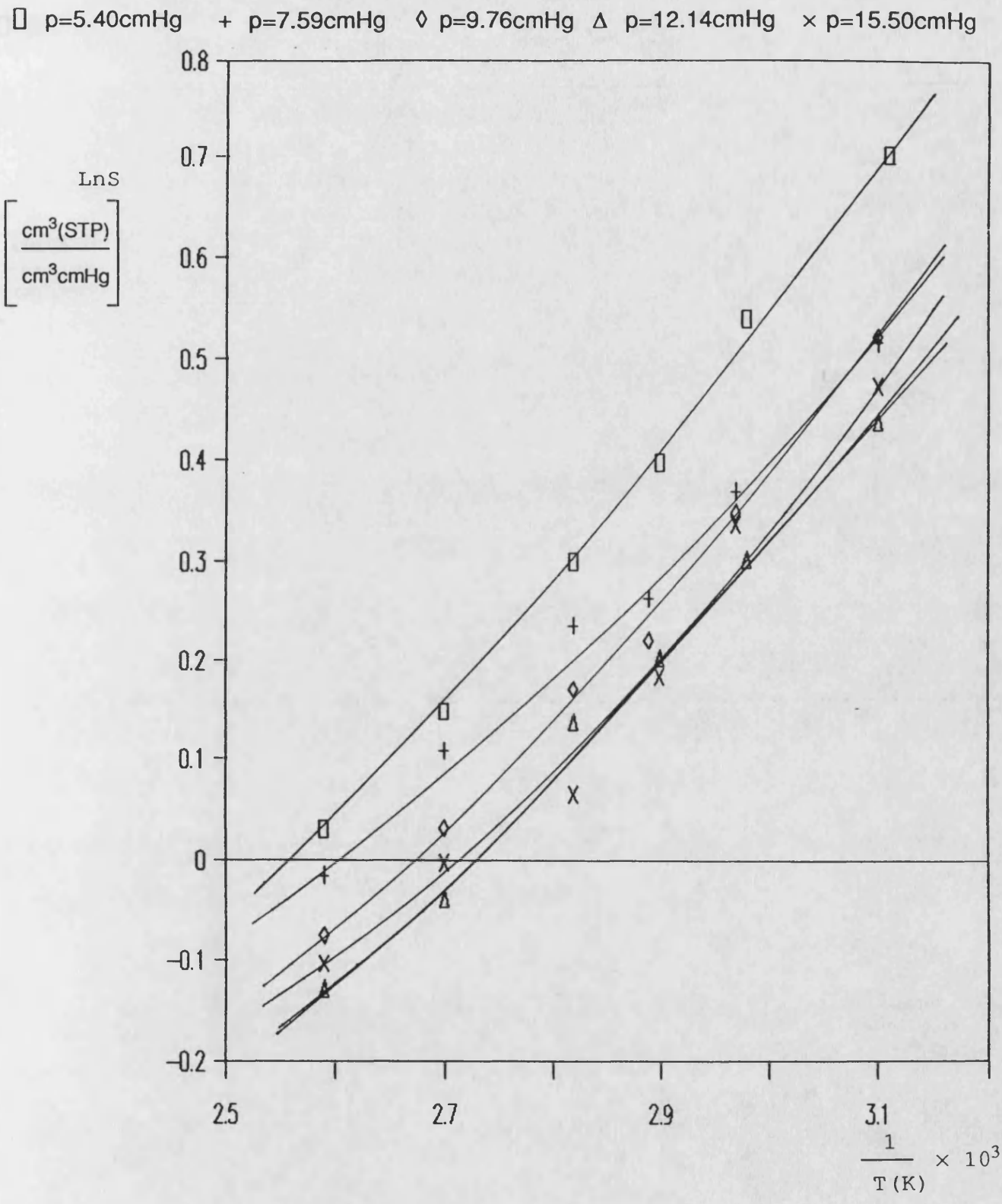

Figure A25 : LnS vs 1/T for Acetone in Filled PDMS.

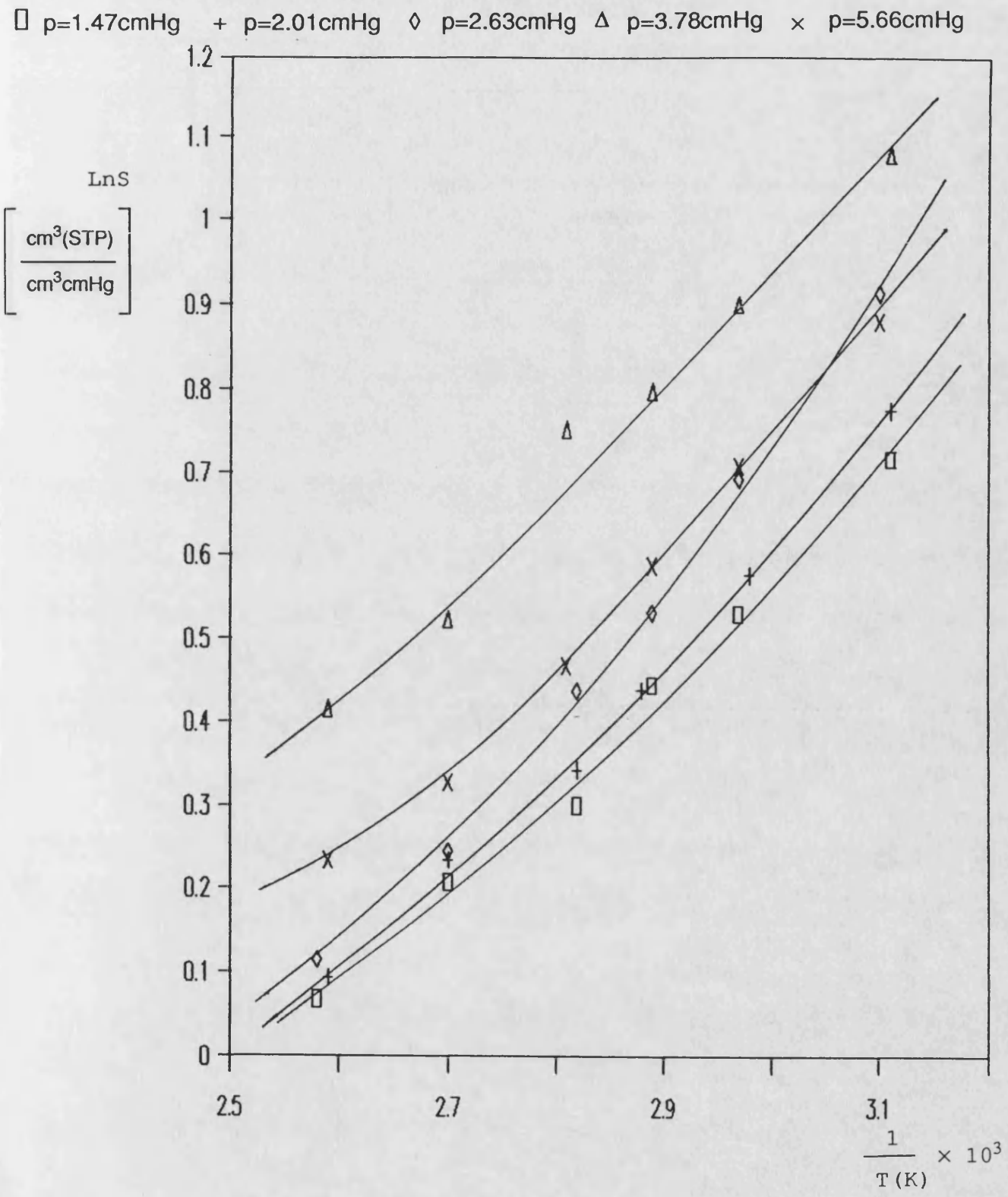

Figure A26 : LnS vs 1/T for Ethanol in Filled PDMS.

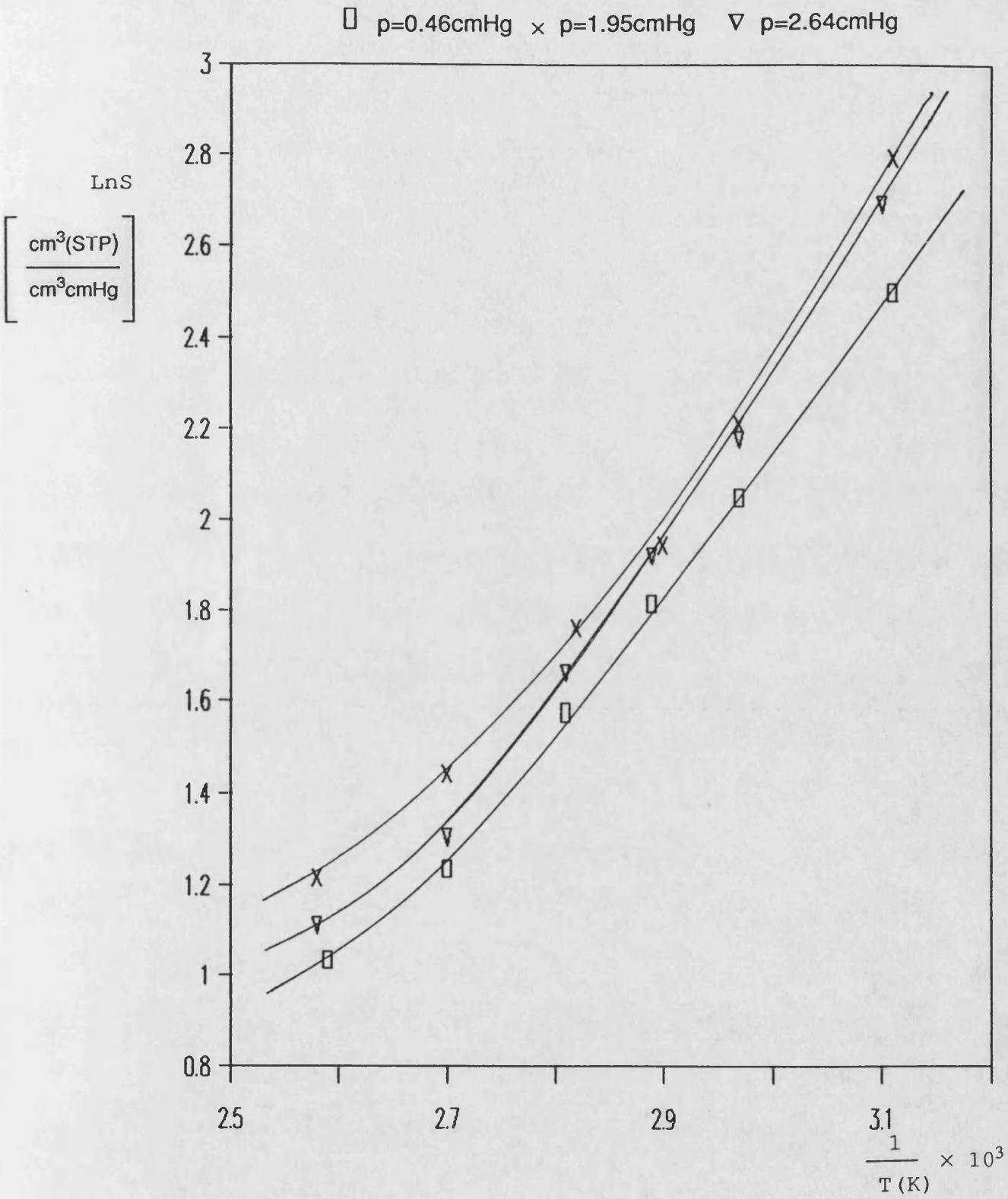

Figure A27 : LnS vs 1/T for Tetrachloroethylene in Filled PDMS.

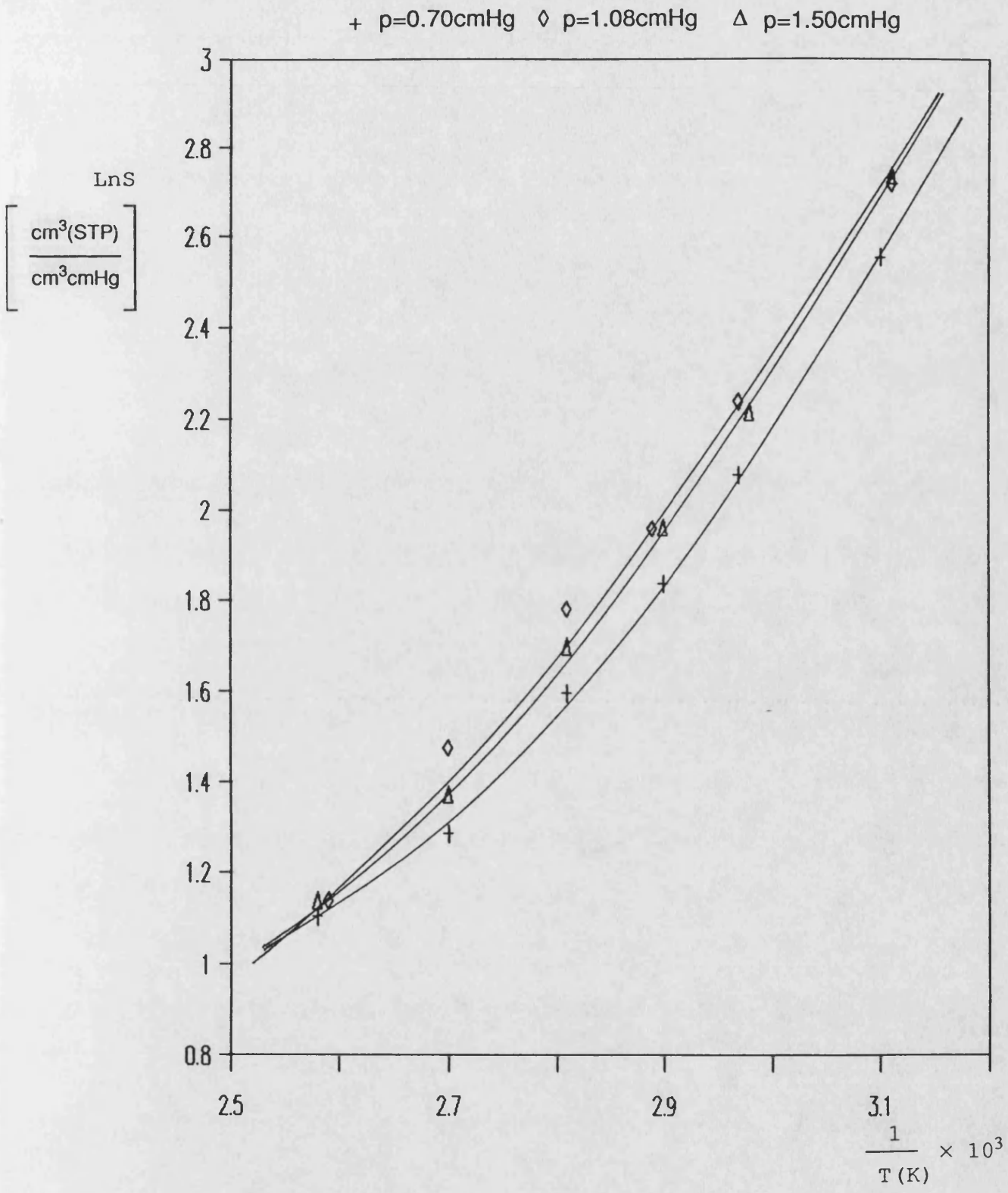

Figure A27a : LnS vs 1/T for Tetrachloroethylene in Filled PDMS.

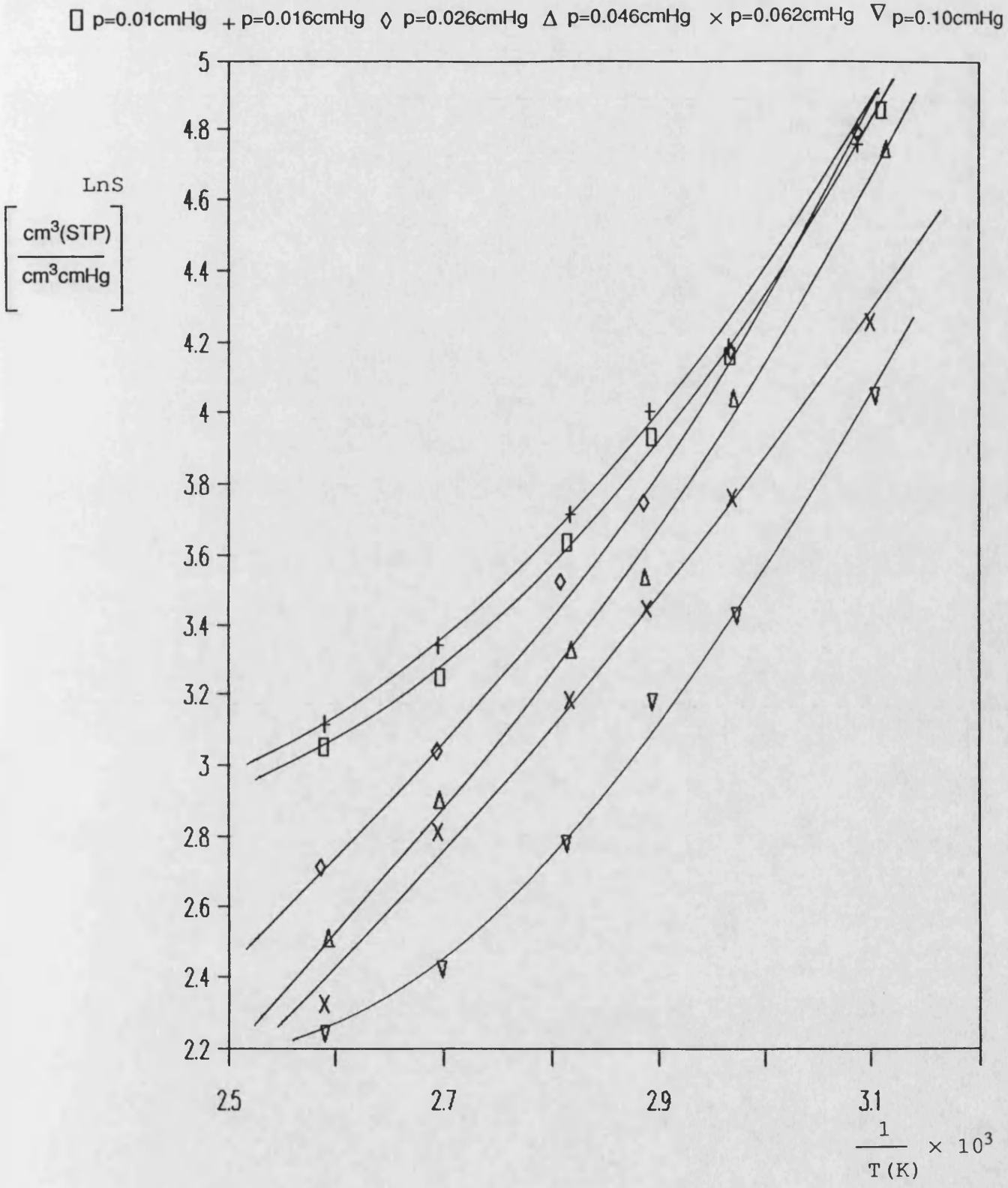

Figure A28 : LnS vs 1/T for Nitrobenzene in Filled PDMS.

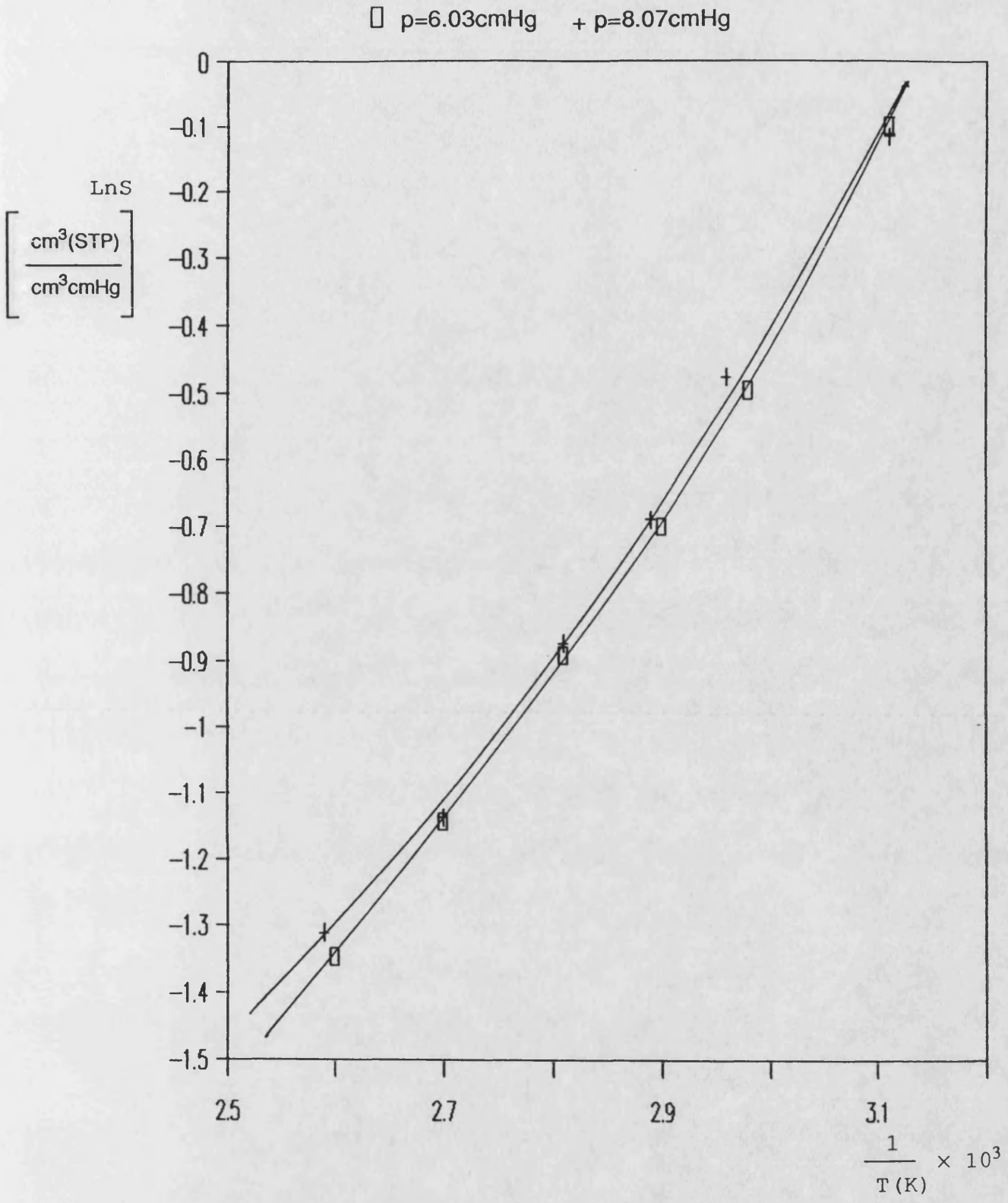

Figure A29 : LnS vs 1/T for Acetone in Unfilled PDMS.

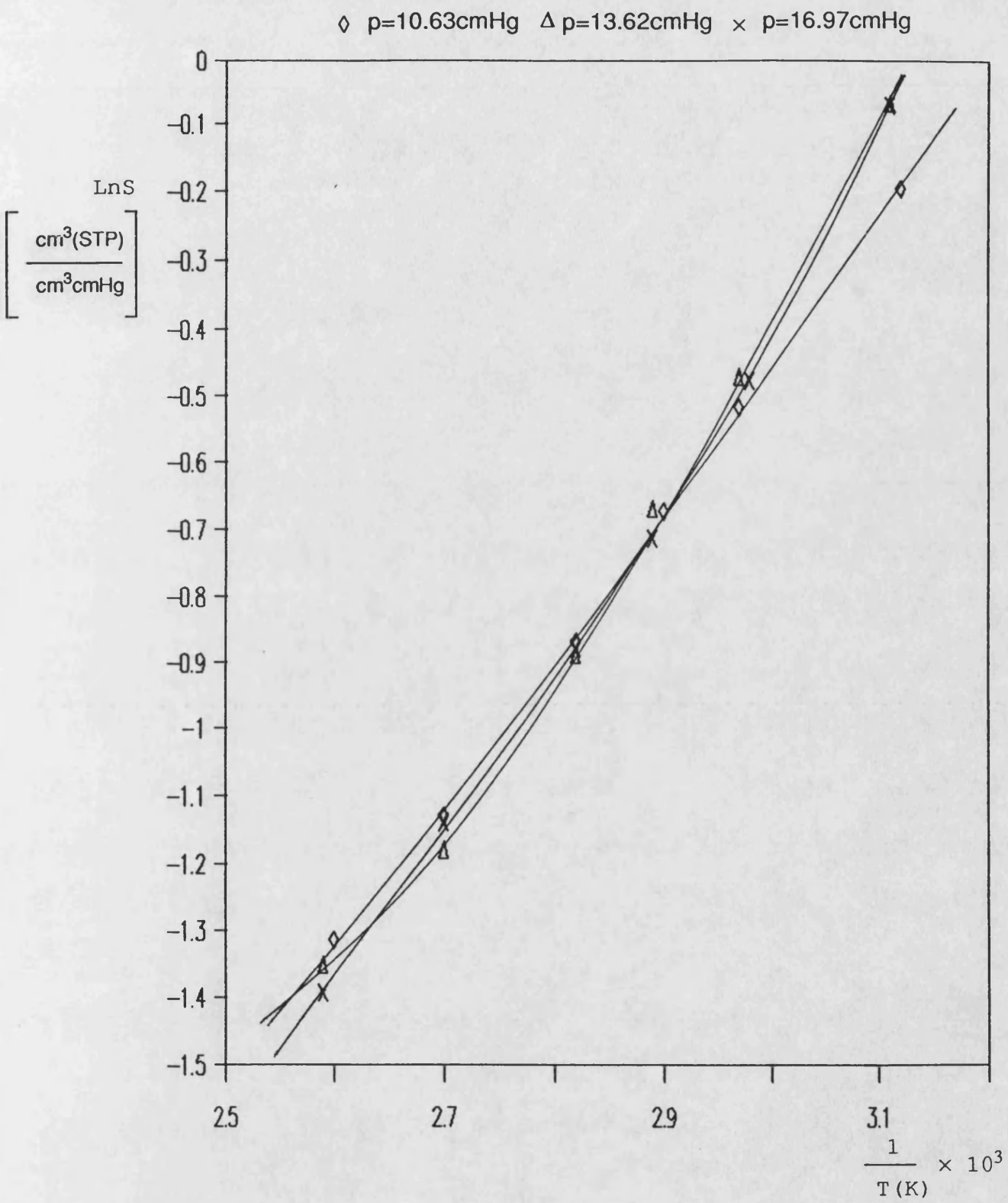

Figure A29a : LnS vs 1/T for Acetone in Unfilled PDMS.

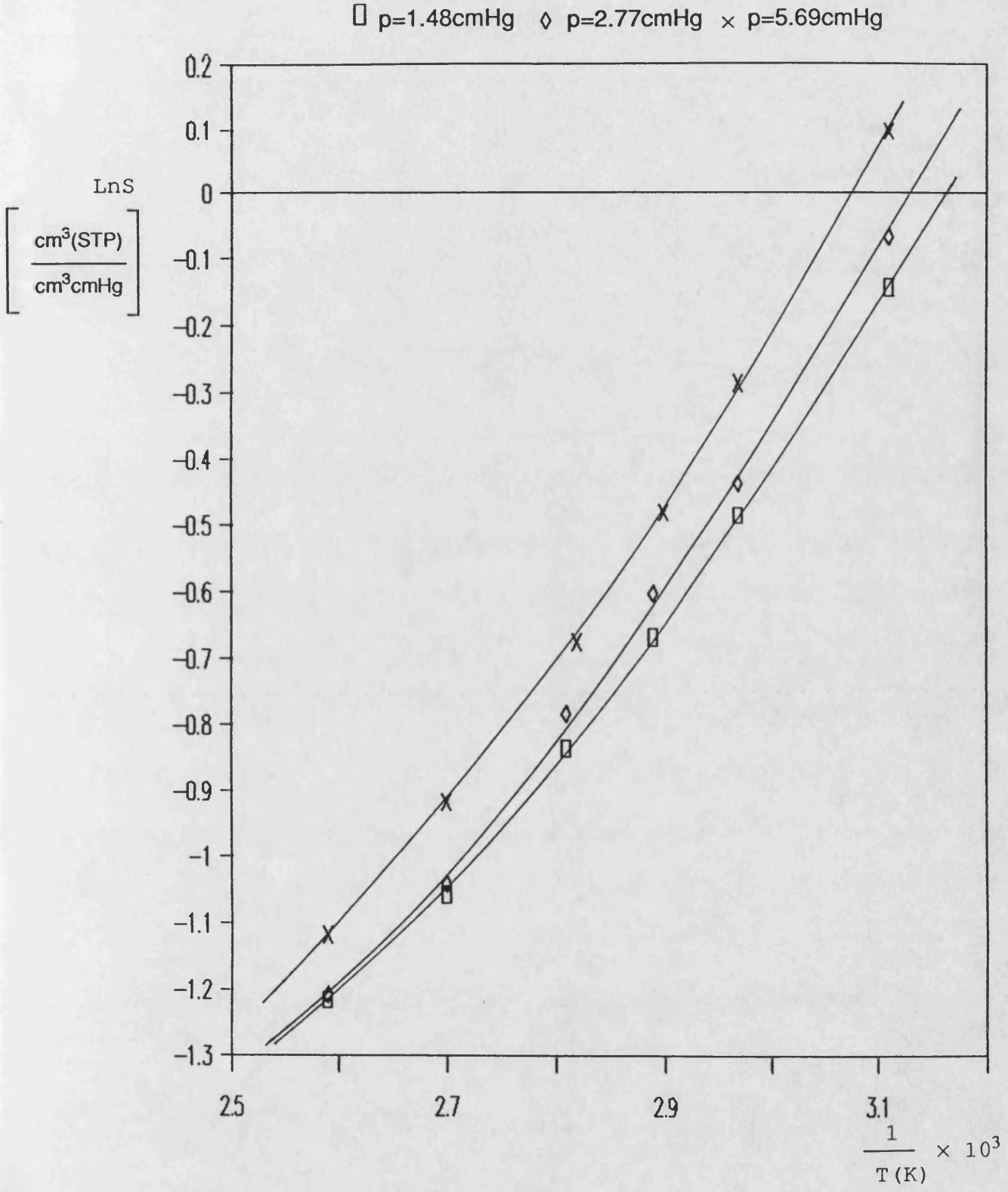

Figure A30 : LnS vs 1/T for Ethanol in Unfilled PDMS.

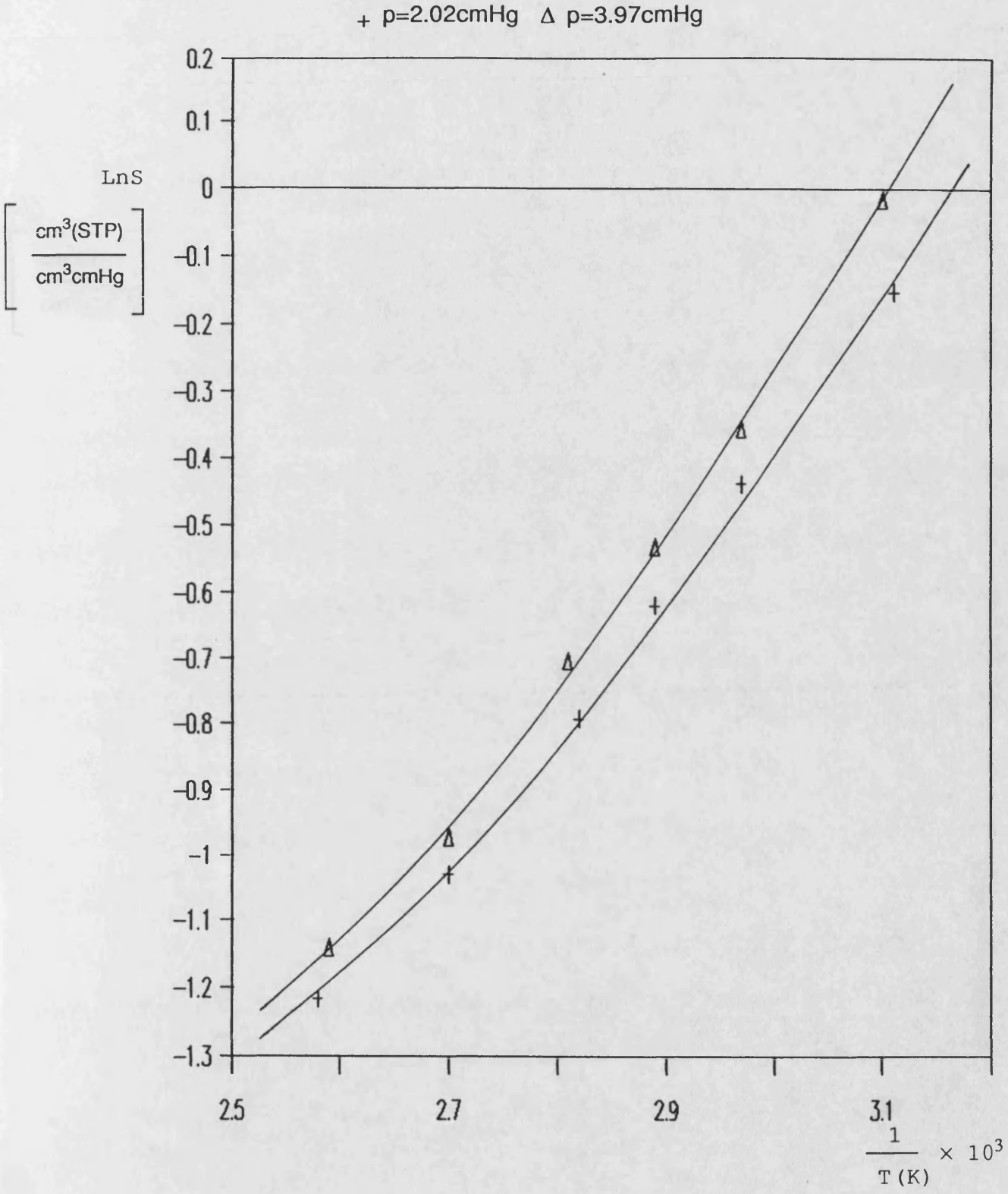

Figure A30a : LnS vs 1/T for Ethanol in Unfilled PDMS.

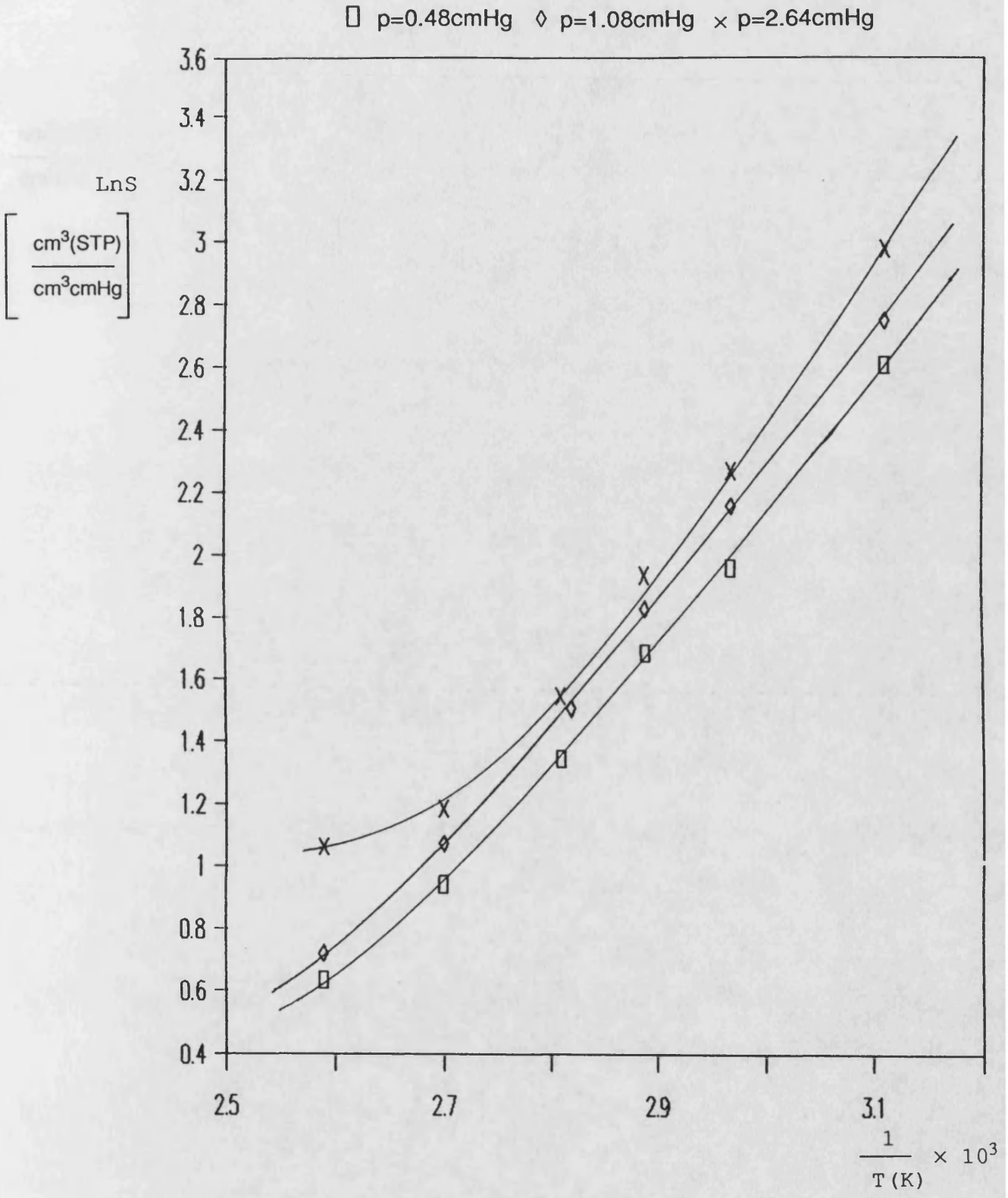

Figure A31 : LnS vs 1/T for Tetrachloroethylene in Unfilled PDMS.

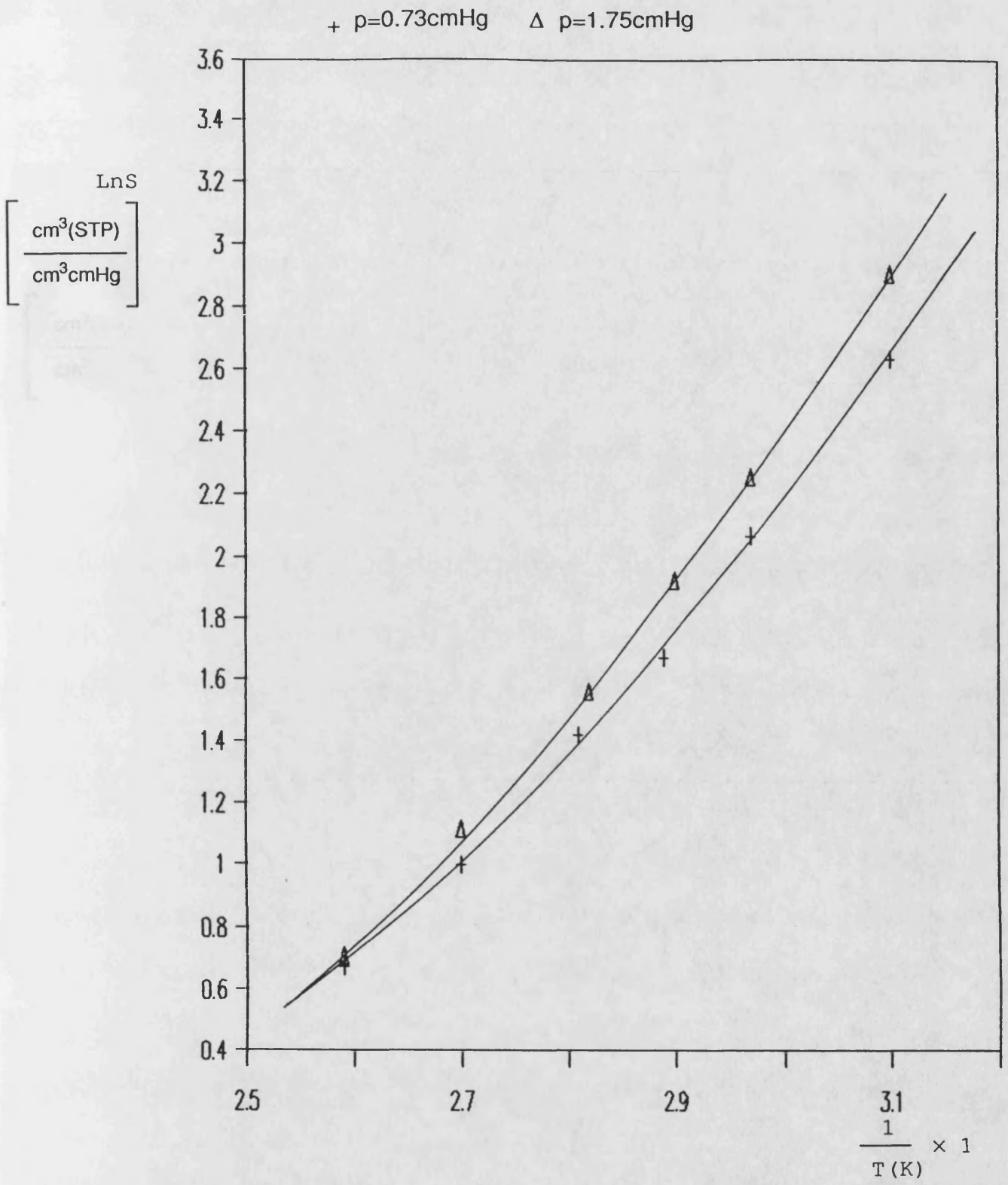

Figure A31a : LnS vs 1/T for Tetrachloroethylene in Unfilled PDMS.

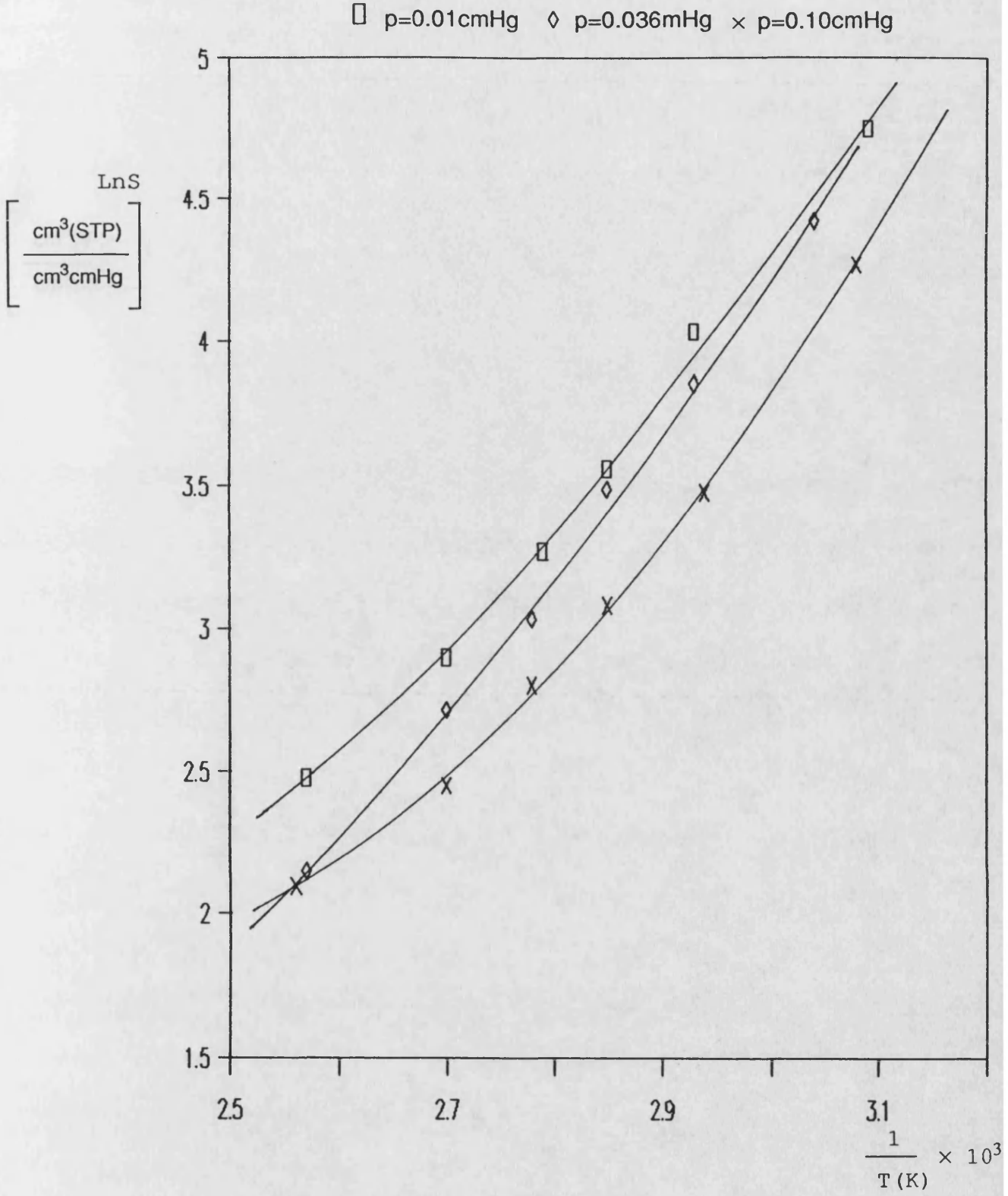

Figure A32 : LnS vs 1/T for Nitrobenzene in Unfilled PDMS.

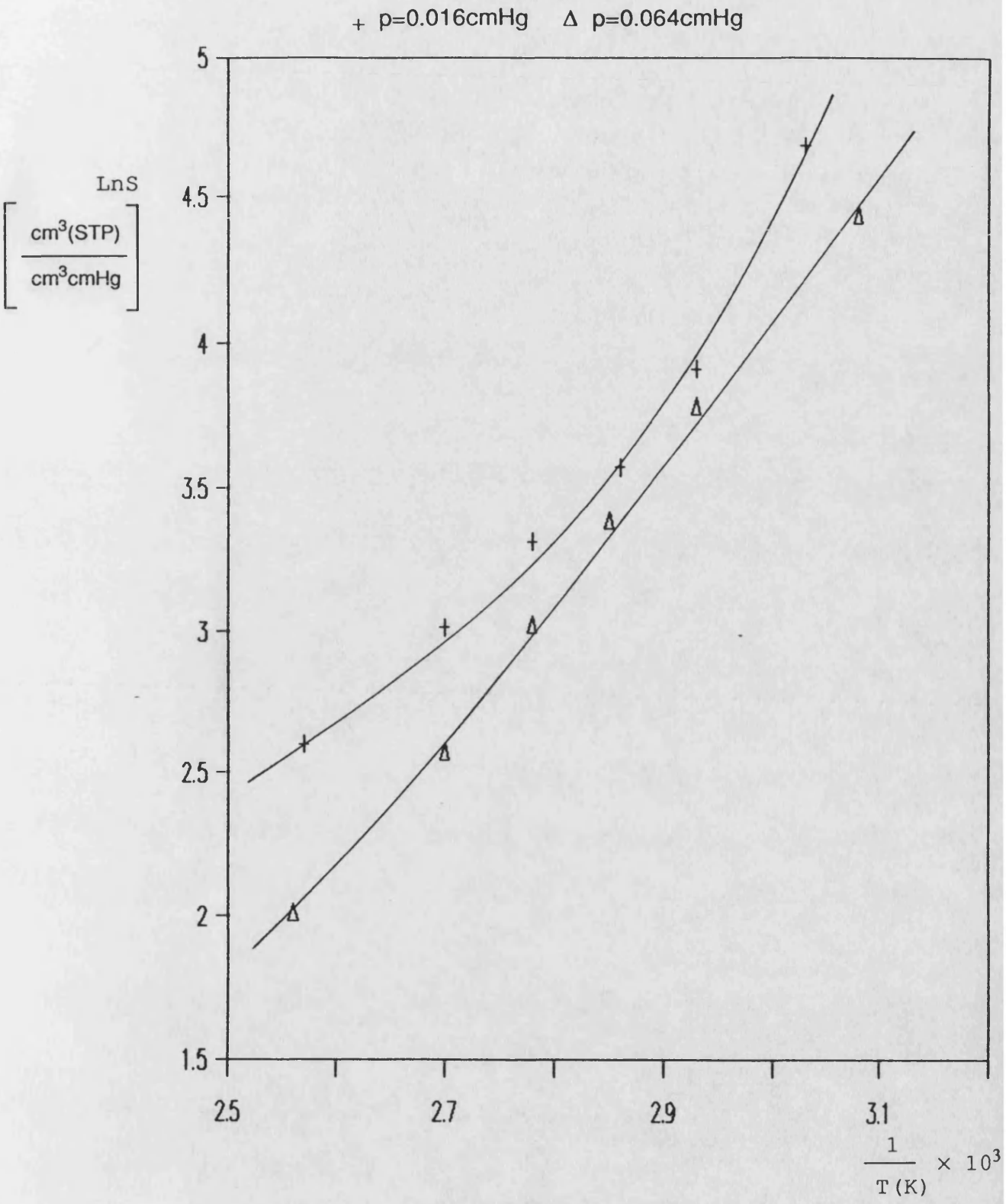

Figure A32a : LnS vs 1/T for Nitrobenzene in Unfilled PDMS.

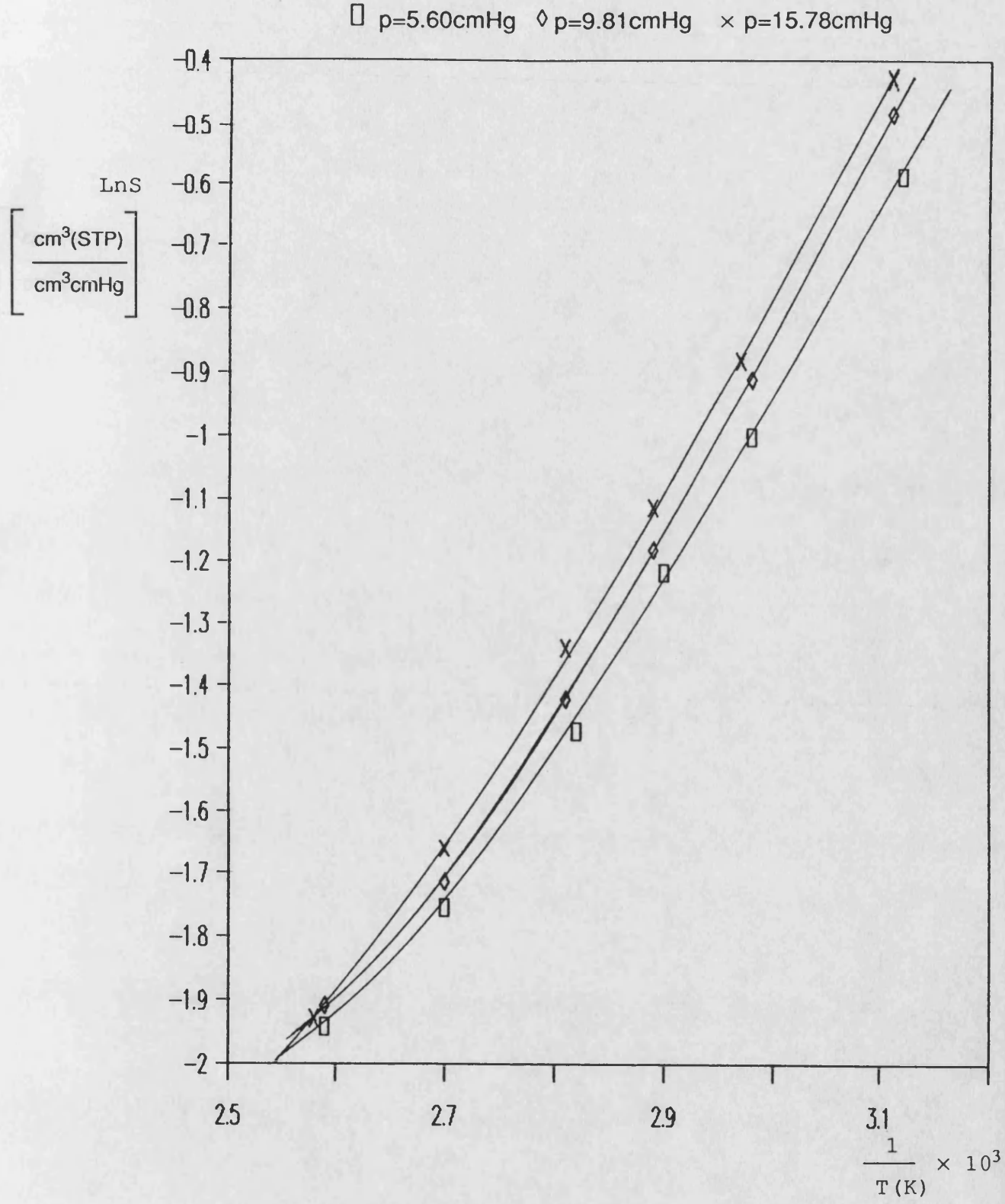

Figure A33: LnS vs 1/T for Acetone in Ester-substituted PDMS.

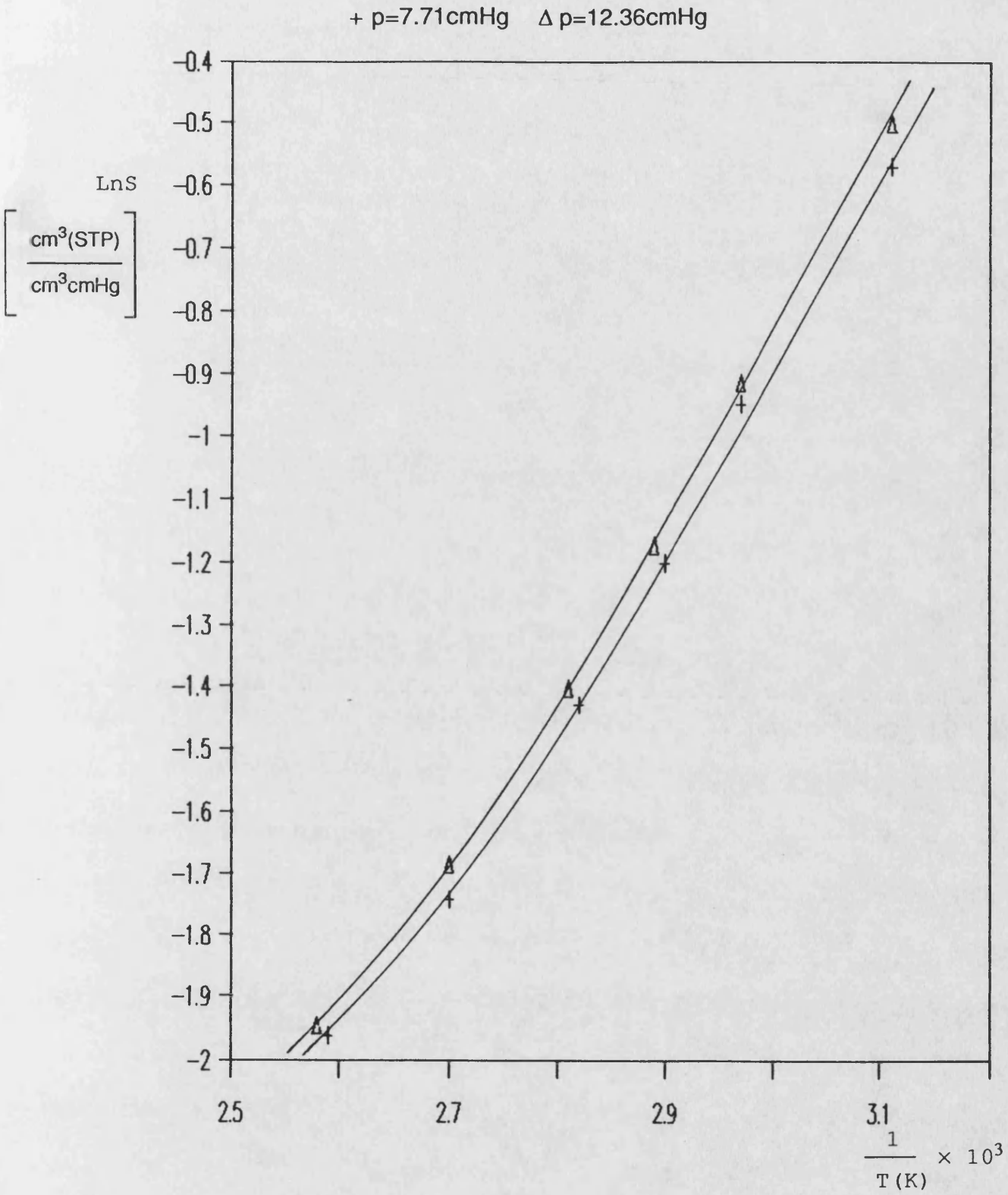

Figure A33a : LnS vs 1/T for Acetone in Ester-substituted PDMS.

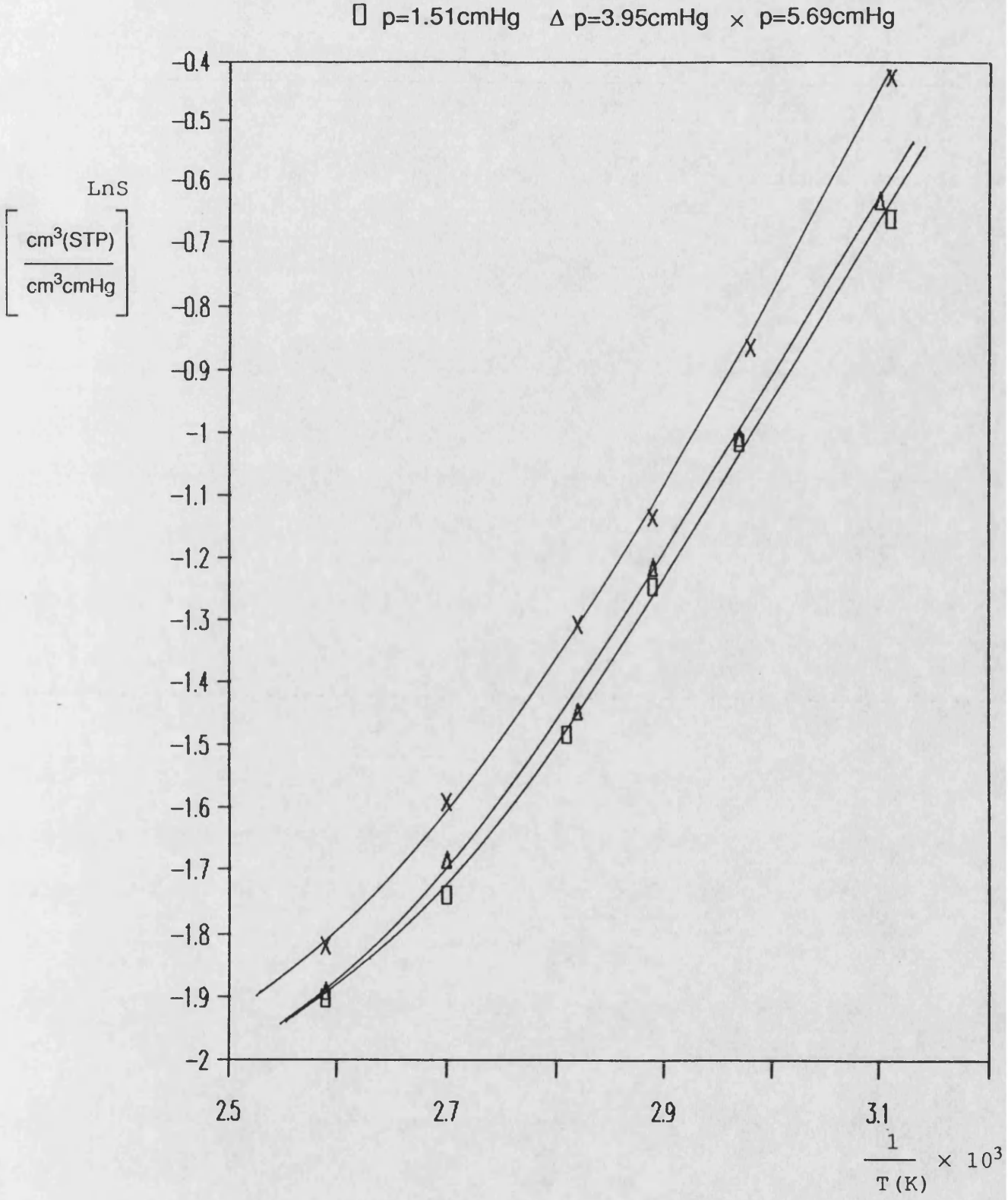

Figure A34 : LnS vs 1/T for Ethanol in Ester-substituted PDMS.

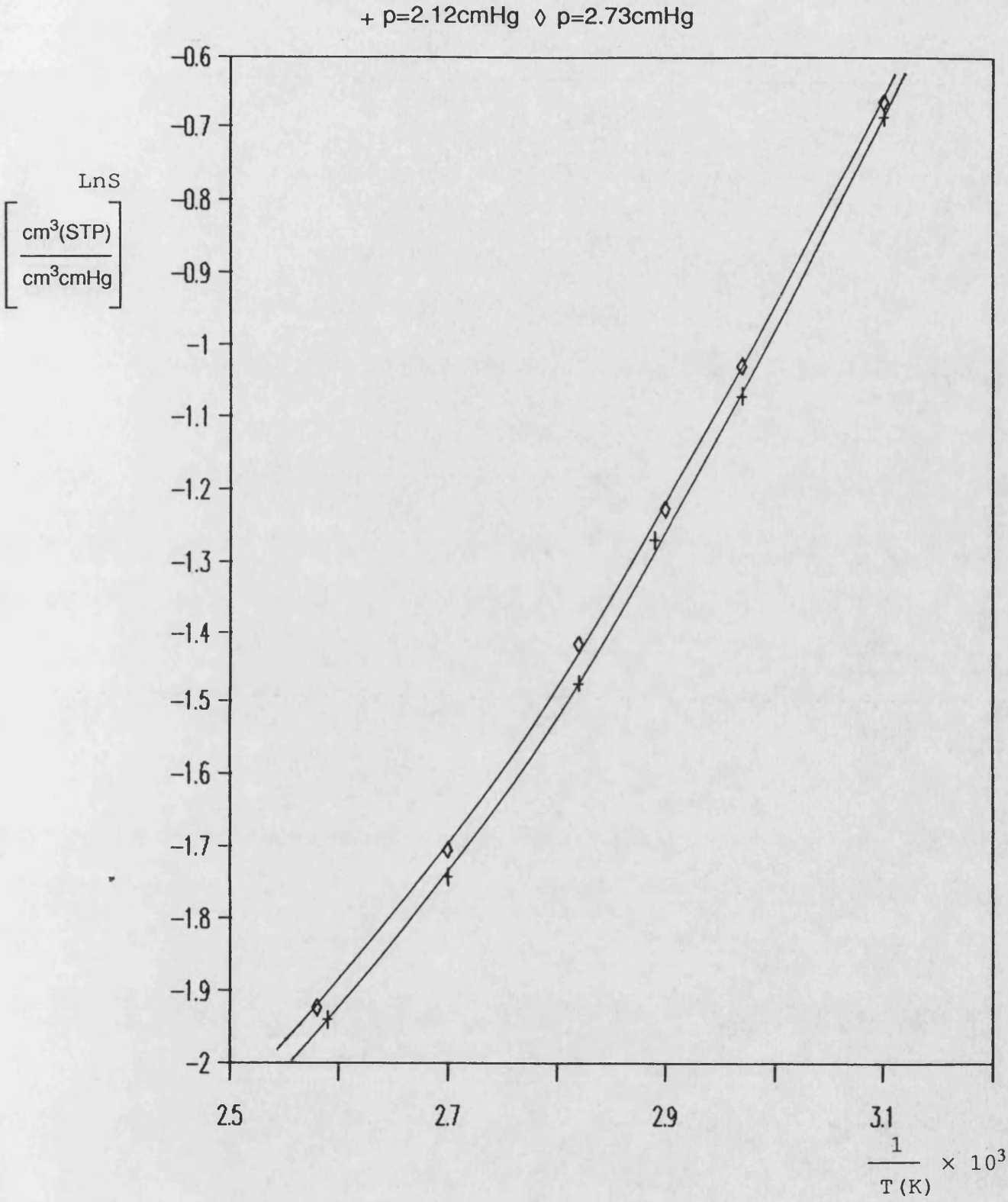

Figure A34a : LnS vs 1/T for Ethanol in Ester-substituted PDMS.

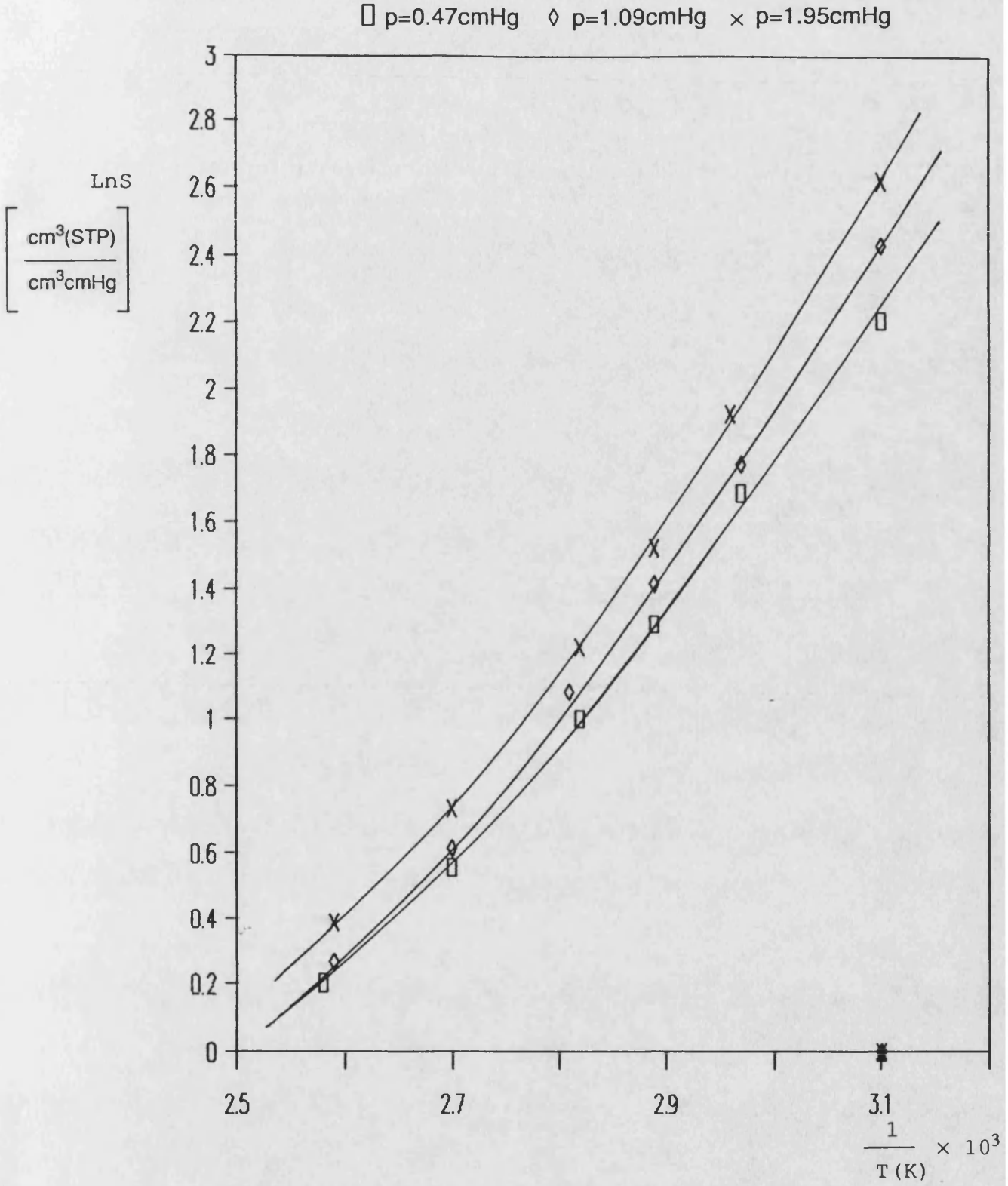

Figure A35 : LnS vs 1/T for Tetrachloroethylene in Ester-substituted PDMS.

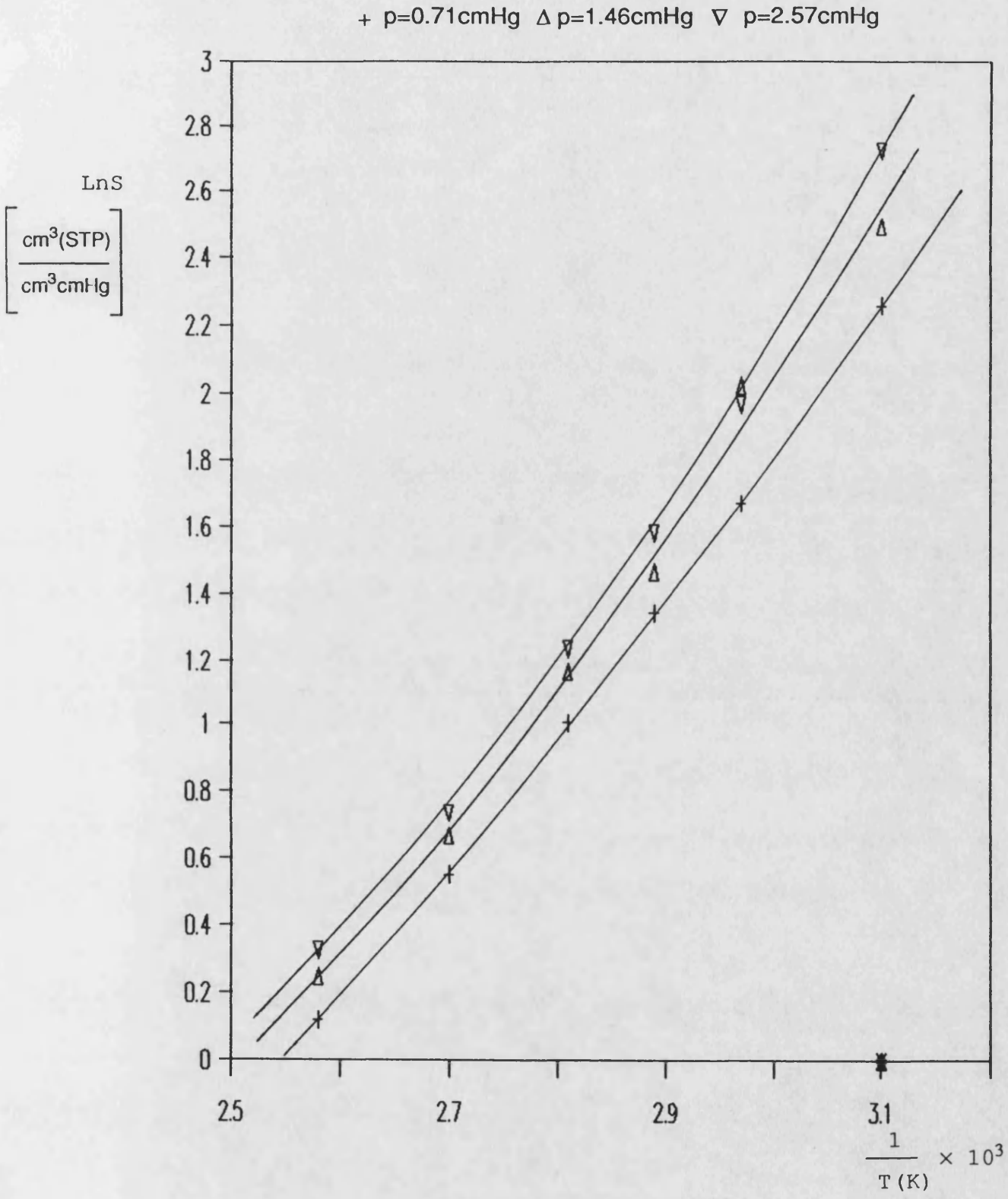

Figure A35a : LnS vs 1/T for Tetrachloroethylene in Ester-substituted PDMS.

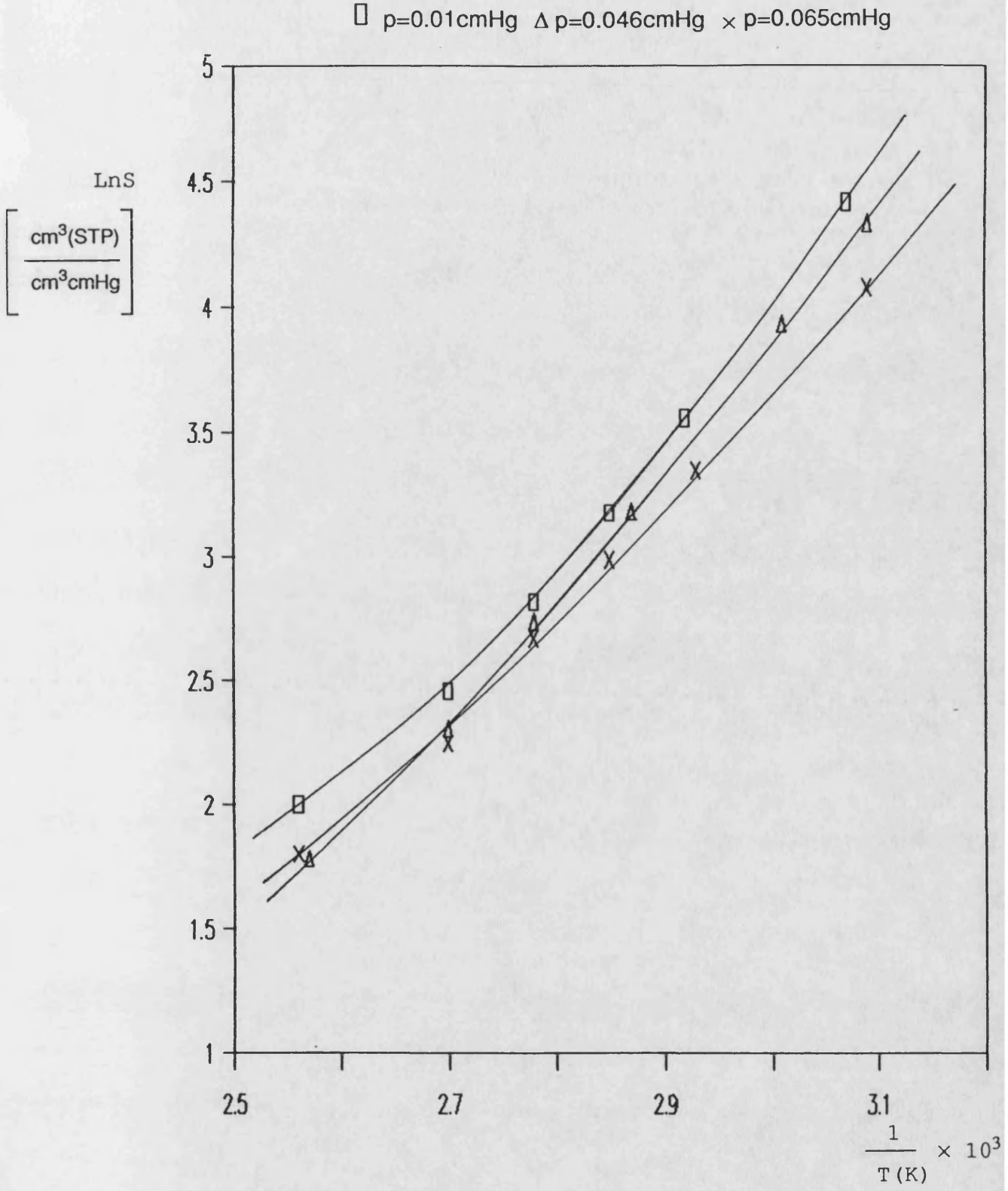

Figure A36 : LnS vs 1/T for Nitrobenzene in Ester-substituted PDMS.

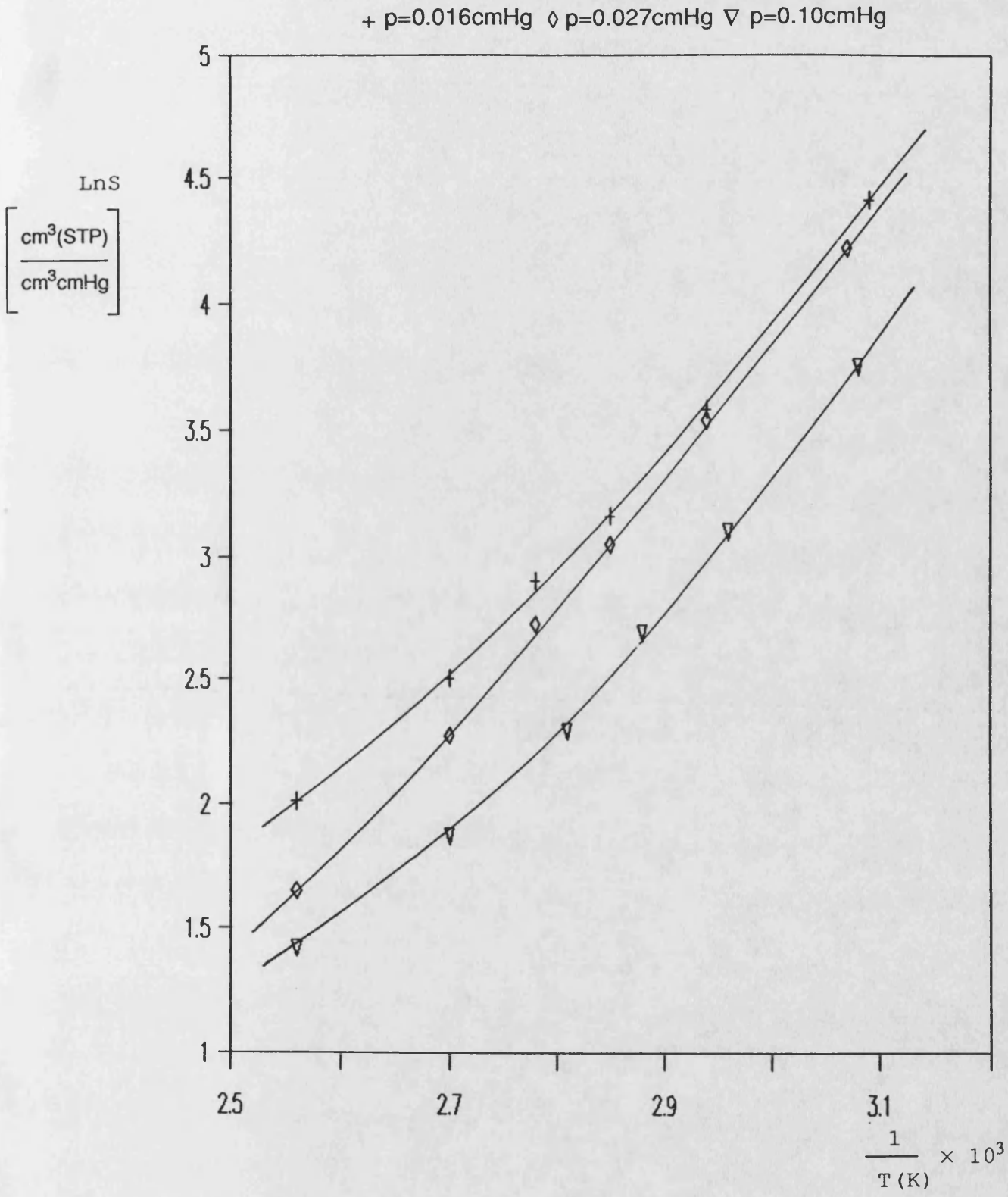

Figure A36a : LnS vs 1/T for Nitrobenzene in Ester-substituted PDMS.

Variation of P, D and S

with Permeant Pressure

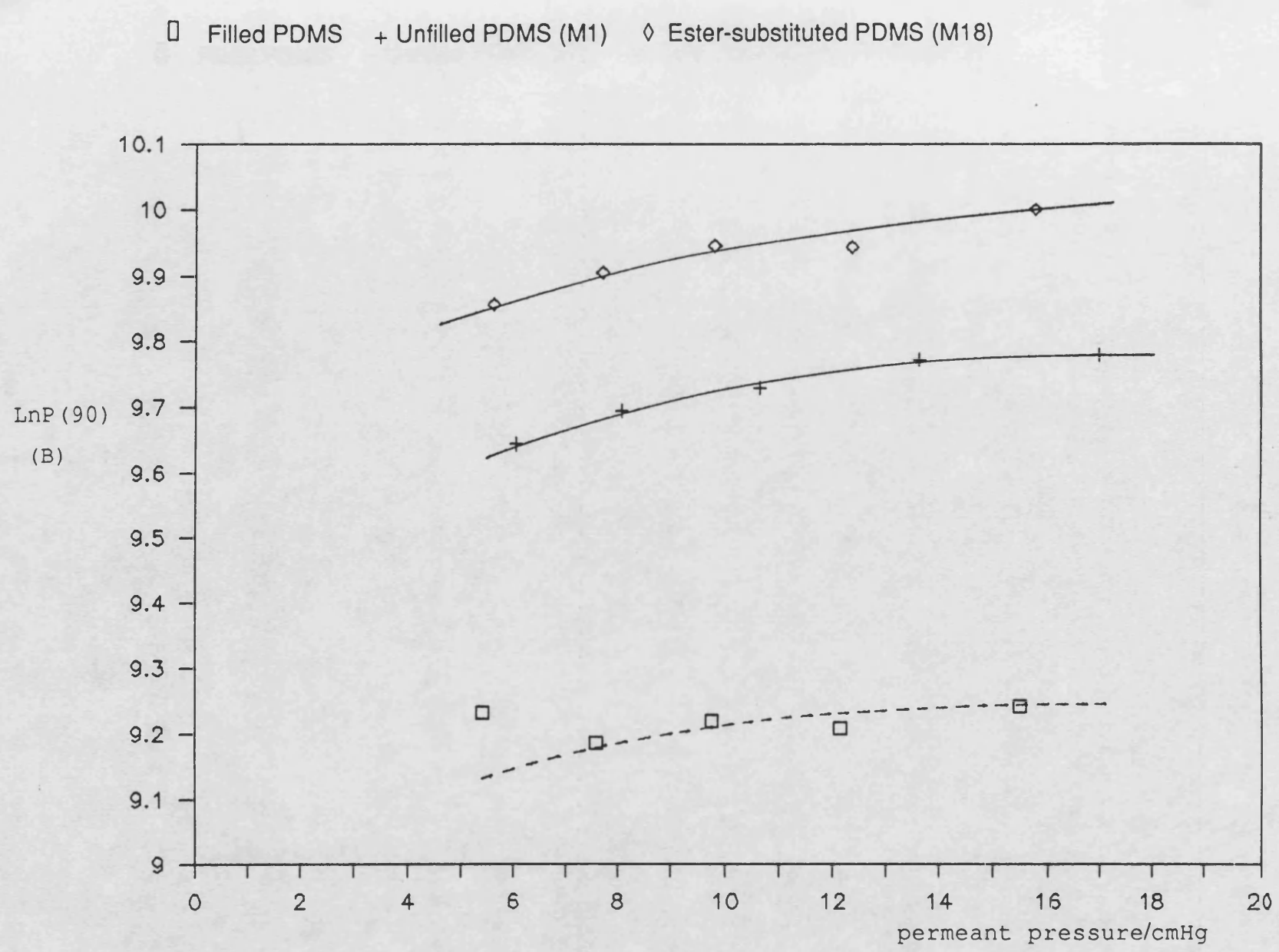

Figure A37 : LnP at 90°C vs Permeant Pressure for Acetone in Polysiloxanes.

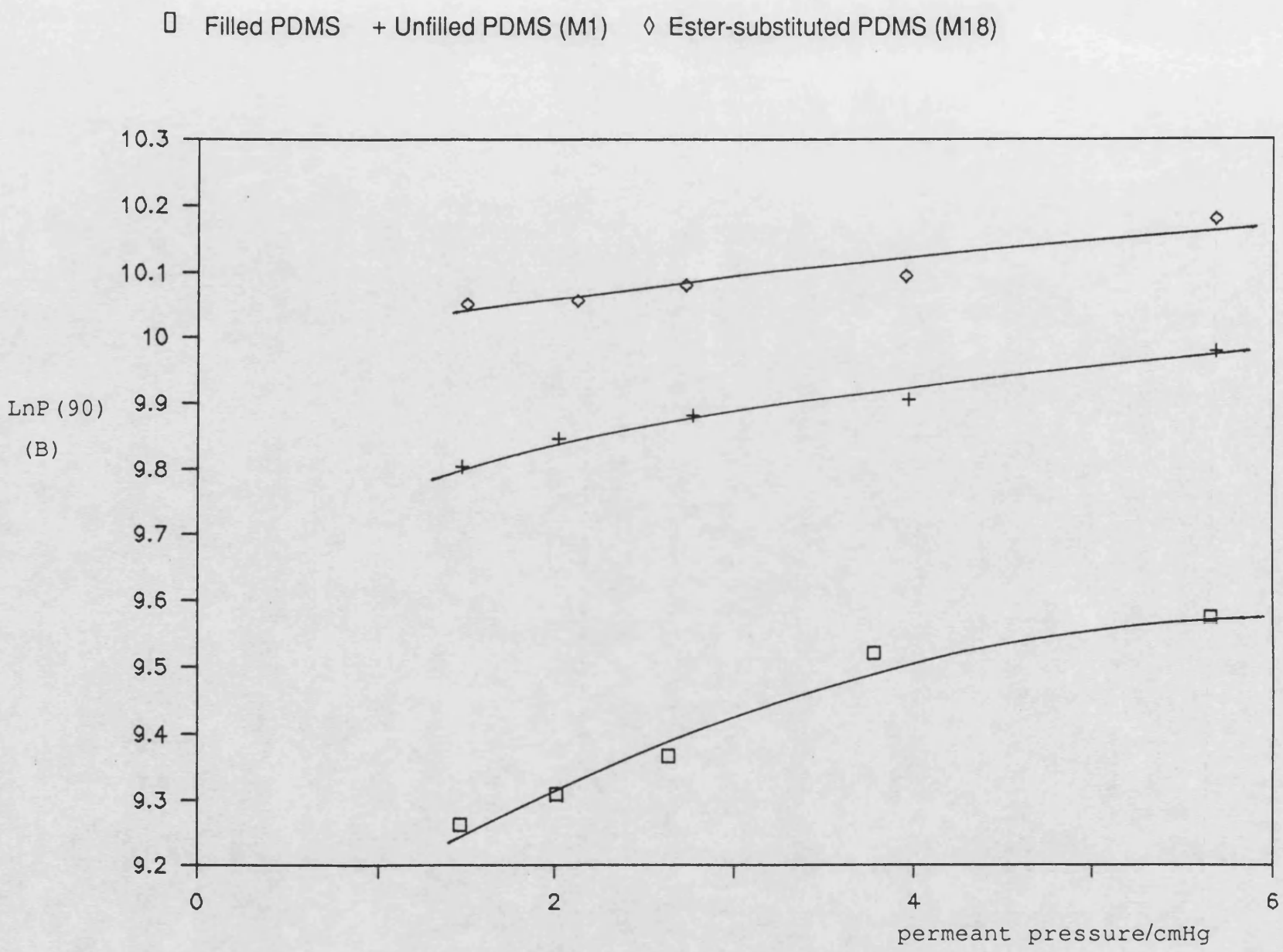

Figure A38 : LnP at 90°C vs Permeant Pressure for Ethanol in Polysiloxanes.

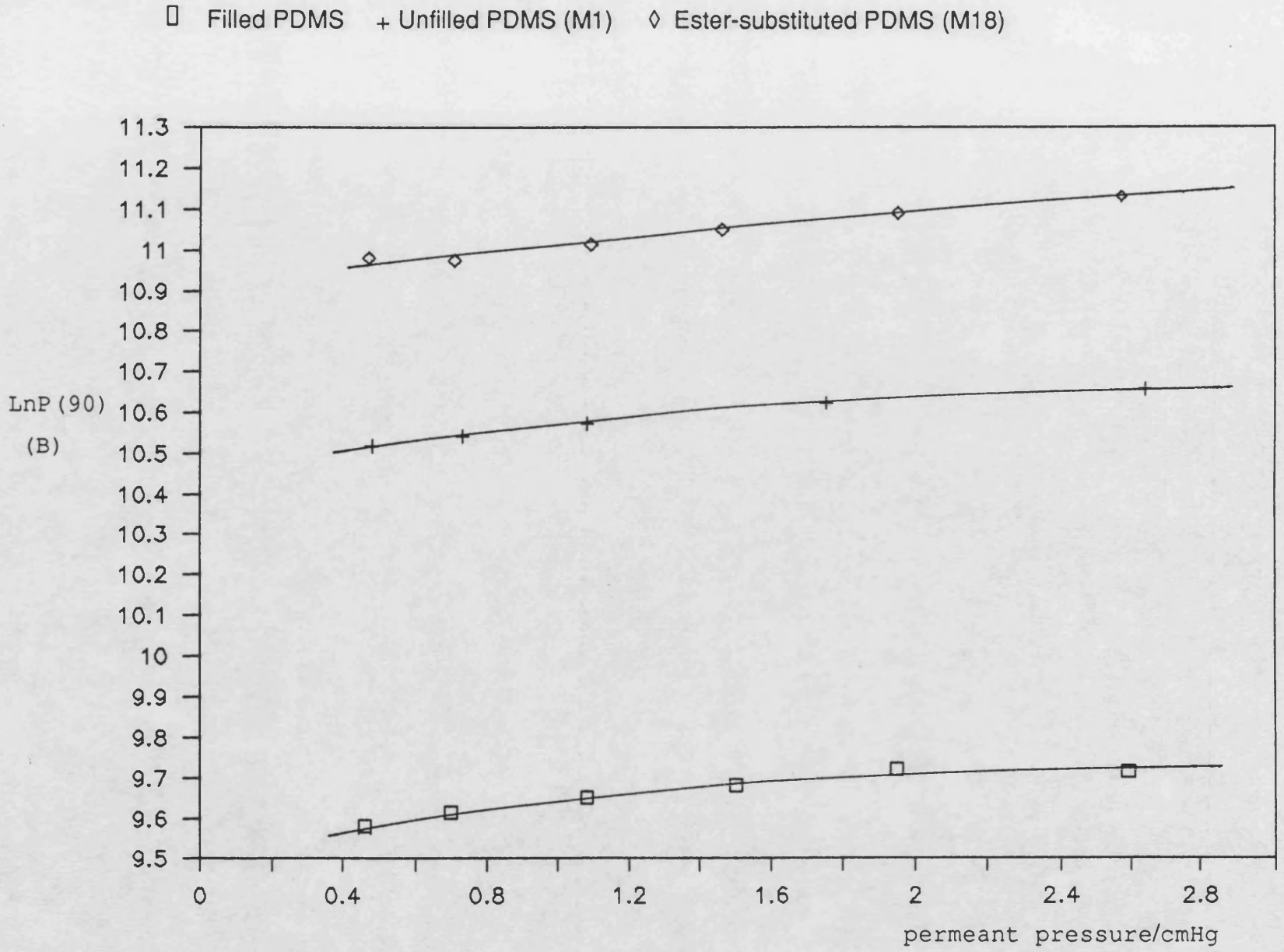

Figure A39 : LnP at 90°C vs Permeant Pressure for Tetrachloroethylene in Polysiloxanes

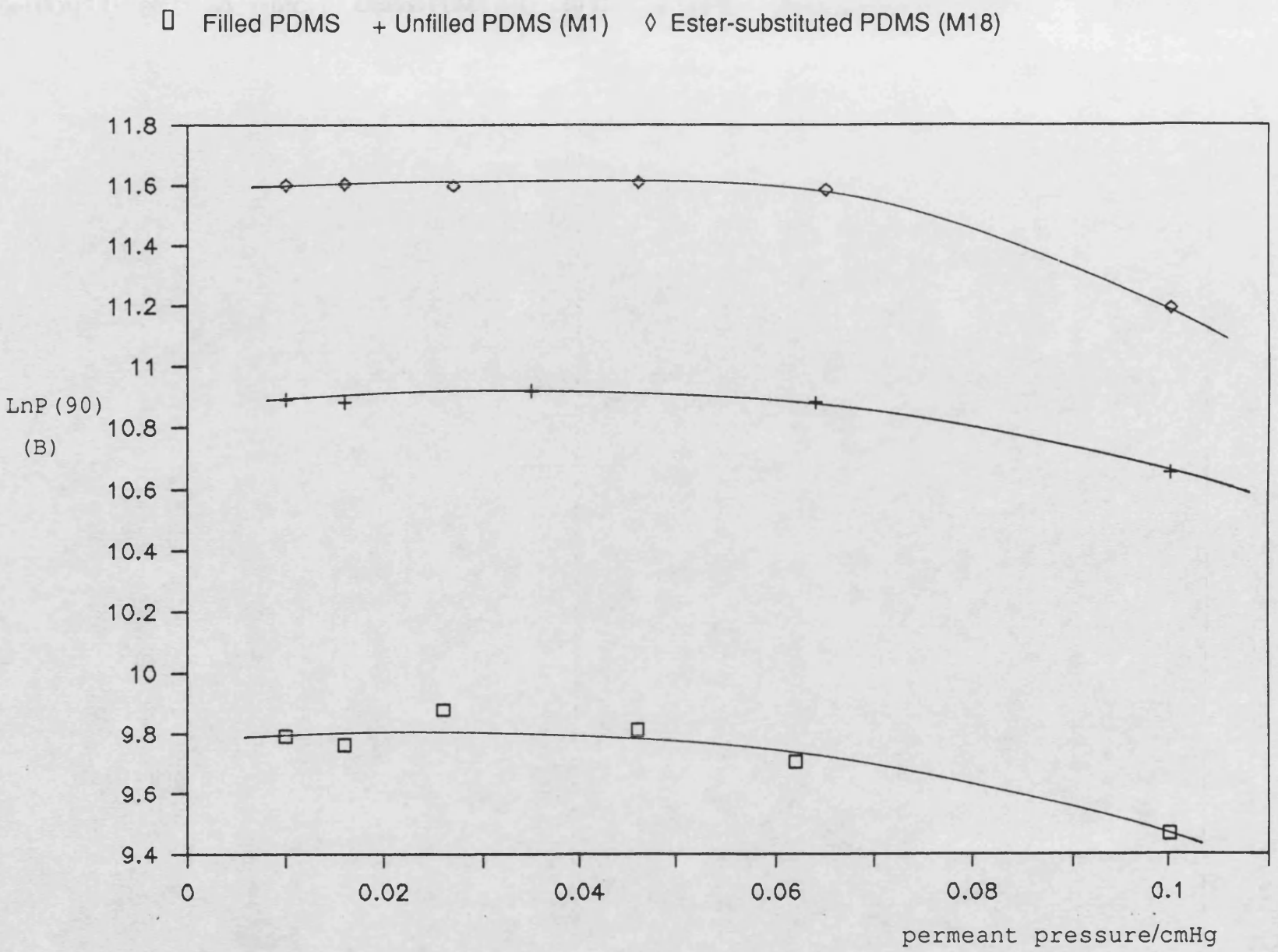

Figure A40 : LnP at 90°C vs Permeant Pressure for Nitrobenzene in Polysiloxanes.

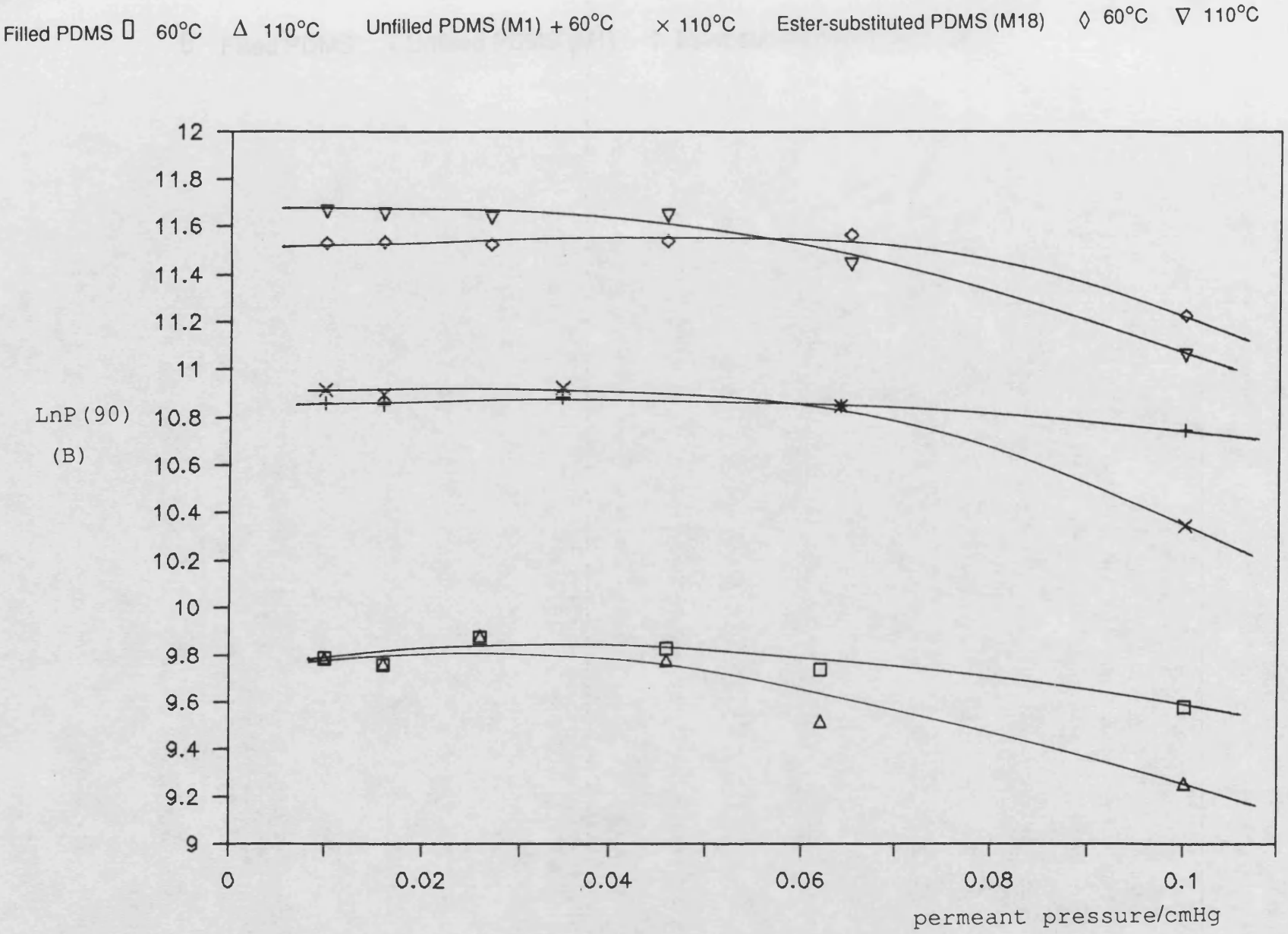

Figure A40a: LnP at 60°C and 110°C vs Permeant Pressure for Nitrobenzene in Polysiloxanes.

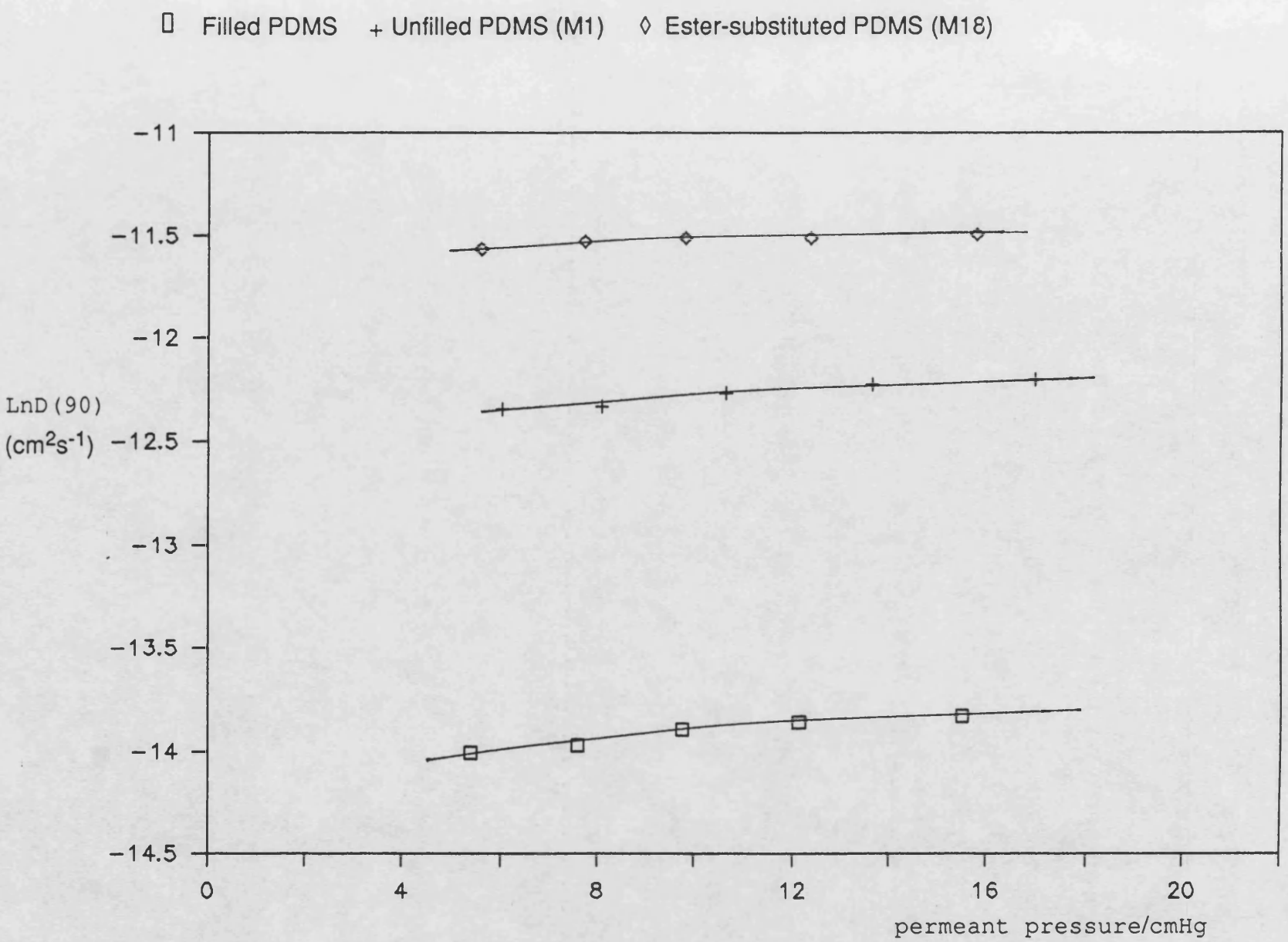

Figure A41 : LnD at 90°C vs Permeant Pressure for Acetone in Polysiloxanes.

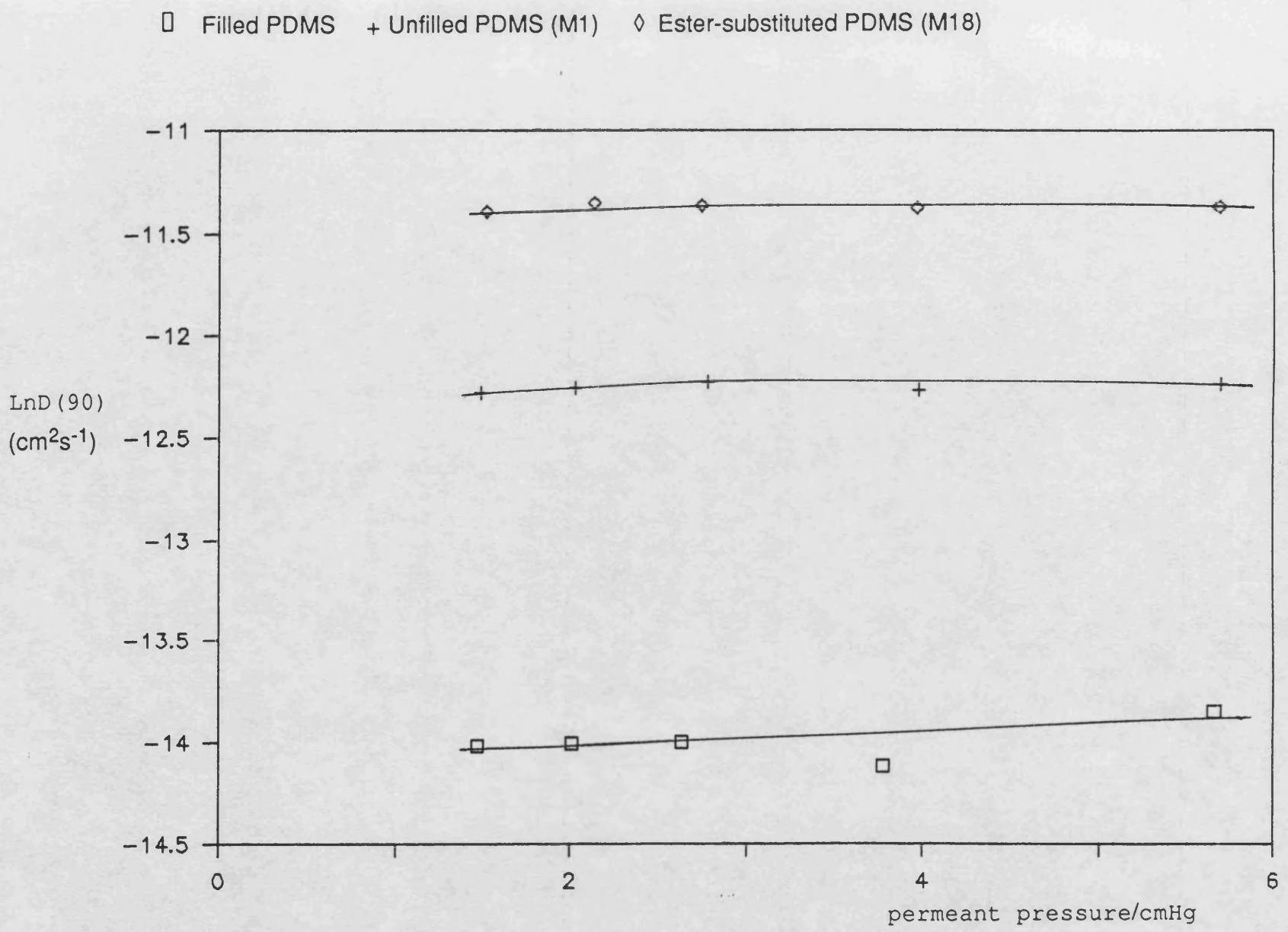

Figure A42 : LnD at 90°C vs Permeant Pressure for Ethanol in Polysiloxanes.

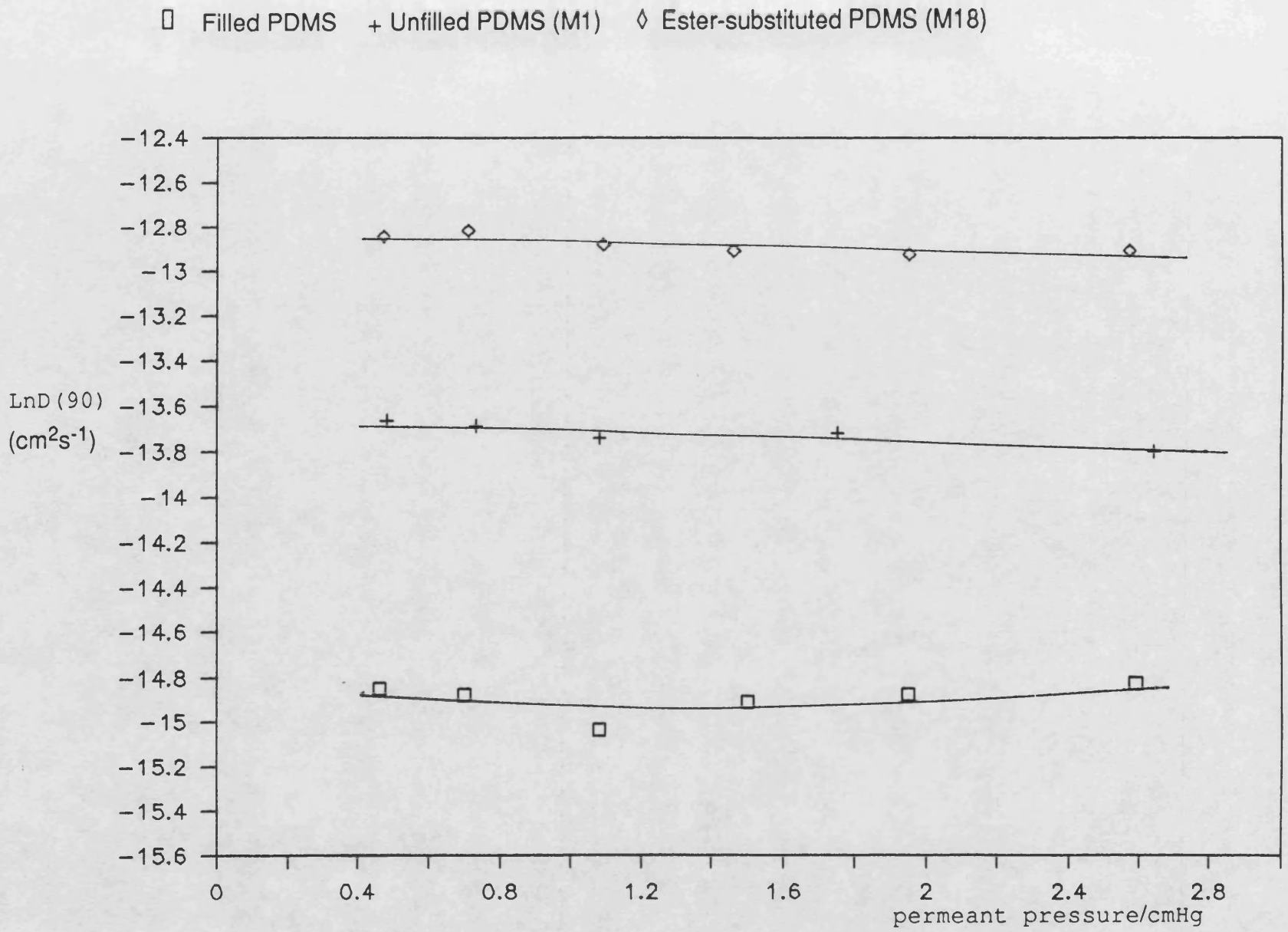

Figure A43 : LnD at 90°C vs Permeant Pressure for Tetrachloroethylene in Polysiloxanes.

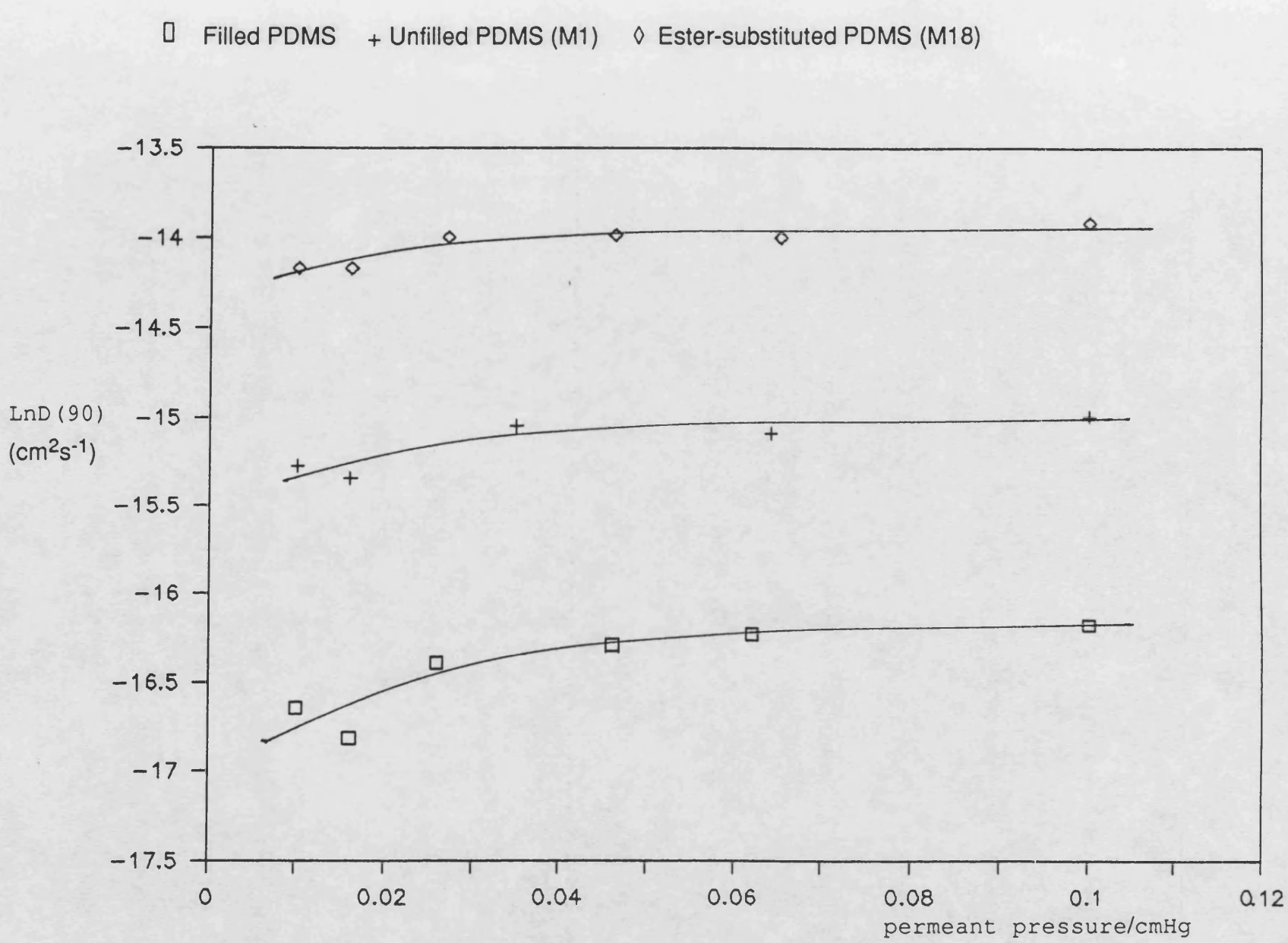

Figure A44 : LnD at 90°C vs Permeant Pressure for Nitrobenzene in Polysiloxanes.

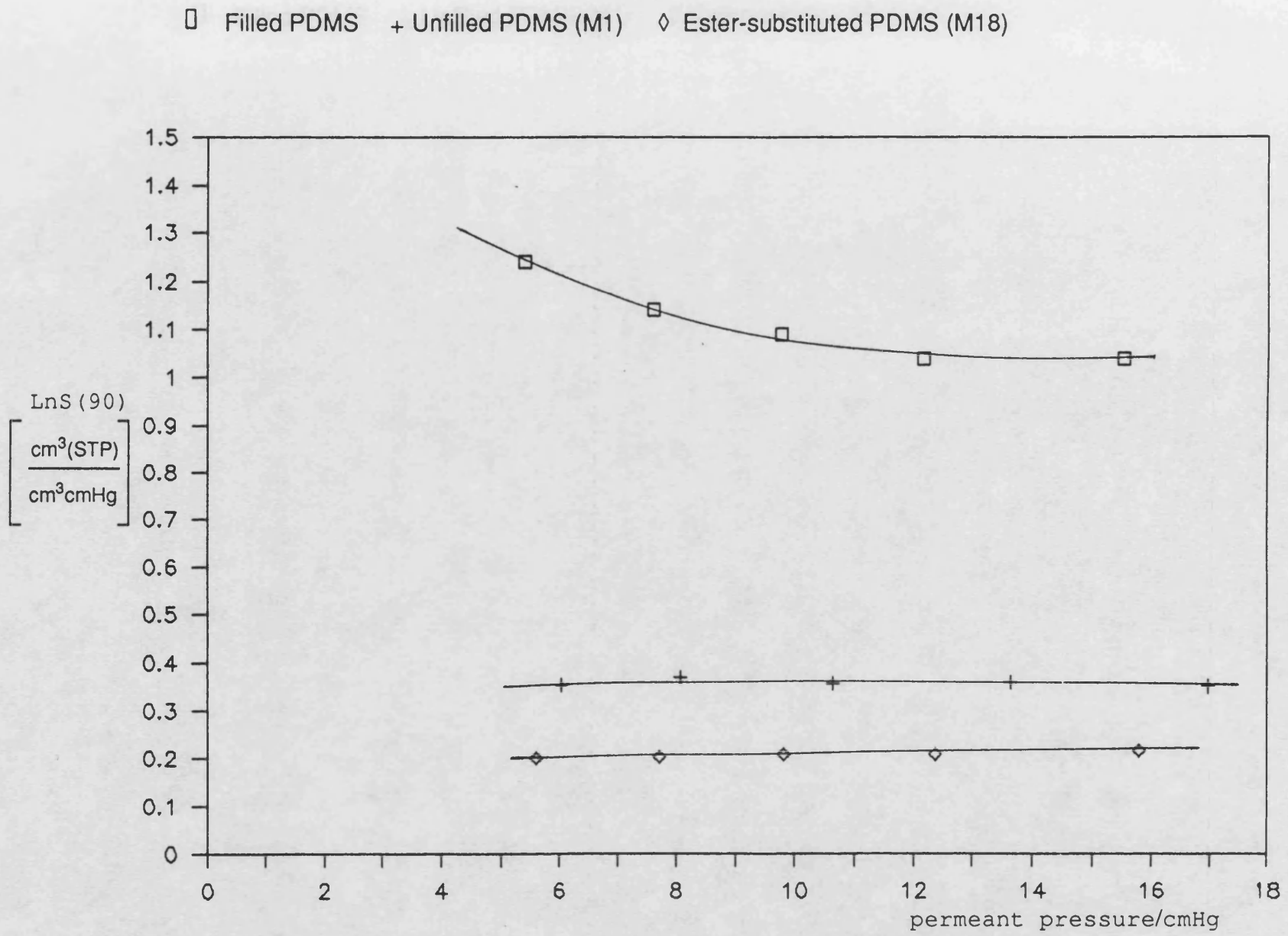

Figure A45 : LnS at 90°C vs Permeant Pressure for Acetone in Polysiloxanes.

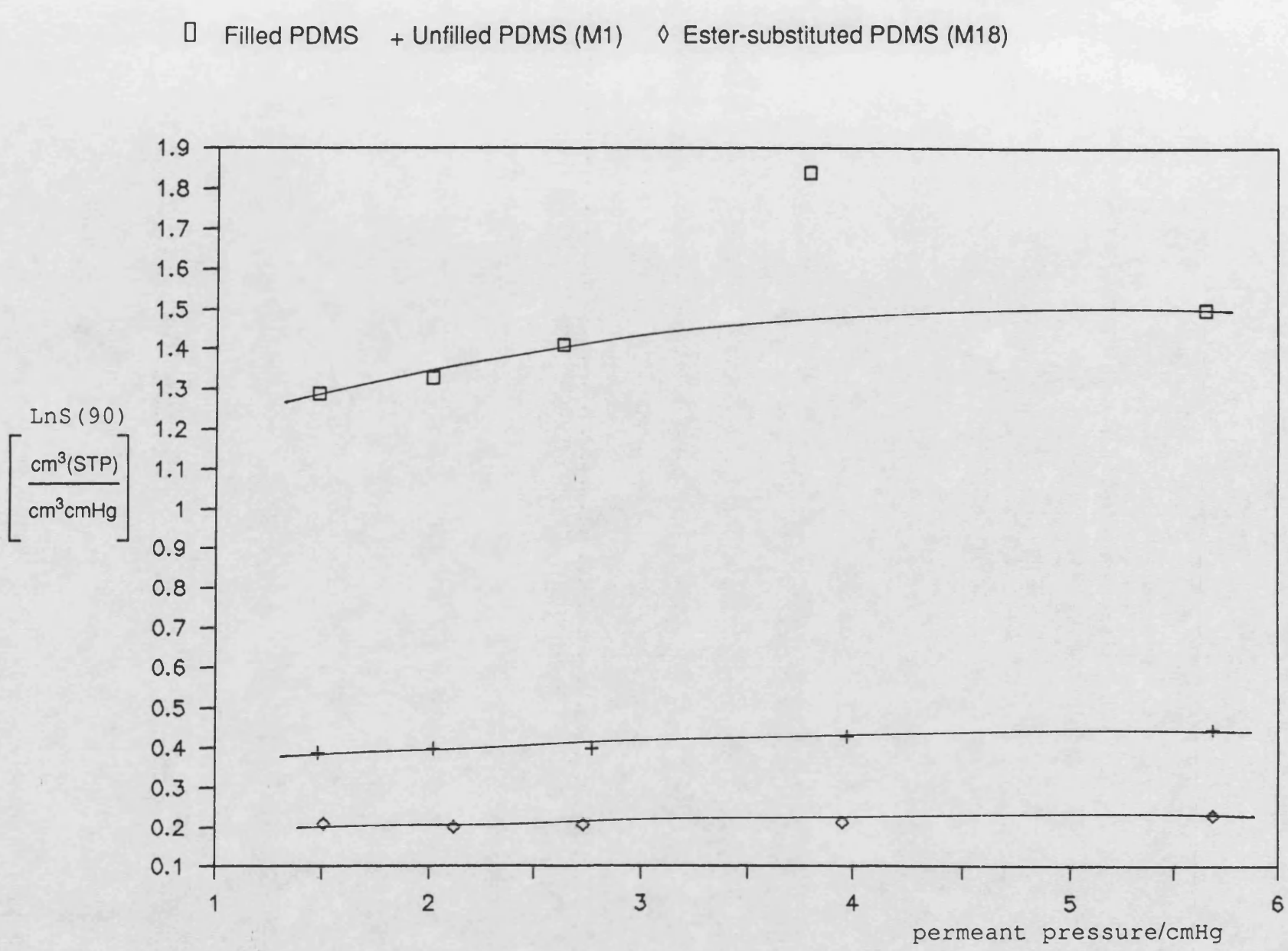

Figure A46 : LnS at 90°C vs Permeant Pressure for Ethanol in Polysiloxanes.

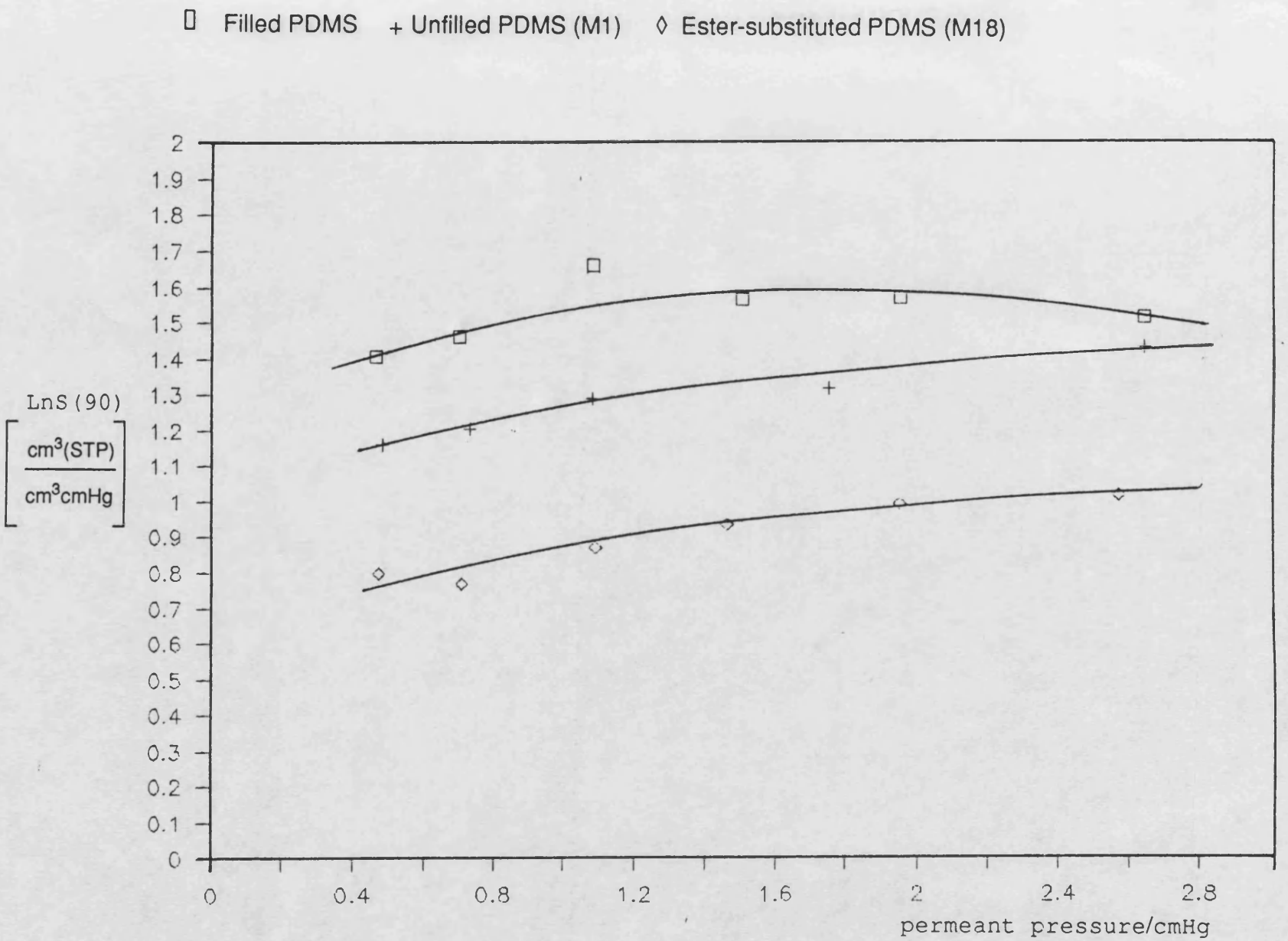

Figure A47 : LnS at 90°C vs Permeant Pressure for Tetrachloroethylene in Polysiloxanes.

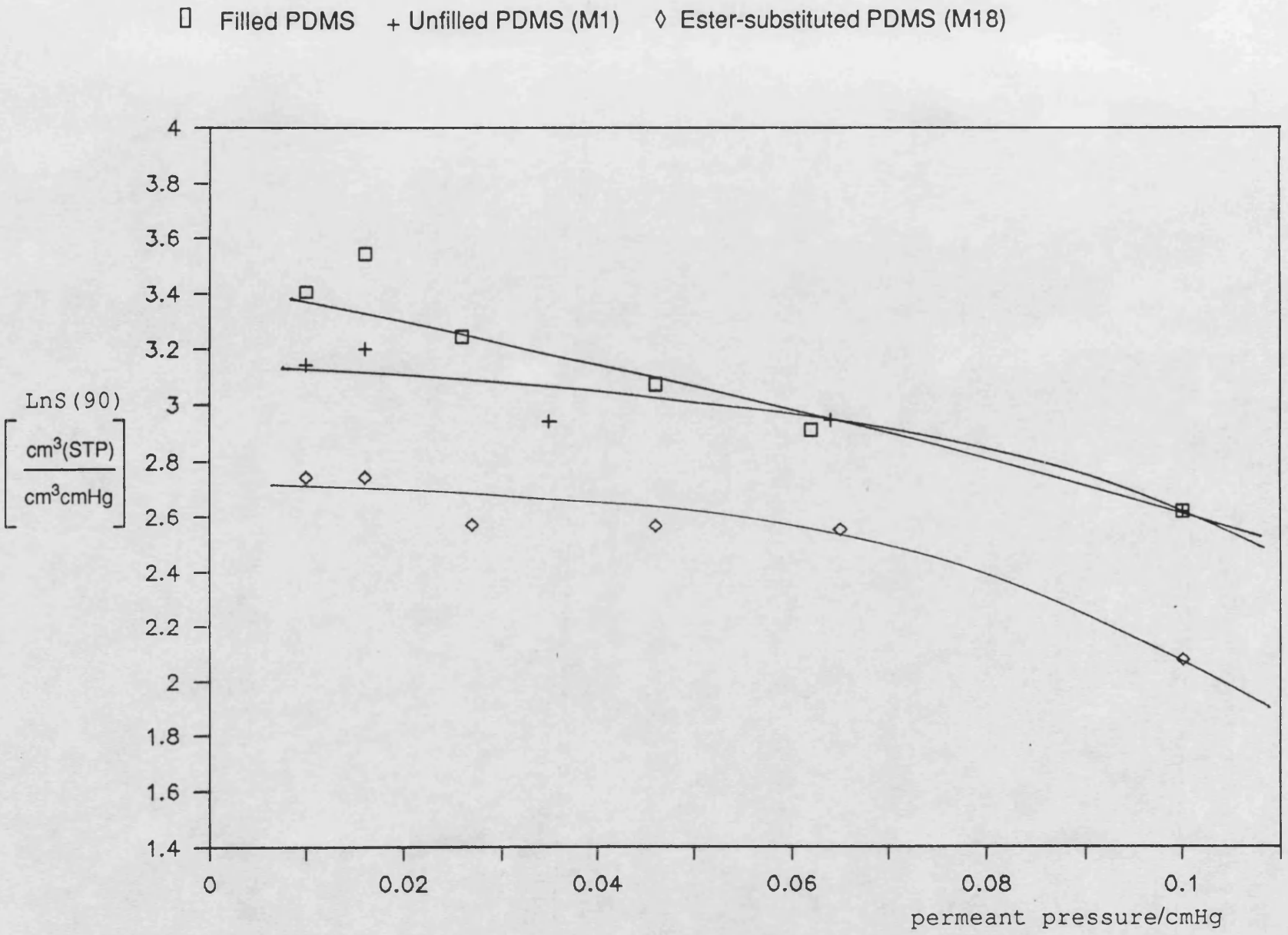

Figure A48 : LnS at 90°C vs Permeant Pressure for Nitrobenzene in Polysiloxanes.